Cellular Pathology and Apoptosis in Experimental and Human Acute and Chronic Compressive Myelopathy

ROWENA ELIZABETH ANNE NEWCOMBE

M.B.B.S. B.Med Sci. (Hons.)

Discipline of Pathology, School of Medical Sciences

University of Adelaide

June 2010

A thesis submitted in partial fulfilment of the requirements for the degree of Doctor of Philosophy

CHAPTER 1

INTRODUCTION

The term “compressive myelopathy” describes a spectrum of spinal cord injury secondary to compressive forces of varying magnitude and duration. The compressive forces may act over a short period of time, continuously, intermittently or in varied combination and depending on their magnitude may produce a spectrum varying from mild to severe injury. In humans, spinal cord compression may be due to various causes including sudden fracture/dislocation and subluxation of the vertebral column, chronic spondylosis, disc herniation and various neoplasms involving the vertebral column and spinal canal. Neoplasms may impinge on the spinal cord and arise from extramedullary or intramedullary sites. Intramedullary expansion producing a type of internal compression can be due to masses created by neoplasms or fluid such as the cystic cavitation seen in syringomyelia. Acute compression involves an immediate compression of the spinal cord from lesions such as direct trauma. Chronic compression may develop over weeks to months or years from conditions such as cervical spondylosis which may involve osteophytosis or hypertrophy of the adjacent ligamentum flavum.

Compressive myelopathies include the pathological changes from direct mechanical compression at one or multiple levels and changes in the cord extending multiple segments above and below the site of compression. Evidence over the past decade suggests that apoptotic cell death in neurons and glia, in particular of oligodendrocytes, may play an important role in the pathophysiology and functional outcome of human chronic compressive myelopathy. The temporal and spatial dimensions of secondary injury involving apoptosis are not yet fully understood. Apoptosis may be reversible depending on progression through the molecular cascade, and an improved understanding of this process in acute and chronic compressive myelopathy may thus be important.

Such knowledge is critical to the development of effective therapeutic intervention strategies designed to limit cellular damage within the spinal cord.

In this thesis major attention is focused on the spinal cord histopathological and apoptotic changes following compression rather than the lesions producing the compression, as few studies on chronic compressive myelopathy have addressed this. Compressive damage to the spinal cord involves not simply a mechanical distortion, but a complex series of molecular events which evolve at varying time intervals after the initial insult. Depending on the site and nature of the inciting injury, neural, glial, axonal, dendritic and vascular

elements may be affected and the pathological changes may vary in time and distance from the direct site of injury. This study aimed to better define the cellular pathology and molecular events, specifically apoptosis, in experimental and human acute and chronic spinal cord injury. Importantly, both spatial and temporal patterns of apoptosis are analysed. The functional alterations, histopathological changes and immunohistochemical markers of neural injury in a rodent model of chronic compression were compared with a rodent model of acute spinal cord injury and human acute and chronic compression.

1.1 Human Chronic Compressive Myelopathy

1.1.1 History

Giovanni Morgagni (1682-1771) was the first to describe paraplegia secondary to intraspinal bony growths and compression of the spinal cord. Cervical spondylotic myelopathy (CSM) was recognised as an important disease process during 1952 by Brain, Northfield and Wilkinson, who suggested that compression of the spinal cord vasculature and ischaemia may contribute to the pathophysiology of CSM. In 1970, Walshe described an 'anaemic and oedematous' cord, with resultant neuronal and myelin sheath damage.

There is sparse literature on the initial recognition of neoplastic tumours as a cause of myelopathy. Harvey Cushing carried out research into tumours of the spinal cord and the development of surgical techniques for excision of intradural spinal tumours during the early 20th Century (Cohen-Gadol et al., 2005). The early recognition of neoplastic spinal cord compression is crucial in the prevention of neurological damage and functional loss.

The term "syringomyelia" is derived, in part, from the Greek word syrinx (Συριγξ) meaning tube or pipe and refers to a fluid-filled, elongated division within the spinal cord parenchyma. In 1764 Dominonco Cotugno described the cerebrospinal fluid surrounding the spinal cord and noted that this fluid connected with intracerebral fluid. This was followed by further description of the CSF by Albrecht Von Haller in 1766. In 1862, William Withey Gull described the clinical manifestations of syringomyelia in his study of a 'case of progressive atrophy of the muscles of the hands: enlargement of the ventricle of the cord in the cervical region, with atrophy of the gray matter'.

1.1.2 Definitions

Three major mechanisms of chronic compressive myelopathy are addressed in this study:

a) Spondylotic myelopathy.
b) Neoplastic myelopathy.
c) Syringomyelia.

Cervical spondylotic myelopathy is defined here as a chronic, degenerative condition affecting the cervical spine involving bone, ligament or soft tissue causing decreased spinal canal diameter and spinal cord compression which is clinically apparent and radiologically verifiable. An example of chronic compressive myelopathy is shown (**Figure 1.1**). Cervical spondylosis has also been termed osteoarthritis deformans, degenerative arthritis, hypertrophic arthritis, osteophytosis, spondylosis deformans, marginal spondylosis, and cervical spondylitis (Epstein, 1976). Cervical spondylosis has previously been defined as degeneration of the components of the spine leading to alterations in neighbouring supportive structures with narrowing of the spinal canal or intervertebral foramen (Cailliet, 1984, Committee on Continuing Education in Neurosurgery, Dunsker (Ed.) 1981).

Spinal tumours may be primary or metastatic and classified according to tissue of origin, benign or malignant, high or low grade, intracapsular or extracapsular. A proposed surgical classification of tumours is the Weinstein-Boriani-Biagini system of staging which indicates intra- or extra-osseous extension (Hart et al., 1997). Neoplastic compression of the spinal cord tissue may result from lesions removed from the cord or from infiltrative lesions.

Three major forms of syringomyelia are recognised; communicating, non-communicating and extracannalicular. Communicating describes a fluid-filled cavity in which there is structural communication between the central canal and the fourth ventricle. This is absent in non-communicating syringomyelia. In extracanalicular or primary parenchymal lesions there is no communication with either the fourth ventricle or central canal. In a review article Milhorat (1997) identifies two exceptions to these criteria, in cases of cyst formation within a malignancy of the spinal cord, and in atrophic cyst formation in myelomalacia. Hydromyelia is a dilatation of the central canal but may be classified alongside syringomyelia. Syringobulbia is used to describe extension of the fluid-filled cavity into the brainstem.

1.1.3 Aetiology and Classification

Spondylotic myelopathy involving the cervical spine most commonly afflicts males of older age, within the sixth or seventh decades (Durrant and True, 2002) and is the most frequent cause of spinal cord dysfunction in older adults (Orr and Zdeblick, 1999). A

combination of sensory and motor deficits may occur, often leading to a loss of dexterity, upper limb weakness and gait difficulties. Cervical spondylosis is characterised by degenerative changes involving bone and connective tissue within joints, ligaments, or the intervertebral disc. Myelopathy may develop anteriorly from degeneration and protrusion of the intervertebral disc or, posteriorly, from degeneration of vertebral joints with osteophytic growths and connective tissue changes. In the latter, there is often ossification of the posterior longitudinal ligament or thickening and dynamic buckling of the ligamentum flavum (Young, 2000). Narrowing of the lateral recesses or intervertebral foramina leads to compression of the nerve roots. In a minority of cases, such narrowing may result in spinal cord compression and myelopathy and it is most often present in the cervical region. Multiple levels, commonly three (Hayashi et al., 1988), are usually involved in CSM and further stenosis is found in the lumbar spine in approximately 5 percent of patients (Epstein et al., 1984). There may be focal involvement of spinal cord tracts. The radiculomedullary artery may be compressed in spondylotic myelopathy and the symptoms vary according to the extent of vascular insufficiency.

Repeated direct load onto the head has been shown to increase the rate of cervical spondylosis (Jumah and Nyame, 1994). Degenerative changes have been demonstrated in rugby footballers, who during a match may experience great pressure to their cervical spine (Newcombe, 1994). Flexion and extension movements cause transient canal stenosis, particularly if pre-existing stenosis is present, and these can lead to shear-type forces (Hayashi et al., 1987). There may be stretch injury to the cord, opposing the stability provided by the dentate ligaments and filum terminale. Stability is also provided by the intervertebral disc articulation, facet articulations and ligaments, notably the interspinous ligaments, ligamentum nuchae and the capsular ligaments of the facet articulations (Bedbrook, 1969). Different movements may cause damage depending on the pattern of the stenosis. A disc prolapse onto the anterior surface of the spinal cord, for example, is likely to be more severe with neck forward flexion, while buckling of the ligamentum flavum may compromise cord movement with neck extension (Rao, 2002). The degree of disc bulging on weight bearing onto the cervical spine has been measured in post-mortem tissue (Chen et al., 1994) although the number of case was small (n=5). The difference on average of disc bulge was 13mm (10.1% canal diameter). This, combined with a 2.68mm ligamentum flavum bulge suggests a potential mechanism for eventual pathological stenosis.

The clinical syndromes associated with CSM include:

a) Transverse compression resulting in damage to corticospinal and spinothalamic tracts, and posterior columns.
b) Central cord syndrome affecting motor and sensory tracts of the upper limb in preference to the lower limb.
c) Brown-Sequard syndrome characterised by asymmetrical or unilateral spinal cord damage affecting the corticospinal tract with contralateral loss of sensation below the level of compression.
d) Motor syndrome with loss of anterior horn cells and corticospinal tract damage.

Compressive myelopathy is a complex, multifactorial disease. Mechanical factors commonly include degeneration of the intervertebral discs, with subsequent loss of interspace and bulging, and are the major contributing factor to narrowing of the spinal canal. These changes occur most commonly after middle age, with approximately half of men and one third of women affected by 60 years (Holt, 1966). With time there are alterations in the biochemical composition of the disc, with progressive loss of disc collagen proteoglycan and water, and with it loss of elasticity (Adams et al., 1996, Rao, 2002). Dehydration leads to a decrease in fluid pressure in the core of the disc with a loss of disc height and subsequent bulging in all directions, or rupture, often towards the midline (Raj, 2008).

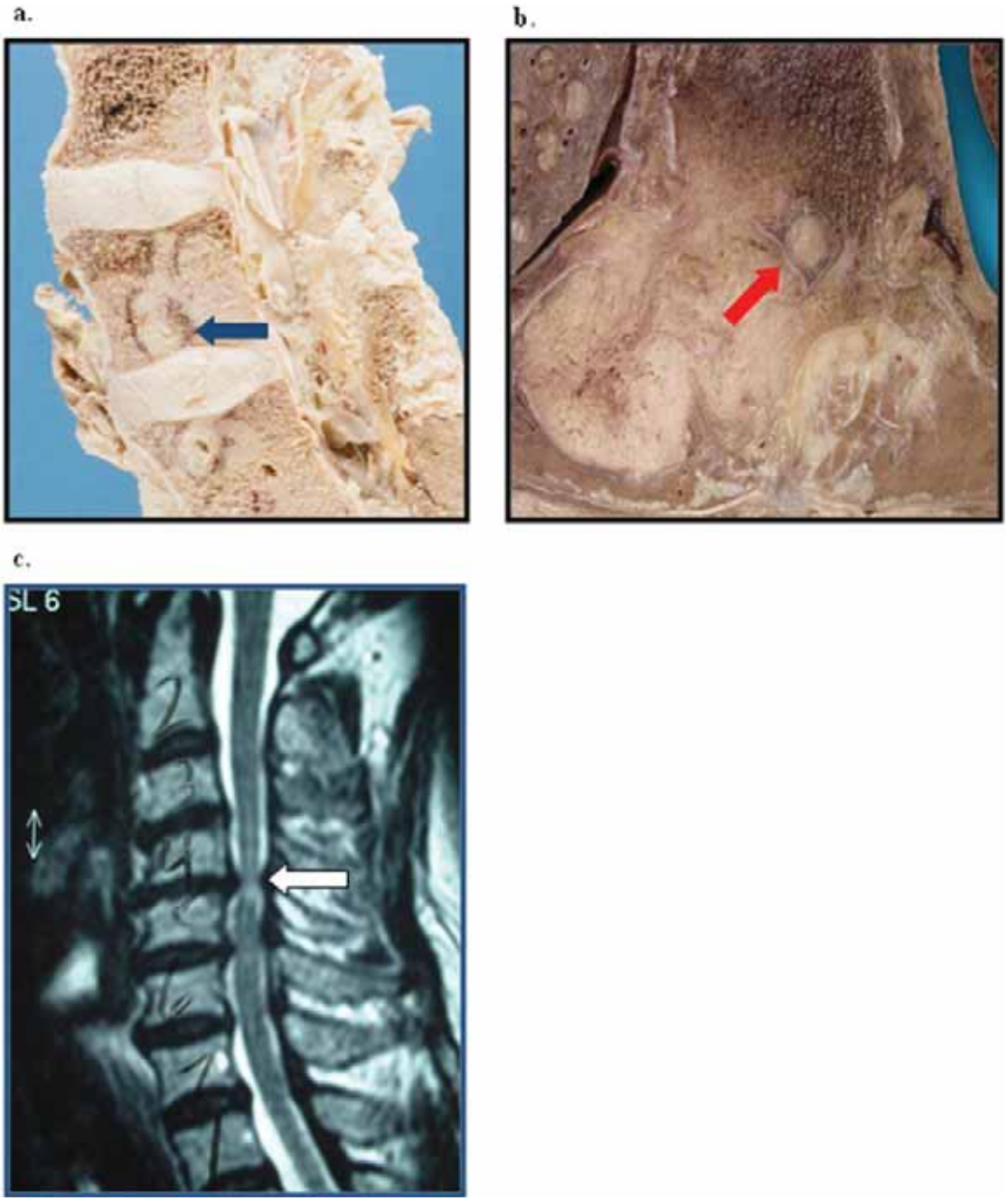

Figure 1.1 Pathological changes in human chronic compressive myelopathy.

A macroscopic sagittal section is shown through the spinal column in a human case of 5 years compressive myelopathy secondary to neoplasm (a). Multiple circular metastases are visible within the vertebral bodies (blue arrow) which may either directly compress the spinal cord or lead to instability and fracture with bony impingement into the spinal canal. In image (b) the tumour is shown encroaching onto the spinal cord (red arrow). In this MRI sagittal view of the spinal column (c) in an elderly patient with cervical spondylotic myelopathy, high signal change is seen within the compressed spinal cord at the junction of the C4/C5 vertebral bodies (white arrow). This may be associated with significant changes on histopathological staining.

The mobility of the spine can vary between cervical segments and this variation appears to contribute to the development of spondylotic myelopathy in the elderly population (Mihara et al., 2000). An association between osteophytes and concave, load bearing areas within the spine was recognised early (Epstein, 1976). Proliferative changes in response to mechanical stress include thickening of the dura, causing adherence to the posterior longitudinal ligament and thickening of the leptomeninges. Late complications of spinal cord injury include arachnoiditis however removal of the arachnoid cysts two levels above and below the lesion may improve outcome (Reis, 2006).

With regard to neoplastic chronic compressive myelopathy, spinal vertebrae are a common site of metastases in systemic neoplasia and can lead to spinal cord compression (Figure 1.1). Some autopsy studies have demonstrated spinal metastases in up to 90% of patients with cancer (Harrington, 1986). Less commonly there is spinal cord infiltration by metastases or there may be direct mechanical compression from extramedullary tumours and this may be highly disabling. A Scottish study of neoplastic spinal cord compression found that the most common sites of primary neoplasm in these patients was lung (29%), prostate (19%) and breast (13%) (n=174). The most common site of compression was the thoracic spine (77%) followed by lumbar (29%), cervical (12%) and sacral (7%) and one-quarter of patients had multiple sites of malignant compression. Median survival has been estimated at 12 weeks once spinal cord metastases are evident (Loblaw et al., 2005). In a Japanese study of compression by metastatic prostate carcinoma, 3.1% of patients had myelopathy leading to paraplegia or quadriplegia (Nagata et al., 2003). Typical primary tumours which metastasise to the spine arise in breast, lung, kidney, gastrointestinal tract or prostate (Schick et al., 2001). It is common for tumours to originate in the extradural space (Mut et al., 2005) although they may less commonly be intradural or intramedullary. There may be direct tumour impingement on, or invasion of the cord. Neoplasm arising from the cord itself is rare (Baleriaux, 1999).

Communicating syringomyelia occurs distal to the fourth ventricle and is often the result of an obstructive process. This may be secondary to Arnold-Chiari II malformation, Dandy-Walker cysts or an encephalocele. Non-communicating syringomyelia may rarely be due to arachnoiditis from infection or inflammation, meningeal carcinomatosis, or masses such as neoplasm or arachnoid cyst. Extracanalicular syrinxes occur as a result of trauma, haemorrhage or radiation necrosis where cavitation occurs separately and in parallel to, the

central canal (Milhorat, 2000).

The prevalence of post-traumatic syringomyelia in spinal cord injured patients has been reported at 51% (Backe et al., 1991). The estimated yearly incidence of syringomyelia inclusive of all types is 8.4 per 100 000 population (Di Lorenzo and Cacciola, 2005). Reports on the incidence of post-traumatic syringomyelia approximate 0.02% with average onset at 5 years (Carroll and Brakenridge, 2005) and this variation may be due to the different reliance on MRI or other imaging modalities for a particular population. Several levels may be affected. In one study, syringomyelia was present in 20 segments of the spinal cord as found using MRI (Hida et al., 1994).

Theories vary according to the aetiology of syringomyelia, for example in Chiari type I malformation the Venturi effect has been proposed as a primary mechanism. This states that fluid velocity increases with narrowing of the channel, such that fluid pressure is decreased. It may be the case that movement of the cerebellar tonsils during systole causes increased velocity of CSF, decreased CSF pressure beyond, and a vacuum effect leading to distension of the spinal cord during diastole (Grietz, 2006). In post-traumatic syringomyelia, a basic pathophysiological mechanism involving inflammation has been proposed. Some studies suggest that altered or obstructed subarachnoid CSF flow is related to arachnoiditis. In an experimental rat model using excitotoxic induced post-traumatic syringomyelia and lumboperitoneal shunt insertion, an increase in subarachnoid space did not cause a measurable effect on CSF flow and did not support the presence of obstructive arachnoiditis as a cause of post-traumatic syringomyelia (Brodbelt et al., 2003). Ventral deformities in post-traumatic syringomyelia can be severe and may decrease the spinal canal diameter by 50% (Holly et al., 2000).

1.1.4 Clinical History and Features

CSM is typically chronic and progressive, often with episodic worsening of symptoms. An acute onset may be seen with traumatic disc prolapse. The onset of CSM is often insidious and may begin as worsening neck stiffness, neck, shoulder or arm pain, which can vary from aching or dull to sharp and severe pain. There may be paraesthesias, often found distally, an asymmetrical weakness of the upper and lower limbs, clumsiness of hand coordination and unsteadiness of gait. Symptoms occurring in a particular nerve

distribution suggest compression of the nerve root or radiculopathy. Rarely, urinary and faecal incontinence may develop. The presentation may be similar to that of metastatic tumour compression of the spinal cord, amyotrophic lateral sclerosis or motor neuron disease, or multiple sclerosis. On examination of the patient, neck flexion may produce an immediate, stabbing pain known as Lhermitte's sign. Muscular atrophy, spasticity and hyperreflexia with upgoing plantar reflex suggest severe or long-standing disease. Several scores have been devised for the evaluation of patient outcomes, such as the Japanese Orthopaedic Association Cervical Myelopathy Score which correlates subjective symptoms, clinical signs, restriction in activities and disturbance of micturition, and appears to have ease of clinical application (Fukui et al., 2007).

Compression of the spinal cord secondary to neoplasm can result in rapid clinical deterioration which is considered a medical emergency (Cher, 2001). Key symptoms include bowel and bladder disturbance, weakness or paralysis, and sensory disturbances. Bony metastases to the spine are common (Perrin, 1992) and may lead to crush fracture and associated back pain.

Syringomyelia usually progresses insidiously over months or years. It is most common in the cervical spinal cord but may occur at any level. Clinical presentation varies widely, but there are often sensory changes such as loss of pain and temperature perception in a cape-like distribution with damage to spinothalamic fibres and loss of light touch, vibration and proprioception as disease extends to the posterior columns. A syrinx may extend to involve the anterior horn causing weakness in the corresponding motor distribution and muscular atrophy. Autonomic changes can occur with progression of the disease leading to bowel and bladder disturbance. Extension of the syrinx into the medulla can damage cranial nerves IX, X or XI leading to dysphagia. Other clinical examination findings may include increased reflexes, increased tone and an upgoing plantar response in the lower limb with severe disease. There may be associated hydrocephalus. Syringomyelia should be considered in any patient presenting with delayed neurological deficit following trauma.

1.1.5 Diagnostic Investigations

MRI has become a useful diagnostic tool and is likely to play a key role in future correlation of histopathological changes with clinical presentation and thus the overall

grading of severity in compressive myelopathy (Loy et al., 2007). Magnetic Resonance Imaging (MRI) analysing for high signal changes and spinal canal pathology continues to be the gold-standard for detailed imaging of the spinal cord in CSM. Degeneration of the spine and subsequent narrowing of the spinal canal are common in the older population, and thus MRI is important in distinguishing intrinsic spinal cord lesions (Adams and Victor, 1993). A computerised tomography (CT) scan is useful for the evaluation of bony narrowing of the spinal canal and may be correlated with MRI findings for disease progression (Freeman and Martinez, 1992). A spinal canal diameter of 13mm has been associated with increased risk for stenosing changes of the cervical discs (Morishita et al., 2009). Early detection is critical in the management of spinal cord compression by solid tumours. MRI is a sensitive imaging technique, particularly for the detection of bony invasion by neoplasm (Traill et al., 1995) although it can be difficult to distinguish between benign and malignant crush fracture (Uetani et al., 2004). Intramedullary lesions may be evident from expansion and enhanced signal on MRI scan (Koeller et al., 2000). Although spinal cord compression may be diagnosed on neurological examination plus plain radiography with high specificity and positive predictive value, MRI is important in determining the best management plan (Husband et al., 2001). Functional MRI has even been used in analysis of cerebral response to cervical decompression within the sensorimotor cortices of the brain (Dong et al., 2008). At the experimental level, diffusion tensor imaging may provide information on axonal changes in chronic compressive myelopathy (Cheung et. al., 2009).

Transmagnetic stimulation has been used in assisting to localise a cervical lesion pre-operatively (Deftereos et al., 2009) although its use is not currently recommended routinely. Plain radiographs may suggest degeneration of the spine but are unable to provide detail on spinal cord pathology. Plain radiographs cannot delineate a syrinx however they can indicate bony abnormalities, instability or abnormalities at the craniocervical junction. CSF pressure may be elevated however lumbar puncture is avoided due to the risk of brain-stem herniation. CT scans provide detailed information on bony impingement into the spinal canal and may indicate spinal cord changes but MRI is the most useful in the detection of syringomyelia particularly using gadolinium contrast for tissue definition. Increasing use of this technique has led to a rise in the reported incidence of Chiari I malformations and syringomyelia. Phase-contrast may be used to show abnormal CSF flow and there is evidence of its predictive value for decompressive surgery

in children with Chiari I malformation (Ventureyra et al., 2003) however other studies have questioned the use of cine phase-contrast due to spatially and temporally heterogeneous results in a similar population (Iskandar et al., 2004). Recent early studies have investigated the potential for detection of apoptotic cell death in vivo using Annexin V or caspase-inhibitors during positron emission tomography and spectroscopy (Blankenberg 2008).

1.1.6 Management and Outcome

Several scales have been developed to determine motor and sensory outcome in compressive myelopathy. Scales used include the well-accepted Japanese Orthopaedic Association Scale for functional assessment of myelopathy, American Spinal Injury Association (ASIA) classification, the Cooper Scale for separate evaluation of upper and lower extremity motor function, and a five-point scale for evaluation of strength in individual muscle groups which have each been well-described (Fukui et al., 2007, American Spinal Injury Association/International Medical Society of Paraplegia, 2001, Chapman et al., 2005). While these human scales and their detailed neurological assessment are not applicable in a rodent model, a battery of testing including locomotor and sensory testing was used in order to quantitatively measure changes following injury.

Surgical intervention in patients with CSM is common and it carries a major community health cost, particularly in view of Australia's ageing population (Rowland, 2003). Surgical outcome is often unpredictable for patients and some indeed become worse following decompression. Traditionally, posterior laminectomy was the mainstay of treatment however during the late 20th Century anterior approaches were recognised as providing improved spinal stability post-surgery (Saunders, 1996) as well as allowing access to osteophytic processes arising from the vertebral body. There is ongoing debate as to whether surgical intervention results in overall better outcomes rather than conservative measures, given that there is a significant risk of surgical morbidity and mortality, although some patients have shown considerable improvement post-operatively (Saunders, 1996, Houten and Cooper, 2003). Estimates suggest that around 18% of patients with CSM will improve spontaneously, 40% will remain stable and about 40% will deteriorate without therapy (Kumar et al., 1999). Furthermore, the association of spinal cord high signal change using MRI scanning with neurological function before or after surgery is not clear.

Some studies suggest that poorer outcome is associated with high signal after decompression (Suri et al., 2003, Wada E, et al., 1999) however this does not always correlate with signal change prior to surgery and further studies assessing the likely cause of signal change (iatrogenic or natural disease progression), its prognostic significance and histopathological correlate are required. Conservative approaches have included immobilisation utilising neck braces, however this is unlikely to lead to improvement and may increase progression of symptoms (Zeidman and Ducker, 1992).

Treatment for compressive myelopathy secondary to neoplasm varies according to the type of neoplasm and stage of invasion but usually includes radiotherapy, chemotherapy or surgical excision of the tumour, often employing multiple approaches. For example, combined radiotherapy and laminectomy in patients with metastatic compressive myelopathy from lung cancer showed significantly improved survival and mobility when compared with those patients treated with only one modality (Bach et al., 1992). In some cancers, radiosurgery can be used for high-dose, focal radiotherapy in the treatment of spinal extradural metastases, with evidence for pain relief and tumour shrinkage in approximately 80% of myeloma cases, however median follow-up was less than one year (Jin et al., 2009).

Surgical excision alone also confers survival benefit in tumours of the cervical spine (Zileli et al., 2007) but there is a high risk of deep venous thrombosis and infection postoperatively in these patients (Xu et al., 2009). Surgical excision is commonly performed using posterior decompressive laminectomy and the further use of spinal fusion is crucial to the management of patients with spinal instability (Preciado et al., 2002, Bock 1991). The development of improved MRI or CT image guidance during spinal surgery is important for both tumour excision and avoidance of key structures (Kalfas, 2001). MRI is useful in determining the suitability of tumours of the spine to surgical excision (Miyakoshi et al., 2003). However, in patients with tumours affecting the spinal cord many other factors may assist in determining whether surgery is required, such as ambulatory status, comorbidities, the effect of radiotherapy, spinal instability and likely surgical complications (Loblaw et al., 2005). The complex interaction of these factors results in often unpredictable outcomes of surgery and improved randomised control trials are required.

In syringomyelia, treatment involves shunting of the syrinx or other decompressive procedures, often in the setting of progressive disease and increasing neurological deficit. Surgical approaches have had unpredictable results (Koyanagi et al., 2005). Arachnoid scarring is a potential complication of post-traumatic syringomyelia, and treatments such as arachnoid lysis have not yet been of proven benefit (Schaller et al., 1999). However there is evidence that if CSF flow and reduction in syrinx size can be demonstrated following surgery then a good outcome may be achieved (Holly and Batzdorf, 2006). Posterior approaches are often used and ventral epidural decompression without shunting has been successful in post-traumatic syringomyelia, although posterior reconstruction may be required for ongoing neurological deficit (Holly et al., 2000).

1.1.7 Spinal Cord Repair

Spinal cord injury often results in a devastating loss of function for the individual, with consequences for carers and the community as a whole. The central nervous system has comparatively little capacity to repair itself compared to the peripheral nervous system (PNS). Much research is aimed at improving knowledge of secondary cell death pathways and developing ways of minimising cellular damage.

A large body of research relates to spinal cord repair with the aim of improving clinical outcome and identifying multiple targets for therapy. A well-accepted, effective therapy is yet to be developed. Regenerative approaches include use of pharmacological agents (Sharma, 2008) to promote neurotrophic factors, synaptogenesis, cytokine regulation, injection of stem cells and hydrogel scaffolds either at the site or peripherally to aid neurogenesis, regulation of intracellular growth factor pathways, inhibitors of axonal degeneration (Coleman, 2005), alteration of remyelination pathways in order to allow for axonal regeneration, and the use of potassium channel blockade for improving conduction along the axon (De Forge et al., 2004).

In axonal regeneration, both oligodendrocytes of the CNS and Schwann cells of the PNS respond through myelin formation and maintenance of myelin along nerve fibres. In the peripheral nervous system, Schwann cells help to maintain the integrity of the axon via tight junctions (Dezawa, 2000). Immune-based therapies which specifically target

neuroinflammatory cascades in order to promote neuroprotection and axonal regeneration carry potential treatment benefit (Donnelly and Popovich, 2008).

The challenge set for current research in the area of degenerative spinal cord injury (SCI) is to define specific clinical circumstances under which of these many techniques may be useful. Potential therapies include the attenuation of oxidative stress and apoptosis by caspase inhibition (Robertson et. al., 2000, Akdemir et al., 2008), tissue engineering and synthetic polymers (Nomura et al., 2006) genetic therapy (Hidaka et al., 2002) and the use of pharmacological agents towards neural repair (Novikova et al., 2002, Zurita, et al., 2002). Cellular transplantation is a novel therapy which has the potential to aid in tissue preservation and complement repair responses (Mikami et al., 2004, Okano et al., 2007, Watson et al., 2009). Viral vectors may be used in the prevention of apoptosis (Lou et al., 1998) and in promoting axonal regeneration and neuronal preservation (Nakajima et al., 2007, Kwon et al., 2007, Ruitenburg et al., 2002). Multiple rather than single therapies are likely to be required. Therapeutic intervention directed at degenerative SCI should determine at which stages in the injury cascade putative neuroprotective agents should be administered to improve clinical outcomes. The pathophysiology of chronic compressive myelopathy with particular emphasis on the role of apoptosis will be reviewed.

1.2 The Apoptosis-Necrosis Continuum

Principal modes of cell death are classically described, apoptosis and necrosis, which have been interpreted as conceptually distinct processes (Majno and Joris, 1995). Since the commencement of this study it has been recognised that not all dying cells conform to this rigid classification and that necrotic and apoptotic processes are part of a spectrum. Multiple forms of programmed cell death (PCD) are classified as types I, II and III PCD. Type I denotes classical apoptosis, Type II autophagic cell death and Type III paraptosis as well as other forms which will be detailed below. A recent article by the Nomenclature Committee on Cell Death (NCCD) revised criteria for determining cell death based not only on morphological criteria, the more traditional means of identifying cell death, but also on biochemical processes. The morphological classification includes 'apoptotic, necrotic, autophagic or associated with mitosis' cell death. An alternate classification can describe enzymatic processes (proteases such as the caspases), functionality, 'programmed or accidental, physiological or pathological' or by immunological versus non-immunological processes (Kroemer et al., 2009).

Necrosis is the premature death of cells after an initial insult. While some elements of programmed cell death have recently been identified in the process of necrosis, it is largely a passive, immediate type of cell death caused by direct insult to the cell, whether by ischaemia, hypoxia, thermal injury, or toxins (Hotchkiss et al., 2009). In apoptosis (Greek: *apo* - from, *ptosis* - falling) injured or superfluous cells shrink and the resulting apoptotic bodies are rapidly deleted, with minimal inflammatory reaction from surrounding tissue. A better understanding of the role of apoptosis, may lead to improved treatment of spinal cord injury.

Morphological criteria have previously been regarded as the most reliable discriminators of cell death in tissues (Majno and Joris, 1995). Secondary morphological changes including nuclear breakdown can be recognised by light microscopy as early as 24 hours following injury. Necrosis falls along a spectrum with apoptosis (cell death by shrinkage) and oncosis (cell death by swelling) (Levin et al., 1999). In apoptosis there is cytoplasmic shrinkage with karyorrhexis, while oncosis (Greek *onkos*: swelling) is characterised by cytoplasmic swelling with karyolysis or pyknosis.

The pathological activation of apoptosis can be caused by multiple processes including viral infection, autoimmune disease, neurodegenerative conditions and carcinogenesis (O'Brien, 1998, Mountz et al., 1994, Yuan and Yankner, 2000, Baretton et al., 1998, Friedlander, 2300). The trigger for this process may be from within the cell, such as mitochondrial dysfunction, or from activation of cell surface receptors such as Fas. Multiple triggers of secondary cell death originating from outside the cell include cell-cell interactions, hypoxia, ischaemia, hormones, genotoxic agents, mechanical forces and immunological reactions. An excessive influx of calcium and generation of reactive oxygen species (ROS) has been demonstrated in both neuronal ischaemia and reperfusion of the tissue. This induces cell death either via the intrinsic, caspase-dependent pathway of apoptosis or necrosis. Insufficient energy production and disruption of the glutamate transporter system lead to excessive extracellular glutamate triggering apoptosis cell death (Park et al., 2004).

Classical apoptosis as described by Kerr (1972) comprises distinct morphological features. Nuclear chromatin is compacted and marginalised to the outer regions of the nucleus. The cytoplasm becomes condensed and there is convolution of both cell and nuclear membranes. Translucent vacuoles may be present in the cytoplasm. With progressing cellular condensation, the chromatin relocates to the periphery, forming crescents. Nuclear fragmentation is then carried out by endonucleases (Kutsyi et al., 1999) into characteristic multiples of 185-200 base pairs (Nakano, 1997) as the cell 'buds', or splits, into apoptotic bodies. Despite these disturbances, the cytoplasmic organelles are preserved in tight configuration. The apoptotic bodies are then engulfed by surrounding phagocytic cells, such as mononuclear phagocytes (Duvall et al. 1985, Savill et al. 1990) and degraded by lysosomes to produce lysosomal residual bodies (Kerr, 1993). This phagocytic reaction is not usually associated with inflammation (Saraste, 1999). Morphological features of apoptosis are the most reliable method for indentifying apoptotic cells but they are not definitive for apoptosis and often supporting biochemical evidence is required. The molecular pathways leading to these changes are widely varied.

Classical apoptosis is a ubiquitous delayed process, occurring in the context of ATP depletion and resulting from a cascade of molecular activation towards cellular dysfunction and eventual cell death. In contrast to necrosis, classical apoptosis is an active secondary form of cell death. The apoptotic process involves self-sacrifice of the damaged cell or

‘cell suicide’, conducted according to a specific molecular cascade that occurs within the cell itself. Apoptosis is often a physiological process, occurring in approximately 50% of neurons during the development of the nervous system, as well as playing a role in atrophy, tissue repair and destruction of inflammatory cells (Chowdhury et al., 2006, Ekshyyan and Aw, 2004).

In apoptosis, compromised or superfluous cells are removed without injury to the cellular microenvironment, whereas oncosis denotes non-apoptotic accidental cell death by ischaemia, hypoxia, toxins or other noxious agents. The apoptotic process (**Figure 1.2**) can be initiated by the cell itself or by extracellular agents causing activation of cell surface receptors in a process known as extrinsic apoptosis. Apoptosis may be intrinsically driven by mitochondrially released proteins, known as intrinsic apoptosis (Gottlieb, 2000). Apoptosis is rapid and may be histologically inconspicuous, whereas cells dying by oncosis take longer (often days to weeks) to be removed and tend to be more readily detectable by light microscopy. Oncotic necrosis initiates an inflammatory response. The cell membrane and mitochondria are damaged and lose their function, leading to cell swelling, cytoplasmic degeneration and eventual lysis (Locke and Brauer, 1991).

Cells undergoing apoptosis may be viable at earlier stages in the pathway, and damage may potentially be reversible. It is currently considered that morphological changes resulting from apoptosis indicate an irreversible component.

Figure 1.2. Intrinsic and Extrinsic Molecular Pathways in Apoptosis.

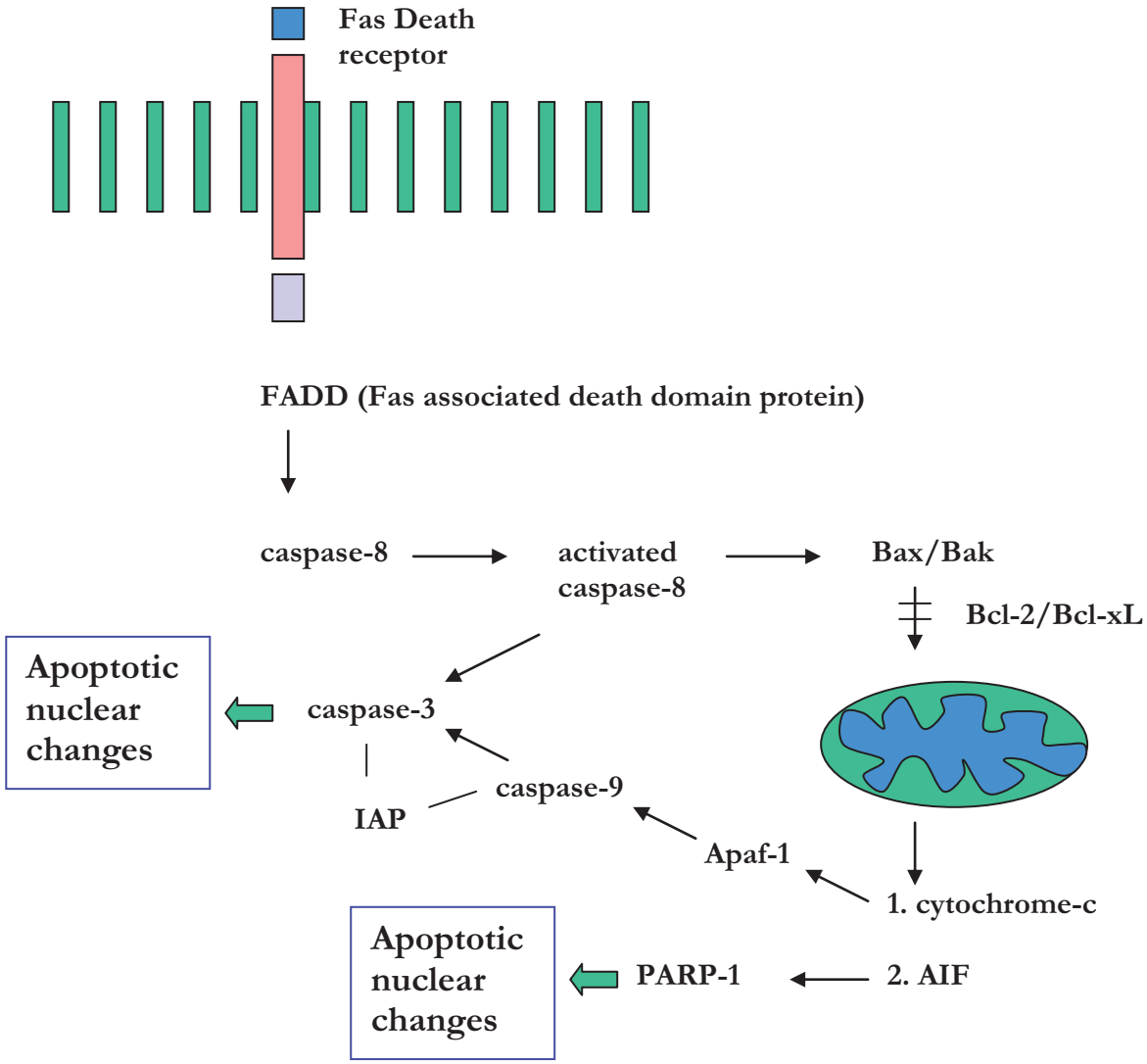

Karyorrhexis, preceded by pyknosis, while not pathognomonic of apoptosis, is a useful diagnostic feature. The shrunken cellular debris resulting from apoptosis or apoptotic bodies are typically engulfed by macrophages or contiguous viable epithelial cells. By contrast, oncosis is characterised by the death of groups of cells which attract an inflammatory reaction, and there is increased membrane permeability (Locke and Brauer, 1991). Unlike apoptosis, DNA in oncosis breaks down in a non-specific manner. This division of cell death is sometimes compromised when apoptosis is severe, because under these conditions, dead cells may occur in large numbers and be associated with inflammation, and cellular enzymes may be released into the circulation.

Under physiological circumstances, apoptosis of sensory and motor-neurons is found in the CNS, while the development of the peripheral nervous system is aided by the deletion of supernumerary neurons (Gschwind and Huber 1997). The inflammatory response is minimal during apoptosis, perhaps due to maintenance of cell membrane integrity.

A major pathway of apoptosis involves activation and release of cytochrome-c from the mitochondria which leads to the activation of the caspase family of proteases. The inactive zymogen of caspase-3 undergoes processing into p18 and p12 subunits. Caspase-3 activity is thought to lead to the major morphological manifestations of apoptosis. However, caspase-independent forms of apoptosis are recognised. The absence of caspase activation in excitotoxic cell death is notable, and the failure of caspase-inhibitors to prevent cell death, but rather to divert to alternative pathways (Johnson et al., 1999; Lankiewicz et al., 2000) is of importance, and suggests that a multifaceted approach to preventative therapies may be needed.

Numerous biochemical, genetic and molecular methods exist to detect apoptosis. These include the use of genetic tools like the microinjection of cDNA into cultured neuronal nuclei and the use of transgenic mice models (Zhang and Le Blanc, 2002). Apoptosis and onconecrosis may be detected by morphological, biochemical and molecular analysis. Imunohistochemistry and immunofluorescent staining in combination with evidence of morphological changes are considered important for the detection of apoptosis. Transmission electron microscopy is important in identifying ‘vulnerable sites’ for intracellular dysfunction during apoptosis and include the plasma membrane, nucleus, mitochondria, endoplasmic reticulum and lysosomes (Ferri and Kroemer, 2001).

There is no single immunohistochemical marker for apoptosis and it is preferable to correlate techniques such as TUNEL staining and a panel of immunohistochemical markers. Alternative methods include non-random DNA cleavage on gel electrophoresis and elevated caspase activity in correlation with morphological evidence of apoptosis. Since the commencement of this study, there have been significant developments in techniques for the detection of apoptosis. Current methodology recommends analysis of: '(1) morphology (time-lapse and transmission electron microscopy and flow fluorocytometry); (2) cell surface markers (phosphatidylserine exposure versus membrane permeability by flow fluorocytometry); (3) intracellular markers (oligonucleosomal DNA fragmentation by flow fluorocytometry, caspase activation, Bid cleavage and cytochrome-c release by western blotting); (4) release of extracellular markers in the supernatant (caspases, HMGB-1 and cytokeratin 18)' (Krysko et al., 2008). Future studies should utilise these new approaches.

Autophagy is a catabolic process involving cellular organelles with potential to enhance cell survival or cause irreversible cell death with the formation of 'excessive' vacuolar autophagosomes. Classical apoptosis was previously known as type I programmed cell death (PCD) occurring as a means of preserving homeostasis of cell number, and paraptosis, previously known as type II PCD, in which death of organelles functions to conserve energy for the cell and preserve its survival. Autophagy is morphologically characterised by visible autophagosomes on transmission electron microscopy in the absence of chromatin condensation. Autophagosomes contain organelle-filled vesicles and thus can be distinguished from the single membrane of apoptotic blebs on microstructural analysis. Adjunctive functional testing for the microtubule-associated protein light chain GFP-LC3 can also aid in the detection of autophagy.

1.3 Human Chronic Compressive Myelopathy

The pathophysiology of chronic compressive myelopathy is complex in part due to the differing compressive lesions and in addition the secondary processes occurring over a variable period of time. It may involve cellular damage due to physical compression, sometimes ameliorated by fluid shift, but also ischaemic, cytotoxic and inflammatory events. Few studies have addressed the question of how apoptosis contributes to the pathophysiology of chronic compressive myelopathy. Studies commonly analyse severe compression at a focal site leading to distinct and severe clinical deficit, such as paraplegia.

Our study provides a detailed and novel analysis of the histopathological and apoptotic changes in chronic cord compression, further defining the pathophysiology in this condition. The number of studies addressing the macroscopic pathological changes affecting the spinal cord in chronic compressive myelopathy is minimal. **Spondylotic myelopathy** was previously regarded as being due to single, planar compression of the cord in association with an absolute cervical canal diameter of 11mm or less (Penning, 1962). There is evidence of dynamic stretching and compression with movement of the spine contributing to the pathophysiology (Henderson et al., 2005). Both compressive forces due to disc bar and tensile forces on the spinal cord via the dentate ligaments during neck flexion have been shown (Levine, 1997). The change in length of the spinal cord during flexion can vary between 4.5 and 7.5 cm, when measured from the dorsal mesencephalon to the conus medullaris (Muhle et al., 1999). Takui et al. (1996) analysed post-mortem tissue from patients with documented evidence of cervical spondylotic myelopathy (CSM) and found atrophic changes in the anterior horn and intermediate zone of the gray matter in the compressed segments and myelin pallor in the lateral and posterior columns, greatest in the lateral region.

Studies of **neoplastic tumour compression** of the spinal cord are few overall and address the molecular pathways underlying the survival and progression of the neoplasm itself, or the inflammatory responses involving surrounding cells of the meninges (Weisieler-Frank et al., 2006), rather than apoptosis. An improved understanding of delayed processes of cell death in chronic compressive myelopathy may assist in knowing whether early surgical decompression is likely to be beneficial.

The pathophysiology of **syringomyelia** remains uncertain and there are few specific studies of the role of apoptosis. Syringomyelia may be associated with cervical spondylotic myelopathy (Kaar et al., 1996) although the underlying mechanisms may vary. During the past decade a 'pre-syrinx state' has been recognised whereby there is myelopathy in the absence of trauma with enlargement and elongation of spinal cord segments demonstrated radiologically but no evidence of cavitation. This state is potentially reversible (Fischbein et al., 1999, Muthukumar et al., 2005). The fluid within a syrinx is thought to consist of CSF, although it has been suggested that this may instead be extracellular fluid (Grietz, 2006). An increase in CSF pressure has long been proposed as the underlying mechanism (Newton, 1969), related to a rise in pulse pressure (hydrodynamic and pressure-wave propagation theories) but strong evidence is lacking (Elliot et al., 2009).

Histopathological changes in **neurons** have been described in few **human** studies of chronic compressive myelopathy. Zhang et al (2007) performed a thorough morphometric assessment in four cases of human CSM compared to four normal controls. Fehlings et al. (2006) assessed changes in the spinal cord in 8 cases of human cervical spondylotic myelopathy (age range 61-89 years). A prominent loss of anterior horn cells (AHCs) was consistently found. Parameters included the number, average transverse area and perimeter of anterior horn cells in lamina 9 at C3, C5-6 and L1, the number and average transverse area and perimeter of axons in the posterior funiculus at C3 and L1, measured under high magnification with oil immersion. A decrease in the number and area of AHCs was shown however this was not consistent across all levels analysed. A significant decrease in the number and area of axons of the posterior columns was found, as was a decrease in the number of axons in the corticospinal tracts at L1. In the rat the corticospinal tract (motor) and dorsal ascending tract (sensory) transmit signals in opposing directions within the dorsal columns and are thus both vulnerable to damage from posterior compression. Distant to the lesion, axonal damage as part of Wallerian degeneration can occur in sensory tracts above, and motor tracts below the site of compression (Yu et al., 1988).

The neuron and its multiple complex synaptic connections provide the basis for cellular communication and processing in the CNS. Oxygen homeostasis is fundamental for sustaining the survival of the cell. The ability of the neural tissue to reorganise and recover using a process of neural plasticity after injury is well recognised. There is now evidence supporting the activity of growth factors and cytokines after spinal cord damage in the

capacity to alter cortical plasticity and therefore function (Ding et al., 2005). The overall role of neural plasticity is unclear and the outcome for patients unpredictable. These processes vary depending on the duration of injury (Ding et al., 2005). Spreading depolarisation of neurons and related ischaemia may contribute to secondary injury in experimental chronic compression (Gorji et al., 2004). Oxidative stress results from the production of harmful metabolites known as reactive oxygen species (ROS). In neurodegenerative conditions such as Alzheimer's disease and Parkinson's disease, for example, it is not fully understood whether ROS are the 'cause or merely the consequence' of neuronal death (Andersen 2004). ROS may instead propagate continuing cell death in a cycle rather than a cascade of damaging events (Andersen 2004). Reactive nitrogen species, which have been implicated in secondary neuronal death following SCI (Liu et al., 2000), are thought to trigger apoptosis via the activation of the apoptogenic protein poly (ADP-ribose) polymerase (PARP) both *in vivo* and *in vitro.*

Neurons are highly specialised cells of complicated morphology and the processes involved in cell death are complex. Neuronal differentiation largely relies on intrinsic cellular factors involving transcription and extrinsic mechanisms such as the active secretion of molecules necessary for cell survival. Of such secreted proteins, the neurotrophins are the most widely recognised (Bibel and Barde, 2000). Nerve growth factor (NGF) activity contributes to axonal and dendritic branching as well as neuronal and glial size in the mouse (Angeletti et al., 1971). Apoptosis of cholinergic neurons within the basal forebrain after fimbria-fornix injury is prevented by the administration of NGF within the ventricles (Williams et al., 1986).

Glial cells form the major cellular support for the complex neuronal circuitry of the spinal cord with astrocytes providing a blood-spinal cord barrier and oligodendrocytes the myelination of axons. Axonal signalling has been shown to influence oligodendroglial proliferation, migration, differentiation and myelination (Keirstead et al., 1999, Bozzali and Wrabetz, 2004, Bradl and Lassmann, 2009) and their loss may account for the demyelinative changes found in acute and chronic SCI. Astrocytic tau lesions have been found in association with neuronal tau staining in human CSM (Shimizu et al., 2008).

1.3.1 Apoptosis in Chronic Compressive Myelopathy

Studies of apoptosis in **human** cases of chronic compressive myelopathy are few. Experimental and human studies on cervical spondylotic myelopathy together support a significant role for apoptosis in secondary injury mechanisms (Kim et al., 2003) but the underlying mechanisms are yet to be dissected. TUNEL immunopositive neurons and caspase-3 and P75 immunopositive glial cells were found in 8 postmortem cases (6 male, 2 female: mean age 73, range 61–89 years) of cervical spondylotic myelopathy (Fehlings et al., 2006). There was a loss of AHCs, dorsal root degeneration, and loss of myelinated axons within the dorsal and lateral columns in association with apoptosis of myelin basic protein (MBP) positive oligodendrocytes. Staining for apoptotic markers in oligodendrocytes has been demonstrated to occur at large distances from the site of injury (Shuman et al., 1997, Li et al., 1999). These studies have used small numbers of subjects in addition to a small panel of markers for apoptosis, and the exact pathways of peptide activation, morphological changes within the spinal cord and correlation with clinical evidence was incomprehensively tested. It was proposed that a loss of oligodendrocytes could lead to demyelination of the long tracts, especially as one oligodendrocyte myelinates several axons in the CNS. Yamaura and colleagues (2002) assessed the changes present in a spinal cord from a single case of human cervical myelopathy caused by ossification of the posterior longitudinal ligament. TUNEL immunopositive glial cells, morphologically consistent with astrocytes, were found in one human case, but evidence was insufficient to conclude the presence of apoptosis. Further studies are needed to assess whether proteins involved in alternative pathways may be activated in vivo. The presence of one such peptide, apoptosis inducing factor (AIF), in human chronic spinal cord compression has not previously been evaluated.

There is accumulating **experimental** evidence for the role of **apoptosis** in neuronal loss and dysfunction in chronic compressive myelopathy (Kim et al., 2003). TUNEL immunopositive neurons were found by 6 weeks and maximal at 9 weeks duration of chronic compression in a rodent model with severe motor and sensory deficits (Xu et al., 2008). Evidence has emerged suggesting a role of glial apoptosis in CSM. Yamaura and colleagues (2002) studied the pathophysiological changes after chronic spinal cord compression in 7 twy (tiptoe-walking-yoshimura) hyperostotic mice at 1 and 6 months. These mice developed calcifications posterolaterally at C1, C2 or C3 vertebrae. No

TUNEL positive cells were seen in 1 month old mice, but immunopositivity was maximal at the site of compression after 6 months or longer, with staining in the anterior and posterior horns of the grey matter and in the anterior, posterior and lateral white matter. Caudally, TUNEL-positive cells were present in the anterior and lateral columns and rostrally in both the grey and white matter, consistent with apoptosis. In the same study, Yamaura et al. (2002) found caspase-3 proenzyme immunopositive glial cells in the grey and white matter, maximal at the site of compression. On double staining, TUNEL-positive cells co-localised with the oligodendrocytic marker Myelin Basic Protein (MBP). Yu and colleagues (2009) used the same twy mouse model of ossification of the ligamentum flavum at C2-C3 to analyse Fas-mediated apoptosis at 4 and 5 months duration of compression. The animals developed progressive paralysis. Using TUNEL and Fas labelling new evidence emerged of Fas-mediated activation of caspase-3, -9 and -8 associated with death of neurons and oligodendrocytes and functional deficit. Fas targeted inhibition of apoptosis was proposed as an adjuvant therapy in the treatment of CSM to preserve oligodendrocytes. The above studies assessed apoptosis no earlier than at 3 weeks of compression, in contrast to our studies which analysed changes as early as 24 hours.

1.3.2 Experimental Models of Chronic Spinal Cord Compression

There are distinct differences between human and rodent spinal columns which complicate the development of an accurate injury model. The cross-sectional diameter of the spinal cord varies from 3.5mm in the rat to approximately 10mm diameter in the human at the thoracic level and there is variation in the topographical organisation, homeostatic mechanisms, inflammatory response and functional, behavioural or environmental influences. The major topographical differences of the spinal tracts include posterior column location of the corticospinal tract rather than lateral, relatively smaller area for the spinothalamic tracts than in the human and lateral rubrospinal tract with no anterior extension.

Experimental models of chronic spinal cord compression have been used to study injury over the duration of weeks, months or preferably over a year or more depending on the available resources (Fawcett et al., 2007). Few models overall have been developed and it remains a challenge to replicate the pathophysiological conditions seen in the human. **Large animal** studies have included a canine model using an anterior screw compression

device (Harkey et al., 1995) with cervical vertebral artery occlusion (Hukuda et al., 1988), a cat model using a screw device (Shinomiya et al., 1992) a rabbit model using unilateral screw compression (Ozawa et al., 2004) and a sheep model involving disc degeneration following nucleotomy (Guder et al., 2009). Such models aim to produce progressive and gradual mechanical compression and subsequent clinical deficit combined with consistently repeatable neuropathological changes on histology similar to that which is seen in the human.

In vitro studies have been performed on the mechanical properties of the spinal cord during chronic compression with the use of biosynthetic materials (Kroeker et al., 2009) or to further understand the cellular response to injury such as neuronal regeneration and axonal sprouting (Stavridis et al., 2009).

Plate and screw devices have been accepted as reproducible models of chronic compression, and compression may be applied onto the nerve root or spinal cord within the root or spinal canal respectively. The screw is turned at set intervals, for example once per day, thus causing a step-incline in the compression of the spinal cord. The screw and plate system provides a fixed point of stenosis over which the spinal cord may stretch, in similar fashion to a mass such as an osteophyte. Using a cervical screw device in the feline, Shinomiya and colleagues (1992) showed the onset of myelopathic changes with tightening of the screw every few weeks to a stenosis of approximately 50% of the cervical canal. Xu and colleagues (2008) used such a model in the rat, with tightening of a root canal screw every 7 days for a period of 6 weeks. They were able to verify the position of the screw using radiology and the model represented a progressive injury in which motor and sensory deficits occurred by 3 weeks and paralysis in two rats by 12 weeks. Such a model cannot exclude a compensatory response such as fluid shift or changes in axoplasmic transport above and below the site which may occur prior to the next turn. The spinal cord may have a variable compensatory response to recurrent, incremental mechanical compression compared to a more gradual, progressive compression. Furthermore, such models are unsatisfactory in that each repeated turn of the screw represents a point of interference and risks an acute insult to the neural tissue possibly dependent upon the pressure applied by the experimentalist and skill in application. Glial changes were observed in a Wistar rat model of chronic compressive myelopathy using screw compression at T7-T9 with survival up to 12 weeks. In this model, motor and

sensory deficits were found from week 3, and myelin damage with loss of glia was described (Xu et al., 2008). The number and density of GFAP immunopositive astrocytes has been studied in a rabbit model of unilateral screw compression without paralysis (Ozawa et al., 2004). The densities of GFAP-positive astrocytes in the gray matter and the anterior column were significantly greater in the compressed half. The lateral and dorsal columns showed similar results however between the compressed and contralateral halves. Substantial tissue damage was noted on the compressed side. The study concluded that glial reaction played a significant role in transverse lesion syndrome in unilateral compression myelopathy although the reason for the vulnerability of the grey matter and anterior white matter was uncertain.

Degenerative models such as the hyperostotic Yoshimura (twy) mice display posterior spinal cord compression by 6 months from osteophytes, developing a 'boomerang' shaped spinal cord in which there is cavitation of the grey matter, myelin damage, loss of axons and glia and degeneration of the long tracts above and below the site of compression (Yamaura et al., 2002). However, the compression is asymmetrical, and thus is problematic in controlling for variation between animals. In contrast, our model of polymer compression enables a consistently symmetrical compression of the posterior white matter. In the twy model, osteophytosis occurs at the C1-3 level, leading to progressive paralysis, and thus the model was also inappropriate for testing mild spectrum injury.

Expandable devices for increasing, persistent compression have rarely been used, such as a balloon (Konno et al., 1995) or polymer. The present study modified a new model of rodent chronic spinal cord compression first described by Kim et al. (2004) using an expandable urethane compound polymer at C5 and C6 in male Wistar rats aged 12-14 weeks. The polymer was firstly sutured at one end and threaded underneath the laminae at two levels to overlie the dural surface. Rat locomotion became impaired at 17 weeks. Immunohistochemistry performed at 1, 3, 6, 9, and 25 week time points found a decrease in the number of motor neurons beginning at 3 weeks. Kasahara et al. (2006) used an identical polymer for expansion over the spinal cord at T7 and verified that there was neuronal loss by 6 weeks after the onset of compression, which had progressed by 9 weeks. Secondary cellular insult was suggested by an increase in the compensatory survival factor brain-derived neurotrophic factor (BDNF) at 6 weeks but this declined at 12 weeks. The study analysed the effect of posterior decompression at 6 weeks. They found a greater

number of neurons in the decompression group compared to ongoing compression however these changes were not persistent at the 9 and 12 week time points, raising the question of whether earlier surgery may result in preservation of neurons and improved functional outcome in chronic compressive myelopathy. In a rodent model using Wistar rats and a screw compression device, progressive AHC loss was demonstrated at 6 and 9 weeks (Xu et al., 2008).

1.3.3 The role of surgical decompression

Experimental evidence analysing clinical state suggests that early surgical decompression of chronic cord compression may improve outcome but these findings are not supported in human studies, in which large-scale randomised control trials are lacking. In human studies of conservative versus surgical management of CSM, functional improvement has been supported by radiological evidence of cord enlargement one year after surgery (Takahashi et al., 2006). In one study, posterior cervical decompression and plating involving patients with quadriparesis found significant improvement in functional outcomes ($P = 0.0002$) using several scales of upper limb and lower limb function (Houten and Cooper, 2003). It is uncertain whether oedema may be a confounding factor in the resolution of cord enlargement.

In an early experimental study of canine chronic compressive myelopathy using an anterior and posterior compressive device, Harkey and colleagues (1995) showed a functional improvement in all six animals following decompression. However, three of these animals displayed anterior horn cell (AHC) loss, necrosis, and cystic cavitation despite decompression. A disruption of synaptic transmission with recovery following decompression has been shown during in vitro testing in rodent spinal cord (Yoshida et al., 2004). Xu and colleagues (2009) analysed apoptosis in a rodent model of compression at T10 using a screw device and staining for TUNEL, caspase-3, Bcl-2 and Bax. Compression duration was for 6 or 24 hours in total before removal of the screw and the animals were sacrificed at week 1 or 4 post decompression. Results were analysed both at the site and up to 7.5mm away from the lesion. They found fewer TUNEL-positive cells in the decompression versus persisting compression groups, consistent with reduced apoptosis. In a consensus article published by the American Association of Neurological Surgeons and Congress of Neurological Surgeons on the natural history of CSM (Matz et

al., 2009) it was recognised that severe or long-lasting symptoms are associated with worse surgical outcome. Furthermore, the age of the patient should be taken into account, as acute deterioration is unlikely in those younger than 75 years. Further research in humans in conjunction with large animal experimental research to assist in the development of treatment guidelines is much needed (Fehlings and Perrin, 2006).

This current study aims to assess the effects of decompression in an experimental model of mild chronic cord compression.

1.4 Axonal Injury

Compressive myelopathy, whether acute or chronic, may involve a common pathway of axonal degeneration. In normal spinal cord, axonal conduction relies in part on the myelin coating which facilitates faster depolarisation, repolarisation and therefore, greater conduction velocity (Nashmi and Fehlings, 2001). Transected axons may undergo acute axonal degeneration leading to early scar formation and impairment of regenerating axons (Coleman, 2005). White matter is typically at least partially preserved in the penumbra of injury after experimental acute traumatic contusion of the spinal cord.

The speed of transmission of a nerve impulse is partially related to fibre size and myelination. Axonal tracts are normally elastic in nature but chronic compressive and stretching forces may disrupt integrins, myelin, and the normal cytoskeletal architecture (Henderson et al., 2005). Damage to the myelin sheath can result in slowed conduction. Axonal injury is likely to play an important role in compressive myelopathy. Consequently, prevention of axonal injury and myelin loss after an insult, to a minimum of approximately 10% of axons, is critical to improve clinical outcome (Little et al., 1988) but is often a neglected therapeutic target (Coleman and Perry, 2005).

Severely disrupted axoplasmic transport may be followed by formation of axonal swellings and **axonal retraction bulbs** indicating severance of the axon and **axolemmal degeneration** known as axonal dystrophy, leading to disruption of glial cell function, mitochondrial damage, sodium and calcium influx, loss of cytoskeletal and membrane bound proteins, demyelinative changes and neuronal degeneration (Coleman, 2005). In traumatic SCI, disruption of axoplasmic transport results in an accumulation of membranous organelles and a variety of molecules (Grady et al., 1993), including APP (Stone et al., 2000). This delayed process of cell death shares similarities with apoptosis. The proximal segment of an axon, deprived of the necessary growth factors, may degenerate secondary to the apoptotic cell death of oligodendocytes. Oligodendrocytes require ongoing axonal signalling to survive and a loss of axonal contact during development is associated with apoptosis (Barres et al., 1993). In a Wistar rat model of axonal transection, TUNEL immunopositive glia with morphological changes of apoptosis on electronmicroscopy were present in the dorsal columns (Abe et al., 2004). However, in a mouse model using transection of axons and in axonal degeneration triggered by

neurotrophin deprivation (Finn et al., 2000), no evidence of caspase-3 expression was found using immunohistochemistry or biochemical markers. Furthermore, caspase inhibition resulted in increased neuronal survival but no change in degeneration of the axonal segment. The authors proposed that there existed two distinct molecular pathways for neuronal cell death, one for apoptosis and one for axonal degeneration. An exact molecular link of axonal degeneration and apoptosis is yet to be identified (Raff et al., 2002, Coleman 2005) and caspase-inhibitors have failed to prevent demyelinative changes (Finn et al., 2000).

CNS myelination and axonal function is dependent on the activity of oligodendrocytes. Accordingly, damage to oligodendroglial cells from external stressors such as trauma may affect the function and survival of axons and lead to Wallerian degeneration. There are three main types of neuroglia: oligodendrocytes, astrocytes and microglia. Glia contribute to the maintenance of neuronal homeostasis, therefore neurons are potentially vulnerable if there are deleterious alterations in these cells. Glial cells participate *inter alia* in myelination, the regulation of ground substance composition and consistency, secretion of neurotrophins, maintenance of the blood-brain barrier, and clearance of cellular toxins and debris. Astrocytes in particular, feature prominently in the immediate post-injury phase, influencing neuronal regrowth, stability of ions, excitotoxic damage, and neovascularisation (Panickar and Norenberg, 2005).

Wallerian degeneration is one of the late and major consequences of damage to myelinated axons occurring slowly within the CNS over weeks or months (Vargas and Barres, 2007). This may be associated with damage to the long tracts of the spinal cord and damage to oligodendrocytes with demyelinative changes in the severe spectrum end of injury. The earliest changes are to the axolemma and cytoskeleton with disorientation of microtubules, segregation from their neurofilaments, and accumulation of organelles (Ishise and Rosenbluth, 1986). Wallerian degeneration is a progressive, secondary process of axonal and myelin degeneration of myelinated fibres occurring distal to the site of injury. The demyelinative changes which occur in Wallerian degeneration refer to a pathological process rather than a disease in isolation. Degeneration of the axon may occur within 30 minutes of spinal cord injury (Kerschensteiner et al., 2005). Wallerian degeneration has been demonstrated post-axotomy within the distal axonal segment and axonal swellings may be prominent (Kerschensteiner et al., 2005). A slow Wallerian degeneration mutant

mouse model (*Wld*^{S}) has been used to show that disrupted axonal transport in addition to structural axonal damage can trigger degenerative changes along the axon (Mack et al., 2001).

Amyloid precursor protein (APP) is recognised as an early and sensitive marker of axonal injury and accumulates within axonal retraction bulbs, swellings or spheroids following a disruption in axoplasmic transport (Blumbergs et al., 1994, Sheriff et al., 1994). First described in traumatic brain injury (Gentleman et al., 1993), APP refers to a 695-770 residue neuronal peptide transported anterogradely along the axon by binding to the kinesin light chain subunit of kinesin-I. The gene encoding APP is highly conserved across species and is present on the long arm of chromosome 21. Antibodies directed against APP may target either the N-terminus present in vesicles, which undergo anterograde transport, or the superficial C-terminus (Stone et al., 2000).

The proteolysis of APP in both acute and chronic compressive myelopathy has not previously been described in humans. The physiological function of the amyloid precursor protein and its processing is unclear and may have either neuroprotective or neurotoxic effects under certain conditions. APP is used as a highly sensitive marker of axonal injury, is synthesised in CNS neurons and transported by fast axoplasmic transport (Weidemann et al., 1989, Sheriff et al., 1994). The degradation of the APP molecule has been identified as a potential trigger of caspase-dependent apoptosis in spinal cord injury (Choo et al., 2008).

The APP molecule spans the cellular and organelle membranes and, following maturation in the Golgi apparatus, undergoes fast anterograde transport to the synaptic terminus (Ferreira et al., 1993), where integration into the cell membrane occurs (Weidemann et al., 1989).

First discovered in 1987, APP has several isoforms (Golde et al., 1990) depending on amino acid length. The APP 695 isoform is predominantly synthesised in CNS neurons which undergo fast axoplasmic transport (Weidemann et al., 1989). In compression trauma to the rat spinal cord, APP accumulation correlates with increasing severity (Li, et al., 1995). APP immunoreactivity in humans has been seen up to 99 days after severe head injury (Blumbergs et al., 1995), suggesting ongoing axonal dysfunction. This provides a

window of opportunity for therapeutic intervention before irreversible secondary axotomy occurs (Povlishock, 1992, Blumbergs et al., 1998).

The precise functions of APP have not been fully elucidated but APP may have diverse roles in mammals (Sheetz et al., 1998), including cell to cell adhesion (Smith and Anderton, 1994), cell signalling and receptor activity (Barger and Mattson, 1996), neuritic growth (Moya et al., 1994), neuroprotection and repair (Goodman and Mattson, 1994), synaptic function (Schubert et al., 1991), enzyme regulation (Smith and Anderton, 1994), coagulation and wound repair (Smith and Anderton, 1994), and cell cytotoxicity (Milward et al., 1992). Given this large array of functions, involving both cell protection and damage, the need to fully define the actions of this molecule is clear.

Studies analysing axonal injury after brain trauma suggest a role for caspase-3 in the cleavage of APP (Stone et al., 2002). In addition, caspase-3-mediated cleavage of APP has been found to be associated with the formation of amyloid-beta, a neurotoxic protein believed to contribute to apoptotic cell death in Alzheimer's disease (Allen et al., 2001). In our study it is hypothesised that APP provides a substrate for the caspase-3 enzyme in human acute and chronic spinal cord compression.

As a result of axonal demyelination and degeneration, the post-synaptic target of the cell, such as a muscle fibre, also degenerates or atrophies due to a lack of neural stimulation. There is a gradual decline in myelin basic protein (MBP) and reactive astrocytes may then fill the area of degeneration forming a new, gliotic matrix up to four months post-injury which is unlikely to support axonal regrowth (Buss et al, 2004).

Caspase-mediated cleavage of APP may be triggered via the classical apoptotic pathway, which results in the production of caspase-3-mediated APP proteolytic peptide antibody (CMAP) and Amy-33 amyloid-beta which have been analysed following traumatic brain injury in the rat (Stone et al. 2002). This study found that APP accumulated in injured axons within 6 hours post-injury and CMAP and Amy-33 amyloid-beta immunoreactivity was evident at 12 hours post-injury. Further evidence of the proteolytic role of caspase-3 within the axon has emerged from studies on the activity of caspase-3 in cleaving beta-spectrin (Buki et al., 2000) at later time-points post-injury. In a biochemical and molecular study, Barnes et al., (1998) showed that increased levels of APP within spinal motor

neurons of the chick embryo provide a substrate for caspase-3 and the subsequent demise of the cell.

There is growing evidence that failure of the normal protein-processing role of membrane bound endosomal vesicles in neurons may underlie the accumulation of amyloid-beta peptide following APP proteolysis and associated plaque formation (Tate and Mathews, 2006). Amyloid-beta has been shown to co-localise with APP and neurofilament proteins in human traumatic brain injury, suggesting that damaged axons may 'serve as a large reservoir of amyloid-beta' (Smith et al., 2003). In a non-transgenic rat model of brain traumatic injury, Iwata et al. (2002) demonstrated the long-term accumulation in the thalamus and white matter of amyloid-beta in rodents 1 month to 1 year after injury, whereas APP expression occurred 2 to 7 days following injury.

Little is known of the **proteolytic processing of APP** in compressive myelopathy following its accumulation within the axon. Proteolysis of APP is thought to produce the main constituent of senile plaques, amyloid-beta, in Alzheimer's disease (AD) (Haass and Selkoe, 1993). In a pig model of traumatic brain injury, amyloid-beta peptide was expressed within APP immunopositive axons providing evidence that amyloid-beta may be produced due to proteolytic processing of APP (Smith et al., 1999). In this model, there was co-accumulation within swollen axons of amyloid-beta, APP, beta-site APP-cleaving enzyme (BACE), presenilin-1 (PS-1), caspase-3 and caspase-mediated cleavage of APP (CCA) 6 months post-injury (Chen et al., 2004). Amyloid-beta antibodies were used in the present study to label the amyloid-beta peptide sequence within human APP.

An important part of the present study is the determination of whether APP is associated with caspase-3 in injured axons. Caspase-3, in its active form, is recognised as a major effector molecule of apoptosis (Erhardt et al., 1997). The exact relationship between the proteolysis of APP, the production of amyloid-beta and caspase activity remains unclear. Increased accumulation of amyloid-beta in ischaemic and excitotoxic brain injury is thought to be associated with cleavage of APP by the major effector molecule in apoptosis, active caspase-3 (Gervais et al., 1999). Caspase-3 cleaves the APP aspartic acid residue 720 to produce a new epitope recognised by an antibody termed caspase-3-mediated APP proteolytic peptide (CMAP) (Gervais et al., 1999).

The presence of caspase-3 has been demonstrated in experimental traumatic brain injury and spinal cord injury within axons, neurons, astrocytes and oligodendrocytes (Buki et al., 2000, Casha et al., 2001). In an immunohistochemical study of traumatic axonal injury in the rat, CMAP antibody was found to co-localise on immunofluorescent staining with amyloid-beta (Stone et al., 2002). Furthermore, amyloid-beta peptide may activate not only caspase-3 but two other effector molecules involved in apoptosis, caspase-2 and caspase-6 (Allen et al., 2001, Mattson et al., 1998).

Three major recognition sites for caspase-3 cleavage of APP have been recognised (**Figure 1.3**), with one at the C-terminus (Asp720) associated with the production of amyloid-beta and two at the N-terminus (Asp197 and Asp219) (Tesco et al., 2003). APP may be directly cleaved by either caspase-3, -6 or -8 at the cytoplasmic tail, after amino acid 664 (Bertrand et al., 2001, Gervais et al., 1999). This reaction results in the neo-epitope C31, which has been shown to induce apoptosis *in vitro,* in the N2A and 293 T cell lines (Bertrand et al., 2001). The caspase-cleaved transmembrane fragment of APP has been linked to cell death in Alzheimer's disease as it is thought to result in accumulation of toxic amyloid-beta (A-beta) peptide formation as well as progression of the apoptotic cascade (Gervais et al., 1999, Nishmura et al., 2002, Soriano et al., 2001). It is hypothesised that caspase-3 is inappropriately activated in Alzheimer's disease, although its importance in cell death is unclear (Selznick et al., 1999). Selznick and colleagues investigated the neuronal expression of caspase-3 in human and mouse hippocampal brain sections and found no association of caspase-3 activation with senile plaques and neurofibrillary tangles. Activation of caspase-3 was however present in hippocampal neurons undergoing granulovacuolar degeneration, suggesting a limited pathological role for caspase-3 in neurons associated with learning and memory. Furthermore, caspase cleavage of the cytoplasmic tail of APP may result in a decline in APP internalisation and a subsequent reduction in endocytic proteolysis of APP (Soriano et al., 2001).

Amyloid-beta peptide has been demonstrated in traumatic brain injury (Graham et al., 1995, Horsburgh et al., 2000) and some epidemiological and histopathological evidence suggests that this accumulation may predispose the patient to Alzheimer's disease (AD) later in life (Plassman et al., 2000, Guo et al., 2000, Horsburgh et al., 2000). Neuronal death in AD is associated with the accumulation of amyloid-beta peptide and subsequent activation of the caspase-mediated apoptotic pathway (Roth, 2001) whereby caspase-3

cleaves APP to produce a neoepitope, $\alpha\Delta C^{asp}$-APP. Studies have demonstrated the expression of $\alpha\Delta C^{asp}$-APP in Alzheimer's disease (AD) in humans (Ayala-Grosso et al., 2002). Analysis of caspase activity in cultivated Jurkat J16 T cells has provided further evidence for the role of caspases in the carboxyl-terminal truncation of APP (Weidemann et al, 1999). This relationship has been proposed as a possible mechanism for amyloidosis and neuronal cell death in AD. Using the APPsw transgenic mouse model of AD and analysis of human brain sections, Selznick et al. (1999) found that caspase-3 activation and subsequent cleavage of APP may contribute to a loss of hippocampal neurons involved in learning and memory. Furthermore, tau-immunopositive deposits in astrocytes and neurons have been found in cervical spondylotic myelopathy (Shimizu et al., 2007), suggesting a potential role of tau protein in this condition.

The relationship between caspase-3-mediated APP proteolysis and the production of amyloid-beta is not well understood. At the intracellular C-terminus, caspase-3 actively cleaves APP, whereas the production of amyloid-beta occurs towards the N-terminus, requiring both β-secretase and γ-secretases (Murphy et al., 1999, Sinha et al., 1999). This cleavage occurs at amino acid residues –671 (Sinha et al., 1999) and –713 (Murphy et al., 1999) on the APP molecule respectively, whereas caspase-3 cleavage has been shown to occur at amino acid residue 720 (Gervais et al., 1999, Weidemann et al., 1999). Caspase-mediated cleavage of APP is thought to expose the N-terminal cleavage site for the subsequent production of amyloid-beta (Stone et al., 2002).

Figure 1.3. APP cleavage sites for the production of soluble Amyloid Precursor Protein beta and amyloid-beta 42 protein fragment via beta- and gamma- secretases.

Caspase-3 cleaves the APP molecule at aspartic acid 720 to produce a neoepitope immunolabelled by the CMAP antibody.

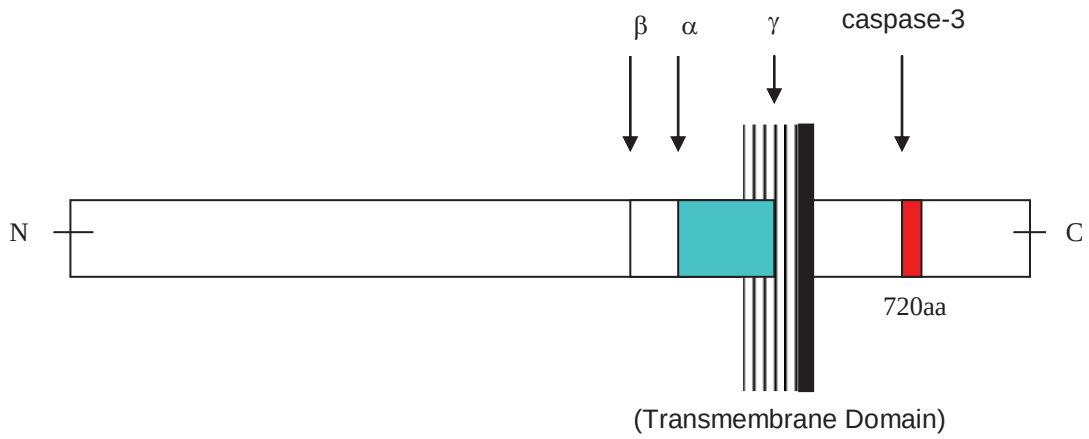

1.5 Human Acute Compressive Myelopathy

1.5.1 History

The first known documentation of spinal cord injury is found in the Edwin Smith papyrus from Thebes, circa 1550 BCE, thought to be written by Imhotep and detailing vertebral subluxation, paraplegia and quadriplegia (Breasted, 1992). Hippocrates (circa 460-370 BCE) reported on several spinal conditions and observed that the limb weakness correlated with the side of injury to the spine (Knoeller and Seifried, 2000). Aulus Aurelius Cornelius Celsus (25 BCE-CE 50) noted that injury to the spinal cord resulted in a poor outcome and that cervical cord injury caused death. Experimental work was thought to have first been conducted by Galen (circa AD 129-210) who noted that the transection of the spinal cord caused motor and sensory loss below the level affected and that transection at the fourth cervical segment caused weakness of the diaphragm (Patwardhan and Hadley, 2001). Knowledge of spinal cord injury was greatly advanced with the advent of histological and new experimental techniques during the 18th Century. In 1850, Marshall Hall was the first to recognise 'spinal shock' resulting from traumatic spinal cord injury.

1.5.2 Definitions

Traumatic spinal cord injury involves an immediate mechanical compression of the enclosed spinal cord within the spinal canal, transection or distraction, and associated primary and secondary tissue changes resulting from direct force such as fracture/dislocation of vertebrae or a penetrating object.

1.5.3 Aetiology and Classification

Traumatic spinal cord injury ranges along a clinical spectrum of mild to severe injury, although an exact classification inclusive of the variation in presentation in correlation with the complex histopathology is yet to be defined. At the more severe end of this spectrum it is a devastating injury with significant morbidity and mortality mostly affecting young males. Over the last decade a trend towards later onset in Westernised countries has been noted, perhaps due to the participation of older people in higher risk activities and the higher incidence of falls in an ageing population. Injury most commonly results from

motor vehicle accidents involving either drivers or pedestrians, falls, or sports related injuries (Lobosky, 1996). In developing countries, vehicle versus pedestrian incidents are emerging as the most frequent cause of traumatic head injury, and contributes substantially to the aetiology of SCI. Traumatic spinal cord and brain injury are a major cause of mortality in the 20-45 year old age group and carry significant social, community and individual cost (Neugebauer et al., 1999). The Australian Spinal Cord Injury Register (ASCIR) reported on 348 newly incident cases from trauma and disease in 2006-07. From that year, '272 new cases of SCI from traumatic causes were registered in Australia, an age-adjusted incidence rate of 14.9 cases per million of population. The most common clinical outcome of SCI from traumatic causes was incomplete tetraplegia (98 cases). Transport related injuries (52%) and falls (29%) accounted for over three-quarters of the 271 cases of traumatic SCI (one case under the age of 15 years was excluded from these analyses). Cases also occurred during sport (n = 21) and working for income, including travel to the workplace (n = 37). Falling was the most common type of event leading to traumatic SCI at older ages' (Spinal Cord Injury, Australia, 2006-07, Cripps R, 2009).

Partial protection of the spinal cord is provided by the adjacent dural sac and vertebrae extending the foramen magnum to the cauda equina at level T12 or L1 in the adult. Nevertheless, the close proximity of structures increases the likelihood that small changes in the diameter of the spinal canal will result in cord compression. Subluxation and hyperextension spinal cord injury is particularly likely to occur at the cervical level, where there is greater mobility of the vertebrae (Walid and Zaytseva, 2009). Cord injury may be focal, involving a single segment of the cord, or diffuse, extending to multiple segments or multiple vertebrae carrying the potential for global deficits.

1.5.4 Clinical Manifestations

The clinical manifestations of acute SCI depend on the segment or segments directly affected through mechanical injury and penumbral areas affected by ischaemia. Clinical symptoms include spinal pain, autonomic dysfunction, motor and sensory loss, and eventual muscular atrophy. Direct damage to one half of the cord usually results in a Brown-Sequard syndrome of hemi-motor and sensory loss, and autonomic dysfunction. In the anterior spinal artery syndrome there is a sudden onset of sharp, penetrating pain, urinary and faecal incontinence, paralysis, and loss of pain and temperature sensation

below the site of compression. Ischaemia secondary to impaired posterior circulation may result in altered vibration sense and proprioception, ataxia, and impaired tendon reflexes. A central cord vascular syndrome can result from a watershed area of ischaemia secondary to mechanical compression or systemic hypotension (Stevens and Lowe, 2000).

1.5.5 Diagnostic Investigations

In the emergency setting plain radiographs showing all cervical vertebrae including C7/T1 junction are used in detecting cervical fracture, subluxation or other bony abnormality. Increased tissue detail is provided by CT scans which often can quickly be obtained in the first instance and may be used to assess spinal cord diameter as well as fine fractures or subluxation. Where soft tissue injuries are suspected MRI is the imaging technique of choice as it can often elucidate parenchymal cord changes secondary to haemorrhage or oedema. Research currently focuses on the application of quantitative and functional MRI for detecting secondary axonal injury and demyelinative changes in experimental and human studies, illustrating motor tract abnormality below the lesion and sensory tract changes above (Kim et al., 2007, Loy et al., 2007, Kozlowski et al., 2008). Narrowing in the spinal cord following traumatic injury has been demonstrated (Schmit and Cole, 2004), however studies of larger cohorts are required.

1.5.6 Management and Outcome

Immediate management is through stabilisation of the patient and immobilisation of the spine. Head injury is often associated with spinal injury and early recognition is important. Hypothermia has been recognised as a potential treatment in traumatic brain and spinal cord injury but the benefits are yet unproven and randomised control trials are lacking. In a retrospective analysis of outcome in 14 patients using femoral catheter-induced intravascular hypothermia for SCI ASIA (American Spinal Injury Association) classification A, Levi and colleagues (2009) found similar complication rates to that of controls. They were able to establish close control of body temperature and effective transmission of cooling to the CSF, associated with a reduction in pulse rate. This was the largest contemporary trial of hypothermia in SCI. Medical therapy may include the use of methylprednisolone, but the benefit of this has not consistently been shown (Fehlings, 2001) and many treatment centres are reluctant to use it within protocols. Some studies

support it as an effective medication at higher doses used within 8 hours after injury (Tsutsumi et al., 2006). Evidence in randomised control trials for the use of methylprednisolone has emerged during the past 20 years and early research, in particular results from the National Acute Spinal Cord Injury Study, suggested an improvement in functional outcome after SCI with administration of the drug within 8 hours (Bracken, 1991, Bracken et al., 1990, Young 1990, Tsutsumi et al., 2006).

Some experimental studies are in support of steroid therapy but the overall evidence is inconclusive. In a rat model of spinal cord contusion by Vaquero and colleagues in 2006, the number of 'apoptotic' neurons and glia was decreased 24 hours post-injury following a single injection of methylprednisolone, however only a single antibody was used, Apostain (anti-ssDNA MAb F7-26). In addition, injection occurred just 10 minutes after injury, an impractical time-frame in the majority of human spinal cord injury cases, especially in the Developing World where emergency transport is often limited. Histopathological changes consistent with decreased inflammation and axonal regeneration have been demonstrated (Oudega et al., 1999). Studies have also shown a functional benefit from the use of methylprednisolone during the first 24 hours after SCI as well as combined therapy such as ensheathing cells or the antioxidant melatonin with methylprednisolone (Cayli et al., 2004, Nash et al., 2002) however it is unclear whether these effects last over a significant duration.

The early administration of methylprednisolone has continued to be been strongly advocated but the validity of these trials has been questioned (Coleman et al., 2000, Short, 2001), citing improper statistical reasoning, biased selection of control groups, and the grouping of mild with severe cases, as weaknesses in the trial. Such methodological errors extend to several other trials for the pharmacological treatment of SCI (Tator, 2006). There does not currently appear to be a pharmacological intervention which has proven benefit after SCI (Hurlbert, 2006). In many centres in the United Kingdom, steroids are still advocated provided administration is prompt, however practice varies and no consistent set of guidelines has been developed (Frampton and Eynon, 2006). As with some other measures for the acutely injured spinal cord, it is difficult to avoid trial of new medication on the basis of risk when clinical hopes of improvement are poor or when there is a desire to leave no stone unturned in possible treatment.

While the current study does not address such pharmacotherapeutic issues, it is an opportunity to review the temporal pattern of pathophysiological changes for the purpose of possible future therapeutic approaches. This is particularly important because of the increasing difficulty in obtaining consent and ethical approval to preserve human material thus making it more difficult to gather more such cases in the future.

There appear to be two main stages of tissue damage within the first 24 hours, immediate mechanical injury to cells and secondary cascades, leading to structural damage within the tissue. Secondary injury mechanisms include ischaemia, ionic imbalances, haemorrhage, oedema, inflammation and production of free radicals, occurring with varying severity and spatial distribution (Walshe, 1970, Emery, 1998).

The **histopathological changes** in human SCI may be divided into zones of varying injury severity (Fleming et al., 2006). Zone 1 is comprised of inflammation and necrosis in short-survival cases, and within days to weeks changing to cystic necrosis. Changes typically occur in the central areas of the cord, as haemorrhage, neutrophil invasion, microglial activation and the development of a necrotic central lesion ensue (Donnelly and Popovich, 2008). Peripheral white matter may be spared. Neutrophil invasion is greatest in the first few days of injury but these cells may appear up to 10 days after SCI. The development of axonal swellings and demyelination occurs in regions which are less severely affected by the injury (Zone 2) and are bordered by intact regions of spinal cord (Zone 3). In the months following injury, post-necrotic cystic change may develop in conjunction with macrophage phagocytic removal of cellular debris and astrocytic gliosis and Wallerian degeneration (Durrant and True, 2002). In a study entitled, ‘The Relationship between Spinal Stenosis and Neurological Outcome in Traumatic Cervical Spine Injury: An Analysis using Pavlov's Ratio, Spinal Cord Area, and Spinal Canal Area’, Song et al. (2009) analysed the above parameters in 212 cervical spinal levels in 53 patients with a distractive-extension injury. An association between narrow spinal canal diameter and poorer neurological outcome was suggested, which was statistically significant using Pavlov’s ratio on plain radiographs.

The cascade of events leading to **neuronal and glial** cell death after spinal cord injury are multiple, complex, and incompletely understood and involve both intra- and extra-cellular signalling. Initially, there is tissue disruption, followed by inflammation, oedema and

ischaemic cell damage (Kakulas, 1999). Ischaemia promotes the accumulation of metabolic products and release of inflammatory cytokines. The inflammatory response involves vascular, molecular and biochemical events which are known to contribute significantly to secondary injury within the CNS (Hausmann, 2003). Inflammatory mediators include the vasodilator substance P, bradykinin, prostaglandins and leukotrienes (Johnson et al., 1983, Durrant and True, 2002). Several factors may contribute to this oedema, including increased microvascular permeability from hypoxia and the release of the vasoactive substances, bradykinin, histamine and acetylcholine. The initial inflammatory response may trigger secondary glial injury, for example the proinflammatory cytokine TNF-α which indirectly regulates the release of glutamate via the AMPAR receptor and is associated with excitotoxic secondary injury (Ferguson et al. 2008).

Phagocytosis of damaged cells is an important part of the injury response yet the precise role of macrophages in SCI is yet to be determined. Frisen et al. (1994) assessed the presence of macrophages rostral, caudal and at the site of incision to the dorsal or ventral fasciculus in rats, finding an increase in the number of macrophages for several weeks following injury. Myelin was removed more rapidly at the site of compression than rostral to it. Ousman et al. (2001) studied the molecular changes within macrophages following the induction of inflammation using lysophosphatidylcholine (LPC). Several proteins, including macrophage inflammatory protein-1α (MIP-1α), macrophage chemotactic protein-1 (MCP-1), granulocyte macrophage-colony stimulating factor (GM-CSF) and tumour necrosis factor-α (TNF-α) were transiently upregulated within the adult mouse spinal cord following LPC injection. Furthermore, neutralisation of these antibodies led to a reduction in recruitment of T-cells, neutrophils, monocytes and macrophages, resulting in decreased demyelination of axons.

Reactive **astrocytes** also play a role by producing proteoglycans during the formation of a scar which can significantly impede axonal regenerative processes (Fitch and Silver, 2008). In severe cases, spinal cord oedema may develop due to the movement of intravascular chloride, sodium and water into the extracellular space (Faden et al., 1987).

Experimental and human research over the past decade supports the role of apoptotic neuronal and glial cell death in spinal cord injury. The exact pathways involved and their

relationship to axonal changes are yet to be fully elucidated.

During the intermediate stages (approximately 72 hours post-injury), macrophages are activated and digest tissue by-products. Neuronal degeneration may commence distal to the site of compression (Durrant and True, 2002). Other factors include the immunological activation of complement, oxidative stress, and mitochondrial dysfunction causing secondary cellular damage and eventual cellular demise (Clarkson et al, 2005). Focal damage to the axon produces excessive calcium influx and subsequent cytoskeletal and mitochondrial damage. Mitochondrial disruption may result in the release of cytochrome-c, an activator of the key apoptotic protease, caspase-3 (Buki et al., 2000).

A cascade of complex events in SCI is thought to cause **neuronal and glial** secondary cell death, including apoptosis (Lu, 2000). Compression can lead to oedema, with ongoing compression of the vasculature leading to ischaemia. Glutamate excess, ionic imbalances and excitotoxic changes can develop (Nashmi and Fehlings, 2001), triggering calcium influx and possible apoptosis (Prophyris et al., 2004). Emery and colleagues (1998) studied apoptosis in a series of 15 human cases with documented survival between 3 hours and 2 months. Immunopositive cells for caspase-3 and TUNEL were present in 14 cases. There was co-localisation of staining for caspase-3 and the oligodendroglial marker, CNPase, and these cells contained apoptotic nuclei. A marker of oligodendrocytes (MO3.13) was used in a recent study of SCI and apoptosis (Austen and Fehlings, 2008). Apoptosis via Fas mediated activation of caspase-3, -8 and -9 was suggested by immunopositivity to these markers. In addition, the novel marker apoptosis inducing factor (AIF), cytochrome-c and TUNEL staining was shown to occur in glia. There was early dissipation of mitochondrial membrane potential (DeltaPsim) which temporally coincided with mitochondrial outer membrane permeability (MOMP), suggesting a role for intrinsically mediated apoptosis. It is important to ascertain whether these secondary processes are reversible or irreversible in order to develop effective research strategies for SCI therapies. Cell death may be ongoing for weeks or months following injury.

Experimental models of acute spinal cord compression are increasingly used to improve understanding and therefore aid in the development of improved therapies for human SCI. Experimental research into acute SCI has investigated pathophysiological aspects such as cell death, tissue oedema and the blood brain barrier (BBB), ischaemia, ionic imbalances

and excitotoxicity. These models commonly replicate the contusion aspect of acute compressive injury and the different types are discussed at the end of this chapter.

An accurate model should encompass both the primary mechanical injury and secondary degeneration and cell death, replicating the initial haemorrhage, necrosis and oedema, which over time develop towards repair and finally reorganisation of the tissue. Studies of spinal cord regeneration must be developed in consideration of the greater distance over which axons must travel in the human compared with the rat (Courtine et al., 2007). Furthermore, the pathological manifestation of injury may vary according to species, such as the common development of post-injury cystic necrosis in the rat (Sroga et al., 2003).

A model that most closely resembles true injury, while minimising variables, and having the advantage of being able to institute early and novel therapeutic regimens is critical in producing accurate data. There have been numerous models of spinal cord injury developed over the last two decades. Acute models typically use an immediate or rapid insult to the cord, and subacute injury may involve onset over hours or days. The use of such models has increased with the aim of better understanding the cellular and molecular cascades involved in cell death. These models also often aim to demonstrate tissue repair, axonal sprouting, remyelination and neuronal survival in correlation with better outcomes of motor, sensory and autonomic function. Even partial preservation of the long spinal tracts may result in functional gains. Research using larger animals such as non-human primates has potential to improve the junction between rodent and human research with regard to the timing of decompressive surgery.

In vivo experimental models of acute SCI are typically divided into complete and partial injury. In experimental models, complete spinal cord transection is commonly performed using a microknife or needle to incise the cord, and thus replicate transection secondary to vertebral dislocation, iatrogenic injury or foreign body insertion such as a knife-injury or shrapnel. These models have the advantage of causing focal injury to specific axonal tracts (Kerschensteiner et al., 2005), but such models do not encompass the combination of contusion and static loading in which the timing of impact is prolonged in addition to shear forces or incisive damage which characterises human SCI (Sheng et al., 2004).

Partial injury can occur through many methods such as partial transection, contusion via weight drop, planar clip compression, hypoxia/ischaemia, extreme temperature, radiation, toxin exposure, and laser. Injury may involve populations of neurons, oligodendrocytes, microglia and astrocytes. Such models have been classified into mild, moderate and severe types (Fehlings and Tator, 1995). A more detailed grading system of injury according to pathological changes and correlated with functional studies may in future allow for easier comparison between different injury models.

Partial transection has been predominantly used for the study of axonal regeneration and dendritic sprouting, due to the clearly defined planes of injury. Partial models allow for localised, precise anatomical deficits that allow the animal some preservation of function during recovery, such as bowel and bladder function. By definition, this model may result in only partial transaction of axons in the region of intended injury, thus facilitating axonal regrowth.

The majority of human acute SCI injury results from **contusive** or blunt trauma to the cord. Therefore many models of acute SCI aim to replicate these blunt mechanisms with resultant diffuse primary cellular and tissue changes. Injury can often involve multiple vertebrae and segments. The clip compression device has long been used as a reliable model of contusive cervical acute compressive myelopathy. The clip compression model is well characterised for functional analysis and histopathological changes such as lesion size, loss of white matter, gliosis, oedema and axonal swellings, however the laminectomy required is extensive and lesions using the aneurysm clip are severe in nature (Von Euler et al., 1997). Poon and colleagues (2007) have characterised a thoracic model of compression at the T2 level using a modified aneurym clip technique of 20, 26, and 35grams and compared histopathological and functional measures including the Beattie Basso Bresnahan score (BBB score). A progressive deficit was demonstrated ranging from mild to severe injury.

A standardised **weight drop model** of SCI was pioneered by Allen in 1911 and has since been developed to more closely simulate acute human SCI in a controlled manner. Gruner (1992) developed an impactor in which a 10 gram rod was dropped from between 6.25 to 50mm, with correlation of functional deficits using the Beattie, Basso, Bresnahan locomotor score (BBB score). The weight drop simulates the flexion-extension injury with

impact of the spinal cord onto the anterior vertebral body that is thought to occur in the human (Black et al., 1988). This technique carries a standard error of 2.5% of the mean force which may be correlated with the height from which the weight is dropped (Black et al., 1988). In our study, acute traumatic single impact SCI at the T12 level was selected as an injury model as it mimics compression in the human from anterior thoraco-lumbar fractures and lower thoracic hyperextension injuries. This controlled model does not encompass injuries at multiple levels, nor the effect of bony compression of the spinal cord which may involve lacerative as well as compressive forces. A SCI produced using such a weight drop model in our laboratory showed congruent characterisation as evidenced by a standard error of less than 10% of the mean maximal lesion area or length (Yang, 2004).

Small animal models allow temporal as well as spatial analysis of apoptosis after contusional SCI with functional recovery. A larger animal model however could allow for ease of surgical approach to the spinal cord and thus potentially fewer iatrogenic complications, replicate the weight bearing applied to the spine in the human, and if performed using non-human primates such as the Macaque monkey, allow measurement of dexterity which is often affected in mild compressive myelopathy.

Experimental models of human acute SCI commonly replicate the development of a central region of haemorrhagic necrosis followed by expansion of a penumbra of secondary cell death, typically occurring over millimetres in the rodent (Hagg and Oudega, 2006). Clinicohistopathological similarities with human SCI have been identified in the rat using this model (Balentine, 1978, Kakulas and Taylor, Handbook of Clinical Neurology, 1992, Siddall and Cousins, 1995). Central haemorrhage and necrosis of the central grey matter, with subsequent demyelination of axons within the white matter, and development of a central cystic lesion was identified as a typical pattern. In a weight drop model of SCI using a 10 gram weight from 6.25mm, expansion and cavitation of the cord was seen over 7 days (Liu et al., 1997).

Primary and secondary **neuronal** damage contributes to the functional deficit in spinal cord injury. Grossman et al. (2001) quantitatively characterised neuronal changes following spinal cord injury in the rat over a 24 hour period. In this study, the loss of anterior horn cells and anterior column astrocytes and oligodendrocytes was recorded at 15 min and 4, 8, and 24 hours after an incomplete mid-thoracic contusion injury in the rat.

The length of lesion and the area of neuronal loss increased in a temporal pattern. The extent of anterior horn cell loss above and below the site of injury progressed symmetrically with time.

In the above study (Grossman et al., 2001), neuronal loss was associated with a loss of glial cells in anterior white matter that was significant at the lesion site by 4 hours after injury. Again, a temporal pattern of increasing loss was demonstrated and cell loss occurred at the 24 hour time point, the earliest used in the current study. In another study of severe contusive injury in the rat, oligodendroglial apoptosis was evident at 3 and 14 days post injury (Yong et al., 1998). This study described an increase in microglial cell number, likely reactive microglia, by day 1 post-injury. Activated microglia are considered to be associated with the release of cytokines such as tumour necrosis factor alpha (TNF-α) which may be detrimental to oligodendrocytes but further research is required (Beattie et al., 2002). Recently, the role of autophagy in traumatic SCI using a mouse model of cord hemisection has been suggested (Kanno et al., 2009).

Experimental evidence suggests that **glial** cells, in particular oligodendrocytes, are vulnerable to apoptosis in acute SCI (Shuman et al., 1997, Li et al., 1999, Tagaki et al., 2003, Beattie et al., 2002). Using an extradural clip compression rat model, Casha et al (2001) demonstrated TUNEL-positive oligodendrocytes in grey and white matter. Glial apoptosis was evident by morphological analysis and DNA laddering on agarose gel electrophoresis. Similar TUNEL staining was seen in a study of traumatic SCI in the rat analysing the excitatory amino acid release mediated by N-methyl-D-aspartate (NMDA) receptors. Inhibition of the receptor appeared to decrease the absolute number of TUNEL-positive cells at 24 hours and 7 days post-injury, however the presence of apoptosis in this study could not be satisfactorily confirmed using a single marker (Wada S. et al., 1999).

Injury models of persisting rather than a single, brief impact have also supported a role for **apoptosis**. For example, Xu and colleagues (2009) studied the effect of surgical decompression after SCI using a rodent model of acute compression from a screw applied to the cord at the T10 level for 6 hours or 24 hours. Reduced numbers of TUNEL positive glial cells were seen at the site with decompression at 1 day, and in the rostral and caudal regions at 3 weeks and 4 weeks. Caspase-3 immunopositivity correlated with Bax and TUNEL staining. The study concluded that decompression reduces neural cell apoptosis

following SCI (Xu et al., 2009). Impairment of oligodendrocyte function and possible cell death has been demonstrated to occur by 3 days post contusive spinal cord injury in the rat (Tripathi and McTigue, 2007). Results from the study indicated an association between oligodendroglial proliferation and progenitor NG2 cells, and that numbers of glia were comparable to those found in the normal spinal cord (Tripathi and McTigue, 2007). In a rodent model of posterior column cordotomy at T8, there was an association between apoptosis and regions of Wallerian degeneration, which occurred distant to the lesion site from T3-T12 segments, however only the TUNEL marker was used for detecting apoptosis.

There is evidence that suggests that programmed cell death plays a crucial role in traumatic SCI. The administration of dexamethasone to rats resulted in decreased apoptosis-related cell death within the spinal cord (Zurita, 2002). Activation of apoptosis occurred at early time points. In a rat model of spinal contusion, apoptotic neurons and glia were detected using Apostain antibody (anti-ssDNA MAb F7-26) as little as 4 hours post-injury. A key regulator of the secondary injury cascade is the transcription factor, NF-kappaB. During such injury, activation of NF-kappaB-dependent genes are increased and inhibition of astrocytic NF-kappaB signalling was protective in a mouse model of SCI (Brambilla et al., 2005). The extracellular accumulation of the neurotransmitter glutamate, has been shown to underlie excitotoxic cell damage and ionic imbalance (Park et al., 2004). In a rodent model of acute SCI, morphological features of apoptosis in neurons were correlated with cell cycle related genes, showing a role of cell cycle in apoptosis (Di Giovanni et al., 2003). Stem cell therapy and the upregulation of neuroprotective genes may be of benefit in minimising apoptosis after experimental SCI in the rodent (Dasari et al., 2009).

Evidence supports a role for the intraperitoneal administration of methylprednisolone. The numbers of apoptotic cells were decreased at the site of injury at 24 hours (Vaquero et al., 2006) but this is yet to be affirmed in the clinical setting. There is evidence that the inhibition of Fas using soluble Fas receptor (sFasR) may decrease cell death and improve outcome in SCI and Fas-deficient mice showed better locomotor recovery, axonal sparing and preservation of oligodendrocytes and myelin (Casha et al., 2005). The use of soluble Fas was assessed in a clip-compression model of SCI and was associated with preservation of oligodendrocytes, nerve tracts, decreased levels of apoptosis and improved functional

outcome, while *in vitro* studies using sFasR found decreased cell death (Ackery et al., 2006).

1.6 Aims and Hypotheses

In the current thesis, it was hypothesized that:

1. Cellular pathology and apoptotic cell death is maximal at the site of compression in acute and chronic compressive myelopathies.
2. Ongoing axonal changes and white matter degeneration follow both chronic and acute compressive SCI.
3. Functional abnormalities, cellular pathology and apoptosis are reduced by decompression.
4. Early decompression (24 hours) produces a greater reduction in cellular pathology and apoptotic cell death than late decompression (3 weeks).

The principal aims of the study were:

i. To assess the functional disturbance, cellular pathology and role of apoptosis in a rodent model of chronic spinal cord compression.
ii. To assess the long term effects of decompression of the cord after 24 hours and 3 weeks of compression.
iii. To assess the cellular pathology and role of apoptosis in human chronic spinal cord compression.
iv. To assess the functional disturbance, cellular pathology and role of apoptosis in a rodent model of acute spinal cord injury.
v. To assess the cellular pathology and role of apoptosis in human acute spinal cord compression.
vi. To assess the axonal changes in acute and chronic spinal cord compression using APP as a marker of axonal injury.

CHAPTER 2

METHODS

All experimental protocols used in this study were approved by the Animal Ethics Committees of the Institute of Medical and Veterinary Science and The University of Adelaide.

2.1 Experimental Chronic Compressive Myelopathy

The experimental model of chronic compressive myelopathy used in this study replicates a persisting mechanical compression of a single spinal cord segment which reaches a maximum compression by 48 hours.

2.1.1 Animals

Sprague-Dawley rats were obtained one week prior to the planned initiation of compressive myelopathy. For the duration of the study all rats were group housed with unrestricted access to food and water. Animals were examined daily for unexpected adverse effects and for the possible need for bladder expression. Daily neurological function was assessed using specially designed tests including the rotarod to assess motor function, and neuroscore for neurological function. These tests are currently in use at the nominated institution and show no evidence of inducing pain or distress in animals exposed to date.

Throughout the duration of the study, any animal observed to be suffering pain or distress (e.g. vocalisation, lack of self-grooming, aggressive behaviour) was immediately euthanased. Researchers carrying out experiments were trained under expert supervision to maximise study efficiency.

2.1.2 Experimental Groups of Chronic Spinal Cord Compression

a) A group of 12 animals undergoing spinous processotomy, polymer insertion, recovery and assessment until 24 hours.
b) A group of 12 animals undergoing spinous processotomy, polymer insertion, recovery and assessment until 1 week. 6 animals for histological analysis and 6 for ELISA.

c) A group of 12 animals undergoing spinous processotomy, polymer insertion, recovery and assessment until 3 weeks. 6 animals for histological analysis and 6 for ELISA.
d) A group of 13 animals undergoing spinous processotomy, polymer insertion, recovery and assessment until 9 weeks. 7 animals for histological analysis and 6 for ELISA.
e) A group of 13 animals undergoing spinous processotomy, polymer insertion, recovery and assessment until 20 weeks. 7 animals for histological analysis and 6 for ELISA.
f) A group of 13 animals undergoing spinous processotomy, polymer insertion, recovery and assessment until 24 hours at which time decompression of the cord was performed with recovery and assessment at 9 weeks. 7 animals for histological analysis and 6 for ELISA.
g) A group of 13 animals undergoing spinous processotomy, polymer insertion, recovery and assessment until 3 weeks at which time decompression of the cord was performed with recovery and assessment until 9 weeks. 7 animals for histological analysis and 6 for ELISA.

2.1.3 Control Groups

h) A naïve non-injury subgroup of 12 animals. 6 animals for histological analysis and 6 for ELISA.
i) A sham subgroup of 12 animals undergoing spinous processotomy, recovery and assessment but without insertion of the polymer sheet. 6 animals for histological analysis and 6 for ELISA.
j) A sham subgroup of 12 animals undergoing spinous processotomy, recovery and assessment without insertion of the polymer sheet, and repeat spinous processotomy at 24 hours. 6 animals for histological analysis and 6 for ELISA.
k) A vehicle subgroup of 12 animals undergoing spinous processotomy, recovery and assessment with insertion and immediate removal of the polymer sheet. 6 animals for histological analysis and 6 for ELISA.

Anaesthesia was induced in animals that were fasted overnight using 4% isofluorane in oxygen (3L/min) in an anaesthetic chamber. Rats were positioned prone. Anaesthesia was

maintained with the animal self-ventilating on 1.5% isoflurane in oxygen. Core body temperature was continuously monitored and maintained throughout the procedure at 38 ± 1 ºC by a heating pad. After surgery, anaesthesia was withdrawn and the rat supplied with 100% oxygen for 1-2 minutes before placing the rat in the postoperative recovery cage. All procedures were performed under sterile conditions.

Table 1. Medications administered perioperatively for acute and chronic spinal cord compression in rats.

Drug	**Dosage**
Anaesthetic Agents	Isoflurane: inhaled during induction and maintenance of anaesthesia Lignocaine: 0.5ml 2% subcutaneously before and after surgery; and after injury
Other drugs	Pentobarbital: 100mg/kg intravenous for euthanasia Formalin: 10% for fixation

Rats in the experimental groups (and corresponding controls) underwent spinous processotomy of the T12 vertebrae (**Figure 2.1**) performed utilising the following technique each time. Following induction of anaesthetic, the back area of the animal was shaved and prepared with povidone-iodine solution. Local anaesthetic (lignocaine) was administered to the operative site. Body temperature was maintained throughout surgery using a thermostatically controlled heatpad to 38 ± 1 ºC. T12 vertebra was exposed by reflecting the superficial layers. The T12 spinous process was transversely cut so that the inner medullary bone was exposed. The adjacent spinous processes were stabilised with fine forceps. A 1mm drill tip was then used to drill towards the spinal cord until the dura was visualised, being careful to avoid any contact with the dura.

Animals planned for compression modelling had a precisely measured 1mm x 1mm x 1mm cube shaped polymer (**Figure 2.2**) inserted such that one angle of the polymer rested on the midline of the spinal cord to form a diamond shape in cross section. The polymer was shaped to an exact size using a surgical microscope and measurement using a Mitutoyo Mtg Co. digital micrometer.

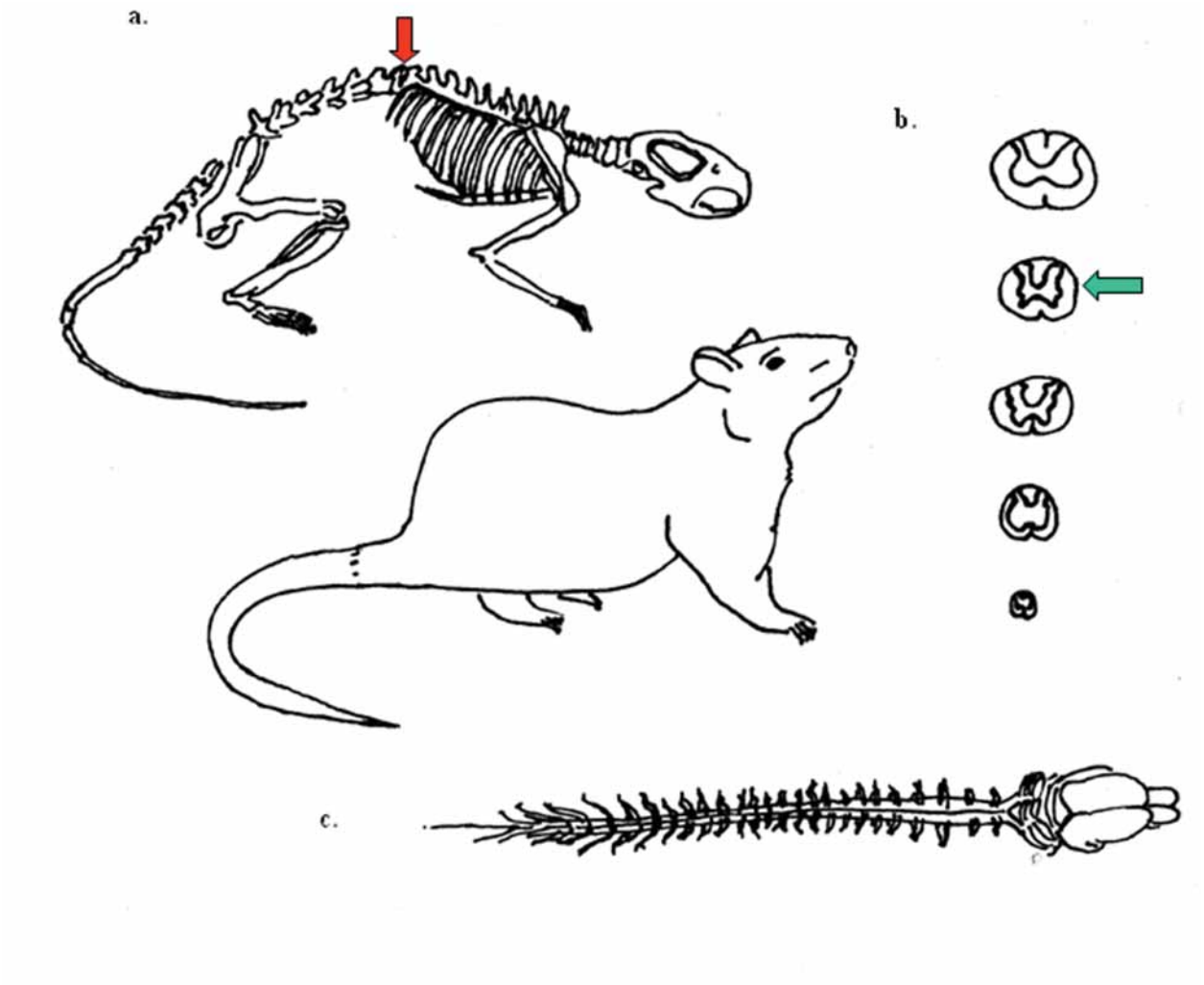

Figure 2.1 Anatomy of the rodent spine and spinal cord.

Surgery in the acute and chronic models was performed at the T12 segment (a) located via palpation of the final accessory rib (red arrow) and illustrated in transection (b) of the spinal cord (green arrow), where cervical, thoracic, lumbar, sacral and cauda equina segments are shown. The intact rodent spinal cord and brain is also shown (c).

Figure 2.2. Polymer preparation.

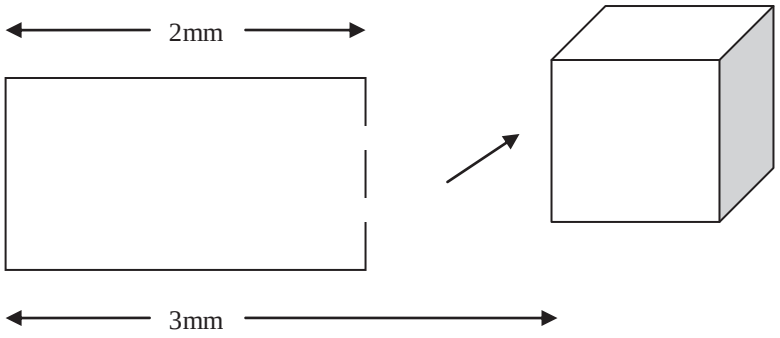

1mm^3 block sectioned from one end of the rectangular polymer.

B)

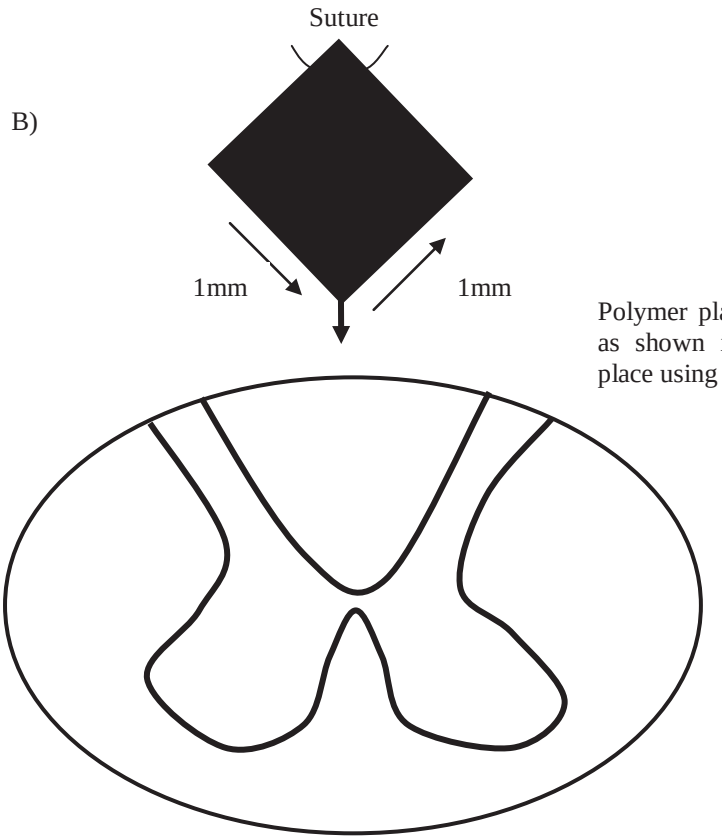

Polymer placed onto posterior surface of dura as shown in cross-section and adjusted into place using the suture and then attached.

Spinal cord in cross-section

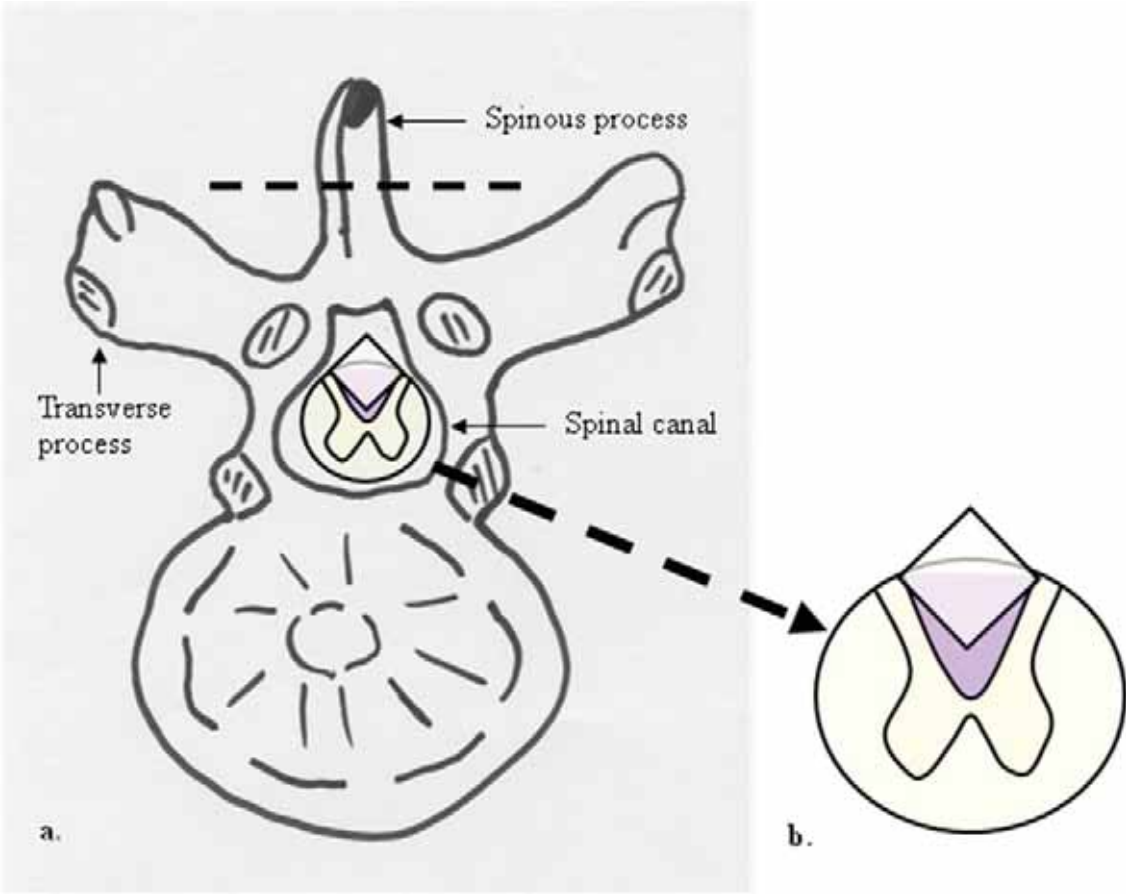

Figure 2.3 Surgical technique for a rodent model of chronic compressive myelopathy.

The T12 vertebra (a) is illustrated. The spinous process is excised horizontally (dashed line). A vertical hole is drilled towards the spinal canal, exposing but not touching the dura. An exandible Aquaprene polymer is inserted, and adhered to the posterior wall of the vertebra using cyanoacetate. The wound is then closed, and the polymer allowed to gradually expand to approximately double its volume and weight (b).

The polymer was made from sheet of expanding water-absorbing urethane-compound polymer (Aquaprene C, Parchem Pty Ltd. Melbourne, Australia) sterilised and inserted transversely into the spinal canal at the level of T12 spinous process. A $1mm^3$ section of polymer was microscopically dissected and measured using a micrometer. A suture was tied across the central part of the polymer in order to help stabilise it during insertion. The polymer was sterilized and carefully inserted under microscopic guidance to avoid acute injury to the spinal cord. The polymer was adjusted using the sutures to lie centrally within the canal (**Figure 2.3**). This ensured that compression was directed towards the posterior sulcus rather than to one side of the spinal cord. The polymer implant was stabilised to the posterior bony surface using cyanoacetate. The wound was closed in layers using 3-0 absorbable sutures.

When placed in a normal saline container the polymer increased weight by 121% after 24 hours, and 157% after 48 hours; and to approximately 2.5 times its original dimensions (**Figure 2.4**) to indent the cord. A 1mm reduction in the spinal canal is compatible with 35-50% of the spinal cord diameter in the rat and has been shown to correlate with the onset of neurological injury (Dimer et al., 1999). Our model consistently resulted in a reduction of the spinal canal by approximately 50%.

Following insertion, the polymer was expected to progressively expand over 24 hours through the absorption of tissue fluid and then remain a constant size. This aimed to replicate the insidious progression of chronic compressive myelopathy in the human. Animals awoke within 30 minutes of surgery and their exploratory behaviour observed within 60 minutes. They required minimal special post-operative care as they feed, self-groom and socialise at normal levels. Rats in the decompression subgroups underwent repeat exposure of the laminae as outlined above but with removal of the polymer sheet, again avoiding leakage of cerebrospinal fluid or mechanical compression of the dura and spinal cord.

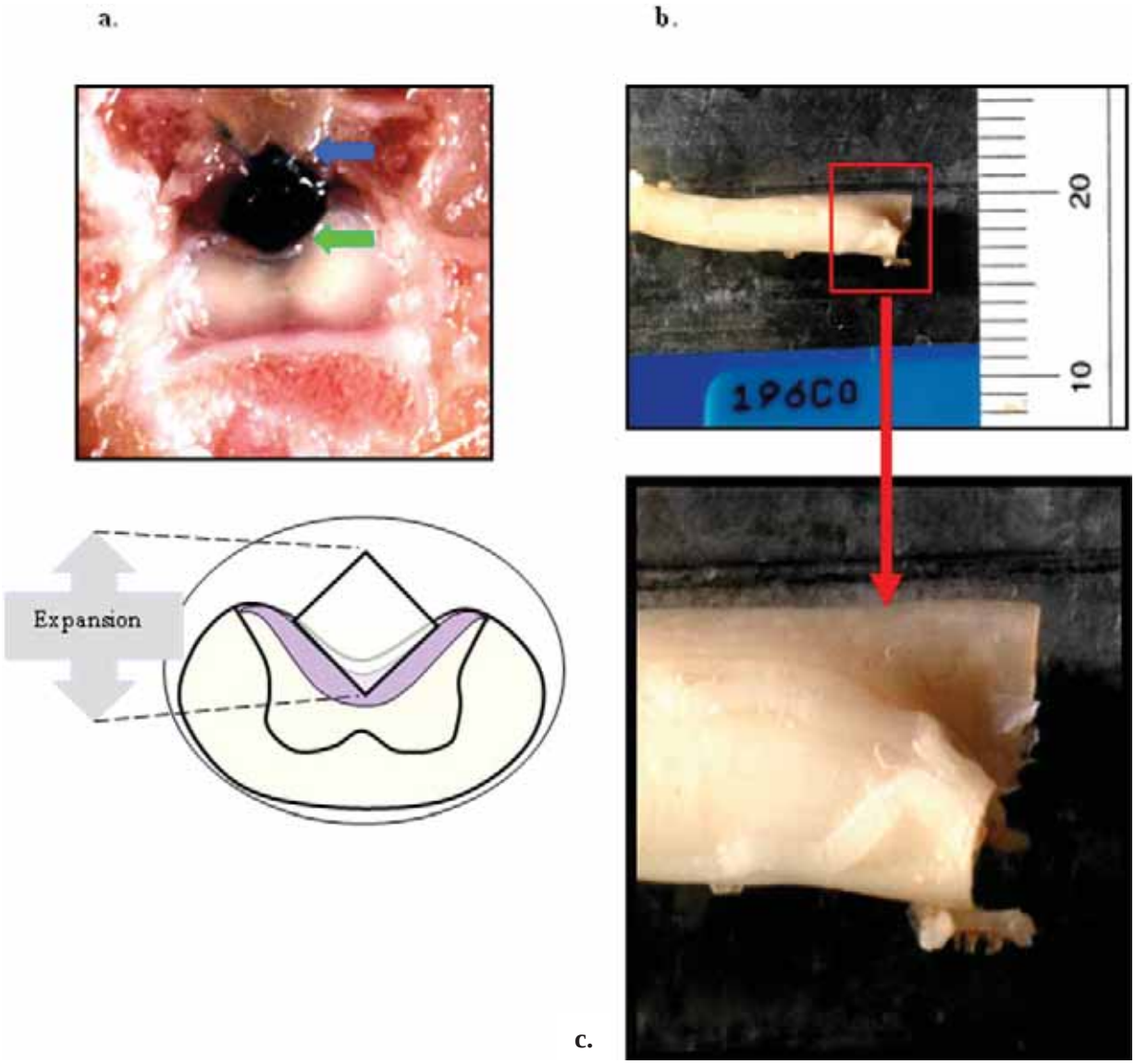

Figure 2.4 The rodent spinal cord in a model of chronic compressive myelopathy.

A cross-section of the rodent spinal cord is shown in macroscopic dissection (a). The Aquaprene polymer was applied to the posterior aspect of the dura (green arrow) adjusted into position using a suture and then adhered to the bony surface posteriorly (blue arrow). The polymer expands to approximately double its size, and 257% of its weight in 48 hours. At pathological dissection, the spinal cord was removed en bloc and the site sectioned (b). In a magnified view of the same image (c) the indentation achieved by the expanded polymer is seen (red arrow).

2.2 Experimental Acute Compressive Myelopathy

In the acute model of spinal cord injury a weight drop model was used. Sprague-Dawley rats were grouped as follows:

a) A sham control group of 12 animals undergoing laminectomy, injury and recovery. 6 animals for histological analysis and 6 for ELISA.
b) A naïve control sub-group using the same animals from the experiment of chronic spinal cord compression with no injury or surgery. 6 animals for histological analysis and 6 for ELISA.
c) A group of 12 animals undergoing laminectomy, injury, recovery and assessment until 24 hours. 6 animals for histological analysis and 6 for ELISA.
d) A group of 12 animals undergoing laminectomy, injury, recovery and assessment until 1 week. 6 animals for histological analysis and 6 for ELISA.
e) A group of 12 animals undergoing laminectomy, injury, recovery and assessment until 3 weeks. 6 animals for histological analysis and 6 for ELISA.

A 3cm incision was made of the superficial layers which were blunt dissected until the paraspinal muscles were reached. These were reflected until the T10-T13 spinous processes and laminae were exposed using a dissecting microscope. A T12 laminectomy was performed exposing a circular region of dura approximately 8mm in diameter. Spinal cord injury was induced using a 10 gram weight of 3mm rounded impact point diameter dropped from a height of 14cm. The circumference of the impact point equated to one spinal segment. The spinous processes adjacent to the weight drop site were stabilised and elevated, thus avoiding impact cushioning from the rat body and minimising respiratory movement which may alter the position of impact. The weight was not allowed to recoil back onto the spinal cord and was instead held in mid-air by the machine. The dural tube was noted to swell after injury. Following injury the wound was closed using 3-0 absorbable sutures and analgesia given.

This weight drop model involved performing a laminectomy at only one level which was sufficient to allow the impounder to impact the spinal cord and avoided the increased trauma that multiple level laminectomies could cause. Previous studies within our laboratory found that by using a 10 gram weight-drop device from heights of 3cm and

12cm at the level of the T12 vertebra, a graded spinal cord injury with varying outcomes of motor function and histopathology could be produced (Yang, 2004). From 3cm the lesion was characterised by multiple microcysts containing axonal swellings in the white matter. An injury from a 12cm height produced subtotal destruction of the grey and white matter.

2.2.1 Functional testing

Functional assessment was performed weekly to determine changes in motor and mixed motor-sensory function using four tests:

a) Basso, Beattie, Bresnahan locomotor score.
b) Acceloratory rotarod.
c) Ledge beam walk.
d) Tail-flick.

Previous studies using a similar model have shown no motor impairment in the rats studied (Kasahara et al. 2004) and so a more broad panel of testing was used. Studies using the same acute model of SCI as used in this study have found evidence of hindlimb paresis but not paraplegia (Yang, 2004).

Methods of rodent neurological assessment include a motor assessment score modified from Tarlov (1972) using an open field locomotion score over five minutes by recording squares crossed in a $1m^2$ grid and open field activity such as rearing, freezing and grooming. The panel of testing used for this study provided a repeatable, easily performed series of sensitive assessments for motor and mixed-motorsensory function. The Basso, Beattie, Bresnahan locomotion score (BBB score) is a reliable, observational measurement of recovery of hindlimb movement originally developed for assessment of pharmacological agents and can be generalised across species (Basso et al. 1995, 1996a, 1996b, McDonald 1999). The BBB score is a reproducible, low cost and sensitive assessment of locomotor function in rodents after SCI (Barros Filho and Molina, 2008) and is based on the 5-point Tarlov score. It is a 22 point (0-21) scale that assesses gait, hindlimb and truncal coordination, foot placement, and weight bearing, recorded over a 2 minute period. A lower BBB score has been well correlated with a loss of tissue away from the site of injury (Bresnahan et al., 1987, Basso et al., 1996). Rotarod time was measured using an

accelerating rotarod to a maximum of 30rpm by 110 seconds, allowing the normal subject to complete a total of 120 seconds. The narrow beam was used as a second assessment of motor strength and coordination, in which rats walk a 1m long beam with ledge and the number of footfalls was counted using video-analysis. The tail-flick test was used as an assessment of motor function (lifting the tail) in response to a sensory stimulus (pain from a laser beam applied to the tail) (**Figure 2.5**).

Animals were trained in the rotarod and narrow beam for 3 days prior to injury. All of these assessments have been well characterised in previous studies (Metz et al. 2000) and provide an efficient and sensitive method of analysing motor function. Gross motor function, spontaneous behaviour and detailed locomotor function are tested using these techniques.

The cross-sectional area of the spinal cord was examined at the site of compression and up to two segments above and below the site in the chronic model using the Nanozoomer HT slide scanner with NDP.scan data acquisition (Hamamatsu Photonics K.K., Japan). Measurements of the total cord cross-sectional area, the posterior column and the ratio of the posterior column to the anterolateral columns was recorded.

Figure 2.5 Tests of motor and mixed motor-sensory function in a rodent model of acute and chronic compressive myelopathy.

Tests are described including the rotarod (a), ledge beam walk (b) and tail flick (c) in which the rat is placed in the clear plastic tube, with tail overlying the heat pad (arrow) through which a laser-beam heat stimulus is applied and the duration of tolerance measured.

a.

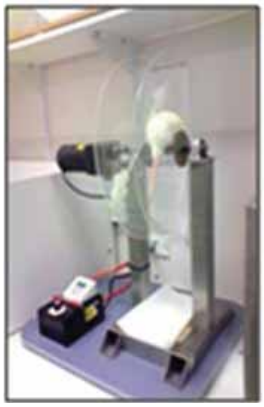

b.

c.

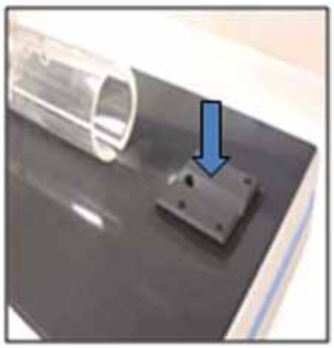

FUNCTIONAL ASSESSMENT	DESCRIPTION
BBB Score	Observation of weakness during locomotion
Rotarod	2 min duration Acceleration Coordination Strength
Ledge Beam	Beam walk 1 metre Gradual narrowing Foot faults recorded during video analysis
Tail-flick	Motorsensory Laser heat-pain stimulus Lift tail in response

Table 2. BBB score categories.

Score	Characteristics	Comment
0	No HL movement observed	HL = hindlimb; FL = forelimb
1	Slight movement 1-2 HL joints	Slight ≤ 50%
2	Extensive movement 1 HL joint and possible movement another	Extensive > 50%
3	Extensive movement of 2 HL joints	Two joints – usually hip and knee
4	Slight movement of all 3 HL joints	Third joint usually the ankle
5	Slight movement of 2 HL joints and extensive movement of 3rd HL joint	
6	Extensive movement of 2 HL joints and slight movement of 3rd	
7	Extensive movement of all 3 HL joints	
8	Sweeping with no weight support or plantar placement with no weight support	Sweeping = rhythmic extensions HL joints, rat on side
9	Plantar placement with weight support in stance only or occasional, frequent or consistent weight supported dorsal stepping and no plantar stepping	Occasional > 1% and ≤ 50%
10	Occasional weight-supported steps with no FL-HL coordination	Coordination = one HL step followed by one FL step, alternating HL steps
11	Frequent to consistent weight-supported steps and no FL-HL coordination	Frequent 51-94% of the time Consistent ≥ 95% of the time,
12	Frequent to consistent weight-supported steps and occasional FL-HL coordination	
13	Frequent to consistent weight-supported steps and frequent FL-HL coordination	
14	Consistent coordinated plantar stepping, predominant paw position is rotated at initial contact and lift-off, frequent plantar stepping, consistent FL-HL coordination and occasional dorsal stepping	Rotation = internal or external rotation of the hindpaw
15	Consistent coordinated plantar stepping, no or occasional toe clearance during forward limb advancement, predominant paw position is parallel at initial contact	Parallel = parallel to the body
16	Consistent coordinated plantar stepping, frequent toe clearance during forward limb advancement, predominant paw position is parallel at initial contact	Frequent toe clearance ≥ 50% of steps have no toe drag sounds
17	Consistent coordinated plantar stepping, frequent toe clearance during forward limb advancement, predominant paw position is parallel at initial contact and lift-off	
18	Consistent coordinated plantar stepping, consistent toe clearance during forward limb advancement, predominant paw position is parallel at initial contact and lift-off	
19	Consistent coordinated plantar stepping, consistent toe clearance during forward limb advancement, predominant paw position is parallel at initial contact and lift-off, tail is down all or part of the time	
20	Consistent coordinated plantar stepping, consistent toe clearance during forward limb advancement, predominant paw position is parallel at initial contact and lift-off, tail is up and trunk instability	
21	Consistent coordinated plantar stepping, consistent toe clearance during forward limb advancement, predominant paw position is parallel at initial contact and lift-off, tail up and consistent trunk stability	

2.3 Human Compressive Myelopathy

Clinical details of each case were obtained from hospital case notes, accident reports and pathology reports. Archival material was obtained from the spinal cords of 16 patients with documented acute or chronic compressive myelopathy during life and definitive evidence of such on post mortem examination; and 8 patients (6 male, 2 female; mean age 55, age range 26-73 years) with documented acute spinal cord injury. The 'duration' of compression was defined as the time from onset of clinical signs and symptoms indicative of compressive myelopathy to death, assuming that the compressive myelopathy was an ongoing process throughout this time. All were subjected to full post-mortem examination.

Chronic cases were divided according to the cause of compression. These were cervical spondylotic myelopathy: 3 male, 0 female; mean age 72, age range 64–77 years; neoplastic compressive myelopathy: 6 male, 1 female; mean age 62, age range 24–79 years; syringomyelia: 3 male, 0 female; mean age 68, age range 55-75 years. In chronic cases, the duration of compression was between 4 months and 22 years. Cases of historically documented traumatic SCI were termed 'acute' due to the mechanisms of injury, although survival time is an important factor in recovery and was defined as the interval between traumatic injury and death ranging from 5 hours to 26 days following injury (age range 26-73 years, mean age 55).

Table 3. Case Summary – Human Cervical Spondylotic Myelopathy.

CASE	AGE	TYPE	VERTEBRAL LEVEL OF COMPRESSION	SPINAL CORD SEGMETNAL INVOLVEMENT	CLINICAL DURATION	CLINICAL DEFICIT
1	77	Prolapsed disc	C3/4	C3, C4, C5, C6	8 years	Quadriparesis
2	64	Osteophytosis	C4/5	C5	14 years	Quadriparesis
3	75	Osteophytosis	C4/5, C5/6	C5. C6. C7	22 years	Quadriparesis

Table 4. Case Summary – Human Neoplastic Compressive Myelopathy.

CASE	AGE	TYPE	VERTEBRAL LEVEL OF COMPRESSION	SPINAL CORD SEGMENTAL INVOLVEMENT	CLINICAL DURATION	CLINICAL DEFICIT
4	50	Oat cell carcinoma, extramedullary	T2, T3, T4	T2, T3, T4	25 days	Paraplegia
5	75	Fibrous histiocytoma, extramedullary	T12	Conus medullaris	4 months	Paraparesis
6	79	Adenocarcinoma, extramedullary	C3, C4, C5	C2, C3, C4, C5	6 months	Right hemiplegia Left hemiparesis
7	59	Osteogenic sarcoma, extramedullary	T11	T12	6 months	Paraplegia
8	74	Squamous Cell Carcinoma, intramedullary	C5, T4, T5, T6	C5, T9, T10	11 months	left sided neck pain
9	24	Ewings Sarcoma with radiotherapy treatment, extramedullary	C5, C6	C5, C6	1 year	Quadriparesis
10	72	Prostate Carcinoma, extramedullary	Odontoid process, C3	C2, C3, C8	5 years	Incomplete quadriplegia

Table 5. Case Summary – Human Syringomyelia.

CASE	AGE	TYPE	VERTEBRAL LEVEL OF COMPRESSION	SPINAL CORD SEGMENTAL INVOLVEMENT	CLINICAL DURATION	CLINICAL DEFICIT
19	75	Traumatic	C7, C8, T1	C6-T5	25 years	Quadriplegia
20	55	Developmental abnormality	Nil	C2-T12	55 years	Paraparesis
21	74	Developmental abnormality	Nil	C2-L1	74 years	Restrictive airways disease

Table 6. Case Summary – Human Traumatic Compressive Myelopathy.

CASE	AGE	TYPE	VERTEBRAL LEVEL OF COMPRESSION	SPINAL CORD SEGEMENTAL INVOLVEMENT	CLINICAL DURATION	CLINICAL DEFICIT
11	73	Fracture/dislocation	C1-C2	C1, C2	5 hours	Quadriplegia
12	48	Fracture/dislocation	C5-T2	C7	24 hours	Quadriplegia
13	30	Fracture/dislocation	C5-C6	C6	88 hours	Quadriplegia
14	67	Fracture/dislocation	T6-T9	T5, T6, T7, T8	6 days	Paraplegia
15	26	Fracture/dislocation	T2-T10	T6, T7	18 days	Paraplegia
16	52	Iatrogenic	C1-C4	C1, C2, C3, C4, C5	26 days	Quadriplegia
17	72	Fracture/dislocation Syringomyelia	C7-T1	C8, T1	32 days	Quadriplegia
18	70	Crush fracture	C7	C8, T1	5 months	Quadriparesis Patchy sensory loss

2.4 Processing of Experimental Tissue

For spinal cords undergoing immunohistochemistry, the spinal column was removed 'en bloc' by firstly sectioning through the sacrum, then removing the head and placing the spinal column in a beaker of 10% formalin for 7 days. Perfusion-sacrifice was used as a technique of tissue fixation in order to minimise cellular changes after death. When each animal was due for analysis they were anaesthetised using 0.3mls pentobarbitone intraperitoneal injection and positioned supine. The thoracic cage was reflected to expose the heart apex into which a 19 gauge needle was introduced and secured in the ascending aorta. Two millilitres of 1000 IU/ml heparin was injected, the right atrium opened and perfusion performed using 10% formalin. Perfusion pressures were generated with compressed air to 80-120mmHg and were monitored using a sphygmomanometer.

Macroscopic images of the lesion site were obtained. The spinal cord was then carefully dissected away for sectioning in 3mm wide sections. Samples were taken for each 3mm, alternating between transverse and longitudinal sectioning. Two transverse sections were taken both caudal and cranial to the site extending up to 6mm away from the site of compression or injury.

For spinal cord to be frozen sectioned, the entire spinal column was removed immediately after perfusion-fixation, snap-frozen in dry ice, and placed in a sterile bag immediately after perfusion. Tissue samples were stored at minus 80ºC until ELISA analyses. The spinal cord was carefully dissected from the spinal column using an anterior approach and placed in 10% formalin.

The macroscopic region of injury was identified and measured. An equivalent region to the macroscopic injury was measured above and below the site and the spinal cord divided accordingly. Specimens were blocked in paraffin wax, labelled and sectioned to 5 micrometre serial sections.

Samples from one half of each experimental and control group underwent immunohistochemical assessment of apoptosis and histopathological changes while the other half were stored at minus 80ºC for use in ELISA assays to investigate changes in the expression of apoptotic proteins.

2.5 Histopathological Assessment

2.5.1 Experimental

Morphological changes were qualitatively assessed at, up to 2 segments above and up to 2 segments below the site in acute and chronic experimental compressive myelopathy using haematoxylin and eosin staining.

2.5.2 Human

In the human series, segments above and below the site of compression were analysed. A marked variation in the spinal cord topography is illustrated in **Figure 2.6 and Figure 2.7**. Demyelinative processes within the white matter at the site were qualitatively assessed with the Weil technique of staining and myelin basic protein (MBP) immunological staining.

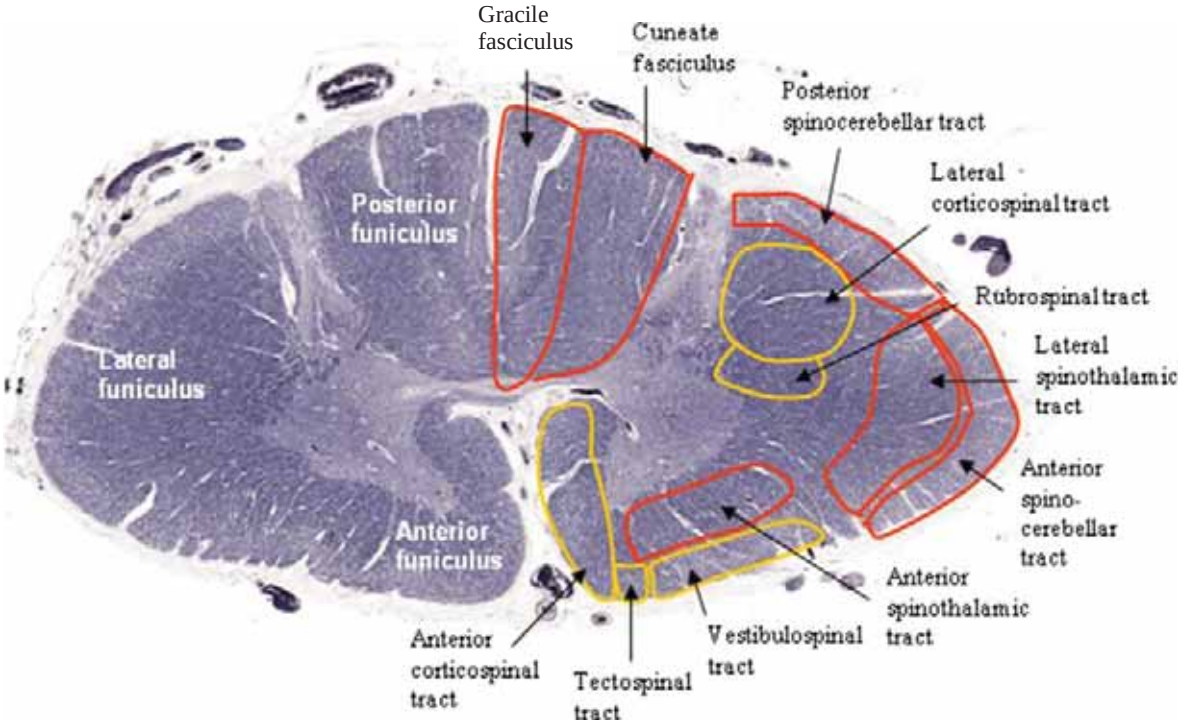

Figure 2.6 Major tracts of the human spinal cord at the mid-cervical level.

In this photomicrograph taken at the level of C4 in normal human spinal cord (Control case 1) the ascending (red) and descending (yellow) tracts are shown on the right. The cord can also be divided into anterior, lateral and posterior funiculi as shown on the left.

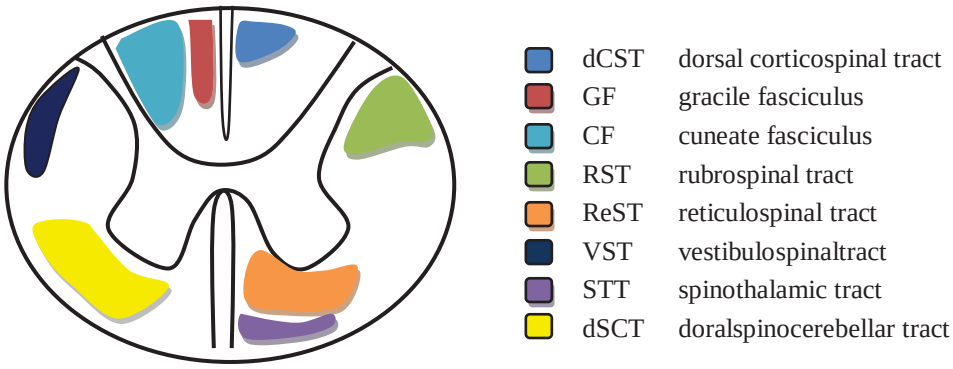

Figure 2.7 Long tracts of the rodent spinal cord.

A diagram of the rat spinal cord in transverse section shows the location of the major tracts. The corticospinal tract is located in the dorsal white matter in contrast with the human in which it is found in the anterior and lateral white matter.

2.6 Immunohistochemistry

All spinal cords were immersion fixed in 40% formalin for a minimum of 10 days and all were examined according to standard neuropathological protocol. Individual cord segments were cut transversely and the segmental level was determined by counting the segments above and below the ventral nerve root of T2, a landmark chosen due to the marked anatomical disparity between T1 and T2 nerve roots.

Qualitative analysis of immunopositive staining using the following antibodies was undertaken in sections at the site of compression, above and below for each case. Haematoxylin and eosin staining was used to examine the histopathological features of all sections. Weil staining was used to differentiate normal myelinated fibres from those with demyelination.

Histopathological and immunohistochemical findings were recorded as follows:

a) Haematoxylin and eosin
    a. Macroscopic findings
    b. Microscopic findings
b) Weil
c) APP
d) Active caspase-3
e) DNA-PKcs
f) PARP
g) Bcl-2
h) Fas
i) Active caspase-9
j) TUNEL
k) Amy-33 amyloid-beta
l) CMAP
m) University of Melbourne amyloid-beta
n) Dako amyloid-beta
o) AIF

Table 7. Antibody Panel.

Antigen	Antibody Clone or Catalogue	Dilution	Pre-treatment	Specificity	Source
APP	22C11 (MM)	1/1000	Citrate	Axonal Precursor Protein	Gift of University of Melbourne
Caspase-3	3015-100 (RP)	1/500	EDTA	Human P17 fragment active Caspase-3	Bio Vision, U.S.A.
DNA DS	AHP318 (RP)	1/10000	TRS	Human DNA-PKcs	Serotec, U.K.
PARP	A6.4.12 (MM)	1/1000	Citrate	Human poly(ADP-ribose) polymerase 116kDa	Serotec, U.K.
Bcl-2	124 (MM)	1/150	Citrate	Human Bcl-2 protein	DAKO,U.S.A.
Fas	NCL-Fas-310 (MM)	1/1000	EDTA	Human Fas (CD 95)	Novocastrian, U.K.
DNA SS and DS	S7101	kit	Kit	3'-OH terminus single and double strand DNA	Intergen, U.S.A.
Caspase-9	3149-100 (RP)	1/1000	EDTA	Cleaved caspase-9 protein 37kDa	Bio Vision, U.S.A.
Amyloid-β	Amy-33 (MM)	1/8000	Citrate	Beta-amyloid peptide 4-5kDa, fibrinogen subunits amino acids 1-28	Seemed, U.S.A.
Amyloid-β	6F/3D	1/100	Formic acid	Human amyloid-beta peptide amino acids 1-42	DAKO, U.S.A.
Amyloid-β	University of Melbourne	1/40	Formic acid	Human amyloid-beta peptide amino acids 1-42	Gift of University of Melbourne
C3-cleaved epitope from APP	AB5942	1/90000	Citrate	Caspase-generated neo epitope of APP	Chemicon International, U.S.A.
AIF 1	AB16501	1/1000	Citrate	517-537a.a. of apoptosis inducing factor molecule	Chemicon International, U.S.A.

Histopathological findings were documented in a variety of forms:

a) A written qualitative statement on each individual section within a particular case (See Appendix).
b) Diagrammatic representation of the spinal cord in longitudinal section and summary of immunohistochemistry at each segment (See Appendix).
c) Semi-quantitative analysis of either rare (3 or less immunopositive cells or axons, occasional 4-10, or frequent > 10 immunopositive cells or axons).
d) Cross-sectional diagram of the spinal cord (See Appendix) as a qualitative representation of staining according to a key (below). Cross-sections were used at the site, above and below the site of compression. Antibodies which were predominantly negative in cases were not included for representation, and thus the following antibodies only were used:
    a. APP
    b. DNA-PKcs
    c. PARP
    d. TUNEL
    e. Amy-33 amyloid-β
    f. AIF
e) Summary of case findings and correlation with clinical data.

Spinal cords from rats without surgical intervention were used as controls. The following antibody panel was used to assess caspase-dependent apoptosis, caspase-independent apoptosis and axonal injury. Immunopositive neurons and glia were qualitatively and semi-quantitatively assessed. Topographical differences are noted between human and rodent spinal cord as illustrated.

2.6.1 Immunohistochemical Markers of Apoptosis

A number of immunohistochemical markers were used in the detection of apoptosis in this study, being chosen according to previous characterisation in the human and rodent spinal cord. The rationale for their selection was as follows:

Fas

Fas/APO-1/CD95 (36 kDa) is a member of the tumour necrosis factor (TNF) receptor family of transmembrane receptors such as the p75 neurotrophin receptor. The Fas molecule is an important mediator of apoptotic cell death as well as being involved in inflammation. Signalling by receptors from the tumour necrosis factor (TNF) family in response to external triggers contributes to a wide range of molecular processes including apoptosis and inflammation. This family comprises at least 32 receptors and of those, Fas is primarily involved in programmed cell death (Muppidi et al., 2004). Membrane bound FasL binds to the receptor within lipid rafts and this triggers downstream activation of FADD and caspase-8 with resultant cell death. Spinal cord ischaemia has been shown to result in activation of neuronal apoptotic mechanisms and activation of Fas as early as 1.5 hours after injury (Matsushita et al., 2000). External apoptotic stimuli result in activation of the Fas receptor and its ligand FasL, in turn activating the Fas-associated death domain protein and caspase-8 (Siegmund et al., 2001). Members of the tumour necrosis factor or 'TNF' death receptor family of molecules play a role in extrinsic apoptosis. They include Fas/Apo-1/CD95, tumour necrosis factor (TNF) receptor 1, DR3 or death receptor 3, TRAIL-R1 (TNF-related apoptosis-inducing ligand receptor 1), TRAIL-R2, DR6, and EDAR (ectodermal dysplasia receptor) (Wajant, 2003). Like Fas and TNF, the p75 structure includes six helices and a death domain classified as 'Type II' (Liepinsh et al., 1997). The domain may be activated in the absence of a ligand (Rabizadeh and Bredesen, 2003). Evidence suggests that these receptors are not only involved in the activation of the apoptotic cascade, but also in non-apoptotic mechanisms (Gentry et al., 2004).

Bcl-2

The Bcl-2 family are key protective regulators of the mitochondrial pathway of apoptosis. Bcl-2 is located within the outer mitochondrial membrane, endoplasmic reticulum and nuclear envelope. In mammalian cells they have been shown to act upstream of caspases and assist in determining the release of pro-apoptotic molecules such as cytochrome-c from the mitochondria (Golstein, 1997). Bcl-2 confers a protective effect on the cell by inhibiting pathways of apoptosis and its expression is increased under apoptotic conditions (Molica et al., 1996). The release of cytochrome-c and mitochondrial permeability are regulated by the Bcl-2 family of proteins. This group is comprised of the anti-apoptotic

Bcl-2 and Bcl-x, and the pro-apoptotic Bax and Bak proteins. Extrinsic induction of apoptosis leads to Bid cleavage and this may be detected using tBid marker (Krysko et al., 2008) in addition to downstream release of cytochrome-c.

Mitochondria provide the critical intrinsic site for respiration and energy production in eukaryotic cells. The production of the cell's energy unit, ATP, from glucose assists with DNA replication and the synthesis of proteins. ATP may be used for kinetic purposes, such as the contraction of actin and myosin in skeletal muscle, or for the growth and repair of tissues. This molecule is unstable and must be used within a short period. In apoptotic cell death, there may be alteration of the electrochemical gradient normally used for the production of ATP (Bernadi et al, 1999).

Subsequently, there is permeabilisation of the mitochondrial membrane by the formation of permeability transition pores, with resulting excessive calcium influx (Zamzami and Kroemer, 2001). Mitochondria play a critical role in the regulation of cell death known as the 'intrinsic' pathway by releasing pro-apoptotic molecules such as apoptosis inducing factor (AIF) and cytochrome-c across this membrane leading to caspase activation (Annunziato et al., 2003). The permeabilisation of the mitochondrial membrane is an important early event during the apoptotic process and causes the release of proteins normally found within the intermembrane space of mitochondria. This process is largely controlled by members of the Bcl-2 family of proteins, Bax and Bak (Degli and Dive, 2003). This allows the activation of an amplification cascade, including the release of cytochrome-c and activation of procaspases-2, -3 and -9 and the apoptogenic protein Smac/DIABLO (Verhagen et al., 2000). Apoptotic cell death was previously classified as capsase-dependent or caspase-independent in nature however it is now recognised that there may be overlap of these cascades in particular with the inhibition of one pathway triggering activation of the alternate pathway.

Caspase-3

The caspase family of proteases both initiate and perform cleavage of a variety of proteins in several intracellular compartments. Initiator and effector caspases are distinct structurally. Initiator caspases include caspase-8, -9 and -10, which in turn cleave and activate caspase-3, -6 and -7. Recent studies suggest that caspases are central not only to

cell death but also other changes in cell state, such as cell differentiation and cell fusion, and are likely to result in irreversible changes (Nhan et al., 2006). Furthermore, the inhibition of caspase activation may divert apoptosis to alternative forms of cell death. This implies that caspase activation cannot simply be equated with apoptosis, but must be considered in the context of other morphological and biochemical evidence.

Caspase-3, in its active form, is a cysteine-aspartic acid protease recognised as a major effector molecule of morphological changes in apoptosis (Erhardt et al., 1997). The caspase-3 gene encodes a proenzyme which undergoes processing by initiator caspases at Asp^{28} and Asp^{175} to form two dimerised subunits to form active caspase-3, which binds to caspase-8 during apoptosis. It is thought that the translocation of caspase-3 from cytoplasm to the nucleus represents a key morphological change during apoptosis (Woo et al., 1998, Zheng et al., 1998) and that this is an active process (Kamada et al., 2005).

Caspases-3 and -9 have been found to be expressed in both mitochondrial and cytosolic compartments of apoptotic Jurkat T lymphocytes and caspase-2 and -3 in the nucleus (Zhivotovsky et al., 1999). In the same experiment, procaspases-2, -3 and -9 were found in mitochondrial and cytosolic fractions of non-apoptotic cells, procaspase-2 in the nucleus, and procaspases-7 and -8 in the cytosol, suggesting that translocation of active caspases may be an important step in apoptosis. Caspase-3 appears to play a key role in both extracellular and intracellular apoptotic mechanisms.

Using knockout mice models, the effect of loss of several apoptotic factors has been documented. Mutation of caspase-3 in the mouse has been shown in perinatal death, T-cell resistance to cytotoxic factors, and altered morphology of apoptotic cells (Kuida et al., 1998, Woo et al., 1998).

Caspase-9

The human caspase-9 gene contains 9 exons and 8 introns and spans approximately 35 kb of the genomic DNA. The caspase-9 precursor procaspase-9 may be cleaved at Asp^{315} and Asp^{330} by granzyme B or following apoptotic triggers by caspase-3. Cytosolic caspase-9 expression has been shown to be ubiquitous in heart, liver, skeletal muscle and pancreas.

Caspase-9 inhibition results in cortical hyperplasia and death in the perinatal phase (Hakem et al., 1998).

DNA-dependent protein kinase catalytic subunit

Immunohistochemical markers of DNA damage and apoptosis were applied to paraffin-embedded sections following dewaxing and dehydration stages. The efficient and adequate repair of DNA strand breaks is crucial for the integrity of the cellular genome. DNA-dependent protein kinase catalytic subunit (DNA-PKcs) is involved in the repair of double stranded DNA breaks in mammalian cells. The DNA-PK molecule contains a heterodimeric DNA-binding subunit (Ku70/80) and a catalytic subunit of 465 kDa known as (DNA-PKcs). Ku is comprised of two proteins of about 70,000 Da (Ku70) and 80,000 Da (Ku80 or Ku86) respectively (Andersen and Lees-Miller, 1992, Andersen and Carter, 1996). DNA-PKcs is a serine/threonine protein kinase activated via the Ku heterodimer where DNA fragmentation exists.

Poly (ADP-ribose) Polymerase

Poly (ADP-ribose) polymerases (PARP) are a family of nuclear proteins found in eukaryotic cells. The functions of PARP include the formation of mitotic spindles (Chang et al., 2004), centromere and centrosomal function, telomere function via the action of Tankyrase, movement of endosomes, DNA strand break detection and repair (D'Amours et al. 2001, D'Amours et al., 1999) and cell death along the spectrum of both apoptosis and necrosis (Burkle, 2005, Koh et al., 2005). PARP activity is central not only for the maintenance of genomic structure but also in carcinogenesis, ageing, neuronal function and inflammatory disorders (Ha et al., 2002, Kim et al., 2005).

18 different genes are known to encode proteins from the PARP family. The first member, PARP-1 (113kDa) is the most abundantly expressed and is located in the nucleus. It assists in DNA repair and the formation of chromatin following gene expression and is active in normal cells. It contains a 20-26 amino acid sequence in the target domain and is thought to bind to non-B DNA structures in chromatin in the absence of DNA strand breaks (Lonskaya et al., 2005), inhibiting the expression of further genes. This process is reversed with the binding of NAD+ to synthesise the long chain polymers, allowing the unbinding

of nucleosomes without change to their internal structure and the further expression of genes (Kim et al., 2005). This is achieved via conserved regions of chromatin specific for the binding of PARP-1, which remain separate from regions of active transcription and the histone-H1 domain. PARP-1 activity is reversed by the catabolic activity of poly (ADP-ribose) glycohydrolase (PARG) (Bonicalzi et al., 2005) and inhibited by ATP.

PARP plays a pivotal role in the regulation of DNA metabolic processes and maintenance of genomic stability as it catalyses the post-translational alteration of proteins. This occurs by a process of NAD+ dependent automodification, whereby PARP specifically binds to nucleosomes, catalyses the covalent attachment of Poly (ADP-ribose) or PAR units to itself and to nuclear acceptor proteins for the modification of chromatin, either directly or indirectly, through the unfolding of chromatin, regulation of cell-cycle and activation of cell survival-cell death molecular pathways. Up to 100 units may be catalysed from NAD+ by PARP's 1-3. A highly conserved 40 kDa carboxy-terminal sequence has been identified and is known to be catalytically active (Simonin et al., 1993).

PARP contributes to cell death by its activation in both the caspase-dependent and more recently, caspase-independent pathways of apoptosis. The MCA1522G antibody against Poly (ADP-ribose) polymerase (PARP) recognises the full 116kD length of the enzyme. PARP-1 has been shown to be cleaved during apoptosis and causes phosphorylation of P53 with resultant DNA damage and induction of apoptosis due to an overexpression of transcription factors. Mild genotoxic stressors may facilitate DNA-repair and cell survival, however severe cytotoxic stimuli result in a rapid increase in PARP and failure to maintain the genomic structure (Skaper, 2003, Virag, 2005). In the presence of coenzyme nicotinamide adenine dinucleotide or NAD+, a cofactor for cell energy and signalling, the enzyme PARP ADP-ribosylates chromatin proteins forming polymers and contributes to the rejoining of DNA strands. This process involves targeting several proteins including histones, DNA topoisomerases, DNA methyltransferase-1 and DNA damage regulatory proteins such as p23, p21, DNA-PK, NF-κB, XRCC1 (Malaga and Althaus, 2005).

PARP may also contribute to cell death by facilitating the recruitment of microglia. In secondary neuronal damage following ischaemic stroke, macrophages and microglia are known to migrate to the site of injury and produce excessive quantities of cytotoxic free

radicals (Love, 1999, Skaper, 2003). PARP is believed to regulate migration of microglia by controlling the expression of integrin CD11a.

Initial evidence of PARP as a sensor and repair enzyme of DNA damage emerged during the 1980s, when use of the PARP inhibitor, 3-aminobenzamide, was shown to cause susceptibility of cells to DNA-damaging agents (Purnell and Whish, 1980, Durkacz et al., 1980). The inhibition of PARP, and studies of animals rendered deficient for the PARP-1 enzyme, have demonstrated the importance of PARP in CNS ischaemic cell damage and reperfusion injury, stroke and trauma (Komjati et al., 2005). PARP inhibition has also been found to decrease cell death in cardiac ischaemia and reperfusion (Szabo, 2005), as well as in several CNS conditions, including brain ischaemia, Parkinsonism (Chiba-Falek et al., 2005, Onyango et al., 2005) and traumatic spinal cord injury (Skaper, 2003). In a model of spinal cord injury in mice using vascular clips, PARP inhibitors, 3-aminobenzamide (3-AB) or 5-aminoisoquinolinone (5-AIQ), significantly reduced the histological severity of inflammation, recruitment of neutrophils, formation of PAR and was associated with decreased levels of apoptosis (Genovese et al., 2005). In experimental focal traumatic injury to the cerebral cortex caused by a cryogenic lesion, the inhibition of PARP and associated nitric oxide synthase achieved using 3-bromo-7-nitroindazole was found to decrease PAR expression in addition to a decrease in lesion volume at 24 hours using 3-AB (Hortobagyi et al., 2003). Such studies provide further evidence of the important role of PARP in neuronal disease. PARP remains a potential therapeutic target in ischaemic and traumatic neuronal insult (Komjati et al., 2005, Skaper, 2003).

Excessive activation of PARP-1 has been shown to occur in neuronal ischaemic and reperfusion injury (Van Wijk and Hageman, 2005, Tanaka et al, 2005). Following the release of the excitatory neurotransmitter glutamate and overexcitation of glutamate receptors, calcium accumulates within the neuron with subsequent activation of potentially lethal proteins. Reactive oxygen species (ROS) and nitric oxide (NO) are associated with widespread DNA-damage. The latter is caused by the activity of nitric oxide synthase (NOS) using the N-methyl-D-aspartate (NMDA) receptor and the damaging effects of NO are reduced in mice deficient for nNOS (Huang et al., 1994, Iadecola, 1997). PARP-1 activation has been shown to greatly increase in focal ischaemic brain injury and its inhibition is crucial in preventing cell death (Chiarugi, 2005). PARP-2 (62 kDa) is a known catalyst in DNA damage to produce polymers of ADP-ribose and is located in the nucleus.

Such pathways may not necessarily lead directly to cell death. In global ischaemia, the activation of PARP may in fact assist in cell survival via activation of the delayed-cell death pathway (Kofler et al., 2005).

Reactive oxygen species (ROS) cause DNA fragmentation and the resultant activation of PARP hydrolyses remaining energy substrate NAD+, depleting ATP and triggering cell death. Activation of PARP-1 may cause release of AIF from mitochondria with subsequent condensation of chromatin, fragmentation of DNA and cell death (Hong et al., 2004). Recently, a rapid communication between nuclear and mitochondrial proteins has been shown. In studies of HeLa cells exposed to methyl-N'-nitro-N-nitrosoguanidine (Cipriani et al., 2005), a DNA-damaging agent, PARP-1 was activated and there was a resultant sharp decrease in NAD+ and ATP. Initially there was an increase recorded in mitochondrial membrane potential and the accumulation of superoxide. This, and the actual death of the cell, was prevented by the prior use of PARP-1 inhibitors. Despite PARP-1 being located in the nucleus, ATP decreased in mitochondria and then the cytoplasm, but rose in the latter phase with PARP-1 inhibition. An alternative pathway is the caspase-dependent apoptotic process, whereby caspases are thought to target the conserved recognition site on the PARP protein known as DEVD. Concomitant with PARP cleavage is the activation of domain and fragmentation nucleases which cleave DNA in characteristic fragment lengths.

Apoptosis Inducing Factor

More recently, a pathway of cell death usually independent of caspase-activation was identified involving activation of a key molecule known as Apoptosis Inducing Factor (AIF). AIF is a flavoprotein (inclusive of the flavine adenine dinucleotide group), encoded by a nuclear gene on the X chromosome, and its precursor is comprised of 612 amino acids (approximately 67 kDa). The crystalline structure of AIF reveals a glutathione reductase-like fold (Mate et al., 2002). It is not surprising therefore, that AIF in mammalian species is found in the mitochondrion, a structure of bacterial evolutionary origin. Post-translational modification of AIF results in the mature form of approximately 62kDa although its exact length and composition is uncertain (Otera et al., 2005, Susin et al., 1999).

AIF has been shown to be ubiquitously expressed in a variety of tissues, including heart and skeletal muscle, bowel wall, liver, skin and bone marrow (Daugas et al., 2000). The molecule is synthesised in the cytoplasm and then moves into mitochondria. In an *in vivo* rat/mouse model of retinal detachment (Hisatomi et al, 2001), AIF was present in normal photoreceptor cells along the inner segment, which has large numbers of mitochondria. AIF was found in the nucleus following retinal detachment.

AIF protein has a dual role of oxidation/reduction. It is essential in the function and production of respiratory chain complexes I and III. It is highly conserved between mammalian species, with more than 95% amino acid match between mouse and human cells (Lorenzo et al., 1999). It is normally located in the mitochondria using the N-terminal mitochondrial localization sequences (MLS). The oxidation of NADH (Miramar et al. 2001) and formation of a superoxide anion, suggest its capacity for electron transfer, although its target in the cell is unknown. Native and recombinant forms of AIF participate in NADH redox reactions.

AIF and its caspase-independent function in apoptosis were first recognised using cytofluorometric assays (Susin et al., 1997, Susin et al., 1999). AIF is released during apoptosis and permeabilisation of the mitochondrial membrane and transported from the mitochondrial intermembrane space via the cytosol to the nucleus, where it causes large-scale DNA fragmentation of approximately 50 kilobase pairs and secondary chromatin condensation. Positive charges on the surface of the AIF molecule allow it to interact with DNA, with preferential binding to single-stranded rather than double-stranded DNA (Vahsen et al., 2006). AIF has been found to play a significant role in the PARP-mediated pathway of cell death, primarily via the Poly ADP-ribosylation activity of PARP-1 (Chen et al., 2004). As detailed above, PARP activation has been shown to contribute to both necrosis and apoptosis and there is evidence of its contribution to cell death after SCI.

The role of AIF in apoptotic processes has been shown to be independent of its role in redox reactions, as NADH oxidation continues to occur under conditions in which AIF-induced DNA fragmentation and chromatin condensation is suppressed. Even mild apoptotic stimuli can trigger the AIF apoptotic pathway, however this process appears to be reversible under such conditions (Dumont et al, 2000).

Nuclear translocation of AIF has been demonstrated in vivo in traumatic brain injury (TBI) (Zhang et al., 2002) and SCI (Austin and Fehlings, 2008) and may play an important role in neurodegeneration (Krantic et al., 2007). In a rat model of traumatic brain injury at 2-72 hour time points, AIF was localised to the neuronal nucleus using immunohistochemical and western blot analysis. AIF protein was increased with longer duration of survival and this was confirmed by increasing numbers of immunopositive cells for AIF in the ipsilateral parietal cortex, dentate gyrus and CA3 hippocampus (Zhang et al, 2002).

Terminal deoxynucleotide transferase dUTP Nick End Labelling (TUNEL)

In situ nick-end labelling (TUNEL) (Intergen, ApopTag S7101) was used as a biochemical marker of apoptotic DNA fragmentation. The TUNEL technique enzymatically labels the free DNA 3'-OH ends of specific DNA strand breaks that are characteristic, though not pathognomonic, of apoptosis. TUNEL may detect early-stage apoptosis prior to the condensation of chromatin (Migheli et al., 1995).

Antibodies used in this study have been well characterised in previous studies and the respective immunolabelling patterns described (Finnie et al., 1995, Muresan, 2004, Susin et al., 1999, Tanaka et al., 2005, Weidemann et al., 1989, Sheriff et al., 1994, Nilsen et al., 1997).

Additional markers

Other markers include tissue polypeptide antigen (TPA), the protein marker ubiquitin, the inhibitory molecule survivin, phosphatidylserine for the recognition of engulfment of dying cells and single-stranded DNA for the detection of early apoptosis, p41, BM-1, Annexin V and finally the sensitive and specific differentiator of apoptotic versus non-apoptotic cells, negative in apoptosis marker (NAPO). It is important to note that the detection of mitochondrial membrane potential using TMRM, rhodamine123, JC-1, Molecular Probes or ROS production (dihydrorhodamine123) does not determine the presence of apoptosis (Krysko et al., 2008). APP and its reputed metabolic breakdown product, Amy-33, were used as marker of axonal injury and amyloid-beta respectively. Histopathology was performed on haematoxylin and eosin-stained sections. Weil's stain was used to demonstrate demyelination.

Section Preparation

Sections were dewaxed in xylene and rehydrated through graded alcohols to water. In all cases, non-specific peroxidase activity was quenched by immersing the sections for 30 minutes in methanol containing 3% H_2O_2. The sections were then microwaved for 10 minutes in the appropriate retrieval buffer and allowed to cool to below 50 degrees Celsius. The sections were then incubated in 30% normal horse serum (NHS) for 30 minutes and subsequently overnight at room temperature in the primary antibody diluted in NHS in a humidified chamber. Each solution was mixed thoroughly before being applied. Bound antibody was visualised by incubation with biotinylated anti-mouse or anti-rabbit immunoglobulin (Vector, U.S.A.), strept-avidin-biotin-horseradish peroxidase (Pierce, U.S.A.) and reaction with 0.01% H_2O_2 and diaminobenzedene. Following DAB staining, the sections were washed in water, counterstained with haematoxylin, dehydrated, cleaved and then mounted. Diaminobenzidene (DAB) was used as a chromagen to visualise the immunological reaction product. The DAB method is based on the oxidation of hydrogen peroxide by peroxidase to form water. During this histochemical reaction, DAB is oxidised and undergoes polymerisation and produces a brown reaction product (Ealey, 1984).

Tissue from lymphoma, human glioma, Alzheimer's disease and traumatic brain injury were used as positive controls, while tissue from histologically normal spinal cords served as negative controls.

2.7 Semi-quantitation

The spinal cord in cross-section was diagrammatically divided into six regions (**Figure 2.8**).

a) Two anterior regions separated by the anterior median fissure on one side and including the anterior corticospinal tract, anterior spinothalamic tract and vestibulospinal tract. These tracts were approximated by a border taken from the lateral portion of the anterior horn perpendicular to the edge of the spinal cord as demarcated by the dotted-line.
b) Two posterior regions separated by the posterior sulcus and enclosed by the posterior and central grey matter.
c) Two lateral regions bound by the posterior horn, anterior horn and the spinothalamic tract.

Axonal immunopositivity was spatially represented according to these six regions as demonstrated (**Figure 2.9**). The presence of neuronal immunopositivity was represented by the dark triangle. Recordings for each case at, above and below the site of compression are provided in the Appendix.

A)

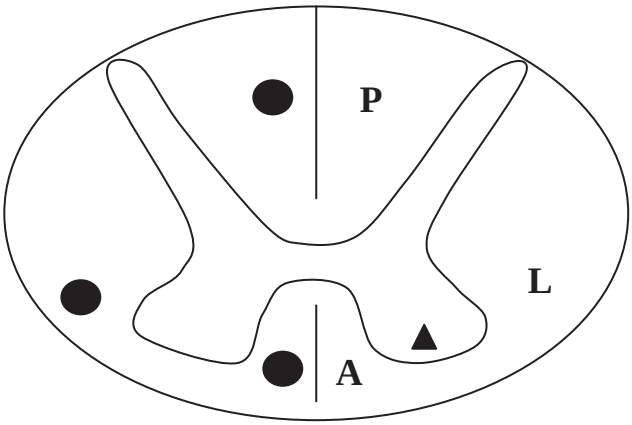

B)

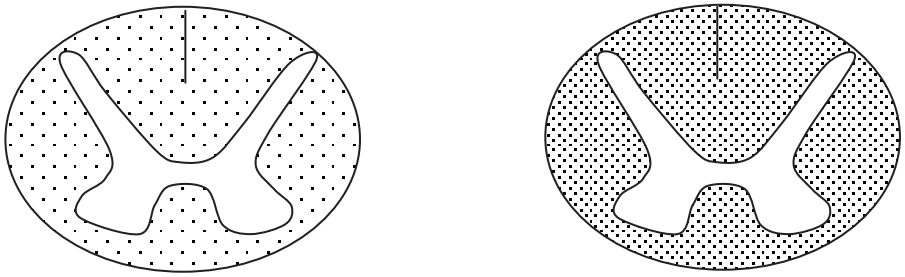

Figure 2.8 Semi-quantitative assessment - Spatial distribution of staining.

Glial immunopositivity was represented by a dark circles (A). An increase in the density of immunopositive glia within a particular case was represented by circles of a closer distance (B) on cross-section as below.

A = Anterior white matter, L = Lateral White Matter, P = Posterior White Matter.

Figure 2.9 Key – Spatial distribution of staining.

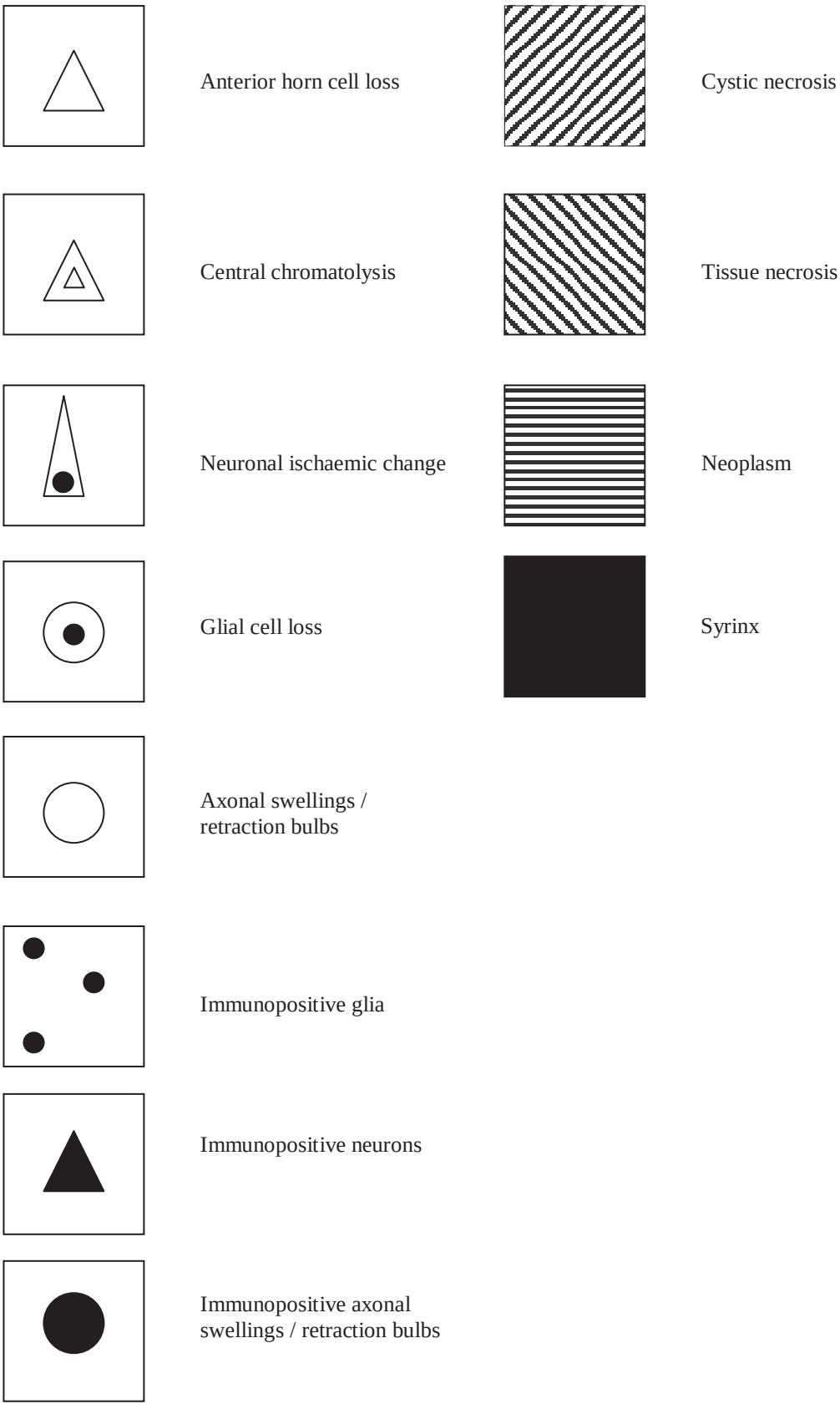

2.8 Laser Scanning Confocal Microscopy

Paraffin-embedded, 7μm, sections were prepared and stained according to the previously described protocol. Fluorescent staining was performed using fluoresceine isothiocyanate (Alexa fluor 488) label for rabbit-polyclonal antibodies, and 5-NN'-diethyl-tetramethylindo di carbocyanine (Cy5) for mouse-monoclonal antibodies. The images were produced using the BioRad Radiance 2100 confocal microscope (Bio-Rad Microscience Ltd, UK) equipped with three lasers: Argon ion 488nm (14mw); Green HeNe 543nm (1.5mw); Red Diode 637nm (5mw) outputs; and an Olympus IX70 inverted microscope. The objective used was a 60x UPLAPO with NA=1.4 oil. The dual labelled cells were imaged with two separate channels (PMT1/2) in a sequential setting. Alexa fluor 488 was excited with Ar 488nm laser line and the emission was viewed through a HQ515/30nm narrow band barrier filter in PMT1. Cy5 was excited with Green HeNe 543nm laser line and the emission was viewed through a long pass barrier filter (E600LP) to allow only far-red light wavelengths longer than 600nm to pass through PMT2. Automatically all signals from PMT 1 and 2 were merged. The image data were stored on a CD for further analysis using a Confocal Assistant software program for Microsoft® Windows™ (Todd Clark Brelje. USA).

The following antibodies were combined using dual-immunolabelling:

1. Caspase-3 / APP
2. Caspase-3 / amyloid-beta
3. AIF / mitochondrial marker
4. AIF / APP

Semi-quantitation

Cells or axons showing immunopositive staining:

0 Negative
0-3 Rare
4-10 Occasional
> 10 Frequent

2.9 Enzyme-Linked Immunosorbant Assay (ELISA)

2.9.1 Preparation of Spinal Cord Homogenate

At sacrifice, rats were anaesthetised with 4% isofluorane in 3L/min O_2 until a surgical level of anaesthesia was reached. The animal was then decapitated and the spinal column removed. The spinal cord was evacuated using forceps away from the injury site. The cord was then dissected as quickly as possible by making two transverse incisions at the segmental margins of the site of injury.

Samples were weighed and homogenised in 10 x spinal region weight of homogenisation buffer (homogenisation buffer with 0.01% Triton X-100), DL-dithioreitol (DTT; Sigma D-9163) and protease inhibitors pepstatin A, aprotinin, leupeptin and phenylmethanesulfonylfluoride (Sigma; P-4205, A-1153, L-9783, P-7626). Homogenised spinal cord regions were kept on ice and vortexed every 5 mins for 20 mins before being centrifuged at 8500 rpm at 4^{o}C for 15 mins. The supernatant was transferred to a clean eppendorf tube and frozen at -80^{o}C.

2.9.2 Protein Estimation Assay

Supernatant from each brain region was rapidly thawed then added in triplicate (5µl/well) to a 96-well plate (Greiner Bio-One) along with triplicates of standards of known protein contents (0, 0.1, 0.2, 0.5, 1, 1.5, 2, 5, 7.5 and 10µg/µl of bovine serum albumin, BSA; Sigma T-8877). 20µl of reagent S (Biorad, 500-0115) was added per ml of reagent A (Biorad, 500-0113) then 25µl of this solution was added to each well. Finally, 200µl of reagent B (Biorad, 500-0114) was added to each well, and the reagents mixed for approximately 20 mins. The plate was then read at 620nm on an Ascent Multiscan plate reader (Thermo Labsystems). The protein content of each spinal cord homogenate sample was determined by producing a standard curve with the known protein content standards then using the equation of the trend line to determine the protein content within the unknown samples. Spinal cord homogenate samples were then diluted with tris-buffed saline (TBS) to 400ng protein per 100µl of TBS.

2.9.3 ELISA for Caspase-3 and Caspase-9

An ELISA assay was used to determine the level of active caspase-3 expression in experimental chronic compressive myelopathy comparing 9 week and decompression groups with controls. It was also used for caspase-9 expression in experimental acute compressive myelopathy comparing 3 week and 24 hour groups with controls. Samples were loaded into each well of a Maxisorp plate (Nunc) in triplicates. Blank wells with no loaded protein were included as positive controls. The protein was allowed to coat the wells overnight at 4^{o}C. Samples were tipped off and blocking agent (0.2% gelatine solution) added to each well until a meniscus formed, before plates were given a gentle agitation at room temperature for 1 hour. Wells were washed in TBS three times (x3) then incubated with 100µl of SP antibody (Chemicon, ab-1566, 1:1000) at 37 ^{o}C for at least 1 hr in a humid container. Following washes in TBS (x3), wells were incubated with 100 µl of secondary anti-rabbit horseradish peroxidise conjugate (HRP; Rockford, 1:1000) antibody for 1 hr in an oven at 37 ^{o}C in a humid container. Wells were washed in TBS (x4) and the liquid substrate system 3,3'-5,5'-tetramethylbenzidine (TMB; Sigma, T-8665) was used to reveal protein expression by adding 100µl to each well. The reaction was then stopped at the same time for each well with 50 µl of 0.5M sulphuric acid (H_2SO_4). The level of SP expression was then determined by reading the absorbance at 450nm on an Ascent Multiscan plate reader.

2.10 Photography

Images of microscopic sections were recorded using a NanoZoomer HT slide scanner with NDP.scan data acquisition (Hamamatsu Photonics K.K., Japan).

2.11 Statistical Analysis

Statistical analysis was performed with the assistance of a professional statistician. The number of animals required was measured with a CV of 15-20%. Applying this to a power calculation showed that for a 30% change, n=6 rats were required in each group. All parametric data are expressed as mean ± standard error of the mean (SEM) and non-parametric data are expressed as the median. In all cases, the number of rats served as the n number. Significance was determined using Student's t-tests and one-way repeated measures of analysis of variance (ANOVA) with Tukey's post hoc analysis; p was set at <0.05.

CHAPTER 3

RESULTS
CHRONIC SPINAL CORD COMPRESSION

The pathological changes in chronic compressive myelopathy, and how these may be modified by decompressive surgery, are not well understood and few studies have addressed the pathophysiological changes present in the spinal cord. This study provides a novel descriptive and semi-quantitative analysis of the spatial distribution and temporal evolution of neural injury in a rodent model of chronic spinal cord compression and the effects of decompression. A thorough observational study of apoptosis and pathological changes in human chronic compressive myelopathy is included and this may assist in providing a basis for future research or the generation of hypotheses in this field. A priority of the study design was the use of multiple immunohistochemical markers of apoptosis, representing differing stages of cell compromise, as well as the key biochemical marker, TUNEL, rather than a single marker. A complete representation of pathological and apoptotic changes in human cases is documented in the Appendix, including an illustrative representation of the spatial pattern of staining.

In the experimental model, the results of insertion of a gradually expandable polymer, as demonstrated in normal saline immersion, in 78 male 12-15 week old Sprague-Dawley rats were analysed. For histological studies, 12 rats in each group were sacrificed at 24 hours, 1, 3, 9 and 20 weeks and divided into histopathology and ELISA groups. Histopathological changes at, above and below the site of compression were correlated with immunohistochemical markers of apoptosis: active caspase-3; TUNEL; PARP; caspase-9; and AIF. Amyloid precursor protein (APP) was used to assess axonal damage. A similar panel of apoptotic markers was used to assess apoptosis in human chronic compressive myelopathy. Cross-sectional areas were used to measure the extent of compression. For functional outcome, surgical decompression was performed at 24 hours and 3 weeks with sacrifice after 9 weeks. Motor-sensory assessment included BBB score, rotarod, and tail flick.

In experimental chronic compressive myelopathy a loss of posterior white matter area was shown, maximal at the site of compression. These changes resolved with decompression (3 week group mean area 3.05mm^2, increasing following decompression at 3 weeks and survival to 9 weeks to 5.75 mm^2). Functional impairment was mild overall. Using the tail-flick, a measure of motorsensory function, a significant increase in measured time versus control was found at 1 week ($p < 0.0001$) and 3 weeks ($p = 0.0015$). A progressive decrease in BBB locomotor score was seen at 1, 3, 9 and 20 weeks ($p < 0.0001$). Functional status

was comparable between 9 week compression and 24 hour and 3 week decompression groups with insignificant changes in tail-flick scores ($p = 0.8401$), rotarod function ($p = 0.2153$) and BBB scores ($p = 0.0666$).

Caspase-9, PARP, AIF and aC3 staining was found in glia at, above and below the site of compression in all groups. Caspase-3 was greater expressed in the 24 hour decompression (mean 0.3167, $p = 0.0108$) and 3 week decompression (mean 0.3099, $p = 0.0182$) groups versus the 9 week compression group (mean 0.1850). A significant increase in posterior white matter area was found above (mean 0.4508, $p = 0.0042$) and below the site of compression at 3 weeks (mean 0.5800, $p < 0.0001$).

APP axonal immunopositivity was present in frequent numbers following decompression. APP immunopositive axonal swellings occurred greatest in number at the site of compression in injury groups, predominantly in the posterior white matter, but were also seen distant from the site of injury. Decreased myelin staining was demonstrated above the site at 20 weeks duration of compression. A loss of Olig2 immunopositive oligodendrocytes was seen at 9 and 20 weeks in the posterior white matter at the site of compression, suggesting cell death in a subset of oligodendroglia. Reactive astrocytosis was indicated by the pattern of GFAP staining in persisting compression and decompression groups and reactive changes were minimal at these time-points. A qualitative increase in Iba1 staining demonstrated a significant presence of resident and likely activated microglia, most profound at 1 week compression. Reactive perivascular microglia were present at 24 hours, 3, 9 and 20 weeks. Comparable patterns were seen in the decompression groups.

In human chronic compressive myelopathy due to spondylosis, malignancy or syringomyelia, TUNEL, DNA-PKcs, PARP and the caspase-independent marker, AIF, were immunopositive in glia, greatest at the site of compression or, in cases of severe necrosis, at the margins of injury. Furthermore, the presence of DNA damage was suggested by TUNEL, DNA-PKcs and PARP immunopositivity. PARP immunopositivity was found in a subset of glia with the morphology of oligodendrocytes. Neuronal immunopositivity was also seen using TUNEL, a key marker of DNA fragments consistent with apoptosis.

In human compressive myelopathy, APP immunopositive axonal swellings were present at, above and below the site of compression. APP immunopositivity in axonal swellings appeared maximal at the site of compression in all areas of the white matter suggesting widespread axonal changes. A subset of enlarged axons was immunopositive for caspase-3 antibody. One marker of amyloid-beta, Amy-33, showed immunopositivity within neuronal nuclei suggesting potential proteolysis of APP into the neurotoxic peptide, amyloid-beta, however this finding was contrasted by the negative staining of University of Melbourne and DAKO amyloid-beta antibodies.

The detailed results of our experimental studies will be described first, followed by those from human tissue using similar methods of analysis. Results are presented in table format for comparison across several groups and as an overview of staining.

3.1 Experimental Chronic Spinal Cord Compression

3.1.1 Histopathology

Table 8. Haematoxylin and eosin findings in a rodent model of chronic compressive myelopathy.

	H&E
24 HR	Macroscopic deformity, axonal swellings, haemorrhage, AHC loss
1 WK	Macroscopic deformity, mild tissue necrosis, lymphocytes, axonal swellings
3 WK	Macroscopic deformity, reduced posterior WM, axonal swellings
9 WK	Macroscopic deformity, reduced posterior WM, axonal swellings, AHC loss, macrophages
20 WK	Macroscopic deformity, axonal swellings
DEC24	No deformity, syrinx, gliosis, axonal swellings, tissue necrosis, central chromatolysis
DEC3	Macroscopic deformity 3/7 cases, cystic change, meningeal thickening, axonal swellings

Dec24 = 24 hour decompression group
Dec3 = 3 week decompression group

Haematoxylin and eosin

Histopathological changes involving the grey matter and white matter are shown in **Figure 3.1** and **Figure 3.2**.

24 hours

Macroscopic deformity was present in all cases, with compression greatest in the posterior white matter. Axonal swellings were found in the majority of cases (4/6 animals in the histology group) in the posterior, anterior and lateral white matter. Mild haemorrhage of the central grey matter extended to the posterior white matter in 4/6 cases and was associated with an acute inflammatory infiltrate of neutrophils. In one case, central chromatolysis of the anterior horn cells (AHC) and anterior horn cell loss was noted.

1 week

Macroscopic deformity was present in all cases. There was mild tissue necrosis and infiltration of lymphocytes within the posterior column in two cases. Axonal swellings were seen in 5 of the 6 cases throughout the white matter, maximal in the posterior column.

3 weeks

There was macroscopically visible compression, distortion and reduction of the posterior white matter which was asymmetrical in 2 cases. In 4/6, axonal swellings extended to the anterior and lateral white matter.

9 weeks

There was macroscopic deformity after 9 weeks of continuous compression by the polymer. There was an associated reduction in area of the posterior white matter and paucity of glial cells. Axonal swellings were present in the posterior white matter, often in the opposing anterior white matter and occasionally in the lateral white matter. Reactive astrocytes were noted within the grey matter. Loss of anterior horn cells and neuronal dark cell changes were a common feature. Central chromatolysis of neurons was noted at the site of compression. Macrophages were present in the damaged white matter. At one segment below the site of compression there was anterior horn cell loss, red cells, vacuolation, paucity of glia, axonal swellings unilaterally and reactive astrocytes. Vacuolation, anterior horn cell loss and paucity of glia were features at 2 segments above the compression. AHC loss, reactive astrocytosis and central chromatolysis of neurons was found 2 segments below the site.

20 weeks

There was macroscopic deformity secondary to polymer compression in cases at 20 weeks survival. There was a decrease in the area of posterior white matter with paucity of glial cells. Vacuolation of the white matter was present in association with occasional (3-10) axonal swellings in the anterior, posterior and lateral white matter.

Decompression at 24 hours, survival to 9 weeks

The perimeter of the spinal cord was normal and there was no evidence of deformity. Histopathological changes were variable in severity. A communicating central syrinx was seen in one case, associated with lymphocytes and macrophages. A cicatrix (meningeal scarring and invasion of the white matter) was found in 2 cases. There was astrocytic gliosis of the grey matter. There were axonal swellings within the posterior white matter in 5 of the 7 cases, These were most numerous in the deep posterior and cuneate fasciculus and were also seen in the lateral white matter in 5 cases, and in the anterior white matter in 3 cases. Axonal swellings were present in cases one segment above and one segment below the site of compression. Central chromatolysis was also found at one segment above. Macroscopic deformity was present in 3 cases by 9 weeks after decompression at 24 hours. Central chromatolysis of neurons and red cell change occurred in one case in which there was also macroscopic deformity left from the polymer.

Decompression at 3 weeks, survival to 9 weeks

Macroscopic deformity of the posterior cord from the polymer was identifiable in 3 of the 7 cases though a restoration of the basic tissue architecture was apparent and this was verified using area measurements. Histopathological changes were variable in severity following decompression. Severe cystic cavitation or vacuolation of the posterior white matter was present (4/7 histology cases), greatest in the deep posterior columns. A central syrinx was noted in one case. There was meningeal thickening suggestive of inflammation. Axonal swellings of the posterior white matter were also seen with associated vacuolation.

GFAP, Iba1 and Olig2

Reactive astrocytes expressed the intermediate filament glial fibrillary acidic protein (GFAP) as early as 24 hours and up to 20 weeks following polymer insertion. Fibrous astrocytes in close proximity to capillary vessels were distributed in the white matter. A qualitative increase in microglial activation was found using Iba1, greatest at 1 week after injury. A qualitative loss of oligodendrocytes was seen using Olig2 at 9 and 20 weeks. There was pallor of the Weil stain above the site of compression at 20 weeks, consistent with loss of myelin.

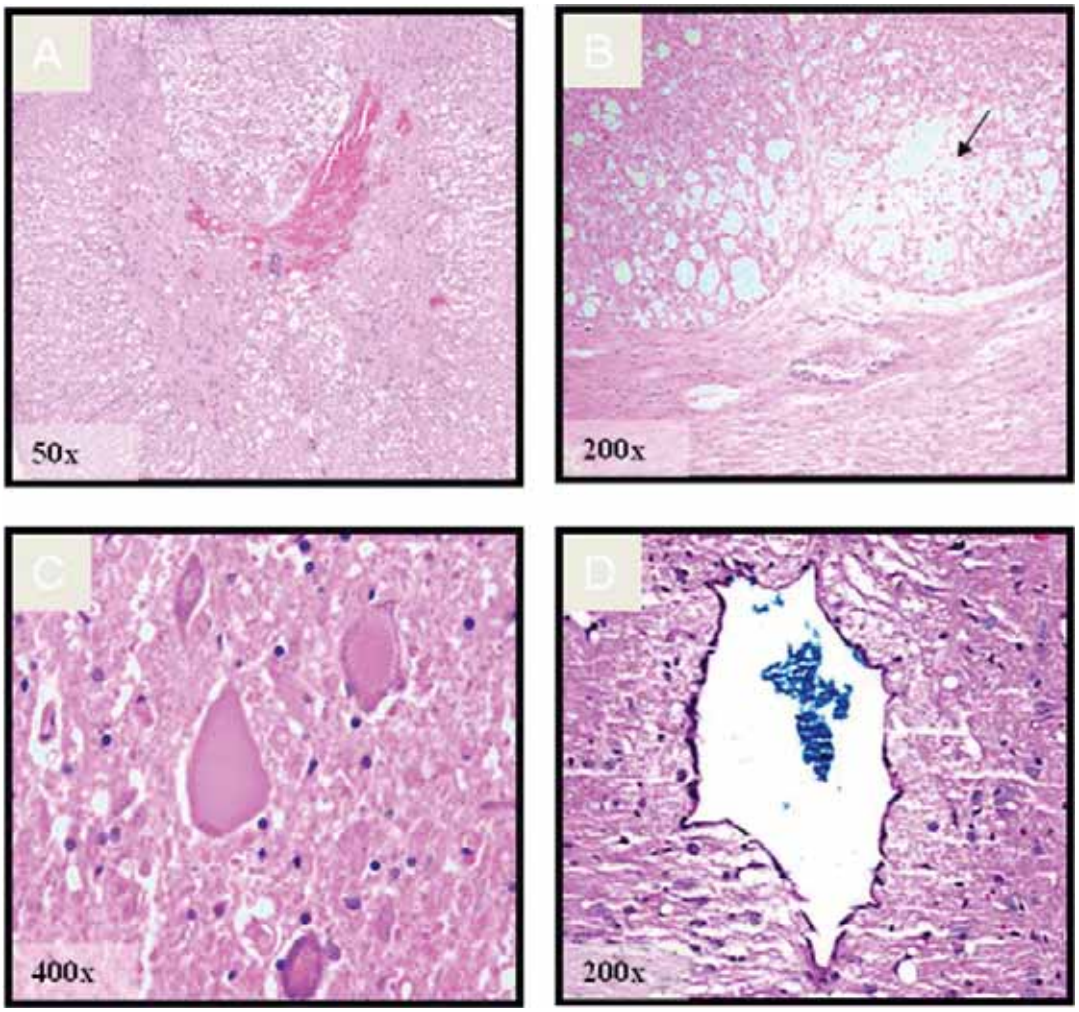

Figure 3.1 Histopathological changes on haemotoxylin and eosin staining in rodent chronic compressive myelopathy.

Photomicrograph (A) shows haemorrhagic necrosis affecting the central grey matter. In (B) there is vacuolation of the deep posterior white matter and early cystic necrosis unilaterally (arrow). Central chromatolysis of neurons suggesting chronic axonal degeneration is shown in (C). A dilatation of the central canal (hydromyelia) is shown at 9 week sacrifice in a Sprague-Dawley rat that underwent surgical decompressive laminectomy at 24 hours duration of compression (D).

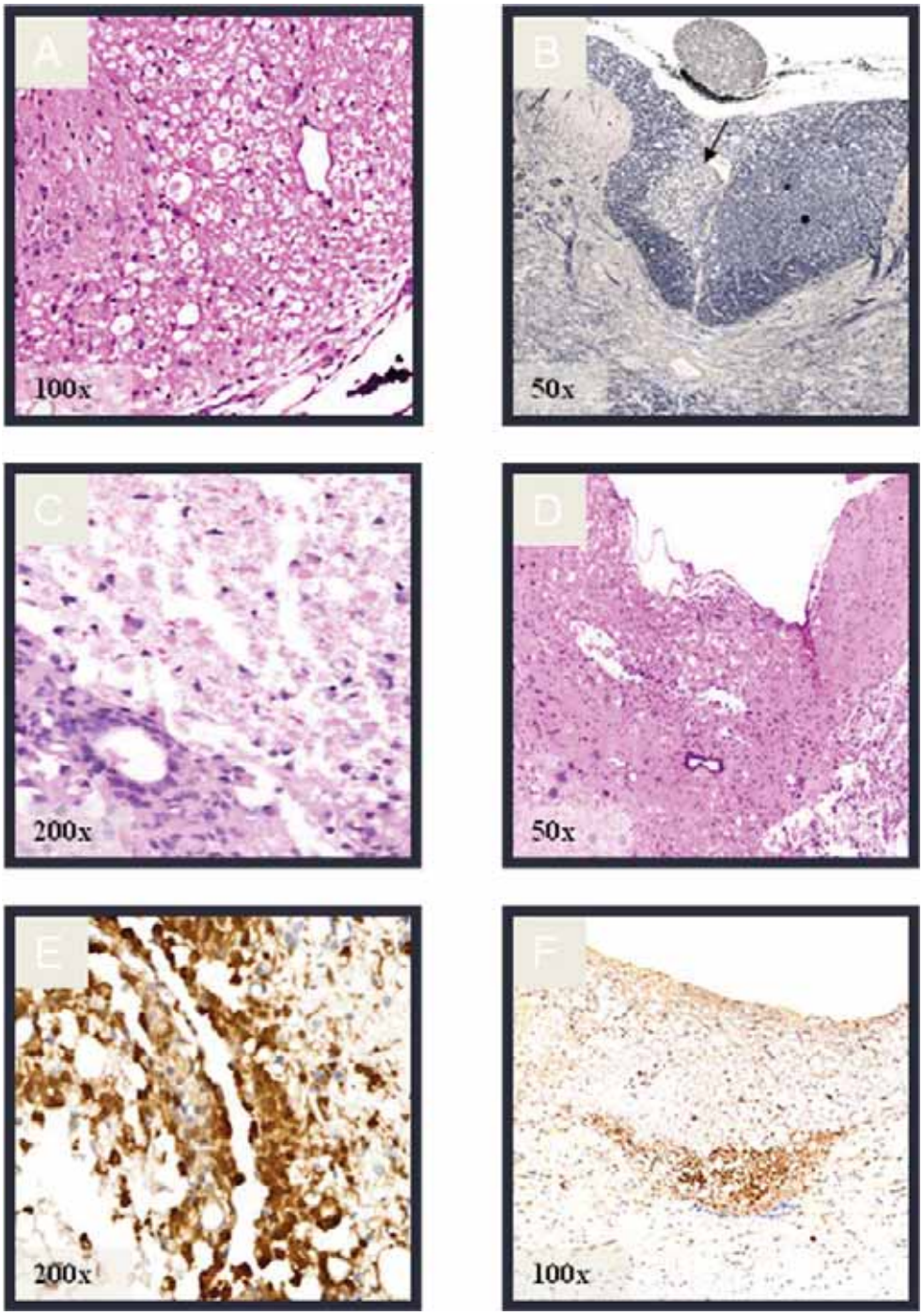

Figure 3.2 White matter (WM) changes in a rodent model of chronic compressive myelopathy.

Axonal swellings are evident in the lateral WM in photomicrograph A (H&E). A loss of myelin was suggested using Weil stain in a case of 20 weeks continuous compression in the posterior WM (B). Mild tissue necrosis was seen in the deep posterior WM (C) (H&E). A loss of posterior WM in (D) (H&E) in addition to mechanical distortion achieved by the polymer. Iba1 immunoreactive microglia suggest possible reactivity at the site of compression by 1 week (E) (Iba1). Focal regions of axonal APP immunopositivity within the deep posterior WM (F) (APP).

3.1.2 Apoptosis

Cells of morphology consistent with glia (oligodendrocytes, astrocytes and microglia) and neurons were rarely immunopositive using TUNEL. Glial immunostaining for caspase-3, caspase-9 and PARP was seen at, above and below the site of compression at 3, 9, and 20 weeks. Caspase-9 and active caspase-3 staining was rare at the site of compression in 24 hour and 1 week continuous compression groups. Apoptotic staining was present after early and late decompression and a quantitative increase in caspase-3 expression was demonstrated. In the decompression groups, histopathological changes were variable, and in some cases, there were more severe changes than in the 9 week continuous compression group. Increased active C3 immunopositive glia were seen in decompression groups. Neuronal staining for active C3, C9 and PARP was present at 9 and 20 week sacrifice. Neuronal and glial reactivity for AIF was widespread in each injury group. Immunostaining for C9 and PARP was similar in compression and decompression groups. Active caspase-3 was greater expressed in the 24 hour decompression (mean 0.3167, $p = 0.0108$) and 3 week decompression (mean 0.3099, $p = 0.0182$) groups versus the 9 week persisting compression group (mean 0.1850). Immunoreactivity for each immunomarker is shown below. The typical immunostaining for our panel of apoptotic markers is shown in **Figure 3.3** and **Figure 3.4.**

Table 9. Immunopositivity in a rodent model of chronic compressive myelopathy.

ANTIGEN	24 HR	1 WK	3 WK	9 WK	20 WK	DEC24	DEC3
APP	+ A	+ A	+ A	+ A	+ A	+ A	-
aC3	+ G	+ G	+ G	+ G/N	+ G/N	+ G	+ G
PARP	+ G/N	+ G/N	+ G/N	+ G/N	+ G/N	+ G/N	+ G/N
TUNEL	-	+ G	-	-	-	+ G	+ G
Caspase-9	-	-	+ G	+ G	+ G	+ G	+ G/N
AIF	+ A/G/N	+ G	+ G/N	+ G/N	+ G/N	+ G/N	+ G/N

+ Immunopositivity **A = Axonal** **G = Glial** **N = Neuronal**

- Negative **Dec24 = 24 hour decompression group**

Dec3 = 3 week decompression group

TUNEL

TIME	24 hour	1 week	3 weeks	9 weeks	20 weeks	Dec24hr	Dec3wk
TUNEL	-	+ G	-	-	-	+ G	+ G

+ Immunopositivity **A = Axonal** **G = Glial** **N = Neuronal**

- Negative **Dec24 = 24 hour decompression group**

Dec3 = 3 week decompression group

Compression

Glial TUNEL immunopositivity was present in the anterior, posterior and lateral white matter at 1 week compression.

Decompression

Glial TUNEL immunopositivity was present predominantly in the lateral but also in the anterior and posterior WM in the 3 week decompression group. In the 24 hour decompression group, rare glial TUNEL immunopositivity was found at the site of compression in the anterolateral white matter of one case, and the lateral white matter of another. In one case, immunopositive macrophages were present.

Active Caspase-3 (aC3)

TIME	24 hour	1 week	3 weeks	9 weeks	20 weeks	Dec24hr	Dec3wk
aC3	+ G	+ G	+ G	+ G/N	+ G/N	+ G	+ G

+ Immunopositivity **A = Axonal** **G = Glial** **N = Neuronal**

- Negative **Dec24 = 24 hour decompression group**

Dec3 = 3 week decompression group

Compression

At 24 hours, rare active C3 glial staining was found above and below the site of compression. Glial staining for active caspase-3 was rare at 1 week compression. Immunopositive glial cells for active caspase-3 were rare at 3 weeks at the site of compression. Greater numbers of immunopositive glia were present in the anterolateral white matter above and below the site of compression. Staining was rarely seen at 2 segments below the level of compression. At 9 weeks, glial immunostaining was found at, two levels above and one level below the site of compression. Neuronal immunopositivity for active caspase-3 was seen at the site of compression and two segments above. Glial staining at 20 weeks was widespread throughout the white matter. Neuronal staining was seen one level above the site of compression.

Decompression

Rare or occasional immunopositive glia were seen at the site of compression in the 24 hour decompression group. Glial immunostaining was present in all regions of the white matter above and below the site of compression and was qualitatively greater in this decompression group than at 9 weeks continuous compression. Rare or occasional immunopositivity in glia was seen in the 3 week decompression group. Glial immunostaining was present in all regions of the white matter above and below the site of compression.

Caspase-9 (C9)

TIME	24 hour	1 week	3 weeks	9 weeks	20 weeks	Dec24hr	Dec3wk
C9	-	-	+ G	+ G	+ G	+ G	+ G/N

+ Immunopositivity **A = Axonal G = Glial N = Neuronal**

- Negative **Dec24 = 24 hour decompression group**

Dec3 = 3 week decompression group

Compression

Glial cytoplasmic immunostaining at 24 hours was found in all regions of the white matter up to two segments above and below the site of compression. At 3 weeks, glial cytoplasmic staining was present in all regions of the white matter at the site of compression and up to two segments above and below. No neuronal staining was seen. At 9 weeks, glial immunopositivity was present at the site of compression and up to two segments above and below. Caspase-9 glial immunostaining was present in all regions of the white matter at, above and below the site of compression at 20 weeks. Some cases showed rare or negative staining in glia, in particular two levels below the site of compression.

Decompression

In the 24 hour decompression group, glial staining was seen in all regions of the white matter at and up to two segments above and below the site of compression. In the 3 week decompression group, glial staining for caspase-9 was consistently seen at and up to two segments above and below the site of compression. Neuronal staining was seen in the 3 week decompression group up to two segments above and below the site of compression.

Poly (ADP-ribose) Polymerase (PARP)

TIME	24 hour	1 week	3 weeks	9 weeks	20 weeks	Dec24hr	Dec3wk
PARP	+ G/N	+ G/N	+ G/N	+ G/N	+ G/N	+ G/N	+ G/N

+ Immunopositivity **A = Axonal G = Glial N = Neuronal**

- Negative **Dec24 = 24 hour decompression group**

Dec3 = 3 week decompression group

Compression

Consistent and widespread glial immunostaining and neuronal staining was seen in all segments in the 24 hour group. Consistent glial immunopositivity in all regions of the white matter was found at 1 week continuous compression. Neuronal staining was present up to two segments above and below the site of compression. At 3 weeks, frequent glial staining was seen in the majority of cases in a homogeneous pattern. Neuronal staining was present at, above and below the site of compression. At 9 weeks, homogeneous occasional glial staining was seen at, above and below the site of compression. Qualitatively fewer immunopositive glia were seen than at 20 weeks. Neuronal staining was present at the site. At 20 weeks, PARP glial immunopositivity was present in all regions of the white matter at, above and below the site of compression. Staining was homogeneous in white matter and oligodendrocytes were identified. Neuronal nuclear staining was identified in all cases at the site of compression and up to two segments above and below.

Decompression

In the 24 hour decompression group, glial immunopositivity was occasionally present in the anterior, posterior and lateral white matter in all segments. The spatial pattern of glial staining was qualitatively greater in this decompression group than at 9 weeks continuous compression. Neuronal staining was seen in approximately half of cases and was present at, above and below the site of compression. In the 3 week decompression group, consistent glial and neuronal staining was present in all regions at, above and below the site of compression. The spatial pattern of glial staining for PARP was qualitatively greater in this decompression group than at 9 weeks continuous compression.

Apoptosis Inducing Factor (AIF)

TIME	24 hour	1 week	3 weeks	9 weeks	20 weeks	Dec24hr	Dec3wk
AIF	+ A/G/N	+ G	+ G/N	+ G/N	+ G/N	+ G/N	+ G/N

+ Immunopositivity **A = Axonal G = Glial N = Neuronal**

- Negative **Dec24 = 24 hour decompression group**

Dec3 = 3 week decompression group

Compression

Widespread glial immunopositivity was found in cases of persisting compression. Neuronal staining for AIF was found at, above and below the site of compression. Immunopositivity in axons was seen in all regions of the WM in the 24 hour compression group.

Decompression

Neuronal and occasional glial staining was present in the decompression groups. There was no staining within axonal swellings.

Control Cases

In the sham, decompression sham, vehicle and naïve controls, staining for AIF, caspase-3, caspase-9 and TUNEL was either absent or rarely present in glia only. Using the PARP antibody, staining was absent in the naïve cases but occasional glial and neuronal staining was seen in the sham, decompression sham and vehicle groups.

ELISA

Active caspase-3 expression
9 weeks compression vs decompression groups

The ELISA results were compared between the four groups (24hrs decompression group, 3 week decompression group, 9 week compression group, control) using a one way ANOVA model. There was a statistically significant difference in ELISA values across the three groups ($p = 0.0159$). Active caspase-3 was greater expressed in the 24 hour decompression (mean 0.3167, $p = 0.0108$) and 3 week decompression (mean 0.3099, $p = 0.0182$) groups versus 9 weeks persisting compression (mean 0.1850). A significant increase in active caspase-3 assay was found in the 24 hour and 3 week decompression groups compared to controls ($p = 0.0181$ and 0.0321 respectively) but there was no difference between 9 week persisting compression and control groups.

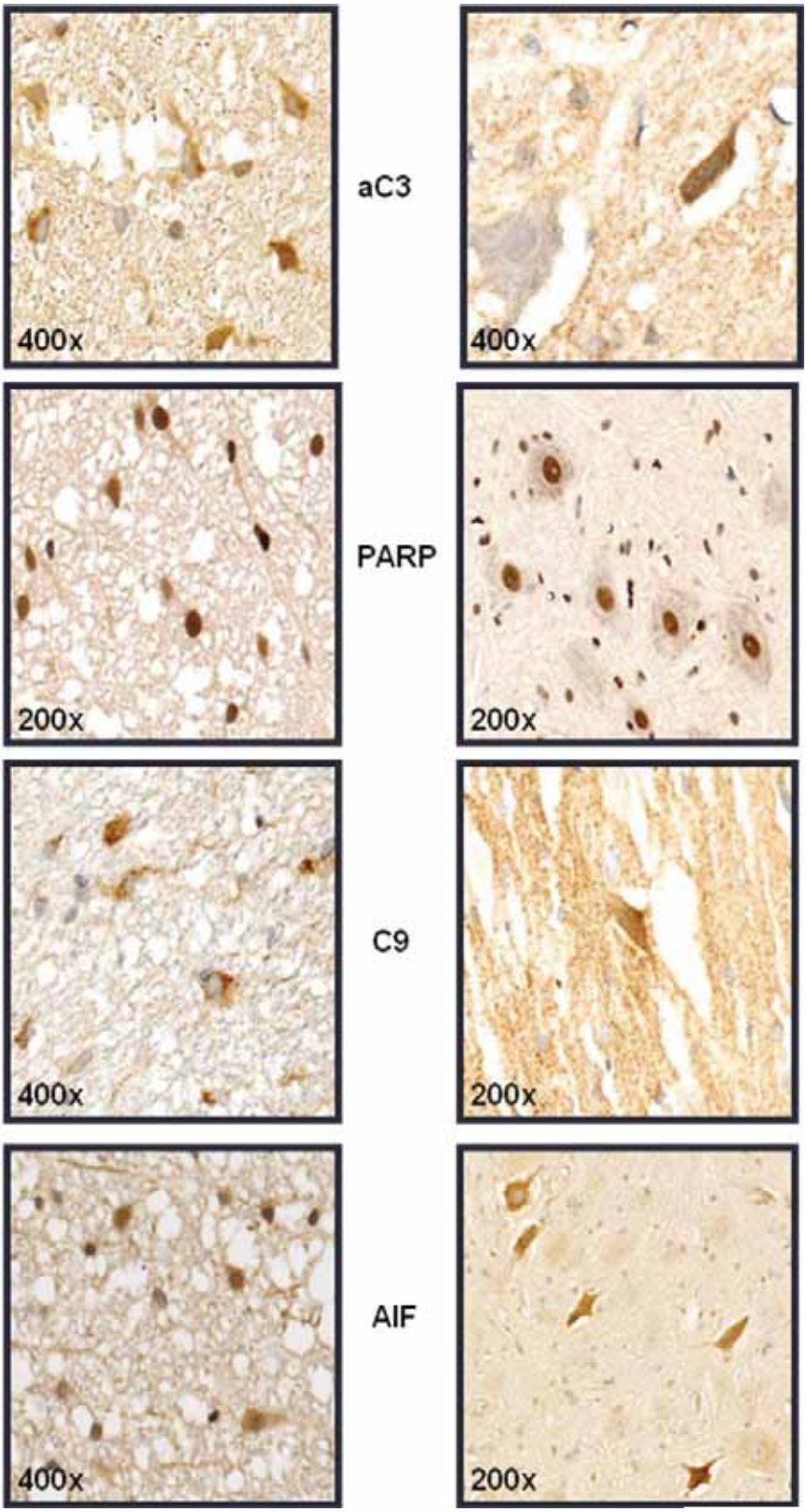

Figure 3.3 Immunohistochemical staining for apoptosis in chronic compressive myelopathy.

Examples are shown of typical staining seen for a panel of markers for apoptosis (listed centrally) in glia (left images) and neurons (right images).

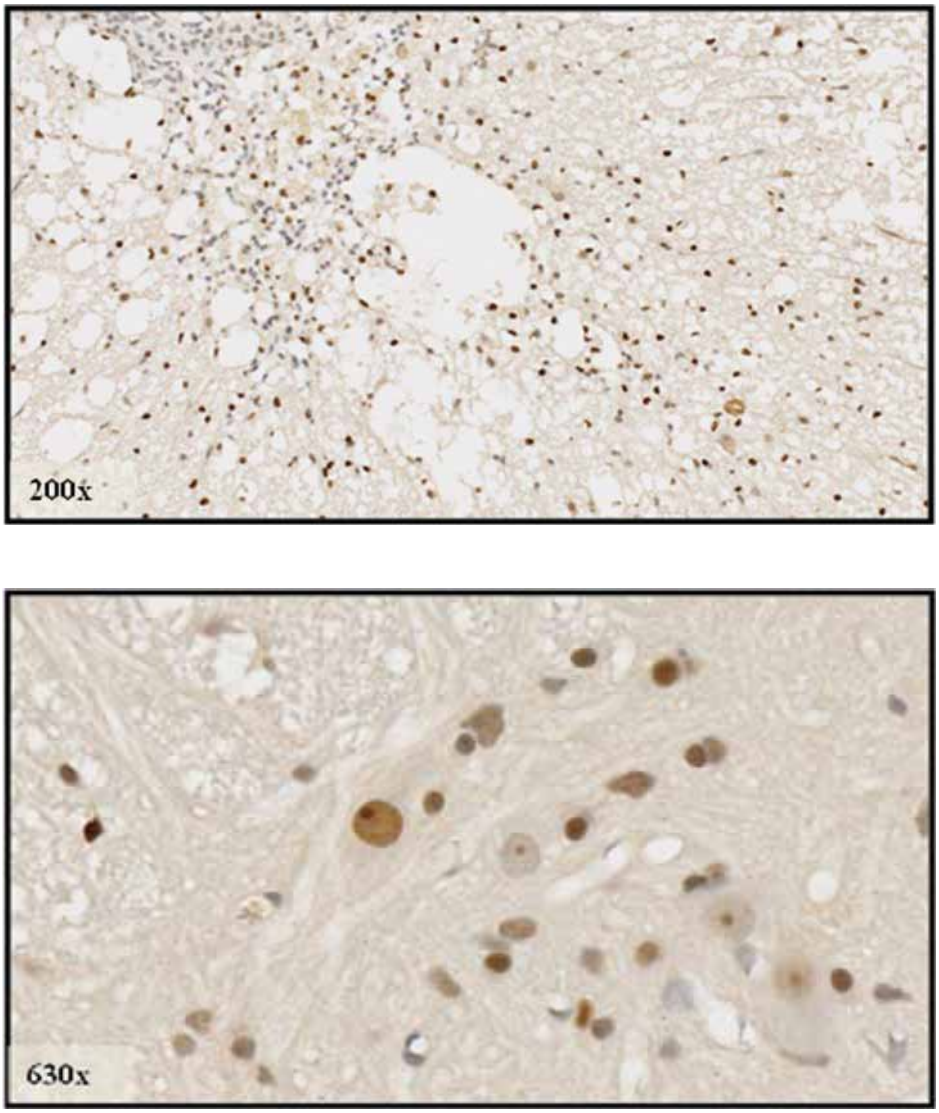

Figure 3.4 PARP immunohistochemical staining following early decompression in a rodent model of chronic compressive myelopathy.

Example of PARP immunopositive glia within the penumbral white matter surrounding a region of necrosis in a case of decompression at 24 hours and survival to 9 weeks (top). The second (bottom) photomicrograph shows a PARP immunopositive neuronal nucleus in a case of continuous chronic compression with survival to 20 weeks.

3.1.3 Axonal Injury (APP)

Amyloid Precursor Protein

TIME	24 hour	1 week	3 weeks	9 weeks	20 weeks	Dec24hr	Dec3wk
APP	+ Ant/Post/Lat	+ Ant/Post	+ Post/Lat	+ Post	+ Lat	+ Ant/Post/Lat	-

+ **Immunopositivity**
- **Negative**

Ant = Anterior white matter
Post = Posterior white matter
Lat = Lateral white matter
Dec24 = 24 hour decompression group
Dec3 = 3 week decompression group

APP axonal immunopositivity was rare or occasionally present in compression groups but was frequently present in the 24 hour decompression group at, above and below the site of compression.

Weil / Myelin Basic Protein (MBP)

At 24 hours, pallor of the deep posterior white matter was seen in 2/6 cases in correlation with APP immunopositivity. There was a normal pattern of staining in other groups. At 1 week compression there was pallor of MBP staining in the deep posterior white matter and the cuneate fasciculus on one side. Three cases at 20 weeks compression (196A, 246D, 196C) showed pallor of the gracile fasciculi above the site of the lesion. There was no pallor involving the motor long tracts. There was pallor on MBP staining in the posterior column unilaterally in one case at 20 weeks, and in one case in the 24 hour decompression group.

3.2 Quantitative Studies – Cross-Sectional Area

The cross-sectional area of the spinal cord was reduced at all time points from 24 hours to 20 weeks in comparison with controls and decompression groups as measured digitally at, above and below the site of compression. In the 20 weeks compression group, the percentage ratio of the posterior column area (PCA) to the anterolateral area (ALA) of white matter was less than controls but did not reach significance (19.6 % at 20 weeks, 21.3% naïve, 20.4% sham). There was minimal change of this ratio at, above and below the site of compression. At 9 weeks, the area was increased above and below the site of compression. At 3 weeks, the greatest relative increase in posterior column area to anterolateral column area was found above and below the site of compression, with greatest loss of posterior white matter at site. In the 24 hour and 1 week compression groups, the white matter area was decreased above and below, compared to site of compression. In the 24 hour decompression group with survival to 9 weeks, the ratio of posterior to anterolateral white matter at the site of compression was comparable to controls, with a small increase at 1 level above and 1 level below, and small decrease in values 2 levels above and below the site. In the 3 week decompression group, the ratio at the site was again comparable to controls, however a significant decrease in the total cross-sectional area was found at the site of compression. In the sham group, a minimal increase in ratio occurred above and below the site of spinous processotomy with up to a 5.9 percentage change above. The naïve group showed an increase in area above and decreased area below T12. In the decompression sham group there was a percentage change of ratio up to -6.7 above and 4.8 below.

3.2.1 Area – Posterior white matter

Statistically, posterior white matter area results were compared between the 7 groups and the 3 levels using a linear mixed effects model. A random rat effect was included in the model to adjust for the dependence in repeated observations from the same rat.

Chronic Spinal Cord Compression

There was loss of the posterior white matter maximal at the site of compression. Necrosis was minimal. A significant interaction was found between groups ($p = 0.0001$) and levels

(p = 0.0001) adjusted for dependence (p = 0.002). A significant decrease in the posterior column area compared to the control was found at 1 week (p = 0.008), 3 weeks (p <0.0001), and 9 weeks (p = 0.0057) with area minimal at 3 weeks compression (**Figure 3.5**) however there was no significant difference compared with the control at 20 weeks.

A significant increase in area was found at 3 weeks continuous compression above (mean 0.451, p = 0.004) and below (mean 0.58, p <0.0001) the site. A significant increase in area was seen above the site at 9 weeks continuous compression (mean 0.618, p = 0.0.003) but not below. A significant increase in the mean posterior column area was present below the site of compression at 20 weeks (mean 0.673, p = 0.015).

Decompression

The total cross-sectional area decreased with time of chronic compression but resolved with decompression (3 week compression group mean 3.05mm^2; decompression at 3 weeks with survival to 9 weeks group mean 5.75 mm^2).

There was no significant difference in the posterior column area at the site for the 24 hour decompression group (p = 0.88) and the 3 week decompression group (p = 0.29) compared with the control group. A significant increase in the area (mm^2) of the posterior column was seen in the 24 hour decompression (mean 0.06, p = 0.01) and 3 week decompression (mean 0.08, p <0.0001) groups compared to the 9 week persisting compression group (mean 0.47). The posterior column area at the site of compression was significantly decreased in the 24 hour decompression group compared to later decompression at 3 weeks (p = 0.004).

At 20 weeks ongoing compression, there was a significant decrease in the area of the posterior column at the site compared to the 3 week decompression group (p = 0.002).

There was no significant difference in the posterior column area above or below the site of compression at 1 week (mean above 0.557, site 0.463, below 0.635), nor in the early 24 hour (mean above 0.617, site 0.623, below 0.685) or late 3 week (mean above 0.712, site 0.756, below 0.708) decompression groups.

Table (a)

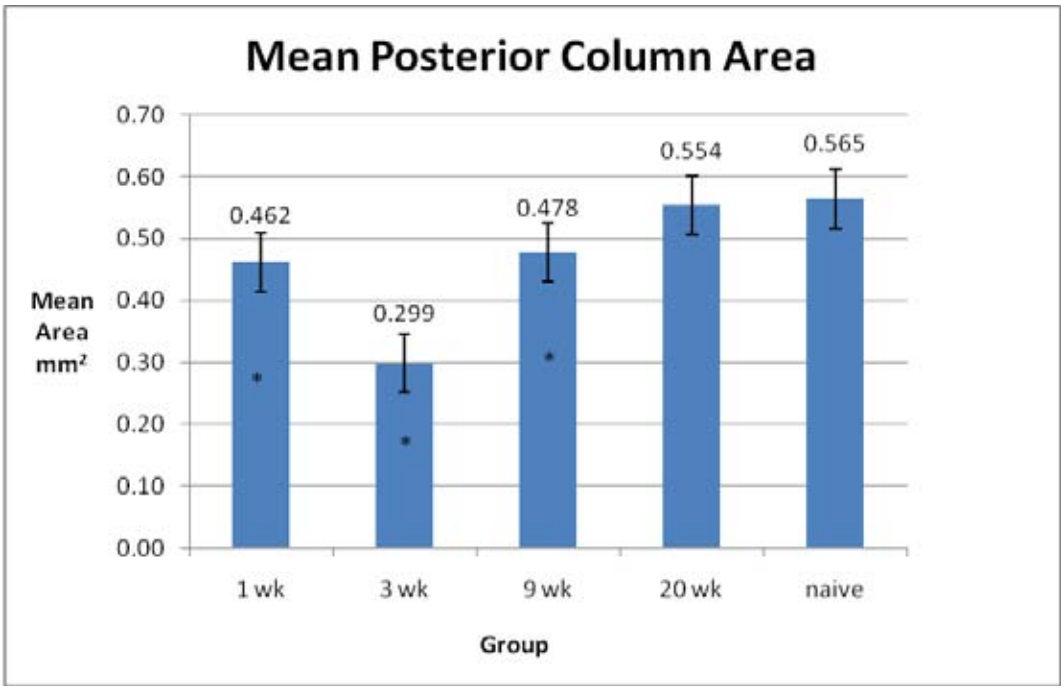

Table (b)

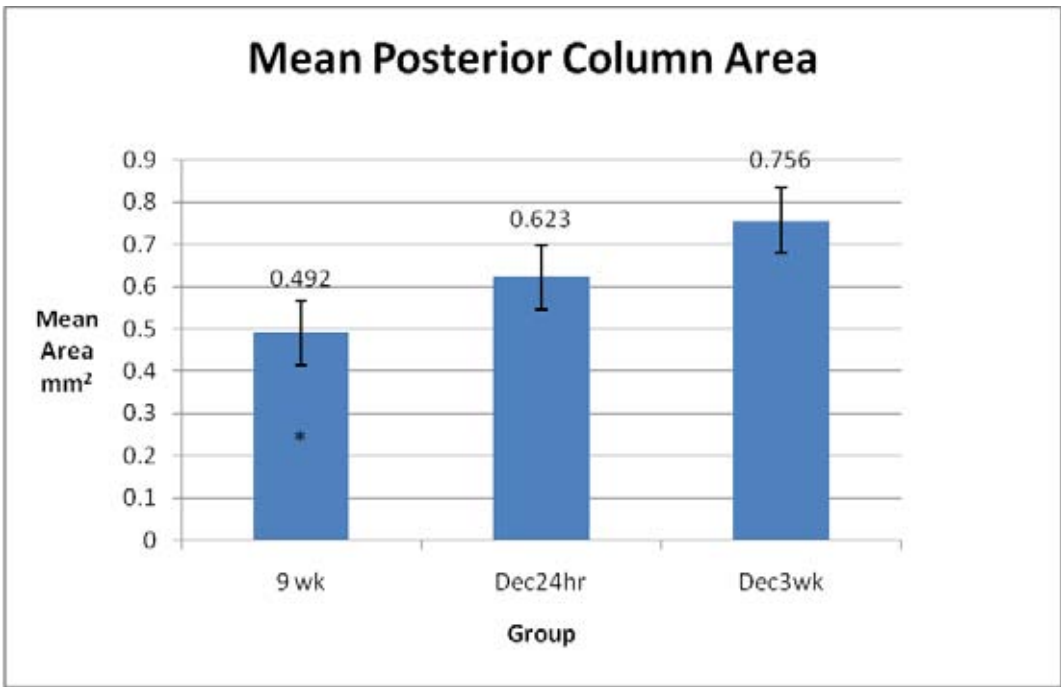

Table 10.

Mean posterior column area (a) for injury groups at 1, 3, 9 and 20 weeks compression and (b) in 9 week compression, 24 hour decompression and 3 week decompression groups.

Significant loss of posterior column area is noted after 3 weeks compression.

3.2.2 Area – Total cross-section of spinal cord (mm^2)

Total area results were compared between the 7 groups and the 3 levels using a linear mixed effects model. A random rat effect was included in the model to adjust for the dependence in repeated observations from the same rat.

Chronic Spinal Cord Compression

There was a significant interaction between groups and levels ($p = 0.001$). A significant decrease in the total spinal cord cross-sectional area was found at the site of compression compared with the control group at 24 hours, 1 week, 3 and 9 weeks ($p = 0.003$, 0.0008, <0.0001 and 0.01 respectively), with total cross-sectional area minimal at 3 weeks compression (mean 3.21). There was no significant difference at 20 weeks compared with the control group. There was no significant difference in the area between the control and 24 hour decompression groups however a significant increase in cross-sectional area was present in the 3 week decompression group (mean 6.48) versus control (mean 5.42, $p = 0.019$).

Cross-sectional area above the site was significantly increased at 1 week ($p = 0.042$) only, and was increased below the site at 1 week ($p <0.0001$), 3 weeks ($p <0.0001$), 9 weeks ($p <0.0001$) and 20 weeks ($p <0.0001$) compared with the control group.

There was no significant change in the ratio of the posterior to anterolateral, or posterior to total spinal cord cross-sectional area between groups. Independently of group, posterior to total cross-sectional area ratios were higher in the level above, compared to the site and levels below ($p <0.0001$). Posterior to total cross-sectional area ratios were higher at the site of compression than the level below (11.17 vs. 10.44, $p = 0.003$).

Decompression

A significant increase in the total cross-sectional area at the site of compression was seen in the 24 hour and 3 week decompression groups versus the 9 week persisting compression group ($p = 0.03$ and <0.0001 respectively). Area above was significantly increased in the 24 hour decompression group ($p = 0.0001$) compared with the site of compression.

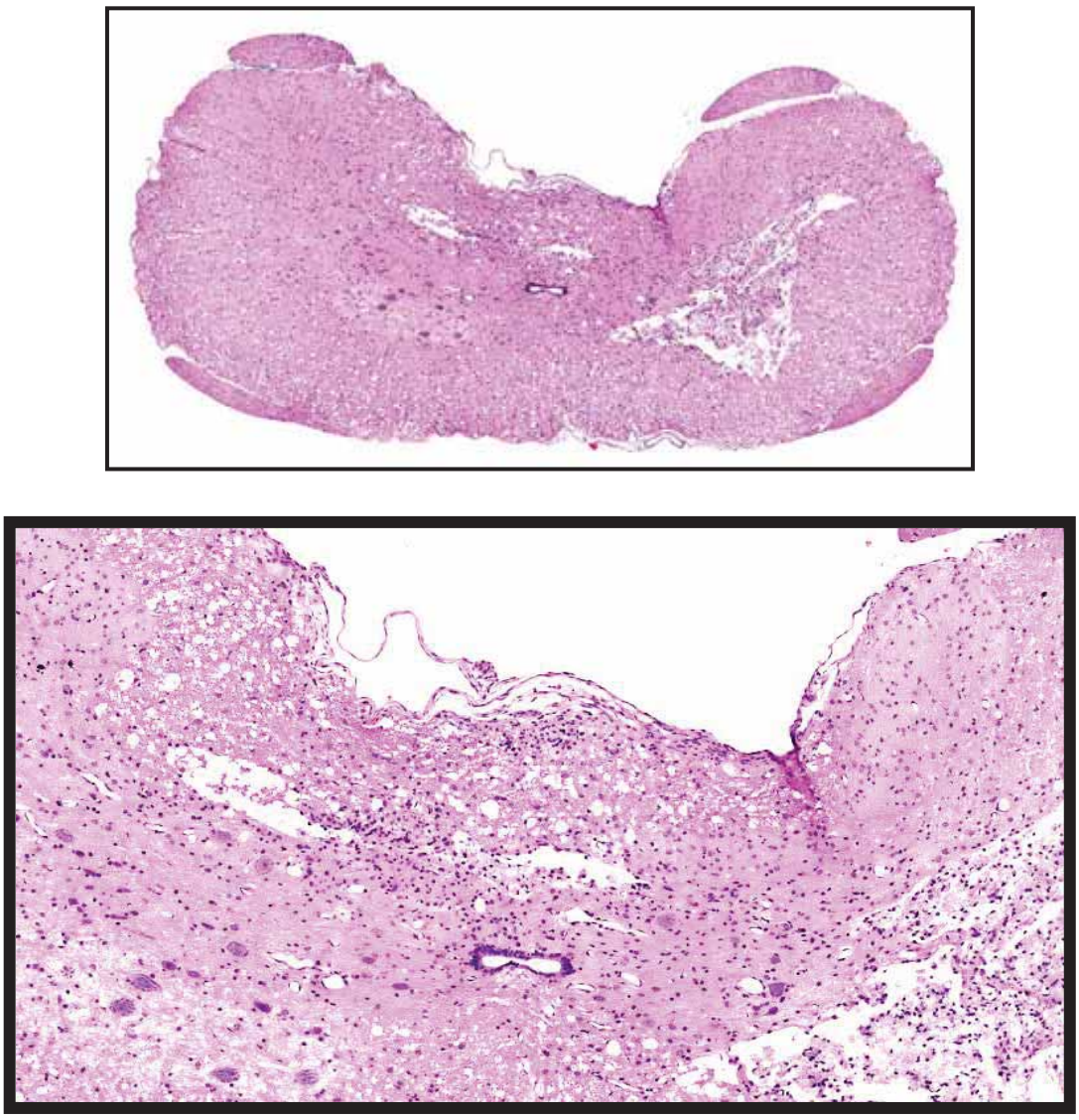

Figure 3.5 Histopathological changes in Experimental Chronic Compressive Myelopathy.

Aquaprene expandable polymer was inserted at T12 level (top) causing indentation of the underlying spinal cord (H&E). In a magnified image of the same case (bottom), loss of the posterior white matter area is demonstrated. Ongoing compression resulted in a decreased posterior white matter area, greatest at 3 weeks (H&E).

3.3 Functional Assessment

3.3.1 BBB Score

In the 24 hour decompression group, peak mean BBB score occurred at 7 weeks (20.3) and was within the normal range (above 20) from the 6 week time point until sacrifice. A decrease below normal was seen in the 9 week compression group, with a peak mean score of 20.77 4 weeks after onset of compression, decreasing to 19.15 at 9 weeks survival. In comparison, the decompression surgery at 3 weeks with survival to 9 weeks group had a peak mean BBB score of 19.92 at the 8 week time point. A decrease in locomotor function, as assessed by the modified Basso, Bresnahan, Beattie Score (Basso et al., 1995), was found in the 20 week chronic compression group. Mean BBB score remained at less than 20, an abnormal reading, at all time points in this group. The peak mean BBB score occurred 2 weeks after polymer insertion (at 19.93 and median 20±1) following recovery from initial surgery and decreased to 18.57 at 20 weeks, median 19±1. Vehicle, naïve, sham surgery and sham decompression surgery groups consistently were recorded as normal BBB scores of 21.

There was a gradual but mild decline in BBB score over 20 weeks. Statistically, the BBB results were compared between the seven groups using a Kruskal-Wallis test. There was significant evidence for a difference in the distribution of BBB results across the groups ($p < 0.0001$). Post-hoc Wilcoxon tests were used to compare the groups two at a time.

A significant decrease in BBB score between treatment and control groups was seen at 1, 3, 9 and 20 weeks ($p < 0.0001$ all). Scores were lower at 9 weeks (median 19) than in the 24 hour (median 21) and 3 week (median 20) decompression groups but this did not reach significance within the cohort ($p = 0.06$ and 0.1 respectively). BBB scores were significantly lower in the 20 week group versus decompression groups ($p = 0.02$ 24 hr decompression, $p = 0.02$ 3 week decompression).

Table 11 (a). Mean and Median BBB scores at sacrifice in Sprague-Dawley rats following spinous processotomy at T12 and insertion of an aquaprene polymer.

Survival	Median BBB score	Mean BBB score
24 hours	13	13.91
1 week	19	18.58
3 weeks	20	19.33
9 weeks	19	19.15
20 weeks	19	18.57
Sham	21	21
Vehicle	21	21
Naïve	21	21

Table 11 (b). Median and Mean BBB scores at sacrifice in Sprague-Dawley rats following decompression laminoplasty for removal of expandable polymer at 24 hours and 3 weeks post insertion.

Decompression Laminoplasty	Median BBB score	Mean BBB score
24 hour decompression	21	20
3 week decompression	20	19.77
Decompression sham	21	21

Table (a)

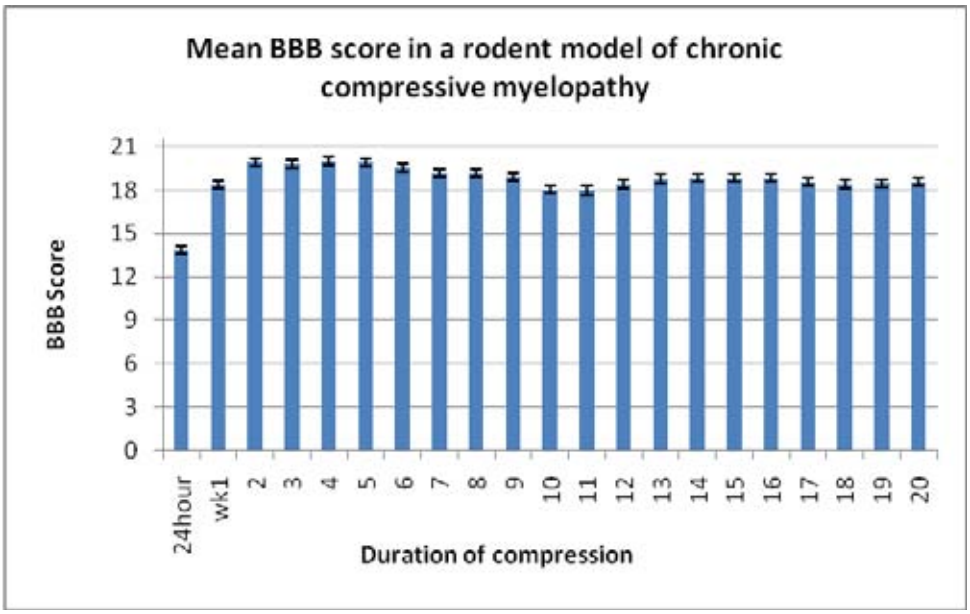

Table (b)

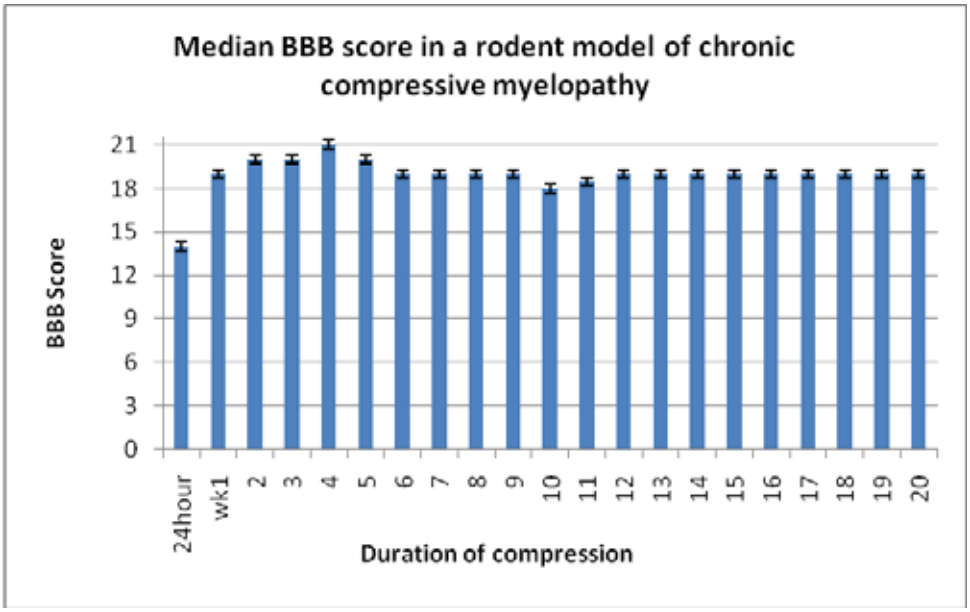

Table 12. (a) Mean and (b) Median BBB score in rat chronic compressive myelopathy up to 20 weeks duration.

A small and consistent reduction in BBB score is evident across weeks 5 to 20, suggesting a mild impairment in motor function with chronic compression. At no time point is the mean naïve BBB score of 21 obtained in the compression groups.

Table (a)

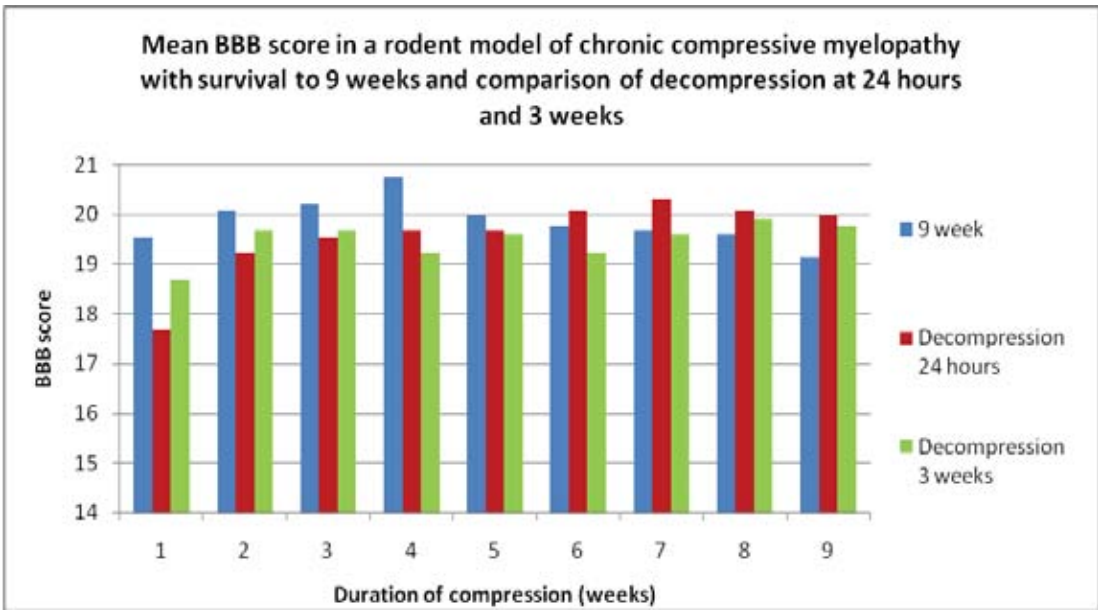

Table (b)

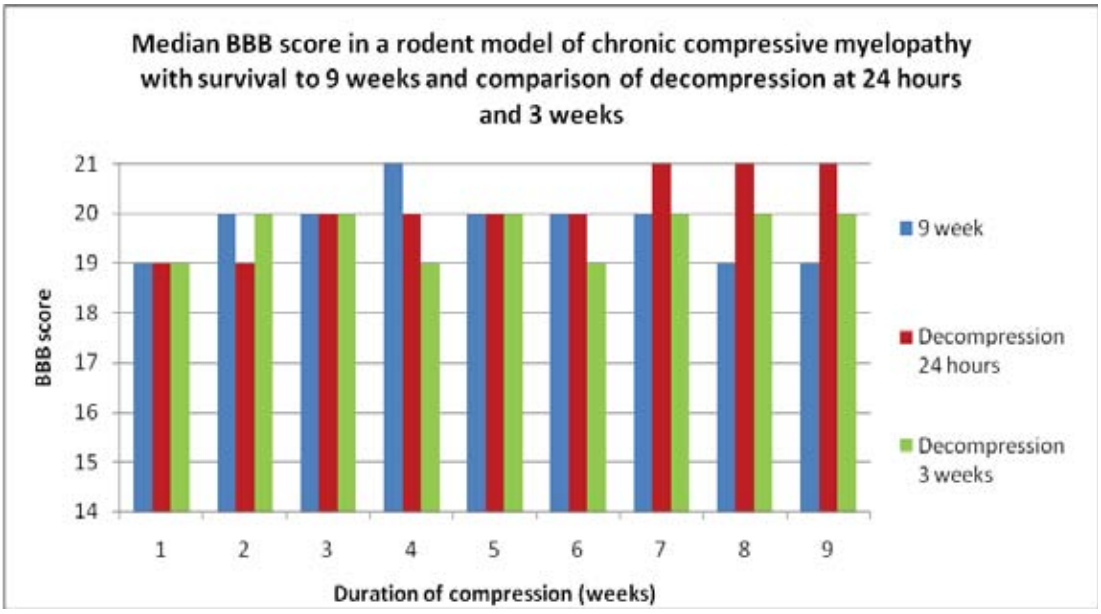

Table 13. (a) Mean and (b) Median BBB scores in the 9 week continuous compression group versus 24 hour and 3 week decompression groups.

At 8 and 9 week time points, the median BBB score reached the normal level of 21 and 20 for the 24 hour and 3 week decompression groups respectively; in contrast to the median BBB of 19 at 9 weeks of chronic compression**.**

3.3.2 Rotarod

The rotarod score was used in the assessment of motor function and coordination. Rats were trained to achieve a standard score of 120 seconds prior to surgery. The rotarod results were compared over time using a Cox proportional hazards model. A robust sandwich estimate of the variance was employed so as to account for the dependence in rotarod measurement from the same rat. A value of 120 seconds was considered to be right censored. There was no evidence for a difference in rotarod times across the 20 weeks of measurement ($p = 0.45$).

There was significant evidence for a difference in the rotarod times across the seven groups ($p < 0.0001$). A gradual increase in mean rotarod score occurred in the 9 week compression group up to 6 weeks (113.29). The highest mean rotarod score of 114.92 occurred at 5 weeks in the 3 week decompression group and 9 weeks (106.61) in the 24 hour decompression group. Measurements in the 3 week and 1 week groups were consistent with recovery after surgery. The mean weekly rotarod score in the 20 week survival group was variable week to week. After initial recovery from surgery, the peak mean score was at 17 weeks (107.14) but a second peak occurred at 5 weeks (100.57 seconds). The lowest mean rotarod score after recovery in the 20 week group was at 10 weeks (78.86 seconds). Vehicle, naïve, sham and decompression sham groups were consistently recorded at 120 seconds.

There was no evidence for an interaction between group and time in the 9 week persisting compression, 24 hour decompression and 3 week decompression groups ($p = 0.22$). Independently of time-point, there was a significant difference in rotarod times between the three groups ($p = 0.02$). Post hoc hazard-ratios for the group term are presented below.

Table 14. Hazard Ratios – Decompression Groups.

Hazard Ratios for group			
Description (Groups)	Point Estimate	95% Wald Robust Confidence Limits	
24hrs decompression versus 3 wk decompression	1.512	1.058	2.162
24hrs decompression versus 9wk compression	1.691	1.143	2.501
3wk decompression versus 9wk compression	1.118	0.761	1.643

The table shows that rats in the 24 hour decompression group had a significantly higher risk of falling off the rotarod (i.e. they had shorter rotarod times) than rats in the 3 week decompression and 9 week persisting compression groups. There was no difference in rotarod times between the 3 week decompression and 9 week treatment groups since the 95% CI includes the null value of 1.

Table 15. Rotarod scores (seconds) at sacrifice in Sprague-Dawley rats following spinous processotomy at T12 and insertion of an aquaprene polymer.

Survival	Median rotarod score	Mean rotarod score
24 hours	24	33.62
1 week	69.5	69.67
3 weeks	79.5	76.75
9 weeks	118	98
20 weeks	101	90.21
Sham	120	115
Vehicle	120	120
Naïve	120	120

Table 16. Rotarod scores (seconds) at sacrifice in Sprague-Dawley rats following decompression laminoplasty for removal of expandable polymer at 24 hours and 3 weeks post initial laminoplasty.

Decompression Laminoplasty	Median rotarod score	Mean rotarod score
24 hour decompression	120	106.62
3 week decompression	120	108.08
Decompression sham	120	120

Table (a)

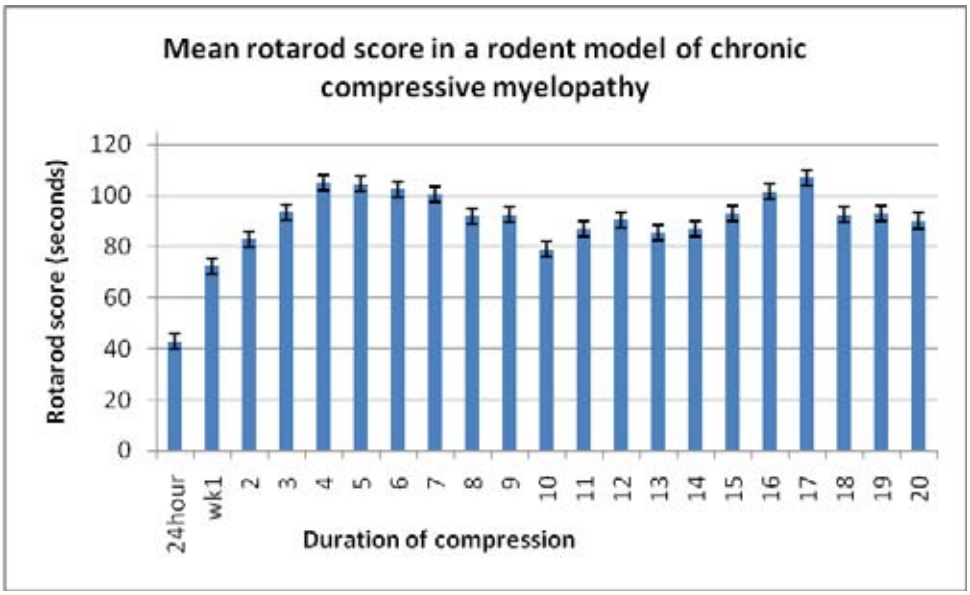

Table (b)

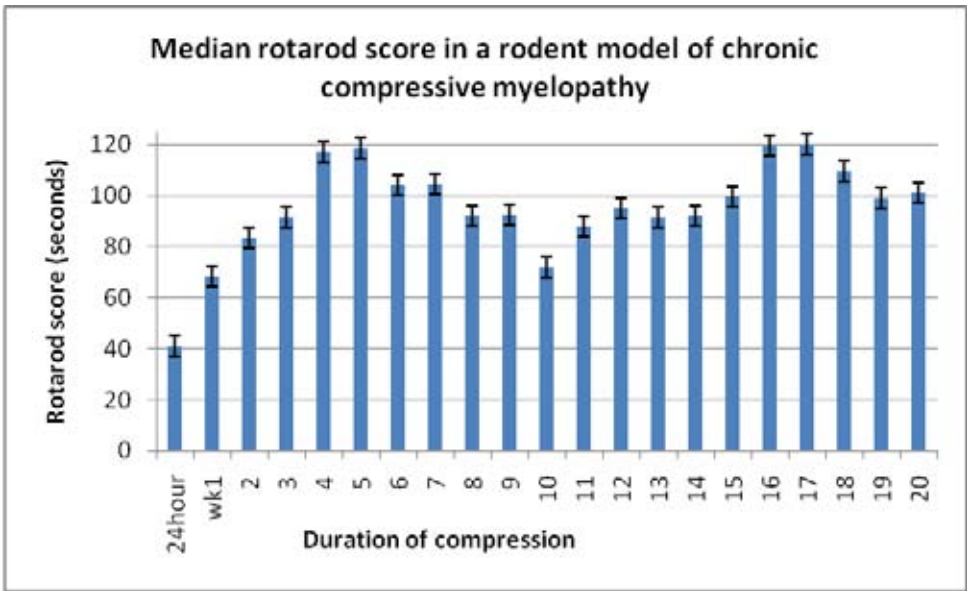

Table 17. (a) Mean and (b) Median rotarod scores in rat chronic compressive myelopathy up to 20 weeks duration.

A biphasic improvement in mean and median rotarod score is evident by 5 and 17 weeks duration of compression. At no stage was a return to the naïve group mean score of 120 seconds obtained.

Table (a)

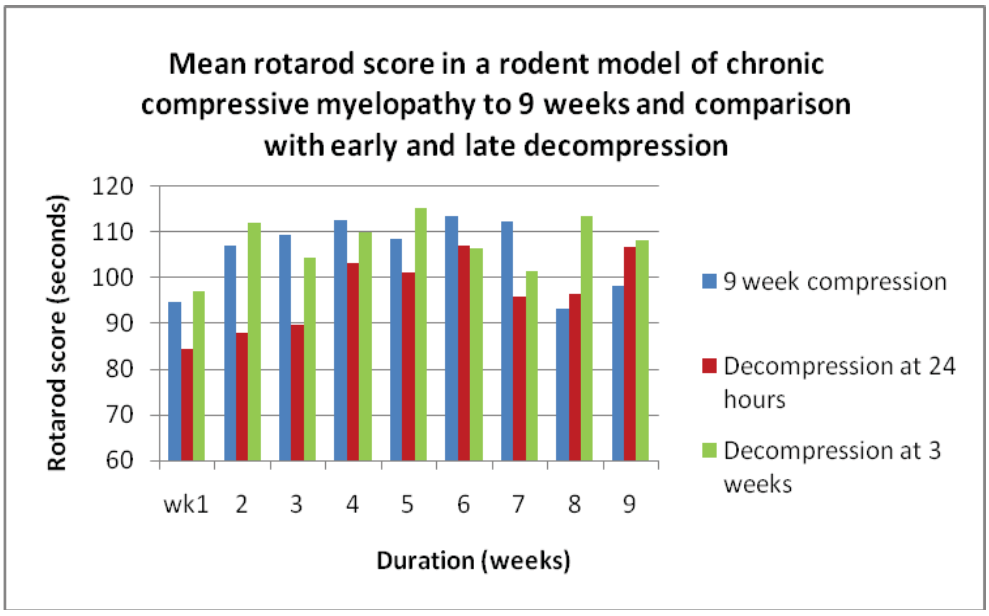

Table (b)

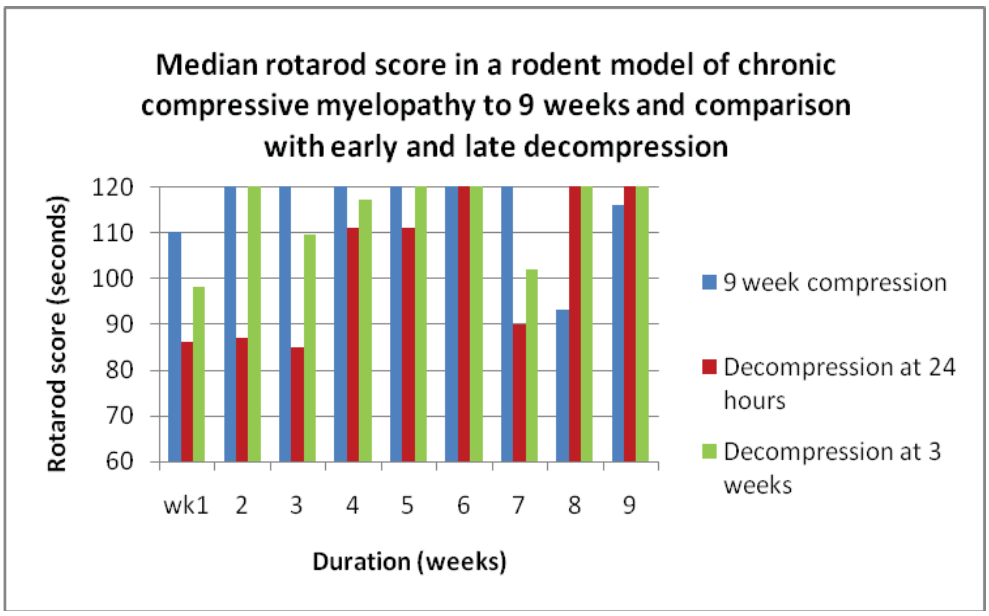

Table 18. (a) Mean and (b) Median rotarod scores in a rodent model of chronic compressive myelopathy.

Similar rotarod scores were recorded for the 9 week compression group versus decompression at 3 weeks in the early weeks but by 8 weeks, late decompression was associated with an improvement in rotarod measured motor function. In the group undergoing decompression at 24 hours, lower rotarod scores than the other groups were measured up to 5 weeks, from which time similar scores were recorded, suggesting a negative but transient effect on motor function with early decompression.

3.3.3 Tail Flick

Tail flick measurements involving a heat-pain stimulus were used in assessment of motor-sensory function. Due to equipment delay, measurements were commenced at the 7 week time point in the 20 week survival group, and at the 5 week time point in the 9 week survival group. Time trends in the tail-flick results of the 20 week treatment group were investigated using a linear mixed effects model. A random rat effect was included in the model to adjust for the dependence in repeated observations from the same rat. Impaired motor function was thought to be indicated by longer tail flicks times, however on review, there appears to be no difference between injury and control groups. Using a linear effects model, there was no evidence for a difference in mean tail-flick results over the time periods of measurement ($p = 0.07$).

The variation of readings across longer time points is reflected in the disparate peak mean scores for each group. This occurred at 19 weeks (4.41 seconds) in the 20 week group, at sacrifice in the 9 week group (4.38), at only 24 hours post decompressive surgery in the 24 hour decompression group (4.27) and at sacrifice in the 3 week decompression group (4.48). Statistically, the tail-flick results were compared between the four groups (24 hours, 1 week, 3 weeks, control) at their final measurement period using a one way ANOVA model.

There was significant evidence for a difference in tail-flick results between the groups ($p <0.0001$). A significant decrease in tail-flick time versus control was found at 1 week ($p <0.0001$) and 3 weeks ($p = 0.002$). There was no significant difference between control and the 9 or 20 week compression groups or the 24 hour or 3 week decompression groups.

A significant increase in the duration of heat-pain stimulus (seconds) suggestive of impaired motor-sensory function was observed in the 1 week group (mean 5.638) compared to the 9 week (mean 4.376, $p = 0.003$) or 20 week (mean 3.854, $p <0.0001$) groups. There was no significant change in tail flick measurements between the 1 week and 3 week groups, suggesting similarly impaired function.

A significant increase in the duration of heat-pain stimulus tolerated was seen in the 24 hour decompression group (mean 4.01, $p = 0.0002$) and 3 week decompression group

(mean 4.46, p = 0.006) compared with the control group. Independently of time, there was no evidence for a difference in tail-flick scores between the 9 week compression, 24 hour decompression and 3 week decompression groups (p = 0.84).

Table 19. Tail flick scores (seconds) at sacrifice in Sprague-Dawley rats following spinous processotomy at T12 and insertion of an aquaprene polymer.

Survival	Median tail flick score	Mean tail flick score
24 hours	6.48	6.86
1 week	5.34	5.64
3 weeks	4.38	5.15
9 weeks	4.4	4.38
20 weeks	3.86	3.85
Sham	4.36	4.33
Vehicle	4.24	3.87
Naïve	3.75	3.66

Table 20. Tail flick scores (seconds) at sacrifice in Sprague-Dawley rats following decompression laminoplasty for removal of expandable polymer at 24 hours and 3 weeks post initial laminoplasty.

Decompression Laminoplasty	Median tail flick score	Mean tail flick score
24 hour decompression	4.12	4.01
3 week decompression	4.63	4.46
Decompression sham	4.34	4.32

Table (a)

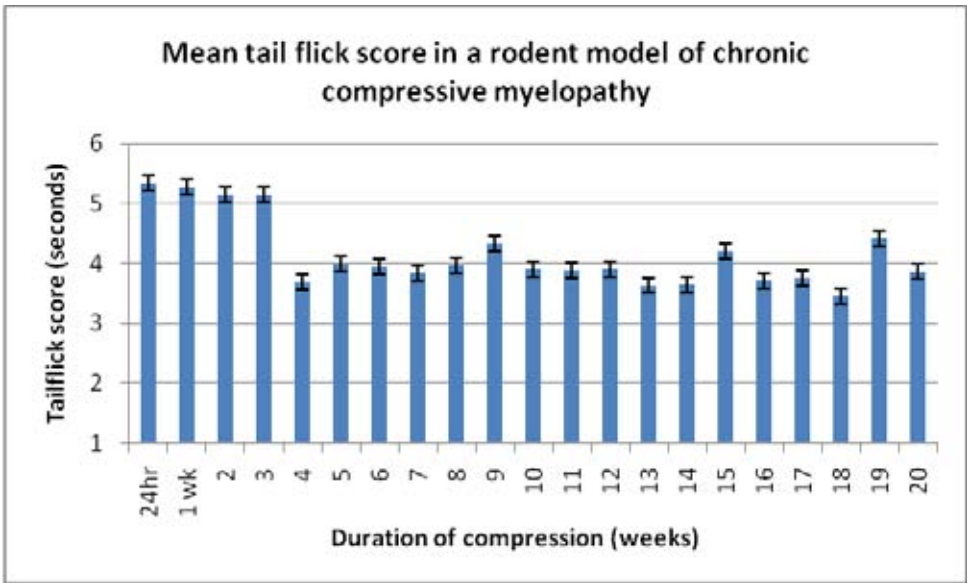

Table (b)

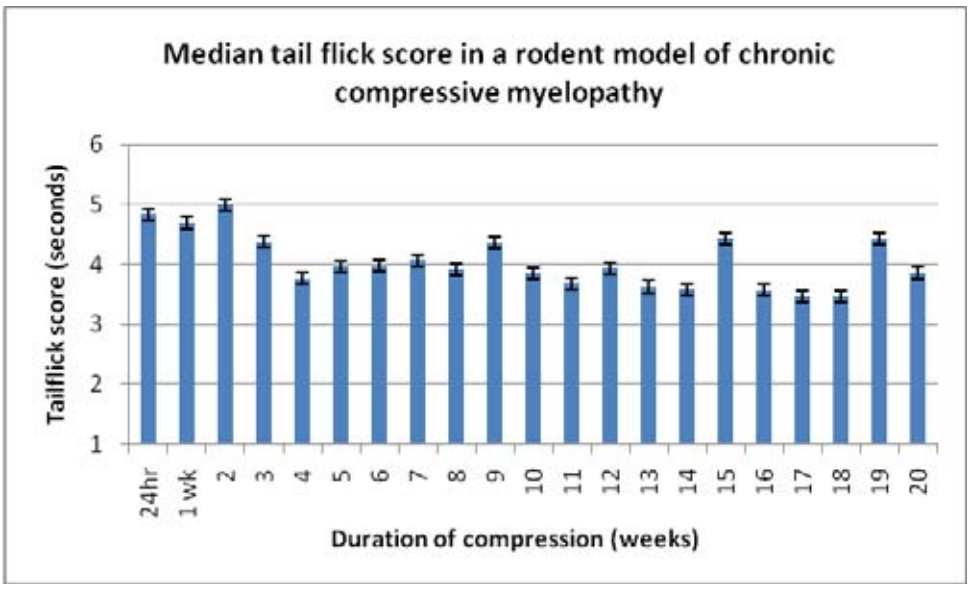

Table 21. (a) Mean and (b) Median tail flick scores in rat chronic compressive myelopathy.

Results include 20, 9, 3, 1, week and 24 hour groups. A decrease in the mean tail flick score and two-point average is seen with increasing duration of compression suggesting an improvement in motorsensory function by 4 weeks after surgery.

Table (a)

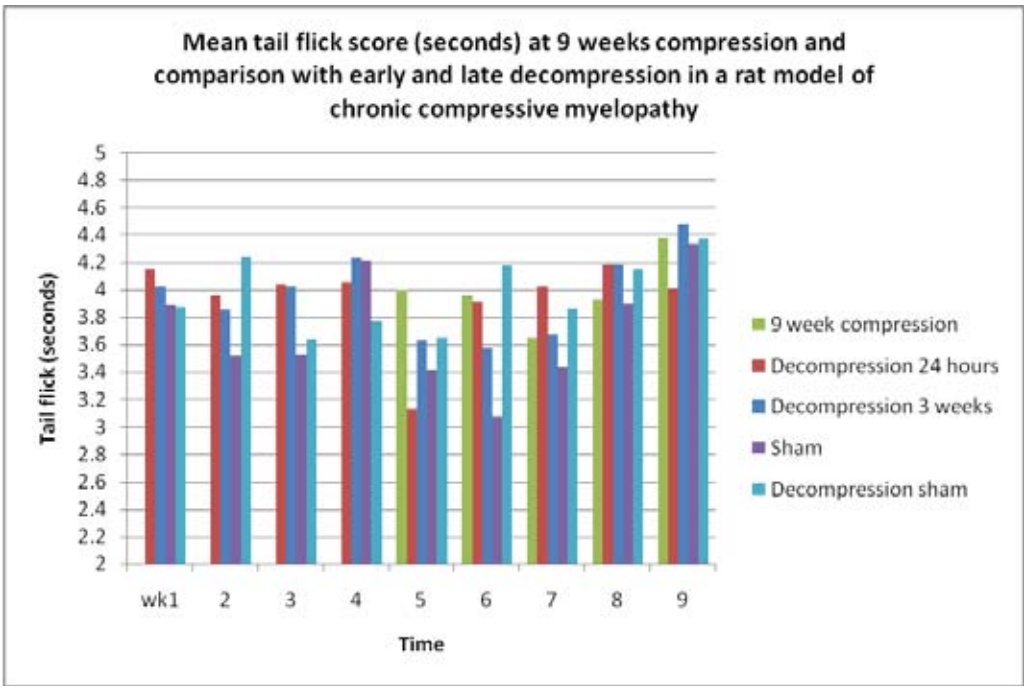

Table (b)

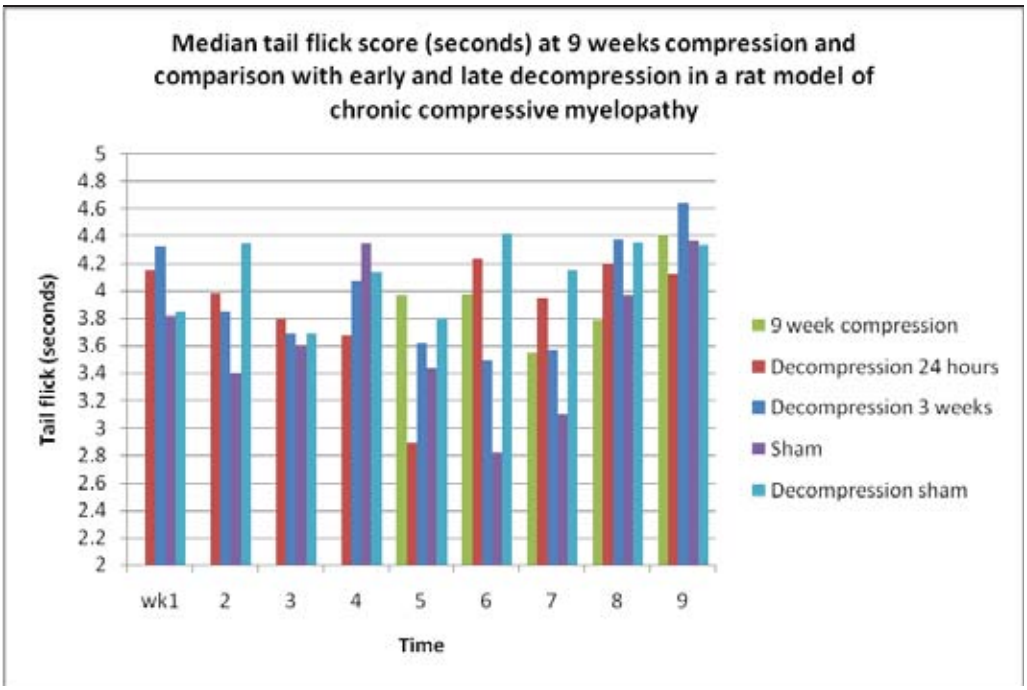

Table 22. (a) Mean and (b) Median tail flick scores in persisting compression versus decompression and control groups.

There was no significant difference in the mean and median tail flick scores between 9 week compression, decompression and control groups in a rodent model of chronic compressive myelopathy. Similar scores are evident at 9 weeks duration of compression compared with earlier time points according to the sensitivity of the tail flick test.

3.3.4 Ledge Beam

For ledge beam, time trends in the ledge-beam results of the 20 week treatment group were investigated using a linear mixed effects model. A random rat effect was included in the model to adjust for the dependence in repeated observations from the same rat. There was significant evidence for a difference in mean ledge-beam falls over the time periods of measurement ($p = 0.004$).

To test for a difference in ledge-beam results between the groups and over time, a linear mixed effects model was fitted to the data. A random rat effect was included in the model to adjust for the dependence in repeated observations from the same rat. A significant group by time interaction effect was found ($p = 0.007$), suggesting that the difference between the groups in ledge beam results varied with the time period since compression.

An increase in the mean number of foot faults at 9 weeks was seen in the 9 week sacrifice group (26.3) versus 24 hour (23.35) and 3 week (16.85) decompression groups but this did not reach significance.

3.4 Chronic Human Spinal Cord Compression

3.4.1 Histopathology

Human Spondylotic Myelopathy

Three cases of human cervical compressive myelopathy, each presenting with severe neurological impairment causing quadriparesis, were examined histologically. Two cases were the result of osteophytosis within the spinal canal and one case was due to compression from a prolapsed disc (see Appendix). All cases were male and aged between 64 and 77 years. There was macroscopic and microscopic evidence of loss of white matter in all cases. Cystic changes and tissue necrosis were present in all three cases in the CSM series with documented cord compression of 8, 14 and 22 years duration. Sections showed a decreased number of glial and anterior horn cells. In all cases there was demyelination in a pattern suggestive of Wallerian degeneration (**Figure 3.6**).

Human Neoplastic Compressive Myelopathy

Seven cases of neoplastic compressive myelopathy were included for study (male:female ratio 6:1, age range 50-79 yrs). Six showed extramedullary compression and one showed intramedullary invasion. Tumour type varied in each case but all were metastatic in nature. Four cases had developed paralysis during their course of illness which was present at the time of death, with a range of symptom duration of 25 days to 5 years. Tissue or cystic necrosis was evident on haematoxylin and eosin staining in approximately half of the cases with survival from 25 days to one year, consistent with mechanical compression and ischaemic injury.

In contrast to cervical spondylotic myelopathy, cases of human neoplastic compressive myelopathy showed a more rapid natural history over weeks or months rather than years, consistent with ‘subacute’ compression. Microscopy revealed axonal swellings, loss of anterior horn cells, and cystic necrosis. Whilst there was an occasional loss of myelin staining, no pattern consistent with Wallerian degeneration was present.

Syringomyelia

Three human cases of syringomyelia were selected for study. The age range was 25 to 74 years and all cases were male. In syringomyelia cases, there were two distinct aetiologies, syringomyelia secondary to trauma resulting in quadriplegia, and syringomyelia as a developmental abnormality or Arnold Chiari malformation with paraparesis.

The patterns of clinical deficit correlated with the histopathological changes. In syringomyelia due to trauma resulting in quadriplegia (Case 19) there was cystic necrosis, loss of glia, loss of myelin staining, effacement of normal architecture, fibrosis, and multiple small cystic spaces above and below the site of traumatic injury. In Case 21, there was post-operative syringomyelia with extensive degeneration and atrophy of the cervical cord above the site of surgery in the upper thoracic region.

Table 23. List of cervical spondylotic myelopathy cases.

CASE	*Age*	*Gender*	*Type*	*Clinical Duration*	*Necrosis*
1	77	Male	Prolapsed disc	8 years	Present
2	64	Male	Osteophytosis	14 years	Present
3	75	Male	Osteophytosis	22 years	Present

Table 24. Summary of histopathological changes in cervical spondylotic myelopathy cases.

Stain	CASE 1	CASE 2	CASE 3
H & E	Macroscopic distortion with tissue degeneration in the posterolateral region, in some segments cystic necrosis of the anterolateral cord unilaterally. Anterior horn cell loss. Large numbers of tissue macrophages are seen in these necrotic areas.	Compression atrophy at C5 and C6, pallor of the posterolateral cord at C2-C6, generalised loss of anterior horn cells, decreased numbers of glia in the posterior cord and lateral corticospinal tract, cystic necrosis of the posterior columns extending to the lateral corticospinal tracts.	Macroscopic compression at the site, cystic necrosis, loss of anterior horn cells, paucity of glia in the lateral white matter.
Weil	Wallerian degeneration	Wallerian degeneration	Wallerian degeneration

Table 25. List of neoplastic compressive myelopathy cases.

CASE	*Age*	*Gender*	*Type*	*Clinical Duration*	*Necrosis*
4	50	Male	Metastatic	25 days	Present
5	75	Female	Metastatic	4 months	Present
6	79	Male	Metastatic	6 months	Absent
7	59	Male	Metastatic	6 months	Present
8	24	Male	Metastatic	1 year	Present
9	74	Male	Metastatic	11months	Present
10	72	Male	Metastatic	5 years	Absent

Table 26. Summary of histopathological changes in neoplastic compressive myelopathy.

Stain	CASE 4	CASE 5	CASE 6	CASE 7	CASE 8	CASE 9	CASE 10
H & E	AHC loss, tissue necrosis, macrophages, axonal swellings	Macrophages, axonal swellings, cystic necrosis	Intradural tumour invasion, asymmetric AHC loss, axonal swellings posterolateral cord, central chromatolysis of neurons	Cystic necrosis, loss AHCs, axonal swellings posterolaterally, Central chromatolysis	AHC loss, Axonal swellings all regions, cystic necrosis lateral spinothalamic tract, lateral corticospinal tract and cuneate fasciculus	Asymmetric distortion, tumour invasion posterolateral cord, axonal swellings throughout, extensive infiltration grey matter, AHC loss	Minor necrosis grey matter, Central chromatolysis
Weil	No pallor	Pallor posterior columns and laterally at the conus	No Pallor	No pallor	Pallor posterior columns and lateral corticospinal tract	No pallor	No pallor

Table27. List of syringomyelia cases.

CASE	*Age*	*Gender*	*Type*	*Clinical Duration*	*Necrosis*
19	75	Male	Fracture/dislocation C7/T1 with secondary syrinx C6-T5	25 years	Absent
20	55	Male	Syrinx C2-T12, developmental anomaly	55 years	Absent
21	74	Male	Decompression surgery for developmental syrinx, residual syrinx C2-L1	74 years	Absent

Table 28. Histopathological changes in human syringomyelia – morphological findings.

Stain	CASE 19	CASE 20	CASE 21
H & E	Healed fracture/dislocation C7-T1. Syrinx communicating with the central canal. Subtotal loss of glia and neurons at site.	Syrinx communicating with central canal. Loss of anterior horn cells.	Residual syrinx. Descending corticospinal tract degeneration, loss of anterior horn cells.
Weil	Pallor above and below	Pallor posterior columns above	Pallor lateral corticospinal tract below

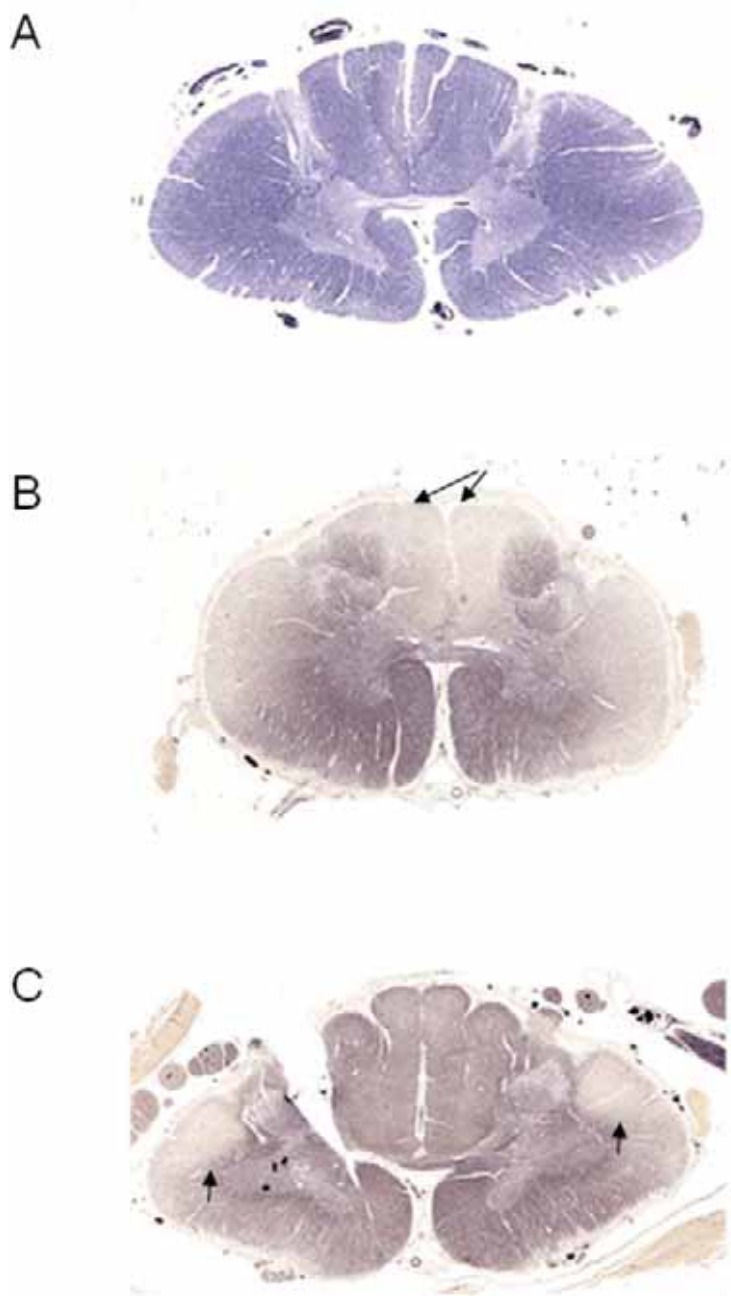

Figure 3.6 Weil staining in human chronic compressive myelopathy.

Photomicrograph (A) shows the normal pattern of myelin distribution surrounding axons using the Weil staining method. Photomicrographs (B) and (C) are taken from Case 2 in which there was myelopathy secondary to cervical spondylosis at the level of C5 and clinical duration of 14 years. Photomicrograph (B) shows Weil staining at C2 and demonstrates pallor of the posterior columns (arrows) consistent with ascending Wallerian degeneration. Photomicrograph (C) shows Weil stain at C8 with degeneration of the descending lateral corticospinal tracts (arrows) consistent with Wallerian degeneration.

3.4.2 Apoptosis

Human Cervical Spondylotic Myelopathy

There was loss of both neurons and glia. Residual anterior horn cells and neurons of the posterior horn were immunopositive for the TUNEL marker. TUNEL immunopositivity in neurons and glia was present above and below the site of compression. In areas of the white matter where glial cells were still present, nuclear immunopositivity to PARP, DNA-PKcs and TUNEL was seen in association with pallor on Weil stain. At the site of compression, where necrosis was present, PARP and DNA-PKcs immunopositive glia were found on the border of necrotic areas. In the preserved areas of white and grey matter surrounding cystic change there was glial immunopositivity to DNA-PKcs and PARP. Staining extended contiguously from the periphery of necrotic areas to the apparently normal neuropil. Neuronal immunopositivity using the Amy-33 marker of amyloid-beta was also a feature. AIF immunopositivity was seen in profiles consistent with both oligodendrocytes and astrocytes. Glial AIF immunopositivity was homogeneously spread throughout the white matter and reduced at the site of compression. AIF immunopositivity was found in profiles consistent with both oligodendrocytes and astrocytes and especially in the subpial region. Neuronal AIF immunopositivity was consistently present. AIF immunoreactivity matched that of mitochondrial protein in immunostaining. Active caspase-3, caspase-9, Bcl-2 and Fas immunomarkers were negative.

Table 29. Summary of immunohistochemical results in human cervical spondylotic myelopathy – immunohistochemical markers of apoptosis and TUNEL.

ANTIGEN	CASE 1	CASE 2	CASE 3
Caspase-3	Negative	Negative	Negative
DNA-PKcs	Positive glia above, below and rarely at site, neurons below	Positive glial nuclei above and below	Positive glial nuclei all segments Positive neuronal nuclei rare at site
PARP	Positive glia at site, above, below	Positive glial nuclei all segments Positive neuronal nucleoli below	Positive glial nuclei all segments
Bcl-2	Negative	Negative	Negative
Fas	Negative	Negative	Negative
TUNEL	Positive glial nuclei above and below Positive neuronal nuclei at site, above, below	Positive glial nuclei above and below Positive neuronal nuclei above, below and rarely at site	Positive glial and neuronal nuclei at site, above and below
Caspase-9	Negative	Negative	Negative
AIF	Glial and neuronal cytoplasmic staining all segments	Glial and neuronal cytoplasmic immunopositivity at, above and below the site	Subpial glial and neuronal cytoplasmic immunopositivity at, above and below
Mitochondrial protein	Heterogeneous glial, neuronal and axonal immunopositivity	Heterogeneous glial, neuronal and axonal immunopositivity	Heterogeneous glial, neuronal and axonal immunopositivity

Table 30. CASE 1 – Compression C3/4 – Immunohistochemical positivity (+) in glial, axonal or neuronal profiles:

Level	Casp-3	DNA-PKcs	PARP	Bcl-2	Fas	Casp-9	TUNEL
C2	-	+	+	-	-	-	+
C3	-	+	+	-	-	-	+
C4	-	+	+	-	-	-	+
C4/5	-	+	+	-	-	-	+
C5	-	+	+	-	-	-	-
C5/6	-	+	-	-	-	-	-
C6	-	+	+	-	-	-	+
C6/7	-	+	+	-	-	-	+
C7	-	+	+	-	-	-	+
C7/8	-	+	+	-	-	-	+
C8	-	+	+	-	-	-	+
T1	-	+	+	-	-	-	+

* Shaded rows represent the site of compression

Table 31. CASE 2 – Compression C4/5 – Immunohistochemical positivity (+) in glial, axonal or neuronal profiles:

Level	Casp-3	DNA-PKcs	PARP	Bcl-2	Fas	Casp-9	TUNEL
C2	-	+	+	-	-	-	+
C4	-	+	+	-	-	-	+
C5	-	-	+	-	-	-	+
C6	-	-	+	-	-	-	+
C8	-	+	+	-	-	-	+

* Shaded rows represent the site of compression

Table 32. CASE 3 – Compression C4/5 and C5/6 – Immunohistochemical positivity (+) in glial, axonal or neuronal profiles:

Level	Casp-3	DNA-PKcs	PARP	Bcl-2	Fas	Casp-9	TUNEL
C3	-	+	+	-	-	-	+
C4	-	+	+	-	-	-	+
C5	-	+	+	-	-	-	+
C6	-	+	+	-	-	-	+
C7	-	+	+	-	-	-	+
C8	-	+	+	-	-	-	+
T1	-	+	+	-	-	-	+

* Shaded rows represent the site of compression

Human Neoplastic Compressive Myelopathy

TUNEL immunopositive glial and neuronal profiles were maximal at the site of compression. Immunopositivity to PARP and DNA-PKcs was found in glia throughout the white matter above and below the necrotic area. DNA-PKcs and PARP glial immunopositivity was maximal in neurons and glia at the site of injury. AIF immunoreactivity was only present in the cytoplasm of neurons. Immunopositivity to aC3 and C9 was seen in axons. AIF immunopositivity in the cytoplasm was congruent with staining using mitochondrial protein.

Table 33. Summary of immunohistochemical results in human neoplastic compressive myelopathy – markers of apoptosis.

ANTIGEN	CASE 4	CASE 5	CASE 6	CASE 7	CASE 8	CASE 9	CASE 10
Caspase-3	Axonal staining	Negative	Rare axonal swellings staining in C2-C5	Axonal stainng L2, L3	Axonal staining above, below site	Negative	Negative
DNA-PKcs	Axonal staining	Occasional glial nuclear immuno-positivity	Glial nuclear staining and axonal swellings at C4	Glial staining all segments, axonal staining L2, L3	Glial and axonal staining at, above and below site	Neuronal nuclear above and below, glial staining at, above and below, axonal staining T3	Glial nuclear staining all, neuronal staining at site
PARP	Glial staining	Glial staining widespread and neurons above site	Glia staining all, neuronal staining C2-C5	Glial staining all, neuronal staining	Glial and axonal staining at and above site	Glial staining all segments, neuronal staining, above and below site	Glial nuclear staining all
Bcl-2	Negative	Negative	Negative	Negative	Negative	Glial staining at, above and below site	Glial staining at and between lesions
Fas	Negative	Negative	Negative	Negative	Negative	Negative	Negative
TUNEL	Glial staining	Neuronal staining L5 and S1, glial staining all	Glial and neuronal staining all	Glial and neuronal staining all	Glial and neuronal staining all	Rare neuronal staining above and below site, glial staining below site	Glial staining all, neuronal staining at, below
Caspase-9	Negative	Negative	Axonal staining	Negative	Negative	Negative	Negative
AIF	Axonal, glial and neuronal staining	Glial and neuronal staining all, axons above	Axonal, glial and neuronal staining	Glial and neuronal staining all, axons below	Glia and neuronal staining all, axons at, above, below	Glial and neuronal staining all	Glial and neuronal staining all
Mitochondrial protein	Glial, neuronal and axonal staining	Glial, neuronal and axonal staining	Glial, neuronal and axonal staining	Glial, neuronal and axonal staining	Glial, neuronal and axonal staining	Glial, neuronal and axonal staining	Glial neuronal and axonal staining

Table 34. CASE 4 – Immunohistochemical positivity (+) in glial, axonal or neuronal profiles:

Level	Casp-3	DNA-PKcs	PARP	Bcl-2	Fas	Casp-9	TUNEL
T2	+	-	+	-	-	-	+
T3	+	+	+	-	-	-	+
T4	+	+	+	-	-	-	+
T5	+	+	+	-	-	-	+

* Shaded rows represent the site of compression

Table 35. CASE 5 – Immunohistochemical positivity (+) in glial, axonal or neuronal profiles:

Level	Casp-3	DNA-PKcs	PARP	Bcl-2	Fas	Casp-9	TUNEL
L5	+	+	+	-	-	-	+
S1	+	+	+	-	-	-	+
conus	-	+	+	-	-	-	+

* Shaded rows represent the site of compression

Table 36. CASE 6 – Immunohistochemical positivity (+) in glial, axonal or neuronal profiles:

Level	Casp-3	DNA-PKcs	PARP	Bcl-2	Fas	Casp-9	TUNEL
C2	+	-	+	-	-	-	+
C3	+	-	+	-	-	+	+
C4	+	+	+	-	-	-	+
C5	+	-	+	-	-	+	+
C6	-	-	+	-	-	-	+
C7	-	-	+	-	-	-	+

* Shaded rows represent the site of compression

Table 37. CASE 7 – Immunohistochemical positivity (+) in glial, axonal or neuronal profiles:

Level	APP	Casp-3	DNA-PKcs	PARP	Bcl-2	Fas	Casp-9	TUNEL	Amy-33	CMAP	AIF
T10	+	-	+	+	-	-	-	+	+	+	+
T11	+	-	+	+	-	-	-	+	+	+	+
T12	+	-	+	+	-	-	-	+	+	+	+
L1	+	-	+	+	-	-	-	+	+	+	+
L2	+	+	+	+	-	-	-	+	+	+	+
L3	+	+	+	+	-	-	-	+	+	+	+

* Shaded rows represent the site of compression

Table 38. CASE 8 – Immunohistochemical positivity (+) in glial, axonal or neuronal profiles:

Level	APP	Casp-3	DNA-PKcs	PARP	Bcl-2	Fas	Casp-9	TUNEL	Amy-33	CMAP	AIF
C3	+	-	+	+	+	-	-	+	+	+	+
C4	+	+	+	+	-	-	-	-	+	+	+
C5	+	+	+	+	+	-	-	-	+	+	+
C6	+	+	+	+	+	-	-	-	+	+	+
C7	+	+	+	-	-	-	-	-	+	+	+
C8	+	+	+	-	-	-	-	-	+	+	+
T2	+	+	+	+	-	-	-	-	+	+	+
T3	+	+	+	+	-	-	-	-	+	+	+
T7	+	+	+	+	-	-	-	-	+	+	+
T8	+	+	+	+	-	-	-	-	+	+	+
T9	+	+	-	+	-	-	-	-	+	+	+
T10	+	+	+	+	-	-	-	-	+	+	+
T11	+	+	+	+	-	-	-	-	+	+	+
T12	+	+	+	+	-	-	-	+	+	+	+
L5	+	-	-	+	-	-	-	-	+	+	+

* Shaded rows represent the site of compression

Table 39. CASE 9 – Immunohistochemical positivity (+) in glial, axonal or neuronal profiles:

Level	APP	Casp-3	DNA-PKcs	PARP	Bcl-2	Fas	Casp-9	TUNEL	Amy-33	CMAP	AIF
C3	+	+	-	+	+	+	+	+	+	+	+
C4	+	+	+	+	-	+	+	-	+	+	+
C5	+	+	+	+	+	+	+	-	+	+	+
C6	+	+	+	+	+	+	+	-	+	+	+
C8	+	+	+	+	-	+	+	-	+	+	+
T2	+	+	+	+	-	+	+	-	+	+	+
T3	+	+	+	+	-	+	+	-	+	+	+
T7	+	+	+	+	-	+	+	-	+	+	+
T8	+	+	+	+	-	+	+	-	+	+	+
T9	+	+	-	+	-	+	+	-	+	+	+
T10	+	+	+	+	-	+	+	-	+	+	+
T11	+	+	+	+	-	+	+	-	+	+	+
T12	+	+	+	+	-	+	+	+	+	+	+
L5	+	+	-	+	-	+	+	-	+	+	+

* Shaded rows represent the site of compression

Table 40. CASE 10 – Immunohistochemical positivity (+) in glial, axonal or neuronal profiles:

Level	APP	Casp-3	DNA-PKcs	PARP	Bcl-2	Fas	Casp-9	TUNEL	Amy-33	CMAP	AIF
C2	-	+	+	+	-	-	-	+	+	+	+
C3	-	+	+	+	+	-	-	+	+	+	+
C4	-	+	+	+	-	-	-	+	+	+	+
C5	-	+	+	+	+	-	-	+	+	+	+
C6	-	+	+	+	+	-	-	+	+	+	+
C7	-	+	+	+	-	-	-	+	+	+	+
C8	+	+	+	+	+	-	-	+	+	+	+
T1	-	+	+	+	-	-	-	+	+	+	+
T2	-	+	+	+	-	-	-	+	+	+	+
T3	-	+	+	+	-	-	-	+	+	+	+

* Shaded rows represent the site of compression

Human Syringomyelia

TUNEL and DNA-PKcs staining in glial cells was present throughout many white matter tracts and predominantly within the central cord. PARP immunopositivity also showed a heterogeneous spatial pattern of staining in glial nuclei. Immunostaining for the AIF antibody was present in glial cells, neurons and ependymal cells across multiple segments involving the syrinx. Staining correlated with mitochondrial protein, suggesting possible translocation of the AIF molecule. AIF was negative in axonal swellings. Active caspase-3 and caspase-9 markers were negative. There was minimal positive staining using the Fas and Bcl-2 antibodies.

Table 41. Immunohistochemical staining using a panel of markers of apoptosis in human syringomyelia – morphological findings.

ANTIGEN	CASE 19	CASE 20	CASE 21
APP	Neuronal staining	Neuronal staining	Negative
Caspase-3	Negative	Negative	Negative
DNA-PKcs	Glial staining all segments, Neuronal staining unilaterally	Glial and neuronal staining all segments	Neuronal staining C5 and C4, Glial nuclei all segments
PARP	Glial staining all segments	Glial staining throughout particularly in subpial region, rare neuronal staining C7	Glial staining throughout particularly in subpial region
Bcl-2	Lymphocyte staining	Lymphocyte staining	Rare glial staining all segments
Fas	Negative	Negative	Negative
TUNEL	Glia staining, rare neuronal staining	Glial and neuronal staining in all segments	Glia staining T7
Caspase-9	Negative	Negative	Negative
AIF	Glial and neuronal immunopositivity at and below the syrinx	Immunopositivity in oligodendrocytes, astrocytes and neurons all segments, positivity in ependymal cells lining the syrinx	Heterogeneous staining in glia and neurons
Mitochondrial protein	Heterogeneous glial, neuronal and axonal immunopositivity	Heterogeneous glial, neuronal and axonal immunopositivity	Heterogeneous glial, neuronal and axonal immunopositivity

Table 42. CASE 19 – Syringomyelia series – Immunohistochemical positivity (+) in glial, axonal or neuronal profiles:

Level	APP	Casp-3	DNA-PKcs	PARP	Bcl-2	Fas	Casp-9	TUNEL	Amy-33	CMAP	AIF
C8	-	-	+	+	-	-	-	-	-	+	+
T2	-	-	+	+	-	-	-	-	+	+	+
T4	+	-	+	+	-	-	-	+	-	+	+
T7	-	-	-	+	-	-	-		+	+	+

* Shaded rows represent the site of compression

Table 43. CASE 20 – Syringomyelia series – Immunohistochemical positivity (+) in glial, axonal or neuronal profiles:

Level	APP	Casp-3	DNA-PKcs	PARP	Bcl-2	Fas	Casp-9	TUNEL	Amy-33	CMAP	AIF
C2	-	-	+	+	-	-	-	+	-	+	+
C3	-	-	+	+	-	-	-	+	-	+	+
C4	-	-	+	+	-	-	-	+	-	+	+
C7	-	-	+	+	-	-	-	+	-	+	+
L2	+	-	+	+	-	-	-	+	+	+	+

* Shaded rows represent the site of compression

Table 44. CASE 21 – Syringomyelia series – Immunohistochemical positivity (+) in glial, axonal or neuronal profiles:

Level	APP	Casp-3	DNA-PKcs	PARP	Bcl-2	Fas	Casp-9	TUNEL	Amy-33	CMAP	AIF
C6	+	-	+	+	-	-	-	+	+	+	+
T7	+	-	+	+	-	-	-	+	-	+	+
L4	+	-	-	+	-	-	-	+	+	+	+
S2	+	-	-	-	-	-	-	+	+	+	+

* Shaded rows represent the site of compression

Human Control Cases

Human lymphoma tissue was used as a positive control for caspase-3, DNA-PKcs, PARP, Bcl-2, Fas, TUNEL, caspase-9, mitochondrial protein, CMAP, Amyloid-beta and AIF antibodies. Human corpus callosum from traumatic brain injury was used as a positive control for APP, CMAP and amyloid-beta antibodies. Cerebral cortex from Alzheimer's disease was used as a positive control for amyloid-beta and CMAP antibodies.

Table 45. Immunohistochemical and histopathological findings in normal human spinal cord cases.

Stain / Antigen	**CONTROL CASE 1**	**CONTROL CASE 2**
H & E	Normal white and grey matter Normal cell morphology and numbers	Normal white and grey matter Normal cell morphology and numbers
Weil	Normal distribution of staining	Normal distribution of staining
APP	Negative in axons	Negative in axons
Caspase-3	Negative	Negative
DNA-PKcs	Negative	Negative
PARP	Rare glial immunopositivity	Rare glial immunopositivity
Bcl-2	Rare glial immunopositivity	Negative
Fas	Rare glial and neuronal staining	Rare glial and neuronal staining
TUNEL	Negative	Negative
Caspase-9	Negative	Negative
AMY-33	Negative	Negative in axons
University of Melbourne amyloid-beta	Negative	Negative
Dako amyloid-beta	Negative	Negative
CMAP	Occasional immunopositivity	Occasional immunopositivity
AIF	Negative in axons	Negative in axons
Mitochondrial protein	Heterogeneous glial, neuronal and axonal immunopositivity	Heterogeneous glial, neuronal and axonal immunopositivity

3.4.3 Axonal Injury

Human Cervical Spondylotic Myelopathy

In contrast to neoplastic compressive myelopathy, APP immunoreactivity was not seen in axons in CSM or syringomyelia. APP immunopositivity occurred in axonal tracts within the white matter and was present within segments affected by cystic necrosis. IHC staining showed many APP positive axons and enlarged axons, either bulbs or swellings, were present at the site of injury. Caspase-3 antibody was negative within all axons. Two of the three antibodies to amyloid-beta were also negative. Amy-33 amyloid-beta antibody was positive within neurons and glia despite the APP marker being negative. CMAP was consistently found in all cell types including ependymal cells and appeared to be non-specific. In the positive control, the DAKO amyloid-beta antibody immunolabelled the core of neuritic plaques (**Figure 3.6** and **Figure 3.7**) whilst the Amy-33 amyloid-beta and APP antibodies showed similar staining within neurites in neuritic plaques on single and double immunolabelling (**Figure 3.8** and **Figure 3.9**)

Table 46. Summary of immunohistochemical results in human cervical spondylotic myelopathy – APP, caspase-3, CMAP and amyloid-beta antibodies.

ANTIGEN	CASE 1	CASE 2	CASE 3
APP	Negative	Negative	Negative
Caspase-3	Macrophages	Negative	Negative
AMY-33	Neuronal staining, rare axonal staining	Neuronal staining at, above and below site	Neuronal and glial staining all segments
University of Melbourne amyloid beta	Negative	Negative	Negative
Dako amyloid beta	Negative	Negative	Negative
CMAP	Heterogeneous staining of glia, neurons, ependymal cells and axons	Heterogeneous staining of glia, neurons, ependymal cells and axons	Heterogeneous staining of glia, neurons, ependymal cells and axons

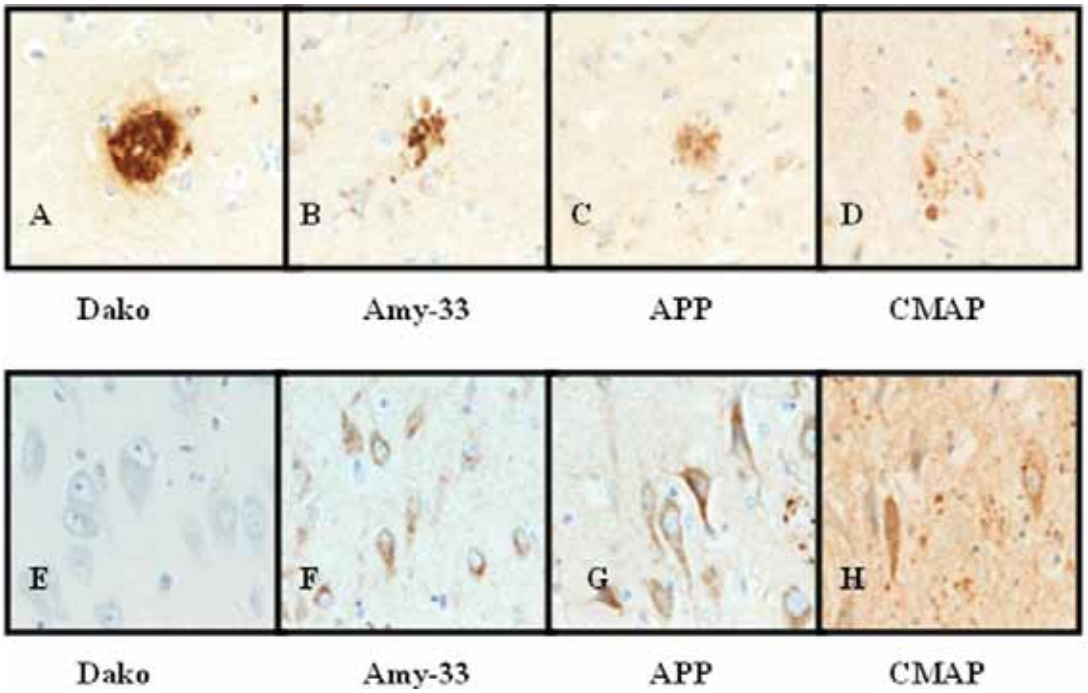

Figure 3.7 Immunoreactivity within cortical neurons of an Alzheimer's disease control case.

The DAKO and University of Melbourne amyloid-beta antibody immunolabelled the core of neuritic plaques (A) and the Amy-33 amyloid-beta, APP and CMAP antibodies show diffuse staining of the neuritic processes of neuritic plaques (photomicrographs B to D). The DAKO and University of Melbourne amyloid-beta antibodies were negative in neurons (E) and Amy-33 amyloid-beta, APP and CMAP antibodies were immunopositive (E to H) (mag. 400x).

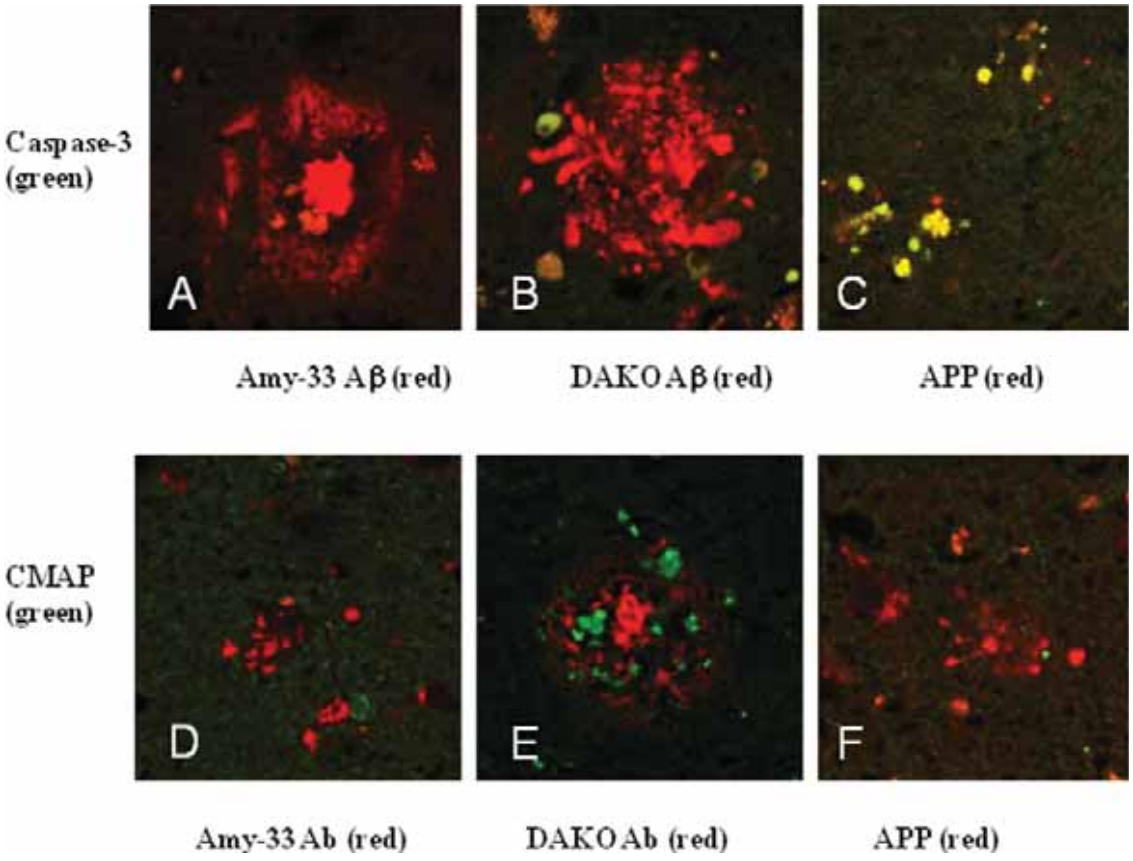

Figure 3.8 APP and Amyloid-beta antibody staining in positive control Alzheimer's disease neuritic plaque.

Human brain with Alzheimer's Disease (mag 400x). The core component of the neuritic plaque is demonstrated in photomicrographs (A) to (F). There is no co-localisation between amyloid-beta antibodies Amy-33 / DAKO and active caspase-3 or CMAP. APP and caspase-3 colocalise within the same neuritic plaque as shown in photomicrograph (C).

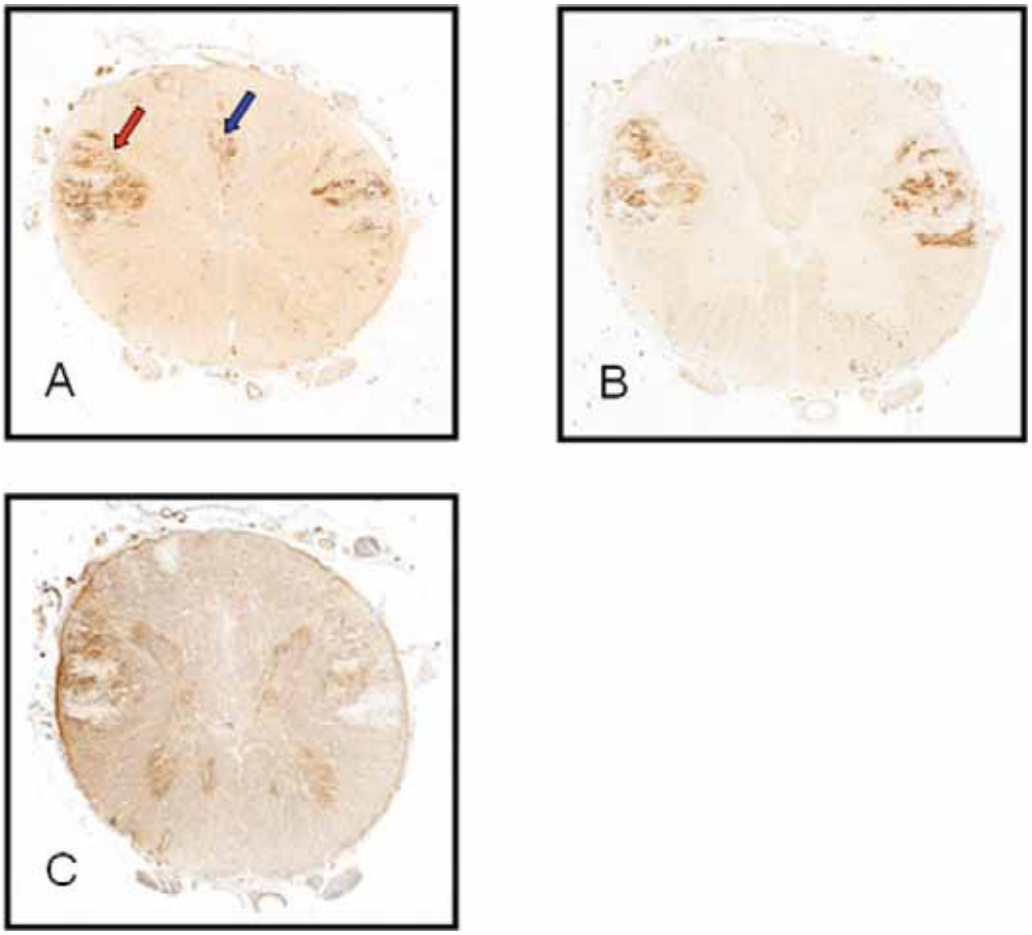

Figure 3.9 APP, AIF and Amyloid-beta antibody staining in human chronic compressive myelopathy.

Cross-section of the human spinal cord showing immunohistochemical staining at the level of L2 in Case 7, a 59 year old male with metastatic compressive myelopathy clinically evident for 6 months. Immunopositive axonal swellings are present in the lateral corticospinal tracts (red arrow) and gracile fasciculi (blue arrow) using APP antibody (A), Amy-33 amyloid-beta antibody (B) and AIF antibody (C). All three markers show similar patterns of axonal immunoreactivity.

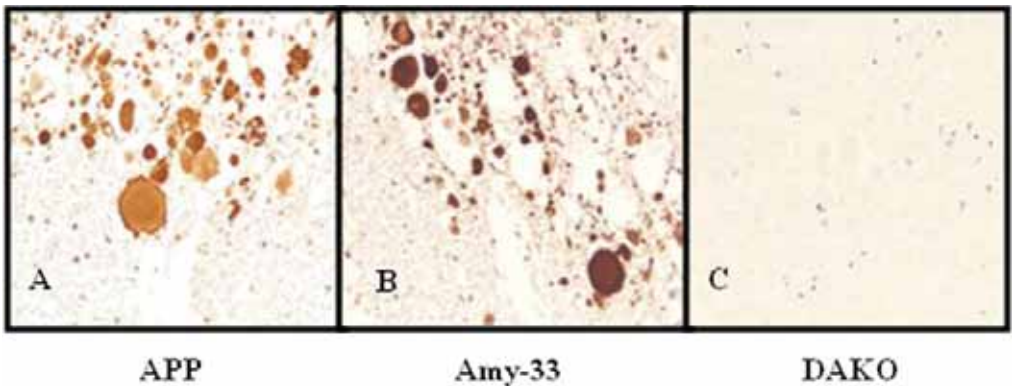

Figure 3.10 APP and Amyloid-beta immunopositivity in human chronic compressive myelopathy.

Axonal immunoreactivity to the APP and Amy-33 amyloid-beta antibodies is present within the damaged white matter (photomicrographs A and B respectively). A negative result was found using the DAKO amyloid-beta antibody (photomicrograph C). (mag.400x).

Table 47. CASE 1 – Compression C3/4 – Immunohistochemical positivity (+) in glial, axonal or neuronal profiles:

Level	APP	Casp-3	Amy-33	CMAP
C2	-	-	+	+
C3	-	-	+	+
C4	-	-	+	+
C4/5	-	-	+	+
C5	-	-	+	+
C5/6	-	-	+	+
C6	-	-	+	+
C6/7	-	-	+	+
C7	-	-	-	+
C7/8	-	-	+	+
C8	-	-	+	+
T1	-	-	+	+

* Shaded rows represent the site of compression

Table 48. CASE 2 – Compression C4/5 – Immunohistochemical positivity (+) in glial, axonal or neuronal profiles:

Level	APP	Casp-3	Amy-33	CMAP
C2	-	-	+	+
C4	-	-	-	+
C5	-	-	+	+
C6	-	-	+	+
C8	-	-	+	+

* Shaded rows represent the site of compression

Table 49. CASE 3 – Compression C4/5 and C5/6 – Immunohistochemical positivity (+) in glial, axonal or neuronal profiles:

Level	APP	Casp-3	Amy-33	CMAP
C3	-	-	+	+
C4	-	-	+	+
C5	-	-	+	+
C6	-	-	+	+
C7	-	-	+	+
C8	-	-	+	+
T1	-	-	+	+

* Shaded rows represent the site of compression

Human Neoplastic Compressive Myelopathy

All seven neoplastic compressive myelopathy cases showed APP immunoreactivity in axonal profiles of predominantly enlarged diameter but also in normal diameter axons. Three of these cases also had immunoreactivity to the active caspase-3 antibody in axonal swellings. Axons were frequently immunopositive to the Amy-33 amyloid-beta in association with APP immunopositivity but not to the DAKO or University of Melbourne amyloid-beta antibodies.

Table 50. Summary of immunohistochemical results in human neoplastic compressive myelopathy – APP, caspase-3, CMAP and amyloid-beta antibodies.

ANTIGEN	CASE 4	CASE 5	CASE 6	CASE 7	CASE 8	CASE 9	CASE 10
APP	Positive axonal swellings	Glial and axonal staining	Positive axonal swellings	Positive axonal swellings, neuronal and glial staining	Axonal staining all segments	Axonal and neuronal staining at, above and below both sites	Rare staining axonal swellings at site
Caspase-3	Positive axonal swellings	Negative	Rare staining axonal swellings	Positive axonal swellings	Axonal staining above, below, greater number at site	Negative	Negative
AMY-33	Positive axonal swellings	Neuronal staining all levels, glial staining S1 and conus	Positive axonal swellings all, neuronal staining	Neuronal staining, axonal staining, glial staining all segments	Neuronal and glial staining at, above and below site	Neuronal and axonal staining at, above and below site	Neuronal staining all, axonal staining between lesions
University of Melbourne amyloid beta	Negative	Negative	Negative	Negative	Negative	Negative	Negative
Dako amyloid beta	Negative	Negative	Negative	Negative	Negative	Negative	Negative
CMAP	Positive glia, neurons, ependymal cells and axons	Positive glia, neurons, axons and ependymal cells	Positive glia, axons and ependymal cells	Positive glia, neurons, ependymal cells and axons	Positive glia, neurons, ependymal cells and axons	Positive glia, neurons, ependymal cells and axons	Positive glia, axons and ependymal cells

Table 51. CASE 4 – Immunohistochemical positivity (+) in glial, axonal or neuronal profiles:

Level	APP	Casp-3	Amy-33	CMAP
T2	+	+	+	+
T3	+	+	+	+
T4	+	+	+	+
T5	+	+	+	+

* Shaded rows represent the site of compression

Table 52. CASE 5 – Immunohistochemical positivity (+) in glial, axonal or neuronal profiles:

Level	APP	Casp-3	Amy-33	CMAP
L5	-	+	-	+
S1	+	+	+	+
conus	+	-	+	+

* Shaded rows represent the site of compression

Table 53. CASE 6 – Immunohistochemical positivity (+) in glial, axonal or neuronal profiles:

Level	APP	Casp-3	Amy-33	CMAP
C2	+	+	+	+
C3	+	+	+	+
C4	+	+	+	+
C5	+	+	+	+
C6	+	-	+	+
C7	-	-	+	+

* Shaded rows represent the site of compression

Table 54. CASE 7 – Immunohistochemical positivity (+) in glial, axonal or neuronal profiles:

Level	APP	Casp-3	TUNEL	Amy-33	CMAP
T10	+	-	+	+	+
T11	+	-	+	+	+
T12	+	-	+	+	+
L1	+	-	+	+	+
L2	+	+	+	+	+
L3	+	+	+	+	+

* Shaded rows represent the site of compression

Table 55. CASE 8 – Immunohistochemical positivity (+) in glial, axonal or neuronal profiles:

Level	APP	Casp-3	Amy-33	CMAP
C3	+	-	+	+
C4	+	+	+	+
C5	+	+	+	+
C6	+	+	+	+
C7	+	+	+	+
C8	+	+	+	+
T2	+	+	+	+
T3	+	+	+	+
T7	+	+	+	+
T8	+	+	+	+
T9	+	+	+	+
T10	+	+	+	+
T11	+	+	+	+
T12	+	+	+	+
L5	+	-	+	+

* Shaded rows represent the site of compression

Table 56. CASE 9 – Immunohistochemical positivity (+) in glial, axonal or neuronal profiles:

Level	APP	Casp-3	Amy-33	CMAP
C3	+	+	+	+
C4	+	+	+	+
C5	+	+	+	+
C6	+	+	+	+
C8	+	+	+	+
T2	+	+	+	+
T3	+	+	+	+
T7	+	+	+	+
T8	+	+	+	+
T9	+	+	+	+
T10	+	+	+	+
T11	+	+	+	+
T12	+	+	+	+
L5	+	+	+	+

* Shaded rows represent the site of compression

Table 57. CASE 10 – Immunological positivity (+) in glial, axonal or neuronal profiles:

Level	APP	Casp-3	Amy-33	CMAP
C2	-	+	-	+
C3	-	+	-	+
C4	-	+	+	+
C5	-	+	+	+
C6	-	+	+	+
C7	-	+	+	+
C8	+	+	+	+
T1	-	+	+	+
T2	-	+	+	+
T3	-	+	+	+

* Shaded rows represent the site of compression

Human Syringomyelia

No APP immunopositivity was found. The Amy-33, Dako and University of Melbourne amyloid-beta antibodies were negative in axons.

Table 58. Immunohistochemical staining in syringomyelia cases – morphological findings

ANTIGEN	CASE 19	CASE 20	CASE 21
APP	Neuronal staining	Negative	Negative
Caspase-3	Negative	Negative	Negative
AMY-33	Neuronal staining at the site	Neuronal staining below the site	Neuronal staining at and below the site
University of Melbourne amyloid beta	Negative	Negative	Negative
Dako amyloid beta	Negative	Negative	Negative
CMAP	Immunopositive	Immunopositive	Immunopositive

Table 59. CASE 19 – Syringomyelia series – Immunohistochemical positivity (+) in glial, axonal or neuronal profiles:

Level	APP	Casp-3	Amy-33	CMAP
C8	-	-	-	+
T2	+	-	+	+
T4	+	-	-	+
T7	-	-	+	+

* Shaded rows represent the site of compression

Table 60. CASE 20 – Syringomyelia series – Immunohistochemical positivity (+) in glial, axonal or neuronal profiles:

Level	APP	Casp-3	Amy-33	CMAP
C2	-	-	-	+
C3	-	-	-	+
C4	-	-	-	+
C7	-	-	-	+
L2	+	-	+	+

* Shaded rows represent the site of compression

Table 61. CASE 21 – Syringomyelia series – Immunohistochemical positivity (+) in glial, axonal or neuronal profiles:

Level	APP	Casp-3	Amy-33	CMAP
C6	+	-	+	+
T7	+	-	-	+
L4	+	-	+	+
S2	+	-	+	+

* Shaded rows represent the site of compression

3.5 Discussion

A more detailed understanding of the pathophysiology of compressive myelopathy will aid in decisions regarding decompressive surgery and the development of conservative treatments. Apoptosis in an experimental polymer model of chronic compressive myelopathy is studied for the first time.

The following hypotheses will be discussed in order:

1. **Cellular pathology and apoptotic cell death is maximal at the site of compression in chronic compressive myelopathy.**
2. **Ongoing axonal changes and white matter degeneration follow chronic compressive SCI.**
3. **Functional abnormalities, cellular pathology and apoptosis are reduced by decompression.**
4. **Early decompression (24 hours) produces a greater reduction in cellular pathology and apoptotic cell death than late decompression (3 weeks).**

1. Cellular pathology and apoptotic cell death is maximal at the site of compression in chronic compressive myelopathy.

The underlying pathophysiology in chronic spinal cord compression is complex, with secondary cell death potentially contributing to the variable response to surgery, and there is potential future therapeutic benefit in addressing the molecular pathways underlying apoptosis. This study aimed to address the question of whether apoptosis occurs in experimental chronic compressive myelopathy and to compare and contrast with evidence in human material.

The majority of research into the pathophysiology of human chronic compressive myelopathy focuses on experimental evidence, but fewer studies analyse the underlying molecular pathophysiology. A large proportion of the literature on the pathophysiology of chronic compressive myelopathies describes in detail the conditions producing compression such as spondylosis where ossification of the posterior longitudinal ligament, calcification and thickening of the ligamentum flavum, disc prolapse and osteophytosis contribute to the pathology. An early study of human compressive myelopathy found that compression of the anterior sulcal arteries anteriorly, and the posterior spinal arteries lead to reduced intramedullary flow affecting primarily the central grey matter (Hashizume et al., 1984). Few studies have focused on the molecular changes present within the cord itself. Following the neuronal activation of glia (Bradl and Lassmann, 2009), ischaemia or the release of toxic factors, axoplasmic transport disruption, axonal degeneration and glial apoptosis has been proposed to contribute to the pathophysiology of cervical spondylotic myelopathy (Fehlings et al., 1998) (**Figure 3.11**) but the spatiotemporal extent of these changes remains unknown.

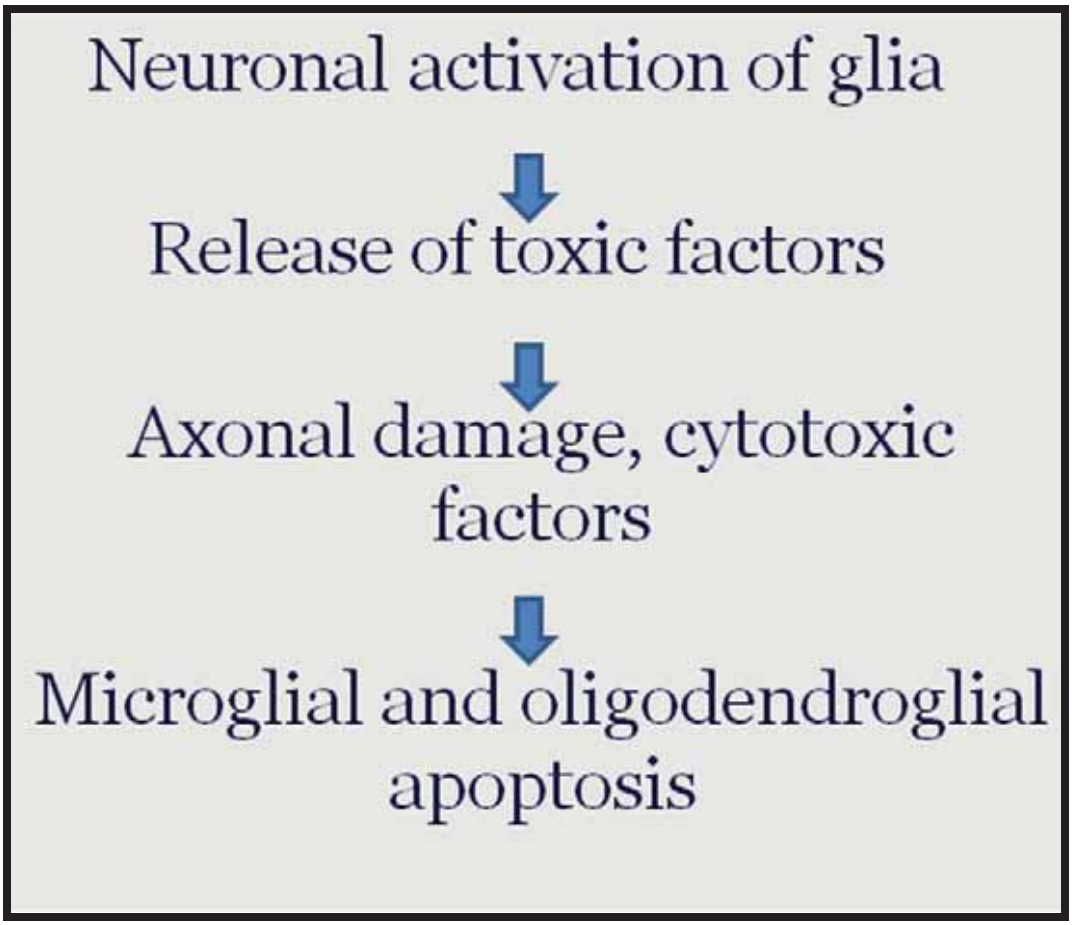

Figure 3.11 Potential role of apoptosis in the pathophysiology of chronic compressive myelopathy.

Fehlings and Skaf. (1998) proposed that the neuronal activation of glia and release of toxic factors such as free radical, cations and glutamate leading to glial apoptosis may be crucial in the pathophysiology of cervical spondylotic myelopathy.

The **rodent model** of **chronic compressive myelopathy** was an inexpensive and reproducible model using a gradually expanding polymer previously characterised in two studies (Kim et al., 2004, Kasahara et al., 2006) in which the polymer was inserted using a suture threaded under the laminae. In our experience, this sublaminar technique created unnecessary risk for direct injury to the dura and spinal cord from the needle tip and compression of the spinal cord from the needle itself. Spinous processotomy is a newly described technique developed in our laboratory for the insertion of the expandable polymer in order to minimise trauma to the dural surface. The model characterised by Kim and colleagues (2004) was further improved by stabilising the polymer to the posterior canal surface in order to replicate the 'fixed' nature of an osteophytic lesion in the human over which the cord moves during neck flexion and extension (Hayashi et al., 1987).

Our study avoided the calculation of a percentage of apoptotic cells which is considered broad, often confusing and unobjective (Kroemer et al., 2008). Furthermore, a panel rather than single immunomarker was used in the detection of apoptosis in this study. **At the site of compression** in the **chronic experimental compression** model, neuronal and glial immunopositivity for apoptotic markers was maximally present. In cases with necrosis present at the site of compression, cells immunopositive for apoptotic markers including the 'gold standard' biomarker of late DNA changes, TUNEL, were maximal in number immediately adjacent to these areas. Glial and neuronal staining was rare using TUNEL but was present at the site of compression in the 1 week injury group. Although not directly comparable, it is interesting to note the smaller spatial distribution of TUNEL-positive cells observed in our chronic experimental studies compared with the human case series. Neuronal staining for markers of early apoptosis, active caspase-3, PARP, and the mitochondrial pathway protease, caspase-9, was again maximal at the site of compression (T12 level).

Neuronal and glial nuclear reactivity for the caspase-independent marker, **apoptosis inducing factor (AIF),** was present in each injury group, suggestive of apoptosis. The spatiotemporal pattern of immunopositivity of AIF has not previously been described in human and experimental chronic compressive myelopathy. AIF immunoreactivity correlated with mitochondrial protein staining in the cytoplasm of neurons, glia and ependymal cells in **chronic experimental compressive myelopathy**. This may represent the mitochondrial translocation of the AIF molecule, which has been suggested to occur

after induction of apoptosis using staurosporin (Susin et al., 1999) or HIV infection (Ferri et al., 2000) and has been observed in the context of apoptotic cell death even in the absence of caspase-activity (Susin et al., 2000, Cecconi et al., 1998, Yoshida et al., 1998).

PARP glial immunopositivity was seen throughout the white matter in all cases and appeared in glia showing an oligodendroglial phenotype. In cases which showed neuronal immunopositivity, PARP expression was visible in both the nucleolus and nucleus. This may reflect active DNA repair within the cell and ongoing protein synthesis as a prominent nucleolus, the organelle of ribosomal production, is indicative of high levels of protein assembly in neurons. In cases without necrosis, DNA-PKcs, PARP and TUNEL immunoreactivity was maximal at the site of compression, providing qualitative evidence of apoptosis maximal at the site of compression in the absence of tissue disruption.

In **experimental chronic compressive myelopathy**, caspase-9, PARP and aC3 staining were found in glia distant to the site of compression, up to two segments (6mm) above and below, in all injury groups, suggesting widespread apoptosis. Furthermore, in regions of tissue necrosis affecting the central spinal cord, glial immunopositivity using these markers was greatest in the penumbra surrounding areas, similar to the pattern seen in our human material. Positive immunoreactivity to apoptotic markers was found in glia and neurons as early as 24 hours and persisted up to 20 weeks of chronic compression. Compression over 20 weeks might be considered comparable to years in the human, given the life expectancy of the Sprague-Dawley rat approximates 3 years (Aleman et al., 1998). Due to ethical considerations, there was a significant age difference between the adolescent or early adult rodent and the average age in our human series of 67 years. The difference in physiological reserve and comorbidities between age groups is noted. A list of comorbidities in each human case is provided in the Appendix. A male predominance was selected for study in our human and experimental studies for control. Although our study was constrained by time limitations, a longer duration of compression in future studies may prove useful in defining the duration of apoptotic changes in chronic compressive myelopathy and the long-term response to decompressive surgery.

Our study of **human chronic compressive myelopathy** was designed to contribute to knowledge in two main areas: the spatial distribution of apoptosis; and the white matter damage involving the axon and myelin sheath. In the human series, results were analysed

qualitatively due to the individual variation in spinal cord size and differing injury severity. The topographical distribution of histopathological changes and apoptosis was recorded in detail for each case at multiple levels (see Appendix). **Histopathological changes in the human** were consistent with the central spinal cord injury often seen in severe chronic compressive myelopathy that may be partially ischaemic in origin (Hashizume et al., 1984, Hashizume et al., 1984). **Glia**, in particular oligodendroglia, are vulnerable under ischaemic conditions in the spinal cord (Crowe et al., 1997).

In **human chronic compressive myelopathy**, PARP-positive oligodendrocytes were consistently present **at, above and below** the site of compression. Oligodendrocytes are active in the process of myelination of axons (Keirstead et al., 1999) and their loss may account for the demyelinative changes in CSM (Fehlings et al., 2006). Oligodendroglial cell death may be secondary to apoptosis in human cervical spondylotic myelopathy (Kim et al., 2003). In a mouse model of osteophytosis (Yamaura et al., 2002) TUNEL-positive cells were observed throughout the grey and white matter maximal at the site of compression. TUNEL-positive cells were found in the anterior and lateral white matter columns caudally, and a small-number of TUNEL positive cells were observed in the grey and white matter in the rostral cord (Yamaura et al., 2002). In the same report, TUNEL immunopositive cells were associated with loss of neurons in a single case of human spondylotic myelopathy at the C5 level. These TUNEL immunoreactive cells were also immunopositive for an oligodendrocyte-specific monoclonal antibody (Olig2) but were negative for GFAP suggesting that oligodendrocytes were a vulnerable glial subtype. In the current human and experimental studies, TUNEL positive oligodendrocytes were maximal at the site of compression but also present above and below. Oligodendrocytes, immunopositive for apoptotic markers, were present in Wallerian degeneration of the ascending tracts above and the descending tracts below the compression site in the human. A loss of oligodendrocytes may be associated with demyelinative changes affecting multiple axons.

In our studies of **human spondylotic myelopathy**, active caspase-3 and rarely, Bcl-2 immunopositivity was seen in macrophages in areas of compressive tissue necrosis. Whilst there was no glial or neuronal staining using these antibodies, their presence in macrophages may indicate the engulfment of cells undergoing apoptosis. TUNEL immunoreactivity was maximal in glia above and below the site of compression in cases of

cystic necrosis, indicating an injury penumbra. This was also true for markers of DNA repair, such as DNA-PKcs and PARP which were maximal above and below the site of compression in cases where necrosis was part of the injury spectrum.

In cases of **neoplastic compressive myelopathy** there was again evidence of apoptosis in regions unaffected by necrosis, and this was maximal either at the site or immediately above and below the site where there was tissue disruption. Central chromatolysis of neurons was seen suggestive of damage due to tumour compression of the anterior nerve roots. Central chromatolysis typically occurs 24-48 hours following injury and may either represent an attempt at increased protein production in response to injury with a disruption of axonal transport or a 'damming' of cytoskeletal elements normally found within the axon (McIlwain and Hoke, 2005). Macrophages and lymphocytes were present in regions of cystic degeneration of white and grey matter, consistent with ongoing phagocytic activity and chronic inflammation. Immunopositivity to active caspase-3 was present in axons and may be associated with an accumulation of proteinaceous material within the disrupted axon. DNA-PKcs glial immunopositivity was seen in the lateral white matter in association with evidence of demyelination on Weil stain. Glial PARP immunopositivity was found in these regions.

In all three cases of **syringomyelia**, a form of compression from within the cord itself, there was significant loss of anterior horn cells associated with DNA-PKcs, PARP and TUNEL neuronal immunopositivity of surviving neurons. In syringomyelia cases, heterogeneous AIF antibody staining of glia, neurons and ependymal cells lining the syrinx was widespread, occurring both at the margins of the syrinx and distant from the affected levels. Furthermore, glial staining for these markers was maximal at the site of the syrinx and often absent away from the syrinx. TUNEL-positive glia were maximal in the deep posterior white matter. PARP staining was widespread in glia throughout the white matter and was present in a sub-population of glia with morphology of oligodendrocytes. DNA-PKcs immunopositivity was found in qualitatively fewer glial cells than PARP. TUNEL immunopositivity was maximal in the central cord. This pattern of immunostaining may represent ongoing DNA damage and subsequent cell death with remodelling in the peripheral white matter or more mildly affected regions. Structural damage to the central cord is described in human chronic compressive myelopathy and in theory may be associated with apoptotic cell death.

Although our results did not suggest the presence of significant AIF-associated apoptosis in **human spondylotic myelopathy**, it does not exclude AIF as a potential early factor in the progression of neuronal and glial cell death at an earlier time-point in these cases. AIF is a bifunctional protein and its role in cell death is thought to be independent from redox activity (Lorenzo et al., 1999). It is beyond the scope of this study to determine if the absence of AIF nuclear staining was due to a lack of activation or the presence of inhibitory factors, as a delay or inhibition of one apoptotic cascade may trigger the activation of an alternative cascade (Johnson et al., 1999; Lankiewicz et al., 2000). Given the increasingly recognised complexity of apoptotic cascades, alternative cascades may as yet be undescribed. Important questions to be answered include whether internal processes are sufficient to cause mitochondrial permeabilisation, and what evidence there is for the mitochondrial release of proteins via predominantly caspase-dependent or caspase-independent pathways.

The occurrence of mitochondrio-nuclear translocation of AIF was also unlikely to occur in **neoplastic compression**. AIF immunoreactivity in neoplastic compression was only present in the cytoplasm of neurons including the axon and there was a total absence of nuclear immunopositivity. AIF translocation to the nucleus and associated apoptotic changes have previously been demonstrated in numerous neurological conditions including traumatic brain injury in the rat (Zhang et al., 2002), where intranuclear localization of AIF was found in the cortex and hippocampus as early as 2 hours after injury and persisted for 72 hours. The shortest duration of survival after onset of symptoms associated with metastatic compression was 25 days. Further analysis of earlier time points after onset of compression is recommended and experimental modelling of metastatic compression may be useful for this purpose. Future studies might include the use of ultrastructural analysis to better localise the AIF molecule.

In contrast to earlier studies of chronic compressive myelopathy, there was minimal immunopositivity for the **Fas and Bcl-2** immunological markers in **experimental and human studies**, and this may indicate the absence of 'extrinsically' activated apoptosis in which there is activation of the Fas death receptor. This receptor initiates apoptosis via the binding of the Fas-associated death domain (FADD) to procaspase-8. The nature of injury in this model may have been insufficient to trigger extrinsic apoptosis. A mild injury in our cases is suggested by the focal nature of changes on light microscopy and the mild deficits

on functional analysis, for example the median BBB score of 19 at 20 weeks compression. A recent study analysed extrinsic apoptotic pathways using a mouse model of hyperostosis of the ligamentum flavum with compression of the C2-3 segments and the development of severe paresis over a chronic period of 4-7 months (Yu et al., 2009). This duration of onset is comparable to clinical progression in human CSM of months to years (Matz et al., 2009). Anti-Fas and anti-FasL immunostaining of frozen sections were correlated with counts of TUNEL positive neurons, glia and macrophages at sites randomly selected form the epicentre of the lesion in cross-section. A loss of neurons (NeuN positive) and oligodendrocytes (anti-CNPase positive) was demonstrated at the severely compressed epicentre. In contrast, an increase in glial cell number was demonstrated above and below the lesion, suggesting a survival or compensatory response to injury. A significant increase in the number of immunopositive glial cells for Fas was demonstrated at the epicentre however this was not the case for neurons, in which a significant increase in Fas positive cells was present only caudally. The study concluded that neurons and oligodendrocytes appear vulnerable to apoptosis in CSM, and that this may contribute to demyelinative changes, although myelin changes were not directly analysed.

Results of our study expand on the few pre-existing studies suggesting a role of glial apoptosis following cord compression in cervical spondylosis (Yu et al., 2009). A novel experimental model was developed and results were compared and contrasted with a human case series. An alternative model for future study is the twy mouse model (Takenouchi et al., 2008) in which hyperostosis and cervical compression develops over months. Results from this model suggest a possible stress-activated / mitogen-activated protein kinase pathway of apoptosis. Although this model is a useful replication of degenerative changes leading to chronic compressive myelopathy, the lesion produced may be asymmetrical, and the severity and onset of compression may vary between animals. Our studies utilise an inexpensive, small animal model of polymer expansion to a repeatable severity. Compression performed at the T12 level, palpable at the base of the thoracic cage, facilitated reproducibility. Larger animal trials may be of benefit in more closely replicating the physiological conditions found in human spondylotic myelopathy.

These studies provide observational and semi-quantitative evidence that neuronal and glial apoptosis occurs in several forms of human compressive myelopathy at various time points of compression and severity. These changes are maximal at the site of injury or, in cases of

severe necrosis, at the margins of injury. Furthermore, the presence of DNA damage was suggested by TUNEL, DNA-PKcs and PARP immunopositivity. PARP immunopositivity was found in a subset of glia with the morphology of oligodendrocytes and may indicate a particular vulnerability of these glial cells to injury. It was beyond the scope of the study to determine glial subtypes due to the absence of a reliable oligodendrocyte marker. Apoptosis of oligodendrocytes has not previously been demonstrated in neoplastic compressive myelopathy or syringomyelia. Further studies could incorporate double-immunolabelling with a panel of different markers as these become available. Changes distal to the site of compression may be accounted for by many mechanisms such as axoplasmic transport disruption, primary cellular damage, oxidative stress, inflammation, calcium and glutamate excess, and membrane damage. Apoptosis may subsequently lead to significant destruction of tissue and cell death. Our study provides novel evidence of apoptosis in the setting of neoplastic compressive myelopathy and syringomyelia in association with axonal changes.

In summary, our studies in the rodent and human correlated histopathological and immunohistochemical evidence of early and widespread apoptosis and functional changes in chronic compressive myelopathy. Apoptotic changes were shown as early as 24 hours following the onset of compression, a finding not previously demonstrated in experimental chronic compression. The gradual and often mild initial stage of chronic compressive myelopathy in the human was replicated using a novel expandable polymer model. Further detailed studies of the temporospatial changes within the spinal cord and the correlation with functional outcome might assist in determining future therapeutic targets. Improved knowledge of the relevant pathophysiological mechanisms is likely to assist in forming effective pharmacological or genetic therapies which may carry the potential to assist in targeting distal apoptosis. The usefulness of, indications for, and timing of surgical decompression requires much ongoing research.

2. Ongoing axonal changes and white matter degeneration follow chronic compressive SCI.

In **experimental mild chronic compressive myelopathy**, there was a striking reduction of the posterior white matter area maximal at the site of compression in association with immunopositivity for apoptotic markers. The total cross-sectional area of the cord at the site of compression, as determined using digital analysis, decreased with the duration of chronic compression and returned to control levels in the decompression groups (e.g. 3 week group mean 3.05mm^2 increasing following decompression at 3 weeks to 5.75 mm^2) associated with visible restoration of the tissue architecture. A maximal reduction in WM occurred at the 3 week time point despite the absence of necrosis. This may have been due to a gradual reduction of tissue volume, whether due to a loss of tissue elements or a reduction in their size, rather than purely mechanical displacement of the white matter laterally. A significant increase in posterior white matter area was found above (mean 0.4508, $p = 0.0042$) and below the site of compression at 3 weeks (mean 0.5800, $p < 0.0001$) which may represent a 'damming up' of axoplasmic flow above and below the site of compression. The apparent restoration of the normal posterior column tissue architecture and tissue volume could be further investigated using weight-based volumetric analysis, structural axonal and myelin changes on electron microscopy to assess the microtubular structure and axolemma, and in vivo imaging to assess the direction of axoplasmic flow and the effect of compression at multiple sites. Therapies aimed at the preservation of axoplasmic transport, myelin and supporting oligodendrocytes may be of benefit in mild spectrum chronic compressive myelopathy.

APP immunopositive axonal swellings were greatest in number **at the site** of compression in injury groups, predominantly in the posterior white matter, but were also seen **distant** from the site of injury. APP immunopositivity was consistent with persisting axonal damage and disruption of fast axoplasmic transport in a subset of axons. APP immunopositive axonal swellings are an important finding, as early disruption of anterograde axoplasmic transport has been associated with axonal swellings with accumulated APP, mitochondrial failure, sodium and calcium influx, myelin changes and axonal degeneration (Coleman, 2005). APP immunoreactive axonal swellings were found at all time points. APP axonal immunopositivity was rare or occasionally present in compression groups but present in frequent numbers in the early (24 hour) **decompression**

group. APP immunostaining was seen in neuronal cytoplasm which may represent physiological processes (Coria et al., 1992).

In some cases, normal WM architecture was seen in surrounding regions, whilst in others there were axonal swellings. Furthermore, there was a loss of myelin staining above the site at 20 weeks duration of compression. It is hypothesised that a disruption in axoplasmic transport occurs in a subset of axonal swellings, greatest in the penumbral region.

A loss of Olig2 immunopositive oligodendrocytes was seen at 9 and 20 weeks in the posterior white matter at the site of compression, suggesting cell death in a subset of oligodendroglia. Reactive astrocytosis was indicated by the pattern of GFAP staining in persisting compression and decompression groups and reactive changes were minimal at these time-points. A qualitative increase in Iba1 staining demonstrated a significant presence of resident and likely activated microglia, most profound at 1 week compression. Reactive perivascular microglia were present at 24 hours, 3 weeks, and less so at 9 and 20 weeks. Similar patterns were seen in the decompression groups however variation between cases was greater, suggesting a variable response of glial cells following decompressive surgery. Changes in axoplasmic transport and demyelinative processes in a subset of axons may be associated with astrocytic and microglial responses.

In **human chronic compressive myelopathy**, irregular, focal axonal swellings were present within the white matter and represent the accumulation of cytoplasmic material due to disrupted anterograde axonal transport. The presence of demyelinative changes on Weil stain, consistent with possible Wallerian degeneration, may be a late change associated with an early disruption in axoplasmic transport and the formation of axonal retraction bulbs (Coleman 2005). Imaging studies have supported the potential for axonal degenerative changes in chronic spinal cord compression (Loy et al., 2007, Cheung et al., 2009). Thus a window of opportunity may exist for treatment, especially in light of evidence that even with preservation of less than 10% of axons, substantial neurological function may remain (Fehlings and Tator, 1995).

In cases of **spondylotic myelopathy**, axonal swellings were not identified on haematoxylin or APP immunostaining. A loss of myelin staining in ascending and descending tracts consistent with Wallerian degeneration was seen.

In cases of **neoplastic compression**, the presence of axonal swellings and APP immunopositive axonal changes were present **at, above and below the site** of compression. APP immunopositivity in axonal swellings appeared maximal at the site of compression in all areas of the white matter suggesting widespread damage. It is beyond the scope of this study to distinguish between primary and secondary changes, nor between axonal swellings and retraction bulbs.

Axonal swellings were also immunopositive using the Amy-33 amyloid-beta antibody, The Amy-33 antibody immunolabels a smaller region on the amyloid-beta peptide than DAKO or University of Melbourne antibodies which label the whole 4-42 amino acid amyloid beta peptide, and therefore there is the potential for cross-reaction with different antigens. Alternatively, the positive Amy-33 immunostaining may indicate the break-down of APP into amyloid-beta peptides in axonal retraction bulbs. Axonal swellings have been associated with amyloid-beta plaque formation in Alzheimer's disease models (Tsai et al., 2004). The C31 fragment of the APP molecule may be a significant mediator of cytotoxic mechanisms (Park et al., 2009).

A subset of enlarged axons were immunopositive for caspase-3 antibody which may represent the accumulation of protein within the damaged axon secondary to disrupted axonal transport. In one case, axonal swellings were immunopositive for caspase-3, DNA-PKcs, caspase-9 and Fas antibodies, possibly due to an accumulation of proteins or organelles such as mitochondria which may be involved in apoptotic pathways. It is outside the limits of this study to assess whether caspase-activation involving mitochondria and release of cytochrome-c occurs at the site of axonal injury or whether upstream apoptotic processes in the cell-body itself might lead to caspase production which is then transported along the axon. It is not known whether there is any molecular interaction between APP and caspase-3 at the site of accumulation.

There were no axonal swellings observed in **syringomyelia**. This is perhaps unsurprising, as their presence is not previously described in this condition, the clinical progression documented in clinical reports was very gradual, and relatively mild histopathological changes were found in comparison to the spondylotic and neoplastic compression cases. There was a loss of myelin staining and PARP immunopositive oligodendroglial cells suggesting possible apoptosis of oligodendoglia. A loss of oligodendrocytes may be

associated with deleterious changes within the myelin sheaths and the potential to compromise axonal transport.

One marker of amyloid-beta, Amy-33, showed immunopositivity within neuronal nuclei suggesting potential proteolysis of APP into the neurotoxic peptide, amyloid-beta, however this finding was contrasted by the negative staining of University of Melbourne and DAKO amyloid-beta antibodies. Further studies are required using alternative markers of amyloid-beta. The specificity of the CMAP antibody was uncertain due to heterogeneous staining of all cell types. Caspase-3 immunopositivity was minimal and is unlikely to be present at these time-points as an enzyme used in the breakdown of APP. There is insufficient evidence for the proteolysis of APP or the production of caspase-mediated amyoid-beta peptide as a neurotoxic process in syringomyelia.

3. Functional abnormalities, cellular pathology and apoptosis are reduced by decompression.

A single level, compressive injury was selected for study with analysis of the effect of a common surgical approach for **experimental chronic compressive myelopathy** - posterior decompressive laminectomy. This *in vivo* study involved a simple direct epidural compression of the spinal cord, with a gradual increase in polymer size over 48 hours, with compression persisting up to 20 weeks, aiming to replicate the insidious nature of chronic spinal cord compression in the human. Decompressive laminectomy was performed at an early time-point, 24 hours, and later time-point, 3 weeks, with survival of these groups to 9 weeks in order to assess the long-term outcome of surgery. Our experimental functional results were consistent with mild locomotor and motorsensory impairment. Using the tail-flick, in which sensory as well as motor function is tested, a significant increase in measured time versus control was found at 1 week ($p < 0.0001$) and 3 weeks ($p = 0.0015$). A progressive decrease in BBB locomotor score was seen at 1, 3, 9 and 20 weeks ($p < 0.0001$). Since our study was performed, the use of a straight-alley with reward assessment of BBB score has been shown to have improved day to day correlation (Wong et al., 2009) and would be used for future studies.

Functional results were comparable between injury and decompression groups despite the immunohistochemical differences already discussed. There was no significant change in tail-flick scores in 9 week compression versus 24 hour / 3 week decompression groups ($p = 0.8401$) and similar rotarod function was found across the three groups ($p = 0.2153$). BBB scores were lower at 9 weeks chronic compression (median 19) than in the 24 hour (median 21) and 3 week (median 20) decompression groups but this was not significant ($p = 0.0666/0.0975$). Foot faults on ledge beam increased in the 9 week compression group compared to both decompression groups but this was not significant. Although further determining studies would be needed, the similarity in functional testing between persisting compression and decompression groups may be due to inadequate sensitivity of the tests used, the preservation of sufficient functioning axons in the decompression groups to allow for signalling along the spinal cord, cellular proliferation, or cellular response to apoptotic pathways enabling survival of the cell. Further studies could use alternative testing such as open field walk or behavioural analyses.

To date, few studies have focused on chronic spinal cord injury in contrast to acute spinal cord compression. Studies on **human chronic compressive myelopathies** such as cervical spondylotic myelopathy have tended to focus on clinical and radiological findings in level II evidence studies, attempting to correlate these with surgical interventions rather than explore further the fundamental pathophysiological changes underlying these conditions. Such studies often aim to address the pressing question of 'when is surgery indicated?' noting the unpredictable outcome after decompression. Previous studies of decompressive laminectomy in humans have documented a variable response to surgery (Fehlings, 2006).

The question of whether irreversible cell death has occurred is critical in determining future diagnostic and management strategies in chronic compressive myelopathy. Suggested criteria include an increase in the number of caspase-3-positive cells. This was difficult to assess in human cases of CSM, syringomyelia and neoplastic compression due to the variability between cases in clinical presentation (e.g. paraplegia versus paraparesis), anatomy (e.g. cord size and level), and pathological findings. There was a difference in the number of immunopositive cells using all apoptotic markers compared with normal controls. Our experimental studies aim to address the question of whether reversible apoptosis occurs in chronic compressive myelopathy using decompression.

At the **site of compression in experimental chronic compression**, tissue necrosis on haematoxylin and eosin staining was minimal in all injury groups but was significantly greater in the decompression groups, possibly reflecting a substantial second insult to the spinal cord due to surgery. This might be explained by the mechanical force of removal of the polymer, removal of the bone, the potential for microvascular and macrovascular compression during surgery, vasospasm or systemic hypotension with subsequent ischaemia, and the increased physiological requirement to endure repeat surgery. Of note is the absence of significant change between negative controls (naïve, sham) and the vehicle group in which the polymer was inserted and immediately removed, nor was there a significant change in the repeat-surgery sham group, negating the hypothesis that the surgery itself is the cause of progressive cellular damage following decompression. Future studies could analyse earlier time-points following repeat surgery, for example at 3, 6, 12 or 24 hours, to determine when these changes occur after decompression.

A previously undescribed reversible reduction of posterior white matter is noted at the site

of compression with swelling of the white matter above and below the site, suggestive of disruption of bidirectional axoplasmic flow. Axonal swellings were present within the WM, however these can occur on axons in which structural continuity is maintained, raising the possibility of reversibility in this condition. Despite a return of normal posterior column architecture in the decompression groups, immunostaining for apoptotic markers was similar or in some cases semi-quantitatively greater following decompression and survival to 9 weeks. A significant increase in posterior white matter area was found above (mean 0.4508, $p = 0.0042$) and below the site at 3 weeks (mean 0.5800, $p < 0.0001$) suggesting possible disrupted axoplasmic transport away from the compression. It is beyond the scope of this study to determine why restoration of the tissue architecture results in worsened apoptotic changes and axonal injury in chronic compression. It is possible that a second surgical insult involving ischaemic or hypoxic conditions, or adverse molecular signalling following restoration of axoplasmic flow may contribute to axonal degeneration. The finding of a negative vehicle control supports a non-iatrogenic cause.

A disruption in axoplasmic transport from the cell body, potentially from early damage to microtubules or demyelinative changes, can cause axonal degeneration (Mack et al., 2001, Coleman 2005). The process of axon death and demyelinative changes is comparable to the delayed cell death of apoptosis (Raff et al., 2002), and indeed axonal changes in this study have been demonstrated to occur in association with apoptosis of glial cells heterogeneously within white matter. APP immunopositive axonal swellings were maximally present in the deep posterior white matter of the spinal cord in cross-section.

Of note is the presence of TUNEL immunopositive glial cells in both decompression groups, in contrast to the 9 and 20 week persisting compression groups in which staining was minimal, suggesting ongoing apoptosis despite decompression of the spinal cord. This was further supported by a qualitative increase in glial staining using another key marker of apoptosis, active caspase-3, in the decompression groups. Using ELISA assay, aC3 was increased in the 24 hour decompression (mean 0.3167, $p = 0.0108$) and 3 week decompression (mean 0.3099, $p = 0.0182$) groups versus the 9 week persisting compression group (mean 0.1850). Glial and neuronal immunostaining for apoptotic markers occurred at, above and below the site of compression in all persisting compression groups. **Decompressive surgery increased apoptosis and axonal injury** in this new rodent model of chronic spinal cord compression despite restoration of posterior column

area. This study suggests that surgical decompression in mild compressive myelopathy may result in increased cellular damage despite restoration of the gross normal anatomy. The usefulness and timing of decompression surgery patients with chronic spondylotic myelopathy remains uncertain, and further studies are required using large animals, larger cohorts, and randomised trials with blinded follow-up evaluation.

Future studies should ideally use prospective, randomised analysis of decompression surgery. The clinical effect of inhibitors of apoptosis is unknown in this area. Future therapy may involve a combination of such inhibitory agents and appropriately timed decompression of the spinal cord. Additional genetic therapies for glial and neuronal (in particular axonal) regeneration, in conjunction with rehabilitation, could further assist in achieving a better outcome.

4. Early decompression (24 hours) produces a greater reduction in cellular pathology and apoptotic cell death than late decompression (3 weeks).

Apoptotic and axonal changes in experimental chronic compressive myelopathy were greater after decompression in contradiction to the stated hypothesis. Although studies of the histopathological changes following decompression in human spondylotic myelopathy have previously been lacking, Harkey and colleagues (1995) studied a canine model of chronic compressive myelopathy with decompression at 45 weeks and survival on average to 62 weeks. Despite improvement in functional outcome following decompression, a 'polarised' histopathology was evident with three animals showing no or very mild histopathological changes after decompression and three animals with anterior horn cell loss, necrosis and cystic cavitation. Our study supported the findings of variable, and in some cases worsened, histopathological changes. We found that despite restoration of the posterior white matter architecture, cystic necrosis was present in this region in the 3 week decompression group. One case in each decompression group exhibited a central syrinx. There was meningeal thickening suggestive of inflammation, and frequent axonal swellings were found, particularly in the posterior white matter, in contrast to the persisting compression groups. In addition, central chromatolysis of neurons was found in the early (24 hour) decompression group suggestive of neuronal damage. Surgical decompression may restore macroscopic changes but it may worsen cellular pathology.

Apoptosis was greater in decompression groups. Using ELISA, active caspase-3 was greater expressed in the 24 hour decompression (mean 0.3167, $p = 0.0108$) and 3 week decompression (mean 0.3099, $p = 0.0182$) groups versus the 9 week persisting compression group (mean 0.1850). Furthermore, a significant increase in active caspase-3 assay was found in the 24 hour and 3 week decompression groups compared to controls ($p = 0.0181$ and 0.0321 respectively) suggesting a pathological expression of caspase-3. On cross-sectional analysis, immunopositivity using a panel of apoptotic markers was found in anterior, lateral and posterior WM glial cells at, above and below the initial site of compression. Maximal apoptotic staining occurred at the site of compression or in the penumbra surrounding tissue necrosis.

Patients with relatively mild radiological and clinical changes may do poorly after decompression and clinical trials have not yet determined accurate selection criteria for

surgery. It is hypothesised that the degree of functional loss, radiological changes including an increased signal on MRI (Suri et al., 2003) and reduction in the spinal canal diameter prior to surgery are important predictors of outcome but this is yet to be definitively demonstrated.

In future, experimental studies that address the timing of decompression and correlation with diagnostic radiological techniques such as MRI may be crucial in identifying indications for surgery based on the severity of stenosis within the spinal canal as well as microscopic and functional changes. A detailed analysis of the histopathological and cell death changes, correlated with clinico-radiological findings in a case series of human spondylotic myelopathy with decompression, would be of great interest. Studies might include analysis of longitudinal axonal fibres, electrophysiological conduction studies, anterograde and retrograde axonal transport, cell-cycle and apoptotic survival proteins such as Bax, Bcl-x and Bak. Experimental models could be developed using larger animals such as the ferret or sheep, or models that ideally replicate the significant weight bearing stresses applied to the spine and the flexion / extension properties of the spinal cord found in the human. Differences in the pathophysiology and surgical management of cervical, thoracic, lumbar and sacral compressive myelopathy should be compared. As the pathophysiology may vary with age, asymmetry of the lesions, fixed versus mobile lesions or ischaemia, future experimental models should account for such variables. Future studies may also consider the current evidence that apoptosis is widespread and occurs distant to the site of compression.

3.6 Conclusions

3.6.1 Apoptosis

This study describes a new rodent model of chronic compressive myelopathy using a gradually expanding polymer inserted with minimal disruption to compress the spinal cord resulting in a mild spectrum injury. Chronic fixed posterior compression resulted in a potentially reversible loss of white matter at the site of compression suggestive of altered axoplasmic transport. Glial and neuronal immunostaining for early and late apoptotic markers was found at, above and below the site of compression in all compression groups and staining was maximal at the site of compression. Decompressive surgery worsened immunostaining for apoptotic markers and severity of axonal injury despite restoration of posterior white matter area. The variable response to surgical decompression in the human may be due to persisting apoptosis.

Apoptosis is maximal at the site of injury or, in cases of severe necrosis at the site of injury, immunoreactivity is maximal in the penumbra surrounding these areas. In human studies, neuronal and glial apoptotic changes were newly demonstrated in spondylotic myelopathy, neoplastic compression and syringomyelia. Apoptosis was maximal at the site of compression and extended to segments above and below. The pathophysiological changes within the spinal cord during neoplastic tumour compression are largely unaddressed within the literature, and this study contributes to our understanding of secondary cell death. In syringomyelia, apoptosis of cells is proposed as a contributory factor in the pathophysiology, in addition to the forces associated with fluid dynamics.

These studies provide novel qualitative and semi-quantitative evidence that early and widespread neuronal and glial apoptosis occurs in chronic compressive myelopathy at various time points of compression. Thus the spatiotemporal pattern of apoptosis may be considered as ‘diffuse’ in chronic compressive myelopathy. As a result, future therapy is likely to be adjunctive in nature, with potential for a combination of surgical, pharmacological and genetic intervention.

3.6.2 Axonal Injury

APP axonal immunopositivity was consistent with persisting disruption of fast axoplasmic transport in a subset of axons. From our human studies, there is evidence that caspase-3 contributes to the proteolytic cleavage of APP in chronic compressive myelopathy. It is theorised that active caspase-3 protein may be transported along the axon and accumulate with disruption of axonal transport in the axonal retraction bulb. It is possible that activation of caspase-3 via secondary injury mechanisms may trigger the apoptotic cascade with the subsequent demise of the cell. This study does not ascertain whether active caspase-3 may be involved in the production of the neurotoxic peptide amyloid-beta via APP proteolysis. The association of caspase-3 cleavage of APP with amyloid-beta accumulation in human compressive myelopathy in uncertain and further study is required. Apoptotic staining using a panel of immunomarkers suggested glial apoptosis in association with axonal injury and Wallerian degeneration.

CHAPTER 4

RESULTS
ACUTE COMPRESSIVE MYELOPATHY

A rodent model of acute traumatic spinal cord injury was used to assess apoptosis and results were compared with the chronic compressive myelopathy model. Tissue from human cases was also studied for apoptosis. This study investigated the histopathological changes in a laminectomy and extradural 10g weight drop model of spinal cord compression causing incomplete injury at the thoracic level. Animals were sacrificed at 24 hours, 1 week and 3 weeks post injury. A panel of sensorimotor testing was used to assess neurological recovery.

Histopathological changes characterised by central haemorrhagic inflammation and APP immunopositive axonal swellings were maximal at 24 hours post surgery and consistent with human traumatic injury. Glial positivity to TUNEL, the "gold standard" biochemical marker of apoptosis, was seen at 24 hours and at 1 week post-injury. Active caspase-3 immunopositive glial cells were present throughout the white matter, extending above and below the site of injury at all three time points, suggesting persisting apoptosis at 3 weeks post-injury. Immunostaining was qualitatively and semi-quantitatively greatest at the site of injury. Apoptosis was also maximal at 24 hours which correlated with worse functional performance. A recovery to near normal functional and histopathological status occurred by 3 weeks. Neuronal and glial apoptosis was seen in all injury groups.

In human acute compression, histopathological changes were greatest in the central cord, with haemorrhagic necrosis and an acute inflammatory infiltrate. TUNEL, DNA-PKcs and PARP immunopositive glia were found at, above and below the site of injury. Axonal swellings, a subset of which were APP immunopositive in longitudinal and transverse profiles, occurred in the penumbra. APP immunopositive axonal swellings were found above and below the site of injury, suggesting widespread changes in fast axoplasmic transport. There was evidence of myelin damage on Weil staining in cases of longer survival post-injury (26 days, 32 days, and 5 months) and this was associated with APP immunopositivity. Novel evidence is provided that caspase-3 may play a role in the cleavage of APP following acute compressive spinal cord injury. Caspase-3 was found to co-localise with APP using confocal microscopy. The Amy-33 amyloid-beta antibody also co-localised with axons expressing APP. However, the specificity of this antibody is contentious as it labelled the neuritic APP positive component of senile plaques and not the central amyloid-beta recognised by other established amyloid-beta antibodies. Our studies therefore suggest that the Amy-33 antibody is not specific for amyloid-beta, but rather is

another marker for APP.

4.1 Experimental Acute Compressive Myelopathy

4.1.1 Histopathology

24 hour survival

At 24 hours survival there was evidence of major white matter and grey matter pathology, primarily of the central spinal cord. Haemorrhagic necrosis was present in the central cord (**Figure 4.1**) involving a variable proportion of grey matter. Microvacuolation was seen throughout the white matter. Axonal swellings were present in these same regions and were most numerous towards the central cord and in particular the deep posterior white matter in the region of the corticospinal tracts. There was neuronal red cell change bilaterally suggestive of ischaemic change, in addition to neuronal karyhorrexis and cytolysis and neuronal dark cell change. Neutrophilic invasion was present in two cases in the central grey and white matter, consistent with acute inflammation. At one segment above the lesions there was mild haemorrhage in the deep posterior white matter columns. Occasional axonal swellings of the anterior white matter were seen below the site of compression.

1 week survival

There was no microscopic abnormality in 3/6 cases at 1 week survival in contrast to all cases at 24 hours post-injury. Tissue necrosis with macrophages was present in two cases, central chromatolysis of neurons in one case and a further case showing prominent neuronal karyorrhexis. Axonal swellings were present in 4/6 cases. Axonal swellings were most numerous in the deep white matter in the region of the corticospinal tracts. Macrophages were present. Central chromatolysis of neurons was seen in one case.

3 week survival

There was no abnormality on light microscopy using haematoxylin and eosin staining in 2/6 of the cases at 3 weeks survival. Axonal swellings were seen in the anterior, posterior and lateral white matter in one case at the site of injury, and the deep posterior columns in another. Occasional (3-10) axonal swellings were observed at one segment above the

lesion in the deep posterior and lateral white matter, and one segment below in the lateral white matter.

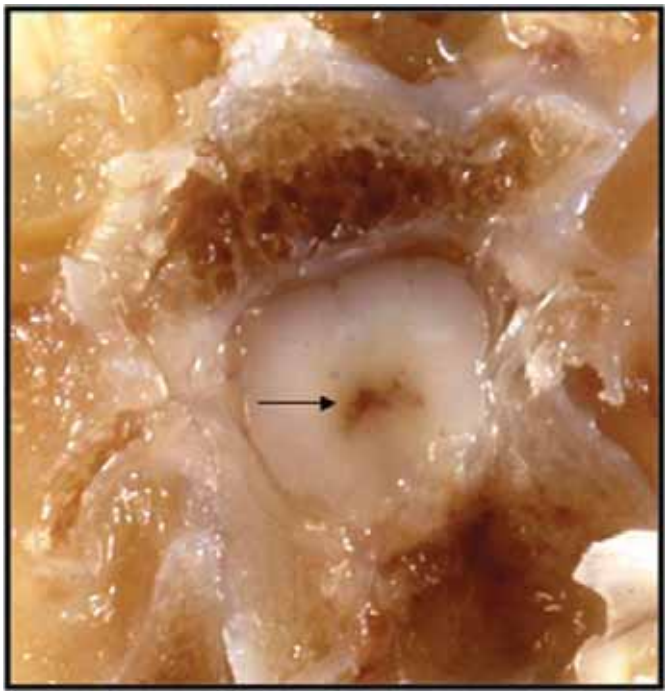

Figure 4.1 Central haemorrhagic necrosis following acute weight drop spinal cord injury in the rodent.

Cross-section of the spinal cord in a case of acute spinal cord injury following weight drop (10g) from a height of 14cm with sacrifice at 24 hours. Haemorrhage is noted within the central cord (arrow).

4.1.2 Apoptosis

Table 62. Immunopositivity in a rodent model of acute compressive myelopathy.

	24 HR	**1 WK**	**3 WK**
APP	+ A	+ A	+ A
Caspase-3	+ G	+ G	+ G
PARP	+ G/N	+ G/N	+ G/N
TUNEL	+ G	+ G	-
Caspase-9	+ G	+ G	+ G
AIF	+ G/A	+ G/N	+ N

+ Immunopositivity A = Axonal G = Glial N = Neuronal

- negative

A typical pattern of immunopositivity is shown in **Figure 4.2**.

24 hour survival

Caspase-9 glial cytoplasmic staining was found in the posterior, lateral and anterior white matter, at, above and below the site of injury in all injury groups. Caspase-3 glial cytoplasmic staining was present in the posterior, lateral and anterior white matter and at 1 and 2 segments above and below the lesion. PARP immunopositive neurons were frequently seen (>10 cells in section) in all glial types and in all regions at, above and below the site of injury. Neuronal and glial staining extended to 2 segments above and below the site of injury. Occasional AIF glial nuclear staining was present in some cases at 24 hours in all regions of the white matter. Axonal swellings also demonstrated AIF immunopositivity, in particular within the lateral white matter. There was no neuronal AIF staining at 24 hours. For TUNEL, one case showed rare glial nuclear staining in the lateral white matter at the 24 hour time point.

1 week survival

Caspase-9 glial cytoplasmic staining was found in the posterior, lateral and anterior white matter. Caspase-3 glial cytoplasmic staining was present in the posterior, lateral and anterior white matter, and at 1 and 2 segments above and below the lesion. PARP immunopositivity was widespread in neurons, in all glial types and in all regions. Neuronal PARP staining was seen up to 2 segments above the site of injury and 1 segment below. Glial PARP staining was seen above and below the lesion. At 1 week, occasional AIF glial cytoplasmic and nuclear staining was present in the anterior, lateral and posterior white matter. Neuronal AIF staining was also seen. At 1 week after injury, widespread glial nuclear staining was seen in one case but all other cases were TUNEL negative.

3 week survival

Caspase-9 glial cytoplasmic staining was found in the posterior, lateral and anterior white matter at, above and below the site of injury. Caspase-3 glial cytoplasmic staining was present in the posterior, lateral and anterior white matter and 1 and 2 segments above and below the lesion. PARP nuclear immunopositivity was widespread in neurons, in all glial types and in all regions. Neuronal and glial PARP staining extended to 2 segments above and below the site of injury. Glial immunopositivity for AIF was rare at 3 weeks. Neuronal AIF cytoplasmic immunostaining was seen. There was no TUNEL positive staining 3 weeks following injury.

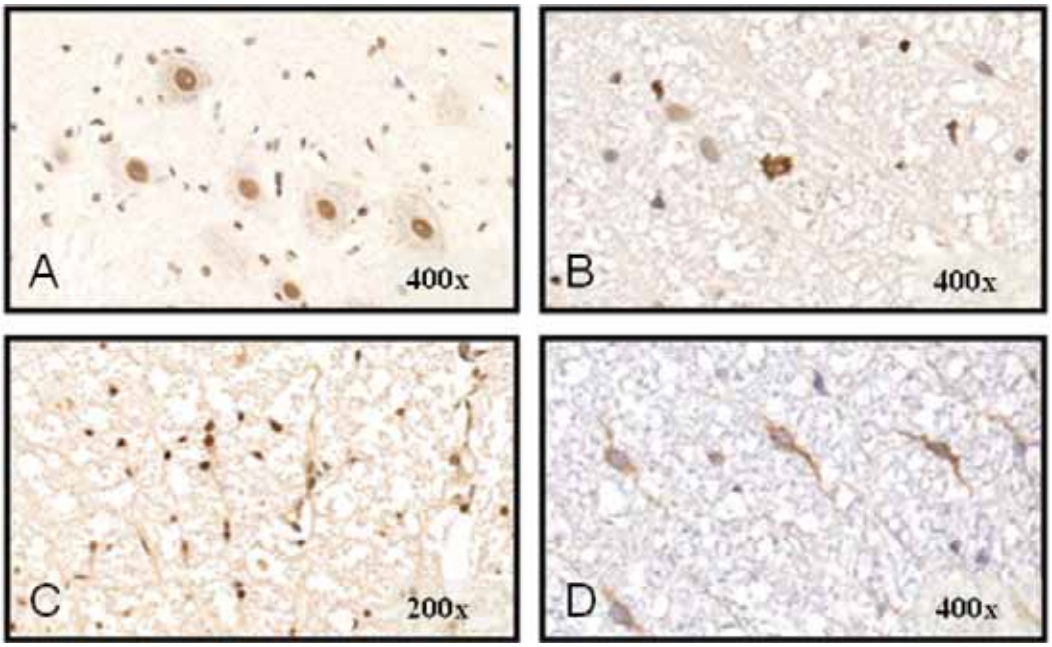

Figure 4.2 Immunohistochemical staining in experimental acute compressive myelopathy using PARP and Caspase-3.

PARP immunopositive neuronal nuclei occur frequently at 24 hours survival (photomicrograph A). An apoptotic glial cell is seen centrally in photomicrograph (B) (mag.400x) and glial nuclear immunopositivity is seen in photomicrograph (C) (mag.200x). Caspase-3 immunopositive glia are present in the lateral white matter at 3 weeks survival (photomicrograph D) (mag.400x).

4.2 Functional Assessment

4.2.1 BBB Score

BBB score increased during the 3 week period following injury to a mean BBB score of 20, within the normal range. Improvement was also seen in the 1 week group from a mean of 14.7 at 24 hours post-surgery to 18 at one week. Physical recovery of the animals after surgery may have caused the initial motor deficit at the earliest time point. The sham laminectomy group had a mean BBB score ranging from 20.8 to 20.9, and the naïve group had a mean of 21.

Table (a)

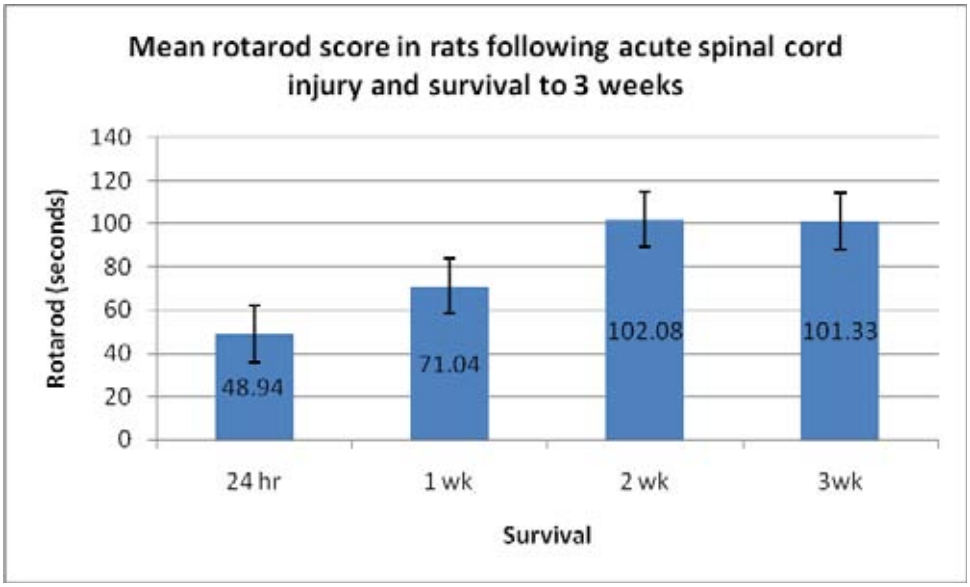

Table (b)

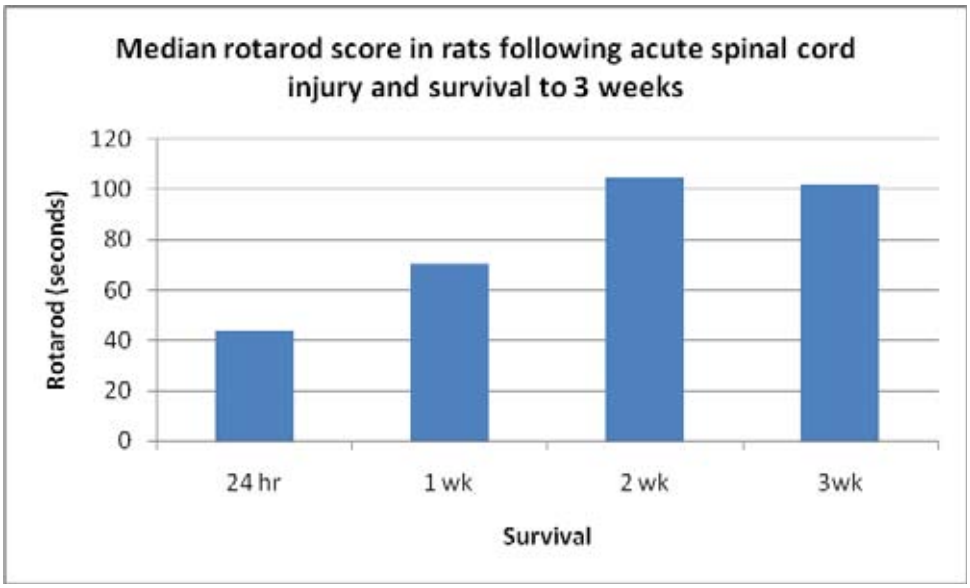

Table 63. (a) Mean and (b) Median rotarod scores in a weight drop model of acute spinal cord injury in the rat.

An increase in rotarod score to near normal is seen by 2 weeks, but the normal score of 120 seconds is not attained.

Table (a)

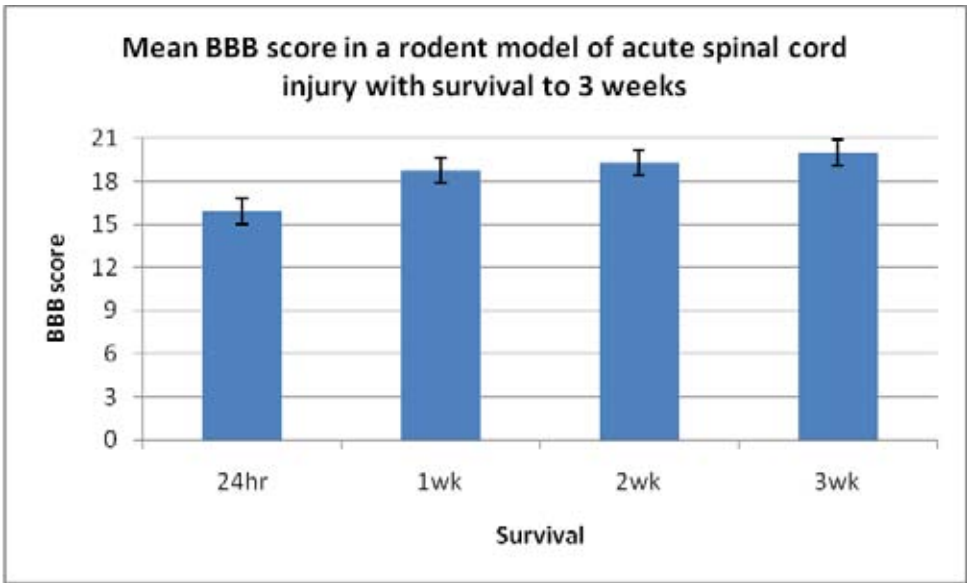

Table (b)

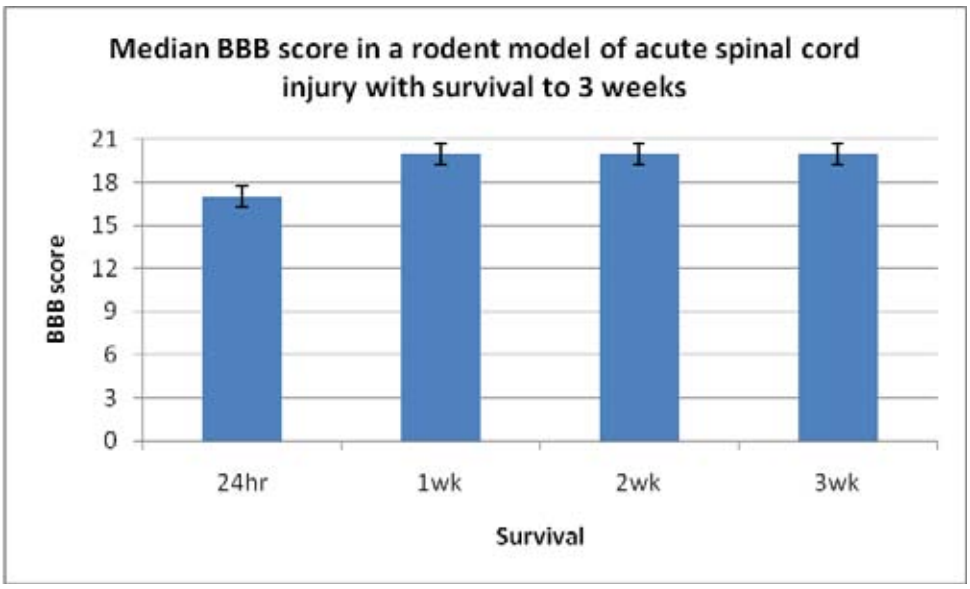

Table 64. (a) Mean and (b) Median BBB scores in a weight drop model of acute spinal cord injury in the rat.

A gradual increase in BBB score is seen after surgery to 3 weeks. Mean and median scores of 20 are reached at 3 weeks, approaching the normal control score of 21.

4.2.2 Tail flick

Between the 1 week and 3 week time points a decrease in the tail flick response was seen suggesting an improvement in motor-sensory function. There was a lengthening of tail flick response between 24 hours and 1 week after injury.

Table (a)

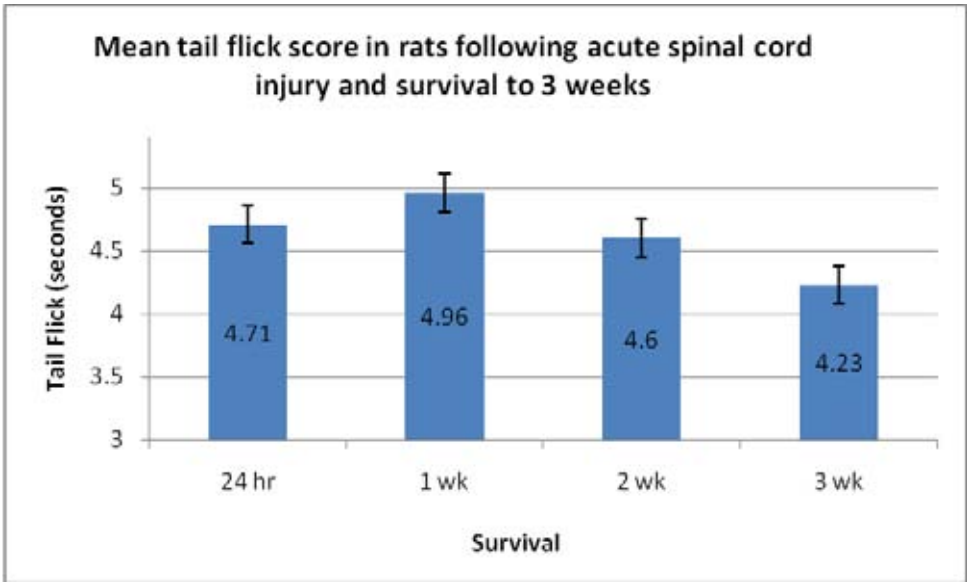

Table (b)

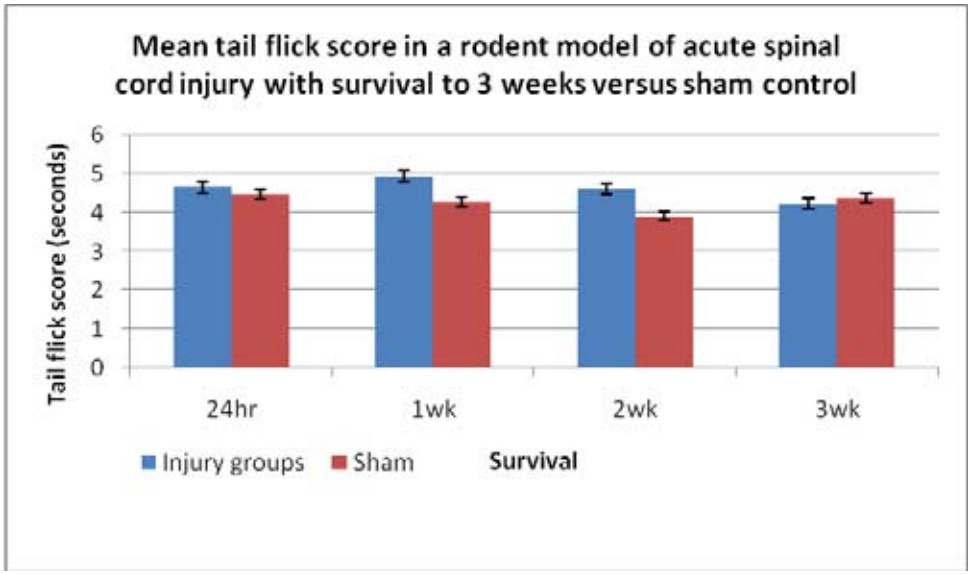

Table 65. Mean tail flick scores (a) by time and (b) versus control in a weight drop model of acute spinal cord injury in the rat.

Table (c)

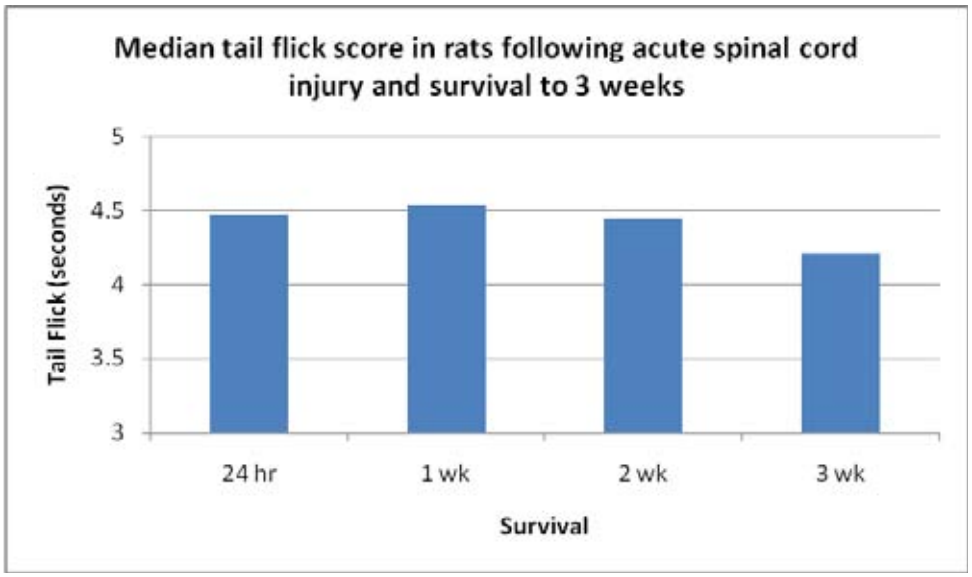

Table (d)

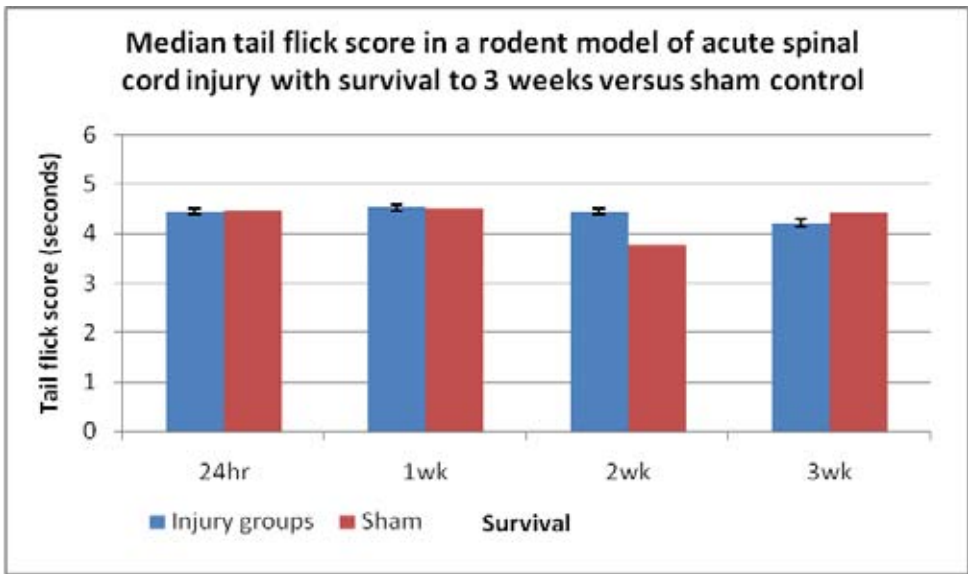

Table 65. Median tail flick scores (c) by time and (d) versus control in a weight drop model of acute spinal cord injury in the rat.

A decrease in tail flick score from 1 week to 3 weeks is seen in the injury groups, which may indicate improved motor-sensory function after recovery from surgery. Scores in the injury groups were not significantly different from sham controls.

4.2.3 Rotarod

Rats were trained to perform the rotarod at a gradually increasing speed to 120 seconds prior to injury. Over 3 weeks there was an increase in the mean rotarod duration from 70.8 at 24 hours post-surgery to 102.1 by 2 weeks maintained at 101.3 at sacrifice. Improved motor function was also seen between 24 hour (mean score 39.5 seconds) and 1 week (61 seconds) time points in the 1 week survival group.

4.3 Axonal Injury

At 24 hours following injury, axonal swellings were seen throughout the white matter and a subset were immunopositive using APP antibody (**Figure 4.3**). Axonal swellings were most numerous towards the central white matter, consistent at all time points and greatest in number at 24 hours. At 3 weeks there were 2/6 cases showing APP positive axonal swellings in the deep posterior white matter. At the 1 week time point, 4/6 cases had axonal swellings including APP-positive swellings, frequently seen in the deep posterior white matter.

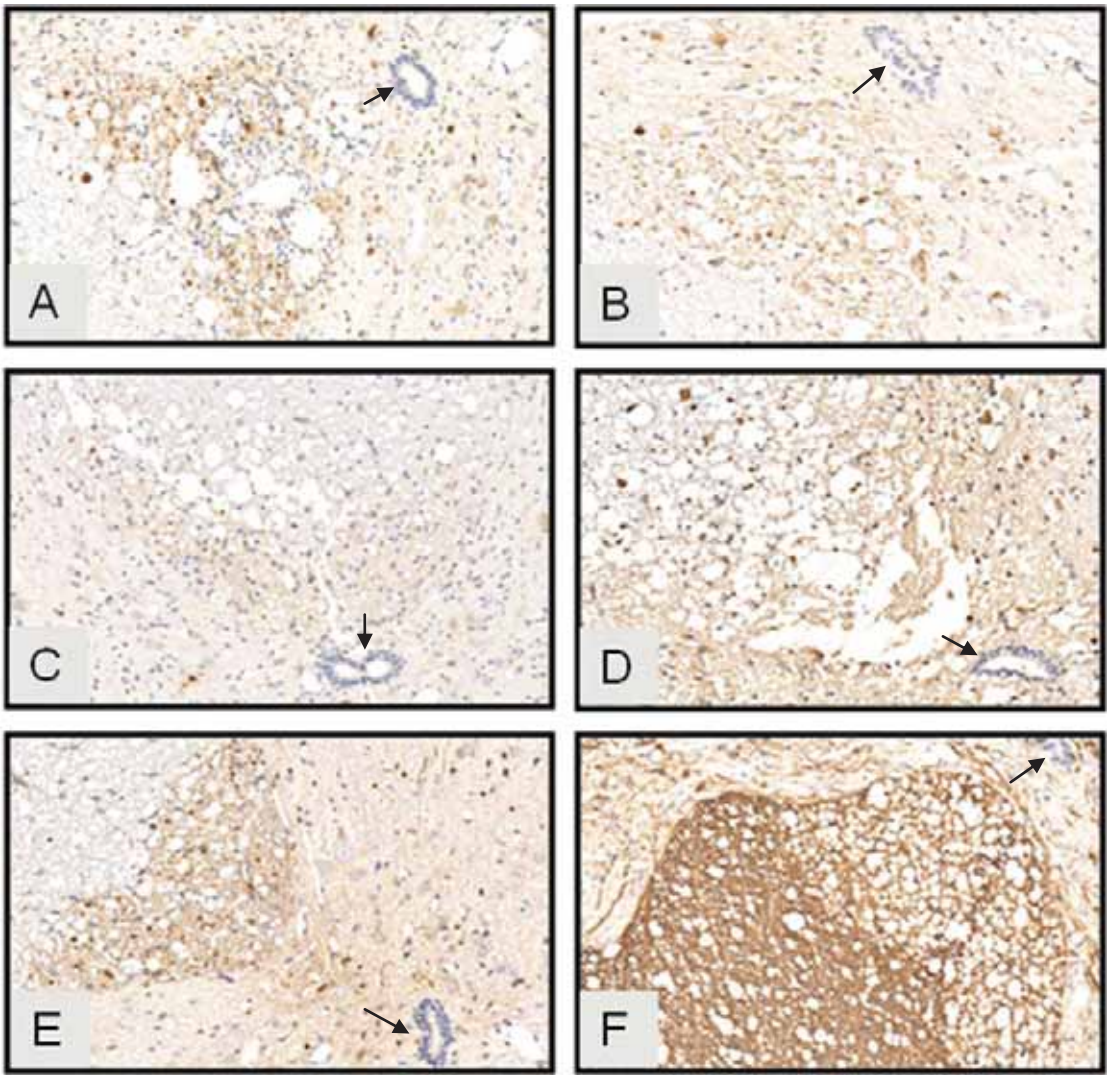

Figure 4.3 APP immunopositivity in axonal swellings in a rodent model of acute spinal cord injury.

APP immunopositive axonal staining is consistently seen in the deep posterior white matter at 24 hours following injury (photomicrographs A to E) (mag.400x). The central canal offers a point of orientation (arrows indicating the orientation of the anterior median fissure). In photomicrograph (F) a loss of myelin staining is seen on the right of the image (myelin basic protein immunostain).

4.4 Human Acute Compressive Myelopathy

4.4.1 Histopathology

All cases of traumatic SCI resulting from motor vehicle accidents had quadriplegia or paraplegia documented in clinical records. Survival post-injury, and thus the recovery time, was wide-ranging (5 hours to 5 months). Only one SCI case in this series was not due to a motor vehicle accident. This patient sustained iatrogenic injury from acute compression of the spinal cord during surgical fusion of C1 and C2 vertebrae for congenital os odontoideum.

Either haemorrhagic or tissue necrosis was present in all cases. Haemorrhagic tissue necrosis with infiltration of neutrophils was present in 5 cases where the survival times ranged from 5 hours to 18 days. Neutrophils were also seen in a case 5 months after crush fracture related compression of the cord. Macrophage invasion was also a feature in cases of longer survival. Cystic necrosis with a significant loss of neural architecture was seen in 2 cases (32 days and 5 months). Neuronal cell loss, particularly of anterior horn cells, and central chromatolysis of neurons was seen.

Significant white matter damage was present in all cases, manifest as white matter vacuolation and axonal swellings. There was variable haemorrhage, numerous APP-positive axonal swellings, and focal and diffuse gliosis. On Weil staining there was pallor surrounding axonal swellings, suggestive of damage to myelin. In cases of relatively long survival, 26 days and 5 months after injury, there was specific pallor of the motor tracts below the site of compression, suggestive of Wallerian degeneration. Post-traumatic gliosis was present within the white matter.

Table 66. List of traumatic spinal cord injury cases.

Case	Age	Gender	Type	Survival	Cause of death	Mechanism	Necrosis
11	73	Female	Fracture/ Dislocation	5 hours	C1/C2 injury	Cyclist versus car	Present
12	48	Male	Fracture/ Dislocation	24 hours	Vertebral artery dissection	Vehicle rollover	Present
13	30	Male	Fracture/ Dislocation	88 hours	Head injury, ventricular fibrillation	Vehicle rollover	Present
14	67	Male	Fracture/ Dislocation	6 days	Multiple trauma	Vehicle rollover	Present
15	26	Male	Fracture/ Dislocation	18 days	Multiple injuries, renal failure	Fall from motorbike	Present
16	52	Male	Iatrogenic	26 days	Bronchopneumonia, cardiac arrest	Surgical complication	Present
17	72	Male	Fracture/ Dislocation, Syrinx	32 days	Unknown	Vehicle rollover	Present
18	70	Female	Crush fracture	5 months	Pneumonia, respiratory arrest	Neoplastic infiltration	Present

Table 67. Summary of histopathological changes in human traumatic spinal cord injury cases.

Stain	CASE 11	CASE 12	CASE 13	CASE 14	CASE 15	CASE 16	CASE 17	CASE 18
H & E	Necrosis, oedema, neuronal loss, red cell change, axonal swellings	Necrosis, central chromatolysis, red cell change, axonal swellings	Necrosis, central chromatolysis, neuronal loss, axonal swellings	Necrosis, central chromatolysis, neuronal loss, axonal swellings	Necrosis, central chromatolysis, neuronal loss, axonal swellings	Necrosis, central chromatolysis, neuronal loss, red cell change, axonal swellings	Cystic necrosis, central chromatolysis, neuronal loss, axonal swellings, syrinx	Cystic necrosis, anterior horn cell and glial cell loss
Weil	No pallor	No pallor	No pallor	No pallor	No pallor	Pallor of the lateral cortico-spinal tract unilaterally below site	Pallor in regions of tissue necrosis	Pallor of the lateral and anterior cortico-spinal tract below site

4.4.2 Apoptosis

TUNEL positivity was found in neuronal and glial profiles (5 cases). Glial staining occurred at, above, and below the site of compression. Substantial TUNEL expression in damaged cords did suggest involvement of apoptosis in cell loss however, the infrequent immunostaining for Bcl-2, caspase-3 and caspase-9 did not support caspase-dependent apoptotic pathways. In Case 12, which showed severe haemorrhagic necrosis, TUNEL staining was minimal at the compression level and may be due to the loss of neuronal and glial cells. TUNEL-positive neurons were present at the site of compression.

Neuronal PARP immunopositivity was found in 2 cases, at the site of compression in one case and above it in the other. Glial nuclear staining was widespread at, above and below the compressed level. PARP positive glia had morphology consistent with oligodendrocytes. PARP immunostaining in neurons was nucleolar as well as nuclear. Neuronal nuclear immunopositivity to DNA-PKcs markers was also present. Immunoreactivity to the Bcl-2 antibody was rare or occasional. Minimal Fas immunoreactivity was observed. Caspase-9 was also rarely seen in axonal swellings in one case.

Cytoplasmic glial AIF immunostaining was found throughout the white matter. Neuronal AIF staining occurred at, above, and below the compression site. AIF staining was also found in APP-positive axonal swellings in 5 trauma cases. In control spinal cords, AIF immunopositivity was widely distributed in glial, neuronal and ependymal cell cytoplasm. AIF co-localised with mitochondrial protein on double-immunolabelling.

Table 68. CASE 11 – Trauma series – Immunohistochemical positivity (+) in glial, axonal or neuronal profiles:

Level	APP	Casp-3	DNA-PKcs	PARP	Bcl-2	Fas	Casp-9	TUNEL	Amy-33	CMAP	AIF
C1-2	+	-	+	-	-	-	-	-	+	+	+
C2	+	-	+	-	-	-	-	-	+	+	+
C3	-	-	-	-	-	-	-	+	+	+	+
C4	+	-	-	-	-	-	-	+	+	+	+

* Shaded rows represent the site of compression

Table 69. CASE 12 – Trauma series – Immunohistochemical positivity (+) in glial, axonal or neuronal profiles:

Level	APP	Casp-3	DNA-PKcs	PARP	Bcl-2	Fas	Casp-9	TUNEL	Amy-33	CMAP	AIF
C3	-	-	-	+	-	-	-	-	-	+	+
C4	-	-	+	+	-	-	-	+	-	+	+
C5	-	-	-	+	-	-	-	-	+	+	+
C6	-	-	+	+	-	-	-	-	-	+	+
C7	-	-	-	+	-	-	-	-	+	+	+
T1	-	-	+	+	-	-	-	-	+	+	+
T2	-	-	+	+	-	-	-	+	-	+	+
T3	-	-	+	+	-	-	-	-	-	+	+
T4	-	-	+	+	-	-	-	+	-	+	+

* Shaded rows represent the site of compression

Table 70. CASE 13 – Trauma series – Immunohistochemical positivity (+) in glial, axonal or neuronal profiles:

Level	APP	Casp-3	DNA-PKcs	PARP	Bcl-2	Fas	Casp-9	TUNEL	Amy-33	CMAP	AIF
C3	-	-	+	+	-	-	-	-	+	+	+
C4	+	-	-	+	-	-	-	-	+	+	+
C5	+	+	+	+	-	-	-	-	+	+	+
C6	+	+	+	+	-	-	-	-	+	+	+
C7	+	-	-	+	-	-	-	-	+	+	+
C8	-	-	-	+	-	-	-	+	+	+	+

* Shaded rows represent the site of compression

Table 71. CASE 14 – Trauma series – Immunohistochemical positivity (+) in glial, axonal or neuronal profiles:

Level	Casp-3	DNA-PKcs	PARP	Bcl-2	Fas	Casp-9	TUNEL
T3	-	-	+	-	-	-	+
T4	-	+	+	-	-	-	+
T5	-	+	+	-	-	-	+
T6	-	+	+	+	-	-	+
T7	-	+	+	-	-	-	+
T8	-	+	+	-	+	-	+
T10	-	+	+	-	-	-	+

* Shaded rows represent the site of compression

Table 72. CASE 15 – Trauma series – Immunohistochemical positivity (+) in glial, axonal or neuronal profiles:

Level	Casp-3	DNA-PKcs	PARP	Bcl-2	Fas	Casp-9	TUNEL
C8	-	-	-	-	-	-	-
T1	-	+	+	-	-	-	+
T2	-	-	-	-	-	-	+
T3	-	-	+	-	-	-	+
T4	-	+	-	-	-	-	+
T5	-	-	+	-	-	-	+
T6	-	-	+	-	-	-	+
T7	-	-	+	-	-	-	+
T8	-	+	+	-	-	-	+
T9	-	+	+	-	-	-	+
T10	-	-	+	-	-	-	+

* Shaded rows represent the site of compression

Table 73. CASE 16 – Trauma series – Immunohistochemical positivity (+) in glial, axonal or neuronal profiles:

Level	APP	Casp-3	DNA-PKcs	PARP	Bcl-2	Fas	Casp-9	TUNEL	Amy-33	CMAP	AIF
C1	+	-	-	+	-	-	-	+	+	+	+
C3	+	-	+	+	-	-	-	+	+	+	+
C4	+	-	+	+	-	-	-	+	+	+	+
C5	-	-	+	+	-	-	-	+	+	+	+
C6	-	-	+	+	-	-	-	+	+	+	+
C7	-	-	+	+	-	-	-	+	+	+	+
L5	-	-	-	+	-	-	-	+	+	+	+

* Shaded rows represent the site of compression

Table 74. CASE 17 – Trauma series – Immunohistochemical positivity (+) in glial, axonal or neuronal profiles:

Level	APP	Casp-3	DNA-PKcs	PARP	Bcl-2	Fas	Casp-9	TUNEL	Amy-33	CMAP	AIF
C3	+	-	-	-	-	-	+	-	-	+	+
C4	+	-	-	+	-	-	-	-	-	+	+
C5	-	-	-	-	-	-	-	-	+	+	-
C7	+	-	-	-	-	-	-	-	+	+	+
C8	+	-	-	-	-	-	-	-	+	+	+
T1	-	-	-	-	-	-	-	-	-	+	+
T2	-	-	-	+	-	-	-	-	+	+	+
T3	+	-	-	-	-	-	-	-	+	+	+
T4	-	-	-	+	-	-	-	+	-	+	+
T11	-	-	-	+	-	-	-	+	-	+	+

* Shaded rows represent the site of compression

Table 75. CASE 18 – Trauma series – Compression C7 – Immunohistochemical positivity (+) in glial, axonal or neuronal profiles:

Level	APP	Casp-3	DNA-PKcs	PARP	Bcl-2	Fas	Casp-9	TUNEL	Amy-33	CMAP	AIF
C6	-	-	-	+	-	-	-	+	+	+	+
C7	+	-	-	+	-	-	-	+	+	+	+
C8	+	-	-	+	-	-	+	-	+	+	+
C8/T1	-	-	-	+	-	-	-	-	+	+	+
T1	+	-	-	+	-	-	-	-	+	+	+
T2	-	-	-	+	-	-	-	+	+	+	+
T3	+	-	-	+	-	-	-	+	+	+	+

* Shaded rows represent the site of compression

Table 76. Immunohistochemical staining in human traumatic spinal cord injury cases – morphological findings.

Antigen	CASE 11	CASE 12	CASE 13	CASE 14	CASE 15	CASE 16	CASE 17	CASE 18
Caspase-3	Negative	Negative	Axonal swellings at site	Negative	Negative	Axons	Negative	Negative
DNA-PKcs	Negative	Glia above and below site, axonal swellings above	Glia at and above site	Glia at, above, below site, Axons at, below, neurons at, above	Axonal swellings above and below site	Glia at and below site	Negative	Negative
PARP	Glia all segments, neuronal staining at, above, below site	Glia all segments, neurons above site	Glia at, above and below site	Glia all segments, neuronal staining at site	Glia at, above and below site	Glia all segments, neuronal staining below site	Glia above and below site	Glia all segments, neuronal at, above, below site
Bcl-2	Negative	Negative	Negative	Neuronal staining at site	Negative	Negative	Negative	Negative
Fas	Negative	Negative	Negative	Axons below site	Negative	Negative	Negative	Negative
TUNEL	Glia at, above, below site	Neurons above and below site	Glia below site	Glia all segments	Glia at, above, below site, neurons above, below	Glia and neurons all segments, maximal below site	Glia, neurons below site	Glia at, above, below site
Caspase-9	Axons below site	Negative	Negative	Negative	Negative	Negative	Negative	Axons below site
AIF	Glia, axons and neurons all segments	Glia and axons at and below site, Neurons, axons above	Glia, axons, neurons at site, Neurons, glia above and below	Glia and neurons all segments, axons at, below site	Glia, axons and neurons above and below site	Glia, neurons at, above site, axons at site	Glia at, above and below site, neurons above, below	Glia and neurons at, above, below site
Mitochondrial protein	Glia, neurons, axons	Glia, neurons, axons	Glia, neurons, axons	Glia, neurons, axons	Glia, neurons, axons	Glia, neurons, axons	Glia, neurons, axons	Glia, neurons, axons

4.4.3 Axonal Injury

APP axonal staining was typically maximal at the site of compression where tissue damage was greatest, including haemorrhage, necrosis and anterior horn cell loss. There was a paucity of glia in regions of cystic cavitation. A loss of anterior horn cells was noted. Axonal immunopositivity using APP was found in focal regions within the white matter, in both longitudinal and transverse profiles.

With double immunolabelling fluorescent microscopy, there was consistent co-localisation of AIF and mitochondrial protein in axonal swellings. Double immunolabelling was performed using active caspase-3, APP, CMAP and amyloid-beta. Axons showing co-localisation of caspase-3 and APP immunopositivity was present, at, above and below the site of compression. Amy-33 amyloid-beta immunoreactivity was found within the same axons which were immunopositive for APP and in an additional population of axons not labelled by APP. DAKO / University of Melbourne amyloid-beta antibodies were negative within axonal, glial or neuronal profiles. CMAP immunoreactivity was present in all axonal profiles of normal and enlarged diameter and was present in the ependymal cells of the central canal and in neuroglia.

Anterior horn cells showed cytoplasmic immunoreactivity to amyloid-beta, CMAP and APP. In the Alzheimer's disease control case, the Amy-33 antibody recognised the APP immunopositive neuritic component of senile plaques but not the amyloid-beta core recognised by the well-characterised DAKO antibody. University of Melbourne amyloid-beta showed a similar central pattern of staining to the DAKO amyloid-beta antibody. Cortical neurons in the Alzheimer's and traumatic brain injury controls showed positive Amy-33 amyloid-beta and APP immunostaining, but DAKO and University of Melbourne amyloid-beta antibodies were negative.

Double-immunostaining in axonal swellings using APP and AIF immunomarkers was performed. Co-localisation of antibodies within both neurons and axons was demonstrated using immunofluorescence for caspase-3 with APP, and caspase-3 with amyloid-beta. Double-immunolabelling was performed using AIF/APP and AIF/mitochondrial marker. The morphology of the anterior horn cells and axons were readily identified, but it was difficult to distinguish between glial types.

Table 77. CASE 11 – Trauma series – Immunohistochemical positivity (+) in glial, axonal or neuronal profiles:

Level	APP	Casp-3	DNA-PKcs	PARP	Bcl-2	Fas	Casp-9	TUNEL	Amy-33	CMAP	AIF
C1-2	+	-	+	-	-	-	-	-	+	+	+
C2	+	-	+	-	-	-	-	-	+	+	+
C3	-	-	-	-	-	-	-	+	+	+	+
C4	+	-	-	-	-	-	-	+	+	+	+

* Shaded rows represent the site of compression

Table 78. CASE 12 – Trauma series – Immunohistochemical positivity (+) in glial, axonal or neuronal profiles:

Level	APP	Casp-3	Amy-33	CMAP
C3	-	-	-	+
C4	-	-	-	+
C5	-	-	+	+
C6	-	-	-	+
C7	-	-	+	+
T1	-	-	+	+
T2	-	-	-	+
T3	-	-	-	+
T4	-	-	-	+

* Shaded rows represent the site of compression

Table 79. CASE 13 – Trauma series – Immunohistochemical positivity (+) in glial, axonal or neuronal profiles:

Level	APP	Casp-3	Amy-33	CMAP
C3	-	-	+	+
C4	+	-	+	+
C5	+	+	+	+
C6	+	+	+	+
C7	+	-	+	+
C8	-	-	+	+

* Shaded rows represent the site of compression

Table 80. CASE 14 – Trauma series – Immunohistochemical positivity (+) in glial, axonal or neuronal profiles:

Level	APP	Casp-3	Amy-33	CMAP
T3	-	-	-	-
T4	-	-	+	-
T5	+	-	+	-
T6	+	-	+	-
T7	+	-	+	-
T8	+	-	+	-
T10	-	-	+	-

* Shaded rows represent the site of compression

Table 81. CASE 15 – Trauma series – Immunohistochemical positivity (+) in glial, axonal or neuronal profiles:

Level	APP	Casp-3	Amy-33	CMAP
C8	-	-	-	+
T1	-	-	+	+
T2	-	-	+	+
T3	+	-	+	+
T4	+	-	+	+
T5	+	-	+	+
T6	+	-	+	+
T7	+	-	+	+
T8	+	-	+	+
T9	+	-	+	+
T10	+	-	+	+

* Shaded rows represent the site of compression

Table 82. CASE 16 – Trauma series – Immunohistochemical positivity (+) in glial, axonal or neuronal profiles:

Level	APP	Casp-3	Amy-33	CMAP
C1	+	-	+	+
C3	+	-	+	+
C4	+	-	+	+
C5	-	-	+	+
C6	-	-	+	+
C7	-	-	+	+
L5	-	-	+	+

* Shaded rows represent the site of compression

Table 83. CASE 17 – Trauma series – Immunohistochemical positivity (+) in glial, axonal or neuronal profiles:

Level	APP	Casp-3	Amy-33	CMAP
C3	+	-	-	+
C4	+	-	-	+
C5	-	-	+	+
C7	+	-	+	+
C8	+	-	+	+
T1	-	-	-	+
T2	-	-	+	+
T3	+	-	+	+
T4	-	-	-	+
T11	-	-	-	+

* Shaded rows represent the site of compression

Table 84. CASE 18 – Trauma series – Compression C7 – Immunohistochemical positivity (+) in glial, axonal or neuronal profiles:

Level	APP	Casp-3	Amy-33	CMAP
C6	-	-	+	+
C7	+	-	+	+
C8	+	-	+	+
C8/T1	-	-	+	+
T1	+	-	+	+
T2	-	-	+	+
T3	+	-	+	+

* Shaded rows represent the site of compression

Table 85. Immunohistochemistry human traumatic spinal cord injury – morphological findings.

Antigen	CASE 11	CASE 12	CASE 13	CASE 14	CASE 15	CASE 16	CASE 17	CASE 18
APP	Axonal swellings at, above, below site	Axonal swellings at and above site	Axonal swellings at, above, below site	Axonal swellings at, above, below site	Axonal swellings at, above site with maximum number below site	Axonal swellings at, above, below site, bordering cystic necrosis	Axonal swellings above, below site, bordering necrotic regions	Axonal swellings at, above, below site
Caspase-3	Negative	Negative	Axonal swellings at site	Negative	Negative	Axons	Negative	Negative
AMY-33	Glia and axons at, above, below site, neurons above and below	Neurons above and below site, axons above	Glia, neurons, axons at, above, below site	Axons at, above, below site	Axons at, above, below site, neurons above	Glia and neurons at, above, below site, axons at and below	Axons at, above, below site, neurons and glial above and below	Axons and glia at, above, below site, neurons above and below
University of Melbourne amyloid beta	Negative	Negative	Negative	Negative	Negative	Negative	Negative	Negative
Dako amyloid-beta	Negative	Negative	Negative	Negative	Negative	Negative	Negative	Negative
CMAP	Glia all segments, neurons below	Glia and axons all segments	Glia and axons at, above, below site	Glia and axons all segments	Glia and axons all segments	Glia and axons all segments	Glia, neurons, axons all segments	Glia all segments, neurons below site

Control cases

Negative and positive controls in human tissue were the same as those used for the study of human chronic compressive myelopathy.

4.5 Discussion – Experimental and Human Acute Compressive Myelopathy

An acute weight drop model of contusive spinal cord injury (SCI) was used to address the following aims:

i. To assess the functional disturbance, cellular pathology and role of apoptosis in a rodent model of acute spinal cord injury.
ii. To assess the cellular pathology and role of apoptosis in human acute spinal cord compression.
iii. To assess the axonal changes in acute spinal cord compression using APP as a marker of axonal injury.

4.5.1 Apoptosis

Experimental

Morphological and immunohistochemical evidence of apoptosis was analysed in a controlled experimental rodent model of acute spinal cord injury (SCI) at 24 hours, 1 week and 3 weeks post injury and compared to the human case material. These time-points were selected for study to improve understanding of the role of apoptosis in mild spectrum acute SCI.

Robins and Fehlings (2008) provided a thorough review of experimental spinal cord injury which emphasised the need for the establishment of the following key principles in experimental models:

1. Multiple outcome measures should be used in order to monitor the effect of therapy.
2. In vivo models may involve many dynamic factors affecting disease progression and models often aim to replicate these processes, but too complex a model should be avoided or alternatively developed in conjunction with in vitro modelling.
3. Traumatic SCI in the human may be incomplete with partial preservation of neural tissue, a situation not replicated by the complete transaction of the cord, and the results must be viewed accordingly.

In our study, multiple small animals could be used within a short time span and the model could therefore be promptly adjusted to replicate injury in the human. In this experimental model we were able to analyse apoptosis after a single level, contusional, extradural injury, with survival to 3 weeks. This model characterised injury along the mild spectrum of severity with subacute resolution of functional and histopathological changes. The classification of injury into mild, moderate and severe categories is now recognised as being overly simplistic, and further research is needed to better define grading within each of these broad classifications. Furthermore, multiple segments are often affected and this may alter the pathophysiology and outcome.

This study investigated the histopathological changes in a focal, extradural impact, weight drop model of spinal cord compression causing incomplete injury at the thoracic level using a 10 gram weight. Histopathological changes were correlated with functional testing. Stability of the spine was preserved and the duration of surgery minimised by performing laminectomy at a single level. The majority of previous models have used severe spectrum injury models involving subtotal or complete damage to the cord, such as horizontal transection. Incomplete injury may be deemed more ethical, in that it allows for better functional outcome in the animal including the ability to maintain adequate hydration, bowel and bladder function, oral intake, and to minimise pain. Incomplete models typically use blunt contusion such as the weight drop used in this study, incision, partial transection, planar compression induced by clips or forceps, hypoxia, thermal radiation or laser induced injury. Functional studies including the BBB score (Basso et al., 1995) have been well described for thoracic injury.

Histopathological changes were reproducible, changes were maximal at 24 hours following injury and had predominantly resolved by 3 weeks, congruent with near-normal motor-sensory function by 3 weeks. Macroscopically visible central haemorrhage and distortion of the posterior surface of the cord was seen at 24 hours, indicative of significant primary injury and tissue disruption on impact. It is thought that the initial impact causes immediate and usually irreversible cell death as a primary process. Traumatic and ischaemic injury causes rapid depletion of energy stores, failure of the sodium-potassium ATP pump, and accumulation of sodium within axons (Agrawal, 1996). Membrane depolarisation occurs resulting in rapid accumulation of calcium, increased activation of enzymes and cytoskeletal injury (Li et al., 1996). This study replicated the grey matter features of human

SCI with evidence of neuronal compromise including red cell change suggestive of neuronal ischaemia, central haemorrhage, and a loss of anterior horn cells. Karyorrhexis, cytolysis and cystic change suggested the presence of necrotic cell death. Haemorrhagic necrosis was minimally present. Ischaemia is a likely contributor to significant secondary injury. The severity of the ischaemic insult may be measured using multiparametric testing and mitochondrial NADH, elevated after traumatic injury to the spinal cord (Simonovich et al., 2008). Changes were consistent with a mild spinal cord injury.

Necrosis after SCI in known to occur rapidly and induces an inflammatory response involving chemotaxis and infiltration of immune cells as well as changes in glia, microglia, neurons and non-cellular components such as inflammatory cytokines (Zhang et al., 1997, Schnell et al., 1999). Necrosis at the biochemical level is usually determined by exclusion of caspase activation, DNA-fragmentation and the release of cytochrome-c. In our study, there was evidence of necrosis in regions negative for TUNEL, caspase-3 and caspase-9.

Neutrophilic infiltration is known to occur as early as 24 hours after injury (Taoka et al., 1997). In this study, neutrophils were visible in the 24 hour and 1 week groups but were seen only in focal areas. No neutrophils were present at 3 weeks. **Macrophages** typically appear in the first week but may persist for months following injury and are involved in the clearance of cellular debris including apoptotic cells (Savill et al., 1990). In this study, macrophages appeared at 1 week following injury but were not a feature at 3 weeks. Resident microglia of the spinal cord have been shown to undergo transformation into phagocytic macrophages within hours after SCI (Popovich et al., 2002), and can persist for weeks after injury. Inflammatory changes such as neutrophilic infiltrate at 24 hours, macrophage infiltration at 1 week and necrosis were seen. Myelin basic protein (MBP) was absent in the region of the corticospinal tract. An association between glial apoptosis and APP expression suggests an axonal transport defect, despite the absence of demyelinative changes on Weil and MBP staining.

Findings using a panel of **apoptotic markers** were consistent with apoptosis in this model of acute SCI. Apoptotic cells were present up to two segments (6mm) above and below the site of injury across all groups, suggesting persisting and widespread apoptosis. The functional deficit in acute SCI was comparable with injury groups in the model of chronic compressive myelopathy. The lesional area was small at the site of injury and was isolated

to the central area of the spinal cord. Secondary processes of cell death are usually seen in the penumbra surrounding the primary injury site, both in the same segment as the injury and also in segments above and below. Secondary damage may be triggered by a multitude of factors, such as enzymatic degradation, ongoing ischaemia, thermal injury, hypoxia or toxins, and damage may be ongoing for many weeks or months following the initial insult. There is cumulative evidence for classical apoptosis after SCI in neurons, oligodendrocytes, microglia and perhaps astrocytes (Beattue et al., 2000). In a rodent model of contusional SCI which analysed effects as early as 30 minutes, Crow and colleagues (1997) found evidence for apoptotic cells from 6 hours post-injury up to 3 weeks, predominantly within the white matter. TUNEL positive cells were counted away from the lesion site, and correlated with cytosolic changes on toluidine blue staining. In this study, apoptosis persisted and the percentage of apoptotic cells was maximal at 8 days post-injury; however current guidelines do not recommend the use of 'percentage' as a term, instead preferring to comment on either the presence of absence of apoptotic cells which have been shown to vary in number over a course of hours. It is of note that no apoptotic cells were seen at the 30 minute time point. In a monkey model (Crow et al., 1997), apoptotic cells were present in the remote degenerating fibre tracts, and it was suggested that chronic demyelination of ascending sensory and descending motor tracts may be at least in part secondary to apoptosis.

Glial positivity using the 'gold standard' biochemical marker of apoptosis, TUNEL, was seen at the earliest time point, 24 hours, and at 1 week following injury. Glial cells immunopositive for active caspase-3 were found in all regions of the white matter, extending above and below the site of injury at all three time points, suggesting persisting apoptosis at 3 weeks post-injury. Immunostaining was qualitatively and semi-quantitatively greatest at the site of compression, supportive of the stated hypothesis. At all three injury time points, apoptosis inducing factor (AIF) immunostaining was found in glia within the white matter and in neuronal perikarya. PARP immunostaining of glial cells with morphological features of oligodendrocytes, astrocytes and microglia was widespread at all three time points. Staining was present at, above and below the site of injury, suggesting the presence of apoptosis away from the site of compression. In addition to its role in apoptosis, PARP may be present in normal eukaryotic cells assisting in the regulation of DNA metabolic processes and maintenance of genomic stability by catalysing the post-translational alteration of proteins (Simonin et al., 1993). Staining for

PARP was absent or rare in control cases, supporting a pathological role in this context. Occasional DNA-PKcs immunostaining of glia was found at, above and below the site of injury. There was minimal Fas and Bcl-2 immunoreactivity in the model of chronic compressive myelopathy and this result was similar to the results from our human material, which contrasts studies of traumatic SCI in the rat that described activation of the Fas receptor and apoptosis (Casha et al., 2001). Bcl-2 activation is mediated, *inter alia*, by the pro-apoptotic release of cytochrome-c and Bax protein. These findings may represent a cellular response to damage via activation of Bcl-2, and DNA repair activity by the PARP enzyme and DNA-PKcs. In our study there was no evidence to support a role for extrinsically activated apoptosis. The temporal pattern of apoptosis was similar to that of our human case series, with survival ranging from hours to weeks.

An increasing number of alternate pathways of secondary cell death are now recognised and these may play a role in the pathophysiology of traumatic SCI, though further studies are needed. Apoptosis is a major cause of cell death, yet other types, along the spectrum between apoptosis and necrosis are known, and may contribute to the pathophysiology of compressive myelopathy. Following the development of spinal cord oedema there may be cell membrane alteration and ionic disturbance (Nashmi and Fehlings, 2001), accumulation of glutamate with excessive activation of its receptor and excitotoxicity (Baptiste and Fehlings, 2006), calcium influx causing release of enzymes and damage to organelles (Liu et al, 1997, Wingrave et al., 2003).

Apoptosis was suggested by neuronal and glial immunopositivity using a panel of apoptotic markers, including TUNEL. The use of ultrastructural analysis in this model at earlier time-points might allow the recognition of changes such as membrane blebbing and apoptotic bodies associated with late stage secondary cell death in conjunction with biochemical changes, as consistent with current definitions of apoptosis (Nomenclature Committee on Cell Death, 2009).

Apoptosis of a subpopulation of oligodendrocytes has been demonstrated in previous studies (Nashmi et al., 2001). Death of oligodendrocytes may result in demyelination due to their central role in myelination within the CNS. Our studies show the presence of active caspase-3, caspase-9, PARP and DNA-PKcs immunopositivity in glial cells with morphological features consistent with oligodendrocytes and astrocytes. Caspase-9

immunopositive staining of glia was widespread in all regions of the white matter and present at, above and below the site of injury. Caspase-9 is an immunological marker of the mitochondrial apoptotic pathway activated following cytochrome-c release. APP immunopositive axonal swellings, indicative of disrupted axonal transport, were noted at the early time points. At 24 hours survival, axonal swellings were semi-quantitatively most numerous in the deep posterior white matter, where the corticospinal tracts are located.

Human Studies

The results in **human** case material are interpreted in light of the wide range in survival time post-injury and thus cases are not directly comparable. Most of the cases represent the severe end of the compression injury spectrum. Significant primary tissue damage is suggested by severe necrosis and compressive forces are assumed to be extreme. In this study of human acute spinal cord injury, haemorrhagic and cystic necrosis was consistently present in the central cord and congruent with the clinical and radiological findings of acute severe traumatic SCI. There was associated central chromatolysis, anterior horn cell loss and red cell change indicating neuronal injury. Histopathological changes were greatest at the site of compression. This severity of histopathological changes lay in contrast to the mild spectrum injury achieved using the rodent model of acute compressive myelopathy.

In this series, 7 patients had either quadriplegia or paraplegia which correlated with severe damage to the motor tracts on histopathological examination. The remaining case had quadriparesis only, had the longest survival-time after spinal cord injury (5 months) and was caused by a typically lower impact mechanism of injury (crush-fracture). This patient's motor loss correlated with less severe changes on histopathology, with occasional axonal swellings in the lateral corticospinal tract which were APP-immunopositive on one side only. No other regions showed evidence for APP. A small region of cystic necrosis was present in the central region of the cord and occasional polymorphonuclear cells suggestive of acute inflammation were seen. There was no apoptotic staining within the penumbra around the area of necrosis in this case, but apoptotic staining was present above and below the site of injury.

Similar to chronic compressive myelopathy, immunopositivity for apoptotic markers in acute SCI was maximal in the penumbra surrounding areas of necrosis, which was often at the site of compression. Staining was widespread in multiple segments above and below the site of compression injury, again consistent with evidence of distant apoptosis in chronic compressive myelopathy. Apoptosis was heterogeneous in cross-section, and was found up to five segments above and below the site of injury in human material, and up to two segments above and below in experimental material, a diffuse distribution. Necrosis was usually haemorrhagic or cystic and associated with axonal swellings in the penumbra, anterior horn cell loss and neuronal red cell changes suggesting significant glial and neuronal compromise. The 'gold-standard' biochemical marker for apoptosis, TUNEL, was immunoreactive in glia in relatively preserved regions of grey and white matter which had maintained an appreciable density of glial cells. Where necrosis was severe at the site of compression, TUNEL glial and neuronal immunopositivity was maximal in the penumbra above or below the injury. DNA-PKcs was seen in all types of glia maximal at the site. TUNEL positive glia and neurons were maximal below the site, as was demonstrated in many of the acute cases. Active caspase-3 immunopositive glia were rare, but on double-immunolabelling co-localisation of caspase-3 and APP within both neurons and axons was demonstrated. In the majority of cases (6/8), PARP immunopositive oligodendrocytes were seen throughout the white matter at, several segments above and several segments below the site of injury, while being maximal at the site. This suggests widespread DNA fragmentation and repair activity. Necrosis extended in some cases above and below the site of injury. In two cases, large numbers of immunopositive glial cells were present below the site, suggesting apoptosis of cells well away from the lesion. DNA-PKcs was also maximal in areas adjacent to necrosis. In regions of tissue necrosis, a neutrophilic and, representative of subacute inflammation, lymphocytic or macrophage infiltration was found at the site. Bcl-2 and Fas staining was negative in the majority of cases. This may represent the absence of externally triggered apoptosis or the absence of this pathway of extrinsic classical apoptosis.

There was insufficient evidence for AIF-induced apoptosis in traumatic SCI due to a lack of correlation between well-characterised markers of apoptosis and AIF expression, the absence of AIF nuclear translocation in neural elements, and substantial AIF immunoreactivity in both injured and uninjured spinal cords. Double immunolabelling confirmed our initial immunohistochemical findings and also provided greater detail on the

spatial relationship of immunopositive cells. AIF was often found aggregated in axonal swellings and was co-localised with mitochondrial protein, but not with the axonal injury marker APP. AIF immunostaining was spatially heterogeneous in a variety of cell types (oligodendrocytes, astrocytes, neurons and ependymal cells) in both traumatically injured and control spinal cords. Moreover, AIF immunoreactivity was invariably intracytoplasmic rather than nuclear; the latter being expected if apoptotic translocation of AIF had occurred. Although not directly comparable, previous experimental models of traumatic brain injury in the rat have shown intranuclear localisation of AIF by 2 hours and persisting up to 72 hours after injury (Zhang et al., 2002). The lack of any correlation between AIF staining and expression of recognised immunohistochemical and biochemical markers of apoptosis also did not support a role for AIF in cell death after traumatic cord injury in our series of patients.

AIF and mitochondrial protein immunostaining was co-localised in axons as early as 5 hours after injury in smaller diameter fibres and persisted in cases of up to 26 days survival. AIF, which is normally present in the mitochondrial intermembrane space, may accumulate in detectable quantities when anterograde transport of this organelle is impeded after a traumatic insult. Immunonegative axonal profiles were also seen, which may indicate preserved axonal transport in these axons. Many axonal swellings were immunostained with APP, the most sensitive marker of axonal injury, but while AIF and APP immunopositivity could sometimes be found in the same axonal swellings, they were present in different regions of reactive axons. This absence of AIF/APP co-localisation may reflect different transport pathways.

Acute inflammation and neutrophilic invasion was present in 5 out of 8 cases of traumatic SCI from 5 hours post-injury to 18 days post-injury. The presence of neutrophils has been shown up to 10 days survival post-spinal cord injury in the human and is associated with severe inflammatory changes (Fleming et al., 2006). It is not typically associated with apoptotic cell death, although apoptosis may be present in the penumbra surrounding necrosis. Activated microglia and neutrophils typically appear early (1-3 days) after injury. The attenuation of this acute inflammatory response, in addition to minimisation of longer term secondary changes, carries potential therapeutic benefit, however the timing of intervention is likely to be complex.

The benefit of immune modulation using steroid therapy following spinal cord injury remains unclear despite intensive study over the past decade. Current guidelines suggest it as an optional but not a recommended part of acute management of SCI. The "National Acute Spinal Cord Injury Study" (NASCIS) trials in the U.S.A. have compared methyprednisolone given over 48 hours and 24 hours after SCI and the antioxidant medication tirilazad mesylate over a 48 hour period. There is evidence from these trials that methylprednisolone administered within the first 8 hours after SCI has a beneficial effect although subsequent studies have not confirmed this finiding.

4.5.2 Axonal Injury

Experimental

In an experimental rodent model of traumatic SCI, APP immunopositive axonal swellings and retraction bulbs were present, especially in the posterior column towards the central cord. APP axonal immunopositivity was most often seen at the site of injury, but was also present above and below the site at 24 hours. In a previous study of traumatic SCI using the Sprague-Dawley rat, increased axonal injury, as evidenced by APP expression, was greater in the fracture-dislocation group when compared to distraction or contusion groups at 3 hours survival. Cytochrome-c release, which may have been related to apoptosis, was found in this fracture-dislocation group as well as in the contusion group, however subject numbers were small (n=2 contusion, n=2 dislocation, n=3 distraction) (Choo et al., 2008). Secondary injury, axonal degeneration and glial apoptosis have been shown after posterior column cordotomy in the rat, suggesting a central role for the supportive glia in the pathogenesis of acute SCI (Warden et al., 2001).

In this study, APP immunopositive axonal swellings were maximal at the site of compression within the penumbra and were associated with PARP immunopositive glial cells, suggesting a possible association between glial apoptosis and disrupted axonal transport. In some cases of severe necrosis, APP and DNA-PKcs axonal immunopositivity was maximal below the site in penumbral areas where glial cells were preserved. DNA-PKcs antibody staining was also present in axonal swellings, potentially due to the accumulation of protein from the cell nucleus or mitochondria following disruption in axonal transport. Caspase-3 immunopositive axonal swellings were also found in

association with APP immunopositivity. TUNEL immunopositivity was seen in oligodendrocytes, astrocytes and microglia in all segments but the subset of oligodendrocytes appeared to be maximally staining.

APP immunopositivity was most often seen at the site of injury but was also present above and below the site at 24 hours, suggesting secondary axonal insult away from the primary impact. APP immunostaining was present in a subset of axons at qualitatively greater number in the posterior columns, towards the central cord. Damage to the motor tracts as evidenced by APP immunostaining in the corticospinal region would be consistent with the motor dysfunction on clinical assessment, greatest at the early time points (median BBB of 16, showing trunk instability, tail and lower limb weakness). Median BBB score improved to near-normal (20) by 3 weeks and functional improvement was also seen using rotarod, tail-flick and ledge beam, suggesting reversibility of motor changes.

Human Studies

A penumbra of damage with axonal swellings was evident, of which a subset were APP immunopositive. APP positive axonal swellings were seen at a range of time-points as early as 5 hours and up to 5 months post-injury. Furthermore, APP immunopositive axonal swellings were seen in segments above and below the site of compression injury, indicating widespread changes in fast axoplasmic transport. The presence of APP-positive axons at the later time points suggests delayed injury to axons.

In human acute SCI there was evidence of myelin damage on Weil staining in cases of longer survival post-injury (26 days, 32 days, and 5 months), and this was associated with APP immunopositivity. The present study provides evidence that caspase-3 may play a role in the cleavage of APP following acute compressive spinal cord injury. Caspase-3 was found to co-localise with APP using confocal microscopy. The Amy-33 amyloid-beta antibody also co-localised with axons expressing APP, however the specificity of this antibody is contentious, as it labelled the neuritic APP positive component of senile plaques and not the central Amyloid-beta recognised by other established amyloid-beta antibodies. Our studies therefore suggest that the Amy-33 antibody is not specific for amyloid-beta, but rather is another marker for APP.

One potential mechanism for delayed axonal injury, is that structural damage to the cell body and its axon, with associated ongoing ischaemia from compression, leads to increased intracellular calcium (Pettus and Povlishock, 1996, Maxwell et al., 1997), altered organisation of neurofilaments, disruption of axonal transport, the formation of axonal swellings and finally the axonal retraction bulb, which indicates a complete blockage of axonal transport (Jarafri et al., 1997). It is of note that both motor and sensory tracts were affected, including the lateral and anterior corticospinal tracts, and gracile and cuneate fasciculi. It is acknowledged however, that in some instances the large degree of necrosis and compression of the cord made distinguishing individual tracts by observers difficult.

There was axonal co-localisation of caspase-3 and APP antibodies, suggesting a possible linkage between the two. The results using CMAP and APP, CMAP and Amy-33 amyloid-beta and caspase-3 and Amy-33 amyloid-beta are equivocal since our subsequent investigations have cast doubt on the specificity of the Amy-33 and CMAP antibodies. The DAKO antibody, which recognises the amino acid segment of the amyloid-beta peptide, showed a different pattern of immunopositivity to that of the Amy-33 amyloid-beta antibody.

4.6 Conclusions – Histopathological Changes in Experimental and Human Acute Compressive Myelopathy

4.6.1 Apoptosis

In this experimental model of an acute compressive impact contusional spinal cord injury, changes consistent with cellular apoptosis were found by 24 hours, maximal in glia and neurons at the site of compression but also widely present above and below this site. Apoptotic staining was present at early and late time points experimentally, and this was congruent with findings in human tissue in which apoptosis was seen across a wide temporal spectrum of survival post-injury. The variable clinical and histopathological changes in the human case material, in correlation with immunohistochemistry, support the presence of glial and neuronal apoptosis across a wide range of injury severity.

4.6.2 Axonal Injury

Disrupted axonal transport, greatest at the site of compression injury, was present in both the experimental and human material. Caspase-3 may contribute to the proteolytic cleavage of APP in acute SCI but further studies are required.

CHAPTER 5

GENERAL DISCUSSION CHRONIC AND ACUTE COMPRESSIVE MYELOPATHY

The pathophysiology of chronic and acute spinal cord injury is yet to be fully dissected; however both conditions appear to involve apoptosis as a common secondary process. Research in this area is important as it may underlie future therapeutic molecular targets. While much research addresses the pathophysiology of acute spinal cord injury, chronic compressive myelopathy, occurring over months or years, carries significance as the most common cause of spinal cord dysfunction in older people. It may be caused by both mechanical compression and stretching due to spondylotic mechanisms, such as disc prolaspse or osteophytosis, spinal cord tumours and syringomyelia (Henderson et al., 2005). The outcome of surgical versus conservative management remains unpredictable and criteria for surgery unclear. An improved understanding of the underlying pathophysiology may lead to effective therapeutic intervention strategies designed to limit cellular damage within the spinal cord. This study provides a novel comparison of acute and chronic compressive myelopathy in both experimental and human tissue. Human material was analysed from pedestrian or motor vehicle incidents (acute) and spondylosis, malignancy or syringomyelia cases (chronic). Two experimental models, one of chronic compressive myelopathy and one of acute traumatic spinal cord injury, were developed to further investigate the presence of apoptosis.

Chronic compressive myelopathy involves a complex series of pathophysiological events which evolve at varying time intervals after the initial insult. Depending on the site and nature of the inciting injury, a wide range of neural, glial, axonal, dendritic and vascular elements may be affected, and damage may occur distant to the original injury site. Compressive myelopathy can be divided into two macroscopic regions of injury: direct mechanical compression at one or multiple levels; and non-compressive factors often extending above and below the site of compression (such as ischaemia or altered axonal transport). Experimental and human studies on cervical spondylotic myelopathy suggest a key role for apoptosis. In one such study by Fehlings and colleagues (2006) TUNEL immunopositive neurons and caspase-3 and P75 immunopositive glial cells were found in 8 postmortem cases of cervical spondylotic myelopathy (6 male, 2 female: mean age 73, range 61–89 years). There was a loss of AHCs, dorsal root degeneration, and loss of myelinated axons within the dorsal and lateral columns in association with apoptosis of myelin basic protein (MBP) positive oligodendrocytes. Staining for apoptotic markers in oligodendrocytes has been demonstrated to occur at large distances from the site of injury (Shuman et al., 1997, Li et al., 1999). The number of subjects used has been minimal and

larger studies are required. Future studies should investigate apoptosis using a wide range if immunological markers in correlation with morphological changes.

In traumatic SCI, two major stages of tissue damage occur within the first 24 hours: immediate mechanical injury to cells; and secondary cascades leading to structural damage within the tissue. The molecular cascade leading to neuronal and glial cell death after spinal cord injury is complex, involving intra- and extra-cellular signalling. Secondary injury mechanisms include apoptosis, ischaemia, ionic imbalances, haemorrhage, oedema, inflammation and production of free radicals, occurring with varying severity and spatial distribution (Walshe, 1970, Emery, 1998).

The principal aims of the present study were to assess apoptosis as a secondary process in acute and chronic compression, describing the nature and spatial distributions of cellular injury (to nerve cell bodies, axons, oligodendroglia, astrocytes, microglia/macrophages) in the white matter and central grey matter in an experimental model. The study aimed to correlate the changes with the immunoexpression of a range of caspase-dependent markers of classical apoptosis in the different cell types in acute and chronic spinal cord compression. In the chronic model, the effect of decompression at 24 hours and 3 weeks was assessed and in addition, a comparison of findings in human tissue is made. In total, 78 male 12-15 week old Sprague-Dawley rats underwent spinous processotomy and insertion of a sheet of expanding water-absorbing urethane-compound polymer (Aquaprene C, Parchem Pty Ltd. Australia) to occupy about 50% of the spinal canal diameter at the T12 level.

The experimental model developed by Kim and colleagues (2004) was modified in our laboratory by stabilising the polymer to the posterior vertebral wall to enable movement of the spinal cord over a fixed mass in replication of human spondylosis. Motor-sensory functional outcome, as assessed by a panel of tests including the Basso, Beattie, Bresnahan Locomotor Rating Scale (BBB score), rotarod, ledge beam walk and tail flick, was used to assess recovery after surgery and progressive impairment with spinal cord compression. For histological studies, 6 rats were sacrificed in each group at 24 hours, 1, 3, 9 and 20 weeks. Posterior decompression was performed at 24 hours and 3 weeks, with survival to 9 weeks. Cross-sectional area measurements of posterior white matter and total cord area further assisted in determining injury severity.

The following hypotheses were addressed in experimental and human studies:

1. **Cellular pathology and apoptotic cell death is maximal at the site of compression in chronic and acute compressive myelopathy.**
2. **Ongoing axonal changes and white matter degeneration follow chronic and acute compressive myelopathy.**
3. **Functional abnormalities, cellular pathology and apoptosis are reduced by decompression in chronic compressive myelopathy.**
4. **Early decompression (24 hours) produces a greater reduction in cellular pathology and apoptotic cell death than late decompression (3 weeks) in chronic compressive myelopathy.**

Apoptosis was maximal at the site of compression in both rodent and human tissue, and was comparable in acute and chronic compressive myelopathy. Furthermore, apoptosis was present in a penumbra up to two segments above and below the site, suggesting a role for secondary cell death in acute and chronic compressive myelopathy in these distal segments of spinal cord. Necrosis was minimal in experimental chronic compressive myelopathy using the polymer model. In human cases of both acute and chronic compression, apoptosis was maximal in the penumbra surrounding areas of tissue necrosis.

Our studies of human material suggested a role for apoptosis in chronic compressive myelopathy due to spondylosis, malignancy and syringomyelia. Using the gold-standard marker of apoptosis, TUNEL, immunopositive neurons and glia were maximal at the site of compression and in penumbral areas. In cases where severe necrosis was evident at the site of compression, TUNEL positive glia and neurons were present in the penumbra above and below. Apoptosis of neural and glial cell types was demonstrated in experimental chronic compressive myelopathy and this was consistent with changes seen in the human. Caspase-9, PARP and active caspase-3 staining was found in glia at, above and below the site of compression in all injury groups. A qualitative increase in aC3 immunopositive glia was seen in decompression groups. Glial and neuronal staining was rare using TUNEL. Neuronal staining for aC3, C9 and PARP was present at 9 and 20 week sacrifice. The presence of widespread AIF immunopositivity in glial and neuronal elements is a novel finding in human compressive myelopathy. Immunostaining for C9 and PARP was similar in compression and decompression groups.

ELISA studies provided quantitative evidence for the presence of apoptosis in chronic compressive myelopathy. Active caspase-3 was greater expressed in the 24 hour decompression (mean 0.32, $p = 0.01$) and 3 week decompression (mean 0.31, $p = 0.02$) groups versus the 9 week persisting compression group (mean 0.19).

In experimental acute SCI, histopathological changes including central haemorrhage and an acute inflammatory infiltrate occurred maximally 24 hours post-injury, with near total resolution by 3 weeks, correlating with an improvement in motor-sensory function. Apoptosis as detected by a panel of immunological markers was qualitatively maximal at the site in human and experimental studies. In our human material, central haemorrhagic necrosis was a feature and this was consistent with the common radiological and pathological changes seen clinically. Apoptosis has previously been demonstrated in neurons, oligodendrocytes, microglia and astrocytes (Beattie et al., 2000) as early as 30 minutes post-injury (Crow et al., 1997). In our study we found that apoptosis was widespread by 24 hours, heterogeneous in cross-section, and occurring up to two segments from the site of injury. These changes persisted despite a resolution of histopathological changes and functional deficits. Thus, ongoing study of apoptosis and its functional effect in both acute and chronic compressive myelopathy is important with a potential focus on the effects of inhibition of the apoptotic cascade and functional outcomes. Of key importance may be the point at which reversible changes in the apoptotic cascade become irreversible in order to prevent cell demise.

Ongoing axonal change and white matter degeneration was demonstrated in human and experimental chronic compressive myelopathy. Oligodendrocytes are vulnerable to a wide range of damaging stimuli resulting in apoptotic cell death including oxidative stress, toxins, radiation, and mechanical injury (Profyris et al., 2004). Their central role in the pathogenesis of progressive neurological diseases such as chronic compressive myelopathies is increasingly recognised (Kim et al., 2003), and their loss may compromise the axon. Demyelinative changes and axonal injury were assessed using the Weil stain and amyloid precursor protein (APP) respectively. Olig2, glial fibrillary acidic protein (GFAP) and ionized calcium binding adaptor molecule 1 (Iba1) were used to assess oligodendrocytes, astrocytes and microglia. In the human studies, APP immunopositive axonal swellings were maximally present at the site of compression, where tissue damage such as necrosis, haemorrhage and anterior horn cell loss, was maximal.

In the chronic experimental model, APP immunopositivity was consistent with persisting axonal damage and disruption of fast axoplasmic transport in a subset of axons. APP immunoreactive axonal swellings were found at all time points. APP axonal immunopositivity was rare or occasionally present in compression groups but surprisingly, it was present in frequent numbers after decompression. APP immunoreactive axonal swellings in the distribution of motor and sensory tracts were a feature of acute spinal cord injury in experimental and human studies. In the chronic experimental model, reactivity within astrocytes using GFAP was seen as early as 24 hours and persisted up to 20 weeks. A qualitative increase in microglial activation was found using Iba1, greatest at 1 week after injury. A qualitative loss of oligodendrocytes was seen using Olig2 at 9 and 20 weeks. There was pallor of the Weil stain above the site of compression at 20 weeks, consistent with myelin changes.

At 24 hours survival in the acute rodent model, axonal swellings were semi-quantitatively most numerous in the deep posterior white matter, where the corticospinal tracts are located. In human acute SCI, APP positive axonal swellings were found in the penumbra surrounding necrosis as early as 5 hours post-injury and extending to 5 months post-injury. APP immunopositive axonal swellings were present at, above and below the site of compression and may represent disrupted fast axoplasmic transport. Furthermore, APP co-localised with caspase-3 on double immunolabelling, suggesting an association.

The apoptosis of glia and axonal changes may be interrelated with neuronal apoptosis. Fehlings and Skaf (1998) proposed that neuronal activation of glia with subsequent release of cytotoxic factors such as glutamate, cations and free radicals may result in microglial and oligodendroglial apoptosis with secondary axonal damage. Whilst it is beyond the scope of this study to assess direct cytotoxicity, our experimental model provides evidence of persisting apoptosis and axonal injury and the associated time points. There was insufficient evidence for the proteolysis of APP or the production of caspase-mediated amyoid-beta peptide as a neurotoxic process in syringomyelia.

Functional abnormalities, cellular pathology and apoptosis were not reduced by decompression. In the compression groups a significant increase in tail-flick time versus control was found at 1 week ($p < 0.0001$) and 3 weeks ($p = 0.002$) suggesting motor-sensory impairment. A progressive decrease in BBB locomotor score was seen at 1, 3, 9

and 20 weeks ($p < 0.0001$). There was no significant change in tail-flick scores between 9 week continuous compression and 24 hour or 3 week decompression groups ($p = 0.84$) and similar rotarod function was also observed across the 3 groups ($p = 0.22$). BBB scores were lower with 9 weeks continuous compression (median 19) than 24 hour (median 21) or 3 week (median 20) decompression, but this was not statistically significant ($p = 0.07/0.1$). Foot faults on the ledge beam were increased in the 9 week continuous compression group versus both of the decompression groups, yet this also was not statistically significant.

In an unexpected finding, decompressive surgery lead to variability and in some cases a worsening of immunostaining for apoptotic markers and severity of axonal injury in a novel rodent model of chronic spinal cord compression. These changes occurred despite restoration of posterior column area following decompression. APP immunopositive axonal swellings were frequently seen in decompression groups. The effect of repeat surgery as a factor in worsening apoptosis was controlled for by a double sham group and it is theorised that other factors, such as reperfusion, fluid shift and axonal transport contributed to re-expansion of the spinal cord and these may be important subjects for future study. In summary, surgical decompression in mild compressive myelopathy may result in a variable outcome with the potential for worsening of histopathological changes.

Early decompression (24 hours) did not produce a greater reduction in cellular pathology and apoptotic cell death than late decompression (3 weeks). Glial and neuronal immunostaining for apoptotic markers was found at, above and below the site of initial compression in the decompression groups, comparable to the chronic compression groups. A newly described loss of the posterior white matter, maximal at the site of compression, appeared reversible with decompression at early (24 hours) and late (3 week) time points. The total cross-sectional area of the spinal cord decreased with with ongoing compression to a minimal area at 3 weeks, suggesting possible disruption in bidirectional axonal transport, but these changes resolved with decompression (3 week group mean $3.05mm^2$ increasing following decompression at 3 weeks with survival to 9 weeks to 5.75 mm^2). At 3 weeks a significant increase in posterior white matter above (mean 0.45, $p = 0.004$) and below (mean 0.58, $p < 0.0001$) the site of compression (compared to the site) was found. Necrosis was minimally present in our model but histopathological changes including central chromatolysis and axonal swellings were variable in both early and late decompression groups. Axonal swellings were frequently seen in the 24 hour

decompression group but not in the 3 week decompression group. These studies suggest that apoptosis plays a significant role in human and experimental acute and chronic compressive myelopathy. This experimental model of chronic compression of the spinal cord is novel and may provide a basis for future study.

In summary, histopathological changes were variable and thus may be less predictable in both decompression groups. Chronic, fixed, posterior compression resulted in a potentially reversible loss of white matter at the site using decompressive surgery. Compensatory changes in area were found above and below the spinal cord which may reflect altered axoplasmic transport.

5.1 CONCLUSIONS

i. **The pathology of mild chronic compression of the spinal cord is different from acute compression of the spinal cord although apoptosis is prominent at both ends of the spectrum.**

ii. **Mild chronic compression of the spinal cord in rats produces potentially reversible alterations in the bidirectional axoplasmic flow to produce a 'damming effect' of axoplasmic flow in the white matter above and below the site of maximal compression, reflected in a reduction of white matter at the site of compression. These alterations in white matter are associated with increased apoptotic cell death of the supporting glia maximal at the site of compression. Necrotic cell death is a minor feature in this mild end of spectrum chronic compressive spinal cord injury.**

iii. **Acute impact compression of the rat spinal cord, titrated to produce a mild reversible functional deficit, results in a spectrum of tissue damage including central haemorrhagic necrosis, apoptotic cell death in the penumbra and surrounding white matter, and axonal injury.**

iv. **Surgical decompression in the rodent model of mild compressive myelopathy results in increased apoptotic cell death and axonal injury compared to animals with non-treated compression, despite restoration of spinal cord anatomy and controlling for the effects of surgery.**

v. **Co-localisation of APP and caspase-3 is present in a subset of axons in human chronic compressive myelopathy.**